Carl von Ossietzky
Universität
Oldenburg

Von der Fakultät VI – Medizin und Gesundheitswissenschaften
Department für Versorgungsforschung
zur Erlangung des Grades und Titels eines

philosophiae doctor (PhD)

angenommene Dissertation

Detecting Movement Abnormalities: Automated Analysis of Periodic Human Movements in Occupational and Clinical Scenarios

von

Pedro Fernando Arizpe Gómez
geb. am 17.11.1988
in Puerto Vallarta, Jalisco, México

Gutachter:

Prof. Dr.-Ing Andreas Hein
Prof. Dr. Med. Karsten Witt
Prof. Dr.-Ing Vanessa Cobus

Oldenburg, Disputation am 27. Februar 2026

Summary/Zusammenfassung

Movement signatures contain invaluable information about the general state of health and the ability to perform daily activities. Quantitative movement analysis helps us understand these signatures and grasp their implications. This dissertation investigates the potential of multisensor motion capture setups, including markerless movement estimation and wearable sensing, for clinical and occupational applications. It proposes analytics pipelines that combine movement information with statistical and machine learning methods to extract key health indicators and insights.

The main contributions to the field of automated movement analysis are: integrating multi-sensor tracking – including depth cameras, wearable sensors, and optical motion capture—with AI[1]-based methods to objectively assess movement irregularities in diverse demographics, including craftspeople and people with neurological movement disorders Parkinson's Disease. It explores best practices for high-precision tracking, bridges clinical and ergonomic applications, and offers a movement analysis framework that can enable early, automated detection of motor disorders and occupational risks. The work provides a foundation for scalable, real-time health monitoring and supports the development of preventive interventions to improve quality of life and workplace safety.

Multisensor movement capture and automated kinematic analysis were key components of this research. Modalities include RGB-D[2] cameras (e.g., AzureKinect[3]), Inertial Measurement Units, and optical Motion Capture. Machine learning supported pose estimation yields joint trajectories that were processed into key movement indicators, including Step Length, Gait Cadence, Gait Velocity, joint ranges, and temporal irregularity (arrhythmicity). For occupational tasks, ergonomic scores (e.g., Rapid Entire Body Assessment) and guideline-based classifications (DGUV[4] 208-033) were automatically computed in different scenarios, including laboratory settings and real-world field environments. Supervised models and statistical tests complement correlation-based validation where appropriate.

In the clinical domain, the validity of RGB-D-based systems was evaluated against a gold-standard (GAITRite[5]) with good agreement for Step Length, Gait Velocity, and Gait Cadence. Upper Extremity mobility was assessed with limited correlation of amplitude/speed with MDS-UPDRS[6], while arrhythmicity was a promising marker. Markerless kinematics quantify task-specific and lateralized effects under Transcranial Temporal Interference Stimulation and enable retrospective MDS-UPDRS analyses from routine video.

In the occupational domain, markerless joint angle estimation was systematically evaluated. The effects of occlusion and viewpoint in markerless sensing were discussed. Wearable sensors and DGUV labeling revealed high knee and back loads for floor-level and bent work. An automated Rapid Entire Body Assessment pipeline combined with Surface Electromyography shows mixed group effects and high inter-individual variability. Transformer-based activity recognition can distinguish complex tasks, with performance depending on label granularity.

Overall, this dissertation demonstrates that the principles of objective, sensor-based assessment extend seamlessly over occupational and neurological health assessment. Both fields aim to mitigate the effects of motor impairments – whether stemming from disease or work-related strain – on individuals' quality of life and productivity. This thesis aims to help pave the way towards a multi-environment prevention-based health monitoring paradigm.

[1] Artificial Intelligence
[2] Color and Depth
[3] Microsoft® Azure™ Kinect™
[4] "Deutsche Gesetzliche Unfallversicherung" [German Statutory Accident Insurance]
[5] GAITRite® Electronic Walkway
[6] Movement Disorder Society's Unified Parkinson Disease Rating Scale

Deutsche Übersetzung

Bewegungssignaturen enthalten wertvolle Informationen über den allgemeinen Gesundheitszustand und die Fähigkeit, Alltagsaktivitäten auszuführen. Quantitative Bewegungsanalyse hilft uns, diese Signaturen zu verstehen und ihre Implikationen zu erfassen. Diese Dissertation untersucht das Potenzial multisensorischer Motion-Capture-Setups – einschließlich markerloser Bewegungsschätzung und tragbarer Sensorik – für klinische und arbeitsmedizinische Anwendungen. Sie schlägt Analysepipelines vor, die Bewegungsinformationen mit statistischen Methoden und maschinellem Lernen kombinieren, um zentrale Gesundheitsindikatoren und Erkenntnisse zu extrahieren.

Die wesentlichen Beiträge zum Bereich der automatisierten Bewegungsanalyse sind: die Integration von Multi-Sensor-Tracking – einschließlich Tiefenkameras, Wearables und optischem Motion Capture – mit AI-basierten Methoden zur objektiven Beurteilung von Bewegungsauffälligkeiten in unterschiedlichen Populationen, einschließlich Handwerksberufen und Personen mit neurologischen Bewegungsstörungen (Parkinson Krankheit). Die Arbeit untersucht Best Practices für hochpräzises Tracking, schlägt eine Brücke zwischen klinischen und ergonomischen Anwendungen und bietet einen Bewegungsanalyse-Framework, der eine frühe, automatisierte Erkennung motorischer Störungen und arbeitsbedingter Risiken ermöglichen kann. Die Arbeit legt damit eine Grundlage für skalierbares, echtzeitfähiges Gesundheitsmonitoring und unterstützt die Entwicklung präventiver Interventionen zur Verbesserung von Lebensqualität und Arbeitssicherheit.

Multisensorische Bewegungserfassung und automatisierte kinematische Analysen waren zentrale Komponenten dieser Arbeit. Modalitäten umfassten RGB-D-Kameras (z. B. AzureKinect), Beschleunigungssensoren sowie optisches Motion Capture. ML-gestützte Pose Estimation liefert Gelenktrajektorien, die zu zentralen Bewegungsindikatoren verarbeitet wurden, darunter Step Length, Gait Cadence, Gait Velocity, Gelenkbewegungsumfänge und zeitliche Irregularität (Arrhythmizität). Für arbeitsrelevante Tätigkeiten wurden ergonomische Scores (z. B. REBA[7]) sowie richtlinienbasierte Klassifizierungen (DGUV 208-033) automatisch berechnet – sowohl in Laborumgebungen als auch in realen Feldszenarien. Überwachtes Lernen und statistische Tests ergänzen korrelationsbasierte Validierungen, wo angemessen.

Im klinischen Bereich wurde die Validität von RGB-D-basierten Systemen gegenüber einem Goldstandard (GAITRite) evaluiert, mit guter Übereinstimmung für Schrittlänge, Ganggeschwindigkeit und Gangkadenz. Die obere Extremität wurde betrachtet mit begrenzten Korrelationen von Amplitude und Geschwindigkeit mit MDS-UPDRS, während Arrhythmizität ein vielversprechender Marker war. Markerlose Kinematik quantifiziert aufgaben-spezifische und lateralisierten Effekte unter Transcranial Temporal Interference Stimulation und ermöglicht retrospektive MDS-UPDRS-Analysen aus Routinenvideos.

Im arbeitsmedizinischen Bereich wurde markerlose Gelenkwinkelabschätzung systematisch bewertet. Die Auswirkungen von Okklusion und Blickwinkel in markerlosen Verfahren wurden diskutiert. Tragbare Sensorik und DGUV-Labeling zeigten hohe Knie- und Rückenbelastungen bei bodennahen und vorgebeugten Tätigkeiten. Eine automatisierte REBA-Pipeline kombiniert mit Surface Electromyography weist gemischte Gruppeneffekte und hohe interindividuelle Variabilität auf. Transformer-basierte Activity Recognition kann komplexe Tätigkeiten unterscheiden, wobei die Performance von der Labelgranularität abhängt.

Insgesamt zeigt diese Dissertation, dass sich die Prinzipien objektiver, sensorbasierter Bewertung nahtlos sowohl auf arbeitsmedizinische als auch auf neurologische Gesundheitsbeurteilung übertragen lassen. Beide Felder zielen darauf ab, die Auswirkungen motorischer Einschränkungen – sei es durch Krankheit oder arbeitsbedingte Belastung – auf Lebensqualität und Produktivität abzumildern. Diese Arbeit soll dazu beitragen, den Weg hin zu einem multi-Umgebung, umfassenden, präventionsbasierten Gesundheitsmonitoring zu ebnen.

[7] Rapid Entire Body Assessment

Contents

[8] Contributor Roles Taxonomy

Acronyms

2D Two-Dimensional

3D Three-Dimensional

AB "Aktiebolag" [Corporation]

Adam Adaptive Movement Estimation

ADL Activities of Daily Living

AI Artificial Intelligence

AMD Advanced Micro Devices

ANOVA Analysis of Variance

AzureKinect Microsoft® Azure™ Kinect™

BMBF "Bundesministerium für Bildung und Forschung" [German Federal Ministry of Education and Research]

BT Body Tracking

CA California

Cad Gait Cadence

CAPTIV Tech Ergo Appliquées' CAPTIV System

CIR Clinical Image Retrieval

CNN Convolutional Neural Network

CPR Cardiopulmonary Resuscitation

CPU Central Processing Unit

CRediT Contributor Roles Taxonomy

CSV Comma-Separated Values

CUDA Compute Unified Device Architecture

CUDF CUDA DataFrame Library

DBA Doing Business As

DBS Deep Brain Stimulation

DBSCAN Density-Based Spatial Clustering for Applications with Noise

DGUV "Deutsche Gesetzliche Unfallversicherung" [German Statutory Accident Insurance]

DIP Distal Interphalangeal

DK Developer Kit

DRKS "Deutsches Register Klinischer Studien" [German Clinical Trials Register]

e. V. "eingetragener Verein" [registered association]

FOV Field of View

FPS Frames Per Second

GaitLab Mobile GaitLab - Portabiles HealthCare, Erlangen, Germany

GAITRite GAITRite® Electronic Walkway

GBS German Bionic Systems

GDPR General Data Protection Regulation

GELU Gaussian Error Linear Unit

GB GigaByte

GPU Graphics Processing Unit

GUI Graphical User Interface

HP Healthy Participant

HPC High Performance Computing

HVAC Heating, Ventilation and Air Conditioning

Hz Hertz

ICC Intraclass Correlation Coefficient

ICP Iterative Closest Point

IMU Inertial Measurement Unit

Inc. Incorporated

IPI Inter-Peak Intervals

IQR Interquartile Range

kHz Kilohertz

KinectV1 Microsoft® Kinect™ V1

KinectV2 Microsoft® Kinect™ V2

LLE Left Lower Extremity

LSTM Long Short-Term Memory

LUE Left Upper Extremity

MA Massachusetts

MAE Mean Absolute Error

MCP Metacarpophalangeal

MDS-UPDRS Movement Disorder Society's Unified Parkinson Disease Rating Scale

MHA Multi-Head Attention

MoCap Motion Capture

MP MegaPixel

MRI Magnetic Resonance Imaging

MSD Musculoskeletal Disorders

MVC Maximum Voluntary Contraction

NA Not Applicable

NARS Neuroergonomic Assessment Rating Scale

NASA-TLX NASA Task Load Index

NISO National Information Standards Organization

NFOV Narrow Field of View

NJ New Jersey

ONNX Open Neural Network Exchange

OR Oregon

OWAS Ovako Working Posture Analysis System

PCC Pearson Correlation Coefficient

PD Parkinson's Disease

PIP Proximal Inter-phalangeal

PwPD Participant with Parkinson's Disease

PyTorch Python Torch Deep Learning Framework

Q-Q Quantile-Quantile

REBA Rapid Entire Body Assessment

ReHopE "Reduktion körperlicher Belastungen von Handwerksberufen durch optimierte Exoskelette" [Reduction of physical strain in skilled trades through optimized exoskeletons]

RESBEPA "Retrospektive Studie zur Quantifizierung von Bewegungsparametern bei Parkinson Patienten" [Retrospective study to quantify movement parameters in Parkinson's patients]

RGB-D Color and Depth

RGB Red, Green and Blue

RLE Right Lower Extremity

RMSE Root Mean Square Error

RNN Recurrent Neural Network

ROI Region of Interest

ROM Range of Motion

RTX Ray Tracing Texel eXtreme

RUE Right Upper Extremity

RULA Rapid Upper Limb Assessment

S-W Shapiro-Wilk

SD Standard Deviation

SDK Software Development Kit

sEMG Surface Electromyography

SIRKA "Sensoranzug zur individuellen Rückmeldung körperlicher Aktivität" [Sensor suit for individual feedback on physical activity]

SL Step Length

Smart-BT "Optimierte Bewegungstherapie durch die Interaktion künstlicher Intelligenz und Videotechnik mit Healthcare Professionals und Patienten" [Optimized movement therapy through the interaction of artificial intelligence and video technology with healthcare professionals and patients]

STN-DBS Subthalamic Nucleus Deep Brain Stimulation

SUS System Usability Scale

TEDIPA "TEleDIagnostik und Verlaufskontrolle bei PArkinson Erkrankungen" [Telediagnostics and progression monitoring in Parkinson's disease]

TETRIS Transcranial Temporal Interference Stimulation of Deep Brain Regions

tTIS Transcranial Temporal Interference Stimulation

UOL "Carl von Ossietzky Universität Oldenburg" [Carl von Ossietzky University of Oldenburg]

USA United States of America

USB Universal Serial Bus

Vel Gait Velocity

WA Washington

WFOV Wide Field of View

WRMSD Work-Related Musculoskeletal Disorder

YOLO You Only Look Once

Part I

Foundations

1 General Introduction

Human movement is a powerful indicator of health and quality of life [BSF21]. With the increasing availability of advanced sensing technologies and computational tools, the analysis of human motion has become more precise, scalable, and accessible. These developments have enabled the detailed assessment of periodic movements –such as gait, hand gestures, and joint rotations– across clinical, occupational, and everyday settings [Ari+20a; Ari+24].

Computer vision and machine learning have played a transformative role in this development. Frameworks such as Google's MediaPipe [Lug+19] and Ultralytics' YOLO[1] [Red16] allow for real-time, markerless video-based human pose estimation, even on consumer-grade devices. These tools facilitate continuous, non-invasive monitoring of motor function, expanding the reach of movement analysis beyond specialized laboratories and into real-world environments.

Movement analysis provides critical insights into neuromuscular coordination, balance, and motor control. In clinical settings, subtle deviations in movement patterns can serve as early indicators of neurodegenerative diseases such as PD[2] [Pag12; Zha+24]. In occupational contexts, repetitive or awkward movements are associated with MSD[3], particularly among aging workers [CV10; Sil08].

The integration of multi-sensor systems –including IMUs[4], RGB-D cameras, and optical MoCap[5]– has enabled the development of robust models for detecting movement abnormalities. When combined with machine learning algorithms, these systems support the extraction of meaningful biomarkers and facilitate the transition from subjective assessments to objective, data-driven diagnostics.

This paradigm shift has broadened the scope of movement science. By quantifying movement variability and identifying deviations from normative patterns, researchers can develop personalized risk profiles and preventive strategies. These approaches are especially relevant in aging societies, where mobility is closely tied to independence and quality of life [Wil+23; BSF21].

This thesis contributes to the evolving field by investigating the automated analysis of periodic human movements in both occupational and clinical settings. It explores the feasibility and efficacy of integrating wearable sensors, RGB-D cameras, and machine learning techniques to assess motor function, detect abnormalities, and support early intervention. The research encompasses multiple studies, including the validation of sensor systems, clinical trials, and field investigations, with the overarching goal of developing scalable, objective, and accessible movement assessment tools.

1.1 Research Motivation

The global trend of population aging has several implications for public health and the availability of qualified workers. According to recent demographic studies, the proportion of individuals aged 60 and older is expected to double by 2050 [Wil+23], reaching an unprecedented share in human history. This demographic shift brings forward critical challenges in healthcare, particularly in the management and prevention of age-related physical and neurological decline. Among the various health concerns, one of the most significant yet underaddressed issues is the deterioration of motor function, which directly impacts an individual's quality of life, autonomy, and productivity.

For example, PD has age as its highest risk factor [AS16]. In addition, early detection significantly improves the course of the disease [Pag12]. Furthermore, current established methods of diagnosis and monitoring are time-consuming and labor-intensive [Zha+24].

[1] You Only Look Once
[2] Parkinson's Disease
[3] Musculoskeletal Disorders
[4] Inertial Measurement Units
[5] Motion Capture

As people age, the prevalence of movement irregularities, such as gait instability and difficulties in performing certain tasks, becomes more pronounced. These motor abnormalities not only diminish the ability to perform daily activities but also pose significant risks to workplace safety and efficiency, especially in sectors that increasingly rely on an older workforce [Sil08; PG15]. In an aging society, where extended working lives are becoming the norm, understanding and addressing movement abnormalities in the aging population is essential for maintaining productivity and reducing the risk of workplace accidents.

Technological advances in movement analysis, powered by innovations in wearable sensors, computer vision, and machine learning, offer a promising avenue for the early detection and assessment of motor function deterioration. Periodic human movements, such as hand pronation-supination, fist opening and closing, finger tapping, and gait, are particularly well-suited for analysis using these technologies. Precise quantification of movement parameters, including speed, amplitude, and rhythmicity, enables the identification of subtle abnormalities that might be early indicators of neurodegenerative diseases such as PD or essential tremor.

Moreover, by continuously monitoring these movements in real-world settings, it becomes possible to detect irregularities at a stage when intervention can be most effective. The potential of these technological tools to provide real-time, non-invasive, and continuous movement analysis may open new pathways for both clinical practice and preventive healthcare [SKA21]. By identifying motor function impairments early, interventions can be implemented to delay or even prevent further deterioration, ultimately improving the quality of life for the elderly and maintaining a healthy, productive workforce. This research aims to explore the feasibility and efficacy of employing modern movement analysis techniques to assess periodic human movements, measure abnormalities, and evaluate their application for early detection of motor dysfunction in aging populations.

1.2 Research Objectives

The **objective** of this thesis is to investigate movement analysis in the context of movement irregularities, with a specific focus on defining the boundaries of expected variability in movement patterns and identifying pathological deviations. This research aims to bridge the gap between traditional clinical assessments and modern data-driven movement analysis by leveraging multi-sensor tracking, computational models, and machine learning to extract meaningful biomarkers for motor dysfunction and occupational strain.

It is not the aim of this thesis to provide clinical diagnoses or to replace established diagnostic procedures. Rather, the focus is on developing and validating analytical tools that support early detection and risk assessment, thereby complementing, but not substituting, clinical expertise. The intention is to enable objective, scalable, and accessible movement assessment, while recognizing that definitive diagnosis and therapeutic decision-making remain the responsibility of qualified healthcare professionals.

The emphasis on PD arises from its prevalence as a neurodegenerative disorder with significant motor manifestations and its status as a leading cause of disability in aging populations. PD serves as a representative model for studying movement abnormalities due to its well-characterized motor symptoms, the availability of standardized clinical assessments, and the urgent need for improved early detection methods. Insights gained from the analysis of PD-related movement patterns are expected to inform broader applications in both clinical neurology and occupational health.

1.2.1 Quantifying Normal and Abnormal Movement Patterns

To establish a foundation for movement analysis, this thesis seeks to quantify both normal and pathological movement variability across diverse populations. Healthy individuals, individuals with neurodegenerative diseases (PD), and craftspeople performing physically demanding work (who are at higher risk of WRMSDs[6] [Bab+25]) will be analyzed to identify characteristic movement signatures.

[6] Work-Related Musculoskeletal Disorders

A key component of this analysis involves detecting deviations in periodic movements, such as gait, pronation/supination of the hand, finger tapping, and overhead occupational tasks. By defining biomechanical thresholds, this thesis will differentiate between natural variability and clinically significant deviations. These findings will provide an essential basis for early detection of neurological disorders and preventive strategies against musculoskeletal degeneration in occupational settings.

1.2.2 Enhancing Multi-Sensor Tracking for Early Detection

To improve the precision and reliability of movement assessment, this research will validate and compare multiple motion tracking technologies. These include:

- **RGB-D cameras:** such as the AzureKinect (Microsoft Corporation, WA[7], USA[8]), the iPad® and the iPhone® (Apple® Inc.[9], CA[10], USA)
- **IMU sensors:** e.g., CAPTIV[11] (TEA France, Nancy, France), Movella DOTs (Movella Inc., CA, USA)
- **Optical motion capture systems:** e.g., OptiTrack (NaturalPoint, Inc. DBA[12] OptiTrack, Corvallis, OR[13], USA), Qualisys (Qualisys AB[14], Gothenburg, Sweden)
- **sEMG[15] sensors:** e.g., Trigno Avanti Sensors (Delsys, Inc., Natick, MA[16], USA)

The thesis will investigate the advantages and limitations of each system in capturing spatiotemporal movement parameters, joint kinematics, and joint kinetics.

By leveraging machine learning algorithms, this thesis aims to improve anomaly detection in movement, reducing reliance on subjective evaluations and enhancing assessment precision.

1.2.3 Applying Movement Analysis for Prevention and Early Intervention

One of the primary applications of this research is the development of movement risk profiles that facilitate early detection and intervention strategies. In the context of neurodegenerative disorders, machine learning models will be employed to analyze fine motor irregularities, allowing for non-invasive, data-driven early diagnosis.

For occupational health, the thesis will focus on identifying high-risk movement patterns in craftspeople that contribute to long-term musculoskeletal strain. By analyzing the biomechanical effects of repetitive work tasks – such as overhead lifting, kneeling, and load carrying– this research will provide quantitative recommendations for ergonomic adaptations. Furthermore, the integration of data-driven movement assessment tools will pave the way for real-time movement monitoring [SKA21], workplace modifications, and predictive injury prevention strategies.

[7] Washington
[8] United States of America
[9] Incorporated
[10] California
[11] Tech Ergo Appliquées' CAPTIV System
[12] Doing Business As
[13] Oregon
[14] "Aktiebolag" [Corporation]
[15] Surface Electromyography
[16] Massachusetts

1.3 Scope of the Thesis

This thesis focuses on the integration of multiple data sources to enable a comprehensive assessment of human movement, with an emphasis on periodic motor tasks. These tasks provide a structured framework for detecting abnormalities and quantifying movement variability.

The research incorporates:

- **Wearable sensors data** (such as IMUs and sEMG sensors) to capture kinematic and kinetic variables.
- **Image-based detection** (such as RGB-D cameras and MoCap systems) for external validation of movement patterns.
- **Clinically validated assessments**, such as:
  - MDS-UPDRS for PD symptom evaluation [Goe+08a]
  - REBA [HM00] for ergonomic risk assessment
  - OWAS[17] [SL96] for ergonomic risk assessment
- **Machine learning algorithms** for anomaly detection, classification, and predictive modeling.
- **Applications in clinical and occupational settings** to demonstrate the utility of movement analysis for early detection and risk prevention.
- **Controlled experimental conditions** to establish baselines and validate analytical tools.
- **System validation** to ensure accurate and reliable data collection across diverse populations and environments.

While the findings are relevant to clinical neurology, occupational health, and ergonomics, this thesis does not focus on implementing strain reduction interventions. Instead, it aims to develop analytical tools for early detection and risk assessment. Real-world deployment and longitudinal validation are considered future research directions.

1.4 Structure of the Thesis

This thesis is divided into five main parts, each addressing a specific dimension of the research.

1.4.1 Part I – Foundations

This part lays the groundwork for the thesis: General Introduction introduces the motivation, objectives, and scope of the research, followed by an overview of the thesis structure. Global Literature Review presents a global literature review, covering neurological and musculoskeletal movement disorders, classical diagnostic and ergonomic assessment methods, and recent advances in machine learning for human pose estimation. General Methodology outlines the general methodology, including the design of the studies, data acquisition strategies, machine learning techniques, and ethical considerations.

1.4.2 Part II – Human studies on movement analysis for neurodegenerative diseases

This part focuses on clinical applications of automated movement analysis for the early detection and monitoring of PD. It evaluates sensor-based and video-based approaches for quantifying motor abnormalities, validating their effectiveness for objective assessment in clinical neurology.

[17] Ovako Working Posture Analysis System

Chapter 4 - Validation of portable multi-sensor system for movement analysis (TEDIPA study)

This chapter presents the results of a study validating a portable multi-sensor system designed to provide objective gait and repetitive movement biomarkers for PD monitoring and remote assessment. The role of this chapter within the thesis is to establish sensor fusion and robust gait feature extraction methods, demonstrating that wearable and camera-based systems yield concordant gait biomarkers in both healthy and PD populations.

Chapter 5 - Clinical study for Parkinson's Disease symptom and treatment monitoring (TETRIS Study)

This chapter evaluates the sensitivity of movement-derived metrics to short-term modulation (tTIS[18]) and examines the relationship between motor changes and clinical measures. Its role within the thesis is to demonstrate that the developed analysis pipeline is capable of detecting physiologically meaningful changes in repetitive fine motor tasks and establishing a link between digital metrics and intervention outcomes.

Chapter 6 - Planned Retrospective Study on Video-Based Analysis of PD-Related Movements (RESBEPA Study)

In the context of this thesis, this chapter presents only the planned study design for the RESBEPA[19] study. It outlines the intended approach for demonstrating the feasibility of extracting clinically relevant repetitive-movement biomarkers from routine clinical video, thereby expanding the applicability of automated movement analysis to legacy datasets and low-resource environments. No results are presented; rather, the chapter describes how such a retrospective analysis will be conducted to enable scalable re-analysis of standardized clinical assessments.

While the first part focuses on clinical applications of automated movement analysis for neurodegenerative disorders, the same principles of objective, sensor-based assessment are equally relevant in occupational health. Both domains share a common goal: reducing the impact of motor impairments—whether disease-related or work-induced—on quality of life and productivity. The following chapters extend this framework to musculoskeletal disorders among craftspeople, demonstrating how validated methodologies and analytical pipelines can be adapted to real-world work environments for ergonomic risk assessment and prevention.

1.4.3 Part III – Human Studies Related to Musculoskeletal Disorders

This part complements the clinical investigations by focusing on occupational health and ergonomic risk assessment, including WRMSD, thereby integrating clinical and workplace perspectives into a cohesive framework.

Chapter 7 - Validation of Video-Based Movement Assessment (Smart-BT Validation Study)

This study validates the reliability of markerless RGB-D-based BT[20] systems, specially the AzureKinect, against wearable IMU references and optical MoCap systems. The primary contribution of this chapter to the thesis is the establishment of the accuracy, agreement, and operational limits of RGB-D-camera-only tracking and informs sensor selection for movement assessment in diverse contexts. Specifically, the investigation focuses on assessing joint angle estimation accuracy that are relevant for MSD prevention and neuroclinical applications. The results identify conditions in which markerless BT performance degrades (for example, supine tasks, rapid limb motion, occlusions, and infrared interference), thereby guiding future applications of these systems in real-world settings.

[18] Transcranial Temporal Interference Stimulation
[19] "Retrospektive Studie zur Quantifizierung von Bewegungsparametern bei Parkinson Patienten" [Retrospective study to quantify movement parameters in Parkinson's patients]
[20] Body Tracking

Chapter 8 - Observational field study on ergonomic risk with craftspeople (ReHopE Hospitationen Study)

In the context of this thesis, this field study serves to provide real-world validation of occupational strain assessment by observing three skilled trades craftspeople in their natural work environments. Joint angles are captured using wearable IMU sensors (CAPTIV system), and ergonomic risk levels are evaluated according to DGUV208-033 guidelines. The analysis focuses on exposure time across body regions (neck, back, knees, shoulders, elbows) during tasks such as climbing, lifting, floor work, and overhead work, thereby identifying high-risk postures and the body regions most affected by skilled trades work.

Chapter 9 - Markerless Ergonomic Assessment and Strain Analysis with Craftspeople (ReHopE Fokusgruppe Study)

This mixed-methods study evaluates the usability and acceptance of exoskeletons (CrayX, Skelex) in skilled trades through controlled task execution with five workers. Automated REBA scores are computed from video-based pose estimation (Detectron2), and muscle activation is measured via sEMG. Post-task focus groups gather qualitative insights on user experience and design requirements. The contribution of this chapter to the thesis lies in demonstrating the integration of automated ergonomic assessment (REBA, sEMG) with subjective feedback, thereby providing a comprehensive evaluation framework for the effectiveness and user acceptance of assistive technologies in occupational settings.

Chapter 10 - Craftspeople activity recognition with Wearable Sensors (ReHopE IMU-OptiTrack Study)

This chapter establishes the feasibility of automated activity recognition for occupational movements using deep learning methods. In a laboratory-based study with craftspeople and untrained individuals, IMUs and OptiTrack optical motion capture were employed to record physically demanding tasks, including load carrying, overhead work, floor work, and stair climbing. The analysis examines whether modeling temporal dependencies and joint interactions enables early detection of ergonomic risk factors. Furthermore, the investigation evaluates the impact of task granularity on classification performance, with a transformer-based machine learning model achieving up to 96% accuracy.

1.4.4 Part IV – Synthesis and Conclusions

This part synthesizes the findings from the clinical and occupational studies, highlighting their implications for movement science, healthcare, and workplace ergonomics. It discusses the broader impact of integrating multi-sensor systems and machine learning into movement analysis, addressing challenges such as data reliability, scalability, and ethical considerations.

Chapter 11 - Discussion

This chapter consolidates the key results from the thesis, comparing the performance of different sensor systems and machine learning models across clinical and occupational contexts. It evaluates the feasibility of deploying these technologies in real-world settings and identifies areas for improvement.

Chapter 12 - Conclusion

This chapter provides a summary of the thesis contributions, emphasizing the potential of automated movement analysis to transform clinical diagnostics and occupational health. It concludes with a discussion of the societal and scientific relevance of the findings, advocating for continued interdisciplinary collaboration in this field.

2 Global Literature Review

2.1 Neurological Movement Irregularities

Movement irregularities are hallmark symptoms of many neurodegenerative disorders, with PD being a prominent example. Characterized by a progressive loss of dopaminergic neurons, PD manifests a range of motor symptoms including tremor, bradykinesia, rigidity, and postural instability. Accurate and comprehensive assessment of these movement abnormalities is crucial for diagnosis, monitoring disease progression, and evaluating therapeutic interventions [Goe+08b]. Over the years, various methods have been developed and refined to capture these motor complexities, ranging from patient-reported outcomes to advanced sensor-based techniques [Bou25; Kha+25; Ha25].

One foundational method for tracking motor fluctuations in PD patients involves the use of diaries. Historically, paper diaries have been employed, allowing patients to self-report their "on" and "off" states and the presence of dyskinesias throughout the day. While offering valuable ecological insights into a patient's daily experience, paper diaries are susceptible to recall bias, incomplete entries, and "diary fatigue" [Ha25]. The advent of digital health technologies has introduced electronic diaries (e-diaries), which enhance compliance and accuracy, providing a more reliable capture of motor symptom fluctuations over time [Ha25].

A cornerstone of clinical assessment for PD is the MDS-UPDRS [Goe+08a], particularly Part III, which focuses on the motor examination. This standardized scale evaluates a broad spectrum of motor signs, including speech, facial expression, tremor, rigidity, finger tapping, hand movements, pronation-supination, leg agility, and gait [Goe+08a]. Clinicians use MDS-UPDRS Part III to objectively track motor performance and progression, making it an important outcome measure in both daily clinical practice and research trials.

Beyond structured clinical examinations, assessing applied motor skills in ADL[1] provides critical insights into the functional impact of PD on a patient's independence. PD symptoms can significantly complicate everyday tasks such as bathing, dressing, eating, and mobility. Instruments designed to evaluate ADL performance capture the multifaceted construct of daily functionality and are essential for understanding how motor impairments translate into real-world disability, guiding rehabilitative strategies [SGa19].

In recent years, wearable sensors and other sensoric technologies have revolutionized the objective quantification of movement abnormalities in PD. These small, lightweight devices, often incorporating accelerometers, gyroscopes, and magnetometers, can be worn on various body parts to capture continuous, real-time data on movement, tremors, gait, and balance [Bou25]. This objective data provides a highly granular and unbiased assessment of motor symptoms, often revealing subtle changes that may be difficult to detect during intermittent clinical visits. The large-scale, high-dimensional datasets generated by these sensors necessitate advanced analytical approaches. Machine learning algorithms are increasingly applied to extract distinctive kinematic signatures and biomarkers from sensor data, aiding in diagnosis, differential diagnosis, and monitoring disease progression [Kha+25]. These algorithms analyze complex movement patterns, identify subtle anomalies, and can even predict risks such as falls, thereby enhancing the precision and personalized management of PD. The focus of the present thesis lies precisely on developing and applying such algorithms and advanced measurement techniques to deepen our understanding and improve the assessment of movement anomalies in neurodegenerative disorders.

2.2 Musculoskeletal Disorders Among Craftspeople

Work-Related Musculoskeletal Disorders are a significant contributor to disability worldwide, leading to substantial societal costs. The integration of wearable motion capture devices in ergonomic assessments has emerged as a promising approach to prevent WRMSDs. These devices facilitate improvements in exposure and risk assessment and enhance the effectiveness of work technique training [LAF23; Har22].

[1] Activities of Daily Living

Traditionally, the assessment of musculoskeletal risk among craftspeople has relied on observational methods and self-reported questionnaires, such as the Nordic Musculoskeletal Questionnaire [Cra07] or direct workplace observations. While these approaches provide valuable information about symptom prevalence and general risk factors, they are limited by subjectivity, recall bias, and the inability to capture detailed, dynamic movement data [Gon+21].

The adoption of wearable motion capture devices addresses these limitations by enabling continuous, objective monitoring of workers' movements in real-world environments. These devices, equipped with IMUs, accelerometers, and gyroscopes, can record detailed kinematic data, allowing for the identification of hazardous postures, repetitive motions, and forceful exertions in real-time. The resulting data supports a more nuanced understanding of exposure to biomechanical risk factors and facilitates the development of targeted, data-driven interventions [SWL25].

Real-Time Monitoring They enable continuous monitoring of workers' movements, allowing for immediate identification of hazardous postures or motions.

Data-Driven Interventions The quantitative data collected can inform personalized interventions aimed at reducing the risk of injury.

Workplace Adaptations By providing objective feedback, these devices can suggest improvements in workplace conditions to reduce the risk of injury.

However, several challenges remain. Data privacy and security are critical concerns, particularly when collecting sensitive health-related information in occupational settings [FOI25; Bou+22]. Ensuring device comfort, durability, and user acceptance is essential for long-term adoption, especially in physically demanding environments. Additionally, the integration of wearable data into existing occupational health and safety frameworks requires standardized protocols and validation studies.

The future of ergonomic assessment among craftspeople lies in the integration of wearable technology with advanced data analytics and machine learning. These approaches enable the extraction of meaningful patterns from large, complex datasets, supporting predictive modeling of injury risk and the development of proactive prevention strategies [SWL25]. For example, machine learning algorithms can identify subtle changes in movement variability or compensatory strategies that may precede the onset of musculoskeletal symptoms, allowing for early intervention.

The application of wearable motion capture devices aligns with the objectives of this thesis, particularly in establishing movement variability baselines among craftspeople and developing AI-driven movement assessment tools for health monitoring and workplace adaptations. The portability and unobtrusiveness of these devices make them suitable for continuous monitoring in diverse work environments, providing a comprehensive understanding of movement patterns and risk exposures. With the integration of machine learning, these systems can achieve highly accurate motion tracking and risk prediction, supporting the development of effective early detection and intervention strategies.

2.2.1 Occupational Risk Factors

For craftspeople, "the most commonly reported biomechanical risk factors with at least reasonable evidence for causing WRMSDs include excessive repetition, awkward postures, and heavy lifting" [DV10]. These risk factors are prevalent in various industries, such as construction, manufacturing, and healthcare, where workers are exposed to physically demanding tasks that require repetitive movements and sustained postures. The cumulative effect of these occupational risk factors can lead to MSD, including pain in shoulders, elbows, wrists and hands, lumbar spine, knees, and ankles [Siz+04].

2.2.2 Impact on Movement Patterns

Occupational risk factors such as repetitive motions, forceful exertions, and awkward or static postures have a profound impact on the movement patterns of craftspeople [DV10; BP97]. Over time, these factors can lead to compensatory movement strategies, where workers unconsciously alter their posture or technique to minimize discomfort or fatigue [ML07; Kei+11].

Furthermore, the persistent exposure to these risk factors can reduce movement variability, as workers tend to adopt habitual patterns that may not be ergonomically optimal [ML07; SD11]. This reduction in variability is associated with a higher likelihood of overuse injuries, as the same tissues are repeatedly loaded in a similar manner. Conversely, some individuals may exhibit increased movement variability as a coping mechanism, which can also be maladaptive if it leads to inefficient or unsafe work techniques [SD11]. Understanding these changes in movement patterns is crucial for designing effective ergonomic interventions and for the development of sensor-based monitoring systems that can detect early signs of maladaptive movement and prevent the progression of WRMSDs.

2.3 Classical methods for neurological movement irregularity assessment.

This section provides an overview of established clinical and observational methods used to assess neurological movement irregularities. These classical approaches form the foundation for evaluating motor symptoms in neurodegenerative disorders, offering standardized frameworks for symptom quantification and comparison. Understanding these methods is essential for contextualizing recent advances in sensor-based and algorithmic assessment techniques.

2.3.1 Movement Disorder Society's Unified Parkinson Disease Rating Scale

The MDS-UPDRS [Goe+08a] is a comprehensive clinical rating scale designed to assess both motor and non-motor symptoms of PD. It is divided into four main parts, each targeting specific domains of the disease: Part I evaluates non-motor experiences of daily living (e.g., cognitive impairment, mood, and sleep disturbances); Part II assesses motor experiences of daily living, focusing on the patient's self-reported difficulties with activities such as speech, handwriting, and walking; Part III is the motor examination, performed by a clinician, and includes detailed tests for tremor (rest, postural, and kinetic), rigidity, bradykinesia (e.g., finger tapping, hand movements, pronation-supination, leg agility), postural stability, and gait; Part IV addresses motor complications, such as dyskinesias and motor fluctuations [Goe+08a]. Each item is scored on a scale from 0 (normal) to 4 (severe), allowing for a nuanced quantification of symptom severity and progression.

The motor examination in Part III, as highlighted in section 2.1, is particularly important for objectively evaluating changes in motor function. Specific tests within Part III are tailored to detect characteristic motor abnormalities: tremor is assessed at rest and during action, rigidity is evaluated in multiple limbs, and bradykinesia is measured through repetitive movements such as finger tapping and hand opening/closing. Gait and postural stability are examined through walking and balance tasks. This structured approach enables clinicians to systematically capture the range and severity of motor symptoms in PD, supporting both clinical decision-making and research applications [Goe+08a; SGa19].

Its structured scoring and direct observational methodology allow clinicians to quantify disease severity and progression, supporting both routine monitoring and the evaluation of therapeutic outcomes. Due to its clinical robustness, the scale is frequently used as a benchmark in research and serves as a comparative reference for newer, sensor-based or algorithmic diagnostic methods.

2.4 Classical methods for ergonomics assessment

Ergonomic assessment methods are essential tools for evaluating workplace postures and movements to identify potential risks for MSDs. These methods provide structured frameworks for analyzing how workers interact with their environment, allowing for the identification of hazardous postures and the development of interventions to improve workplace ergonomics. While there are numerous ergonomic assessment tools available, this section focuses on three widely used methods: REBA [HM00], OWAS [SL96], and RULA[2] [MC04].

2.4.1 Rapid Entire Body Assessment

The REBA [HM00] is a comprehensive ergonomic assessment tool designed to evaluate the postural risks associated with work tasks, focusing on the whole body. REBA [HM00] systematically assesses the postures of various body segments, such as the neck, trunk, legs, and arms, as well as external factors like force, grip type, and coupling. Each body segment is assigned a score based on its position and the degree of flexion, extension, abduction, or rotation. The final REBA [HM00] score is calculated through a series of formulas that combine the individual segment scores and other task-related variables, categorizing the task into one of five action levels. These action levels indicate the need for ergonomic intervention, ranging from negligible risk to high-risk conditions that require immediate attention.

REBA [HM00] is particularly useful in industrial and healthcare settings, where workers are often exposed to awkward and repetitive postures. It provides a relatively quick and simple way to identify risks that may contribute to MSDs, such as back pain or shoulder injuries. The tool is designed to be used by practitioners with limited ergonomic expertise, making it widely accessible. However, the trade-off for simplicity is the lack of specificity in assessing more subtle or dynamic postural variations, and its effectiveness may decrease in more complex scenarios where movement patterns are highly variable or involve multiple interacting risk factors.

2.4.2 Ovako Working Posture Analysis System

The OWAS [SL96] is an ergonomic assessment method developed specifically to evaluate postural stress during industrial work. It analyzes the worker's posture in relation to the back, arms, legs and the load being handled. The OWAS [SL96] assigns each posture to one of four categories based on the severity of its ergonomic risk, with Category 1 representing a low risk and Category 4 representing a highly harmful posture requiring immediate intervention. These categories provide a guide for employers to redesign work tasks or implement ergonomic changes to reduce physical strain on workers and prevent injuries.

OWAS [SL96] is most effective for continuous work tasks where postures tend to be static or repetitive, such as assembly lines or manual labor in industries like mining and construction. A key advantage of OWAS [SL96] is its simplicity and ease of use, which allows non-experts to quickly learn and apply the method. However, like other observation methods, OWAS [SL96] has limitations, particularly in its ability to assess complex or dynamic work environments. It is less sensitive to details of posture or movement, which may make it less suitable for high-precision tasks or highly variable postures. Nevertheless, it remains a valuable tool for identifying and mitigating postural risks in many industrial settings.

2.4.3 Rapid Upper Limb Assessment

The RULA [MC04] is a specialized ergonomic tool for assessing the risk of MSDs in tasks involving the upper body, focusing on the arms, wrists, neck and upper trunk. Like REBA [HM00], RULA [MC04] assesses

[2] Rapid Upper Limb Assessment

posture, strength and repetition, but is specifically designed for tasks involving hand-held tools, sedentary tasks or tasks requiring fine motor control. The scoring system generates an overall risk level for the task, with higher scores indicating a greater need for ergonomic interventions. The RULA [MC04] approach allows for the assessment of a wide range of occupational tasks, from office work to industrial activities, making it a versatile tool for occupational health and safety.

RULA [MC04] is valuable because it focuses on upper body posture, which is a common cause of workplace injury, particularly in sectors such as healthcare, manufacturing and office environments. The method is quick to apply and requires no special equipment, making it accessible to both practitioners and non-practitioners. However, the simplicity of the RULA [MC04] method also means that it can overlook some complex whole-body movement patterns or fail to account for changes in posture over time. Despite these limitations, RULA [MC04] remains a widely used and effective method for identifying and mitigating ergonomic risks to the upper body.

2.5 Machine learning tools for Human pose estimation

Christian Lins [Lin21] describes the development of evolutionarily optimized posture and movement models based on motion capture data for use in health-related assistance systems. This work details software prototype development and empirical evaluations of feasibility and efficacy. Two use cases are examined. The first addresses classification of postures, where a classifier is developed that classifies postures based on data from an inertial motion capture suit (SIRKA[3]) using the OWAS [SL96] method. The system could be employed in intelligent workwear to warn against health-hazardous postures. The second use case derives training parameters for CPR[4] based on an optical motion capture system (KinectV2[5]). A model computes compression frequency and depth from the movements during CPR, potentially supporting rescuer training. The shortcomings of this work are detailed in the following aspects:

Sensor Errors The motion-capture suit SIRKA introduces inaccuracies due to sensor placement. The sensors are integrated into clothing rather than placed directly on the skin. This results in positional shifts of several centimeters during movement, which vary between repetitions and participants. This inconsistency can lead to different data readings even if the posture appears the same to an observer.

Calibration Issues Calibration is conducted offline and may not fully account for variations in clothing thickness worn under the suit during different measurements. If calibration is inaccurate, it can lead to flawed data collection, affecting posture classification.

Data Labeling and Digitalization The manual process of digitizing posture observations introduces potential errors. If data entries are misinterpreted or incorrectly digitized, contradictions in the dataset can arise, reducing the accuracy of the neural network's posture classification.

Limited Training Data The machine learning models, particularly the neural networks, suffered from overfitting due to limited training data. This was especially noticeable in the classification of leg postures, where the algorithm struggled to generalize rules from the small dataset.

Sensor Noise Sensor data is subject to noise caused by minor manufacturing differences and temperature fluctuations, which affect the accuracy of measurements. Additionally, the lack of magnetometer data in the SIRKA system can lead to errors in orientation estimation, especially during periods of low movement activity.

Jan Vox [Vox22] focuses on the recognition and assessment of body postures and movements using joint angles, supported by motion-capture sensor technology. It explores two main applications: Movement Training and Ergonomic Analysis: The work evaluates alternative motion-capture sensors like RGB-D cameras and Light-

[3] "Sensoranzug zur individuellen Rückmeldung körperlicher Aktivität"
[Sensor suit for individual feedback on physical activity]
[4] Cardiopulmonary Resuscitation
[5] Microsoft® Kinect™ V2

house tracking systems, aiming to offer a more accessible and less costly solution for analyzing movements and postures based on joint angles.

Sensor Accuracy and Algorithms: The research assesses the accuracy of these motion sensors against the gold standard (marker-based optical systems) and delves into algorithms for detecting movements, posture segmentation, and automatic ergonomic assessment. The research aims to develop a framework for automatic recognition and evaluation of postures and movements using these technologies.

Key applications are in supporting movement training, ergonomic analysis, and reducing the risk of MSD at workplaces.

Nevertheless, the work also has some possible areas of improvement:

Accuracy Issues Alternative sensor technologies, such as older RGB-D cameras and Lighthouse tracking systems, show reduced accuracy compared to the gold standard (marker-based systems), especially in joint angle analysis, which is essential for ergonomic assessments and movement training.

Complex Calibration Motion capture systems require detailed calibration, and inaccuracies in this process can severely impact the quality of joint angle estimations, making the data unreliable.

Environmental Sensitivity Certain systems, such as the Lighthouse system, are sensitive to environmental conditions like lighting and obstacles, which limit their use in uncontrolled real-world environments.

Cost and Accessibility Consumer-friendly motion capture systems are more affordable but often sacrifice precision, presenting a challenge in balancing affordability with the high accuracy and robustness required in professional applications.

The work by the International Parkinson and Movement Disorders Society Task Force on Technology [Esp+16] discusses the role of emerging technologies in the clinical management of PD, focusing on both the challenges and opportunities these technologies present. The paper identifies several key issues and contributions.

Key Contributions

Technological Challenges and Opportunities: The authors discuss the challenges related to the integration of different technological platforms, particularly in long-term deployment among elderly patients. They also highlight the gap between the large volumes of data generated by sensors and their clinical applicability. Despite these issues, the authors emphasize the potential of open-source, adaptable technologies that could be used for real-time monitoring and individualized treatment systems for PD patients.

Identification of Technological Barriers: The paper highlights the difficulties in achieving platform compatibility, ensuring long-term monitoring of PD patients, and effectively applying the data collected through advanced technologies in clinical settings.

Opportunities in Open-Source Technologies: The authors advocate for the development of open-source platforms for data collection, which could help in creating more customizable, cost-effective solutions for personalized care and symptom monitoring in PD patients.

Integration of Multichannel Data for Personalized Treatment: The work calls for integrated systems that can capture a wide range of motor and non-motor symptoms in PD, leading to personalized, self-adjusting treatment regimens that could enhance patient outcomes and disease management.

Comprehensive Overview of Challenges and Future Potential: The paper provides a comprehensive overview of the challenges and future potential of technology in the management of PD, offering insights that could guide future research and clinical practice.

Prof. Eskofier's paper [Esk+16] investigates the application of deep learning for monitoring movement disorders, specifically bradykinesia in patients with PD, using data from wearable inertial sensors. The study compares deep learning approaches, particularly CNNs, with traditional machine learning methods, such as decision trees and support vector machines, for classifying motor tasks. The results show that deep learning outperforms other machine learning algorithms by at least 4.6% in classification accuracy. The paper

contributes to the field by highlighting the potential of deep learning for sensor-based assessment of motor symptoms in PD patients, as well as discussing its advantages and challenges.

The three main contributions of this paper are:

1. Comparison of deep learning with traditional machine learning techniques for detecting bradykinesia in PD.
2. Application of deep learning methods, such as convolutional neural networks, to wearable inertial sensor data for automated analysis of movement disorders.
3. Discussion of the advantages and challenges of using deep learning for sensor-based assessment of movement disorders and suggestions for future research.

2.6 Synthesis and Research Gap

The reviewed literature demonstrates significant progress in the objective assessment of movement irregularities and ergonomic risk using both classical and sensor-based methods. Clinical rating scales such as the MDS-UPDRS and established ergonomic tools like REBA, OWAS, and RULA provide structured frameworks for symptom quantification and risk identification. Recent advances in wearable sensor technology and machine learning have enabled more granular, continuous, and objective measurement of motor symptoms and workplace exposures [Bou25; Kha+25; SWL25; Esk+16]. These developments have improved the accuracy and scalability of movement analysis, supporting early detection, monitoring, and intervention in both clinical and occupational settings.

Despite these advances, several challenges remain. Many existing approaches are limited by the need for manual annotation, calibration complexity, or reduced accuracy in uncontrolled environments [Vox22; Lin21]. There is a lack of standardized protocols for integrating sensor-based data into clinical and occupational workflows, and the translation of high-dimensional sensor data into actionable insights is still an open problem. Furthermore, most studies focus on either clinical or occupational populations, with few addressing both domains or leveraging cross-domain methodologies.

This thesis addresses these gaps by developing and validating automated, scalable methods for quantifying movement variability and ergonomic risk using markerless and wearable sensor systems. The work integrates advanced machine learning algorithms with multi-modal sensor data to enable robust, reproducible assessment of movement in both laboratory and real-world environments. By bridging clinical and occupational applications, this research contributes to the advancement of objective, data-driven movement analysis and supports the development of personalized interventions for health monitoring and workplace adaptation.

3 General Methodology

This chapter details the methodologies employed to examine movement irregularities, validate multisensor tracking systems, and develop AI-driven assessment tools. The research integrates data from multiple studies, conducted in collaboration with several institutions:

- Department of Health Services Research of the UOL[1]
- University Clinic for Neurology of the UOL
- University of Applied Sciences Jade Hochschule
- Research Institute OFFIS e. V.[2]

These collaborations occurred in the context of several projects:

- ReHopE[3] (BMBF[4] 02K20D130)
- TEDIPA[5] (OFFIS Internal Funds - Vorlaufforschung)
- Smart-BT[6] (BMBF 16SV8580)
- TETRIS[7] (Funded by Joint MD/PhD Programme Groningen-Oldenburg)

3.1 Collaboration Statements

At the conclusion of each chapter describing the individual studies, a CRediT [22] contribution statement is provided. The CRediT taxonomy defines 14 standardized roles to transparently capture the range and nature of contributions to scholarly work, in accordance with best practices established by the NISO[8] and formalized as an American National Standard (ANSI/NISO Z39.104-2022, approved January 14, 2022). For each study, the specific contributions of all authors are detailed using these roles, ensuring a transparent, consistent, and structured record of scholarly contributions. This practice aligns with international standards and supports the integrity and reproducibility of the research.

3.2 Methodology Overview

Understanding and evaluating human movement in clinical and occupational settings requires a multifaceted methodological approach. This section introduces the overarching strategies and study designs that underpin the research presented in this thesis. The integration of diverse methodologies –from quantitative validation studies to qualitative observational analyses– reflects the interdisciplinary nature of movement science and the need to address complex, real-world problems. Each study was carefully designed to answer specific research

[1] "Carl von Ossietzky Universität Oldenburg" [Carl von Ossietzky University of Oldenburg]
[2] "eingetragener Verein" [registered association]
[3] "Reduktion körperlicher Belastungen von Handwerksberufen durch optimierte Exoskelette" [Reduction of physical strain in skilled trades through optimized exoskeletons]
[4] "Bundesministerium für Bildung und Forschung" [German Federal Ministry of Education and Research]
[5] "TEleDIagnostik und Verlaufskontrolle bei PArkinson Erkrankungen" [Telediagnostics and progression monitoring in Parkinson's disease]
[6] "Optimierte Bewegungstherapie durch die Interaktion künstlicher Intelligenz und Videotechnik mit Healthcare Professionals und Patienten" [Optimized movement therapy through the interaction of artificial intelligence and video technology with healthcare professionals and patients]
[7] Transcranial Temporal Interference Stimulation of Deep Brain Regions
[8] National Information Standards Organization

questions related to movement irregularities, sensor validation, and the development of AI-driven assessment tools.

The studies summarized here were conducted in collaboration with leading institutions and span a range of contexts, including clinical trials, field-based ergonomic assessments, and laboratory-based validation experiments. By combining data from multiple sources and employing both established and novel measurement techniques, the research aims to ensure robust, generalizable findings. The following overview highlights the scientific classification of each study, illustrating the breadth of methodological approaches and their relevance to the thesis objectives.

Table 3.1 provides a comprehensive summary of the different methodologies employed across the studies discussed in this thesis. It categorizes each study according to the specific research approach or technique utilized, such as validation studies, observational studies, design science, and clinical evaluations. This classification helps readers quickly understand the methodological diversity and rigor present in the body of research, highlighting how each study contributes unique insights based on its chosen approach. By presenting this information in a structured format, the table facilitates comparison between studies and supports a clearer interpretation of the overall research landscape.

Table 3.1: Scientific Methodology Classification of Thesis Studies

Descriptive Title	**Scientific Methodology**
Validation of portable multi-sensor system for movement analysis (TEDIPA study)	Cross-sectional comparative validation study using quantitative clinical evaluation
Clinical study for Parkinson's Disease symptom and treatment monitoring (TETRIS Study)	Cross-sectional randomized, double-blind, sham-controlled cross-over trial with quantitative movement analysis
Planned Retrospective Study on Video-Based Analysis of PD-Related Movements (RESBEPA Study)	Planned secondary data analysis using digital phenotyping and retrospective modeling (study design only)
Validation of Video-Based Movement Assessment (Smart-BT Validation Study)	Cross-sectional validation study comparing depth-based tracking with reference systems
Observational field study on ergonomic risk with craftspeople (ReHopE Hospitationen Study)	Cross-sectional quantitative observational field study using MoCap data
Markerless Ergonomic Assessment and Strain Analysis with Craftspeople (ReHopE Fokusgruppe Study)	Cross-sectional small-sample observational study with ergonomic risk tasks and qualitative validation
Craftspeople activity recognition with Wearable Sensors (ReHopE IMU-OptiTrack Study)	Cross-sectional design science study using MoCap-labeled data to train IMU-based ergonomic scoring models

It is important to note that while this classification provides a useful framework for understanding the methodologies employed, it does not fully capture the exploratory nature and focus on specific movement indicators present in many studies. Often, the analysis in this thesis examines subsets of the data or emphasizes the evaluation of particular movement metrics, reflecting the iterative and investigative approach of movement science research. Readers are encouraged to refer to the detailed descriptions in subsequent sections for a more nuanced understanding of each study's design, execution, and contributions.

3.3 Scientific Methodology

The methodological design of this thesis aligns with the *mixed-methods* paradigm, integrating quantitative, qualitative, and computational techniques to address the multidimensional nature of human movement in clin-

ical and occupational contexts. Mixed-methods research is particularly suitable when a single methodological approach is insufficient to fully address a complex research problem [Cre03; JOT07].

The following subsections describe the human studies conducted by the author that contributed to the realization of this thesis.

3.3.1 Validation of portable multi-sensor system for movement analysis (TEDIPA study)

This study follows a **comparative validation study** methodology, grounded in quantitative clinical evaluation and instrument validation protocols [Por20]. It evaluates the AzureKinect-based system against the GAITRite walkway [SK11]. Quantitative gait parameters such as SL[9], Cad[10], and Gait Velocity were extracted and compared using statistical metrics including Pearson correlation and Bland-Altman plots [Ari+24].

3.3.2 Clinical study for Parkinson's Disease symptom and treatment monitoring (TETRIS Study)

This randomized, double-blind, sham-controlled, cross-over study investigates the effects of tTIS on motor and motivational processes in PwPD's[11] and healthy controls (HPs[12]) [DRK25]. tTIS enables non-invasive stimulation of deep brain regions by applying two high-frequency alternating currents (e.g., 2 kHz[13] and 2.1 kHz) via scalp electrodes, generating a lower-frequency interference envelope in deep brain targets (ROI[14]) such as the putamen or nucleus accumbens, producing a low-frequency envelope (e.g., 0.1 kHz) that modulates neuronal activity [Gro+17]. This enables modulation of subcortical oscillations while minimizing cortical stimulation.

The study includes:

- **Motor performance assessment**: Finger tapping and hand open-close tasks analyzed with RGB-D video kinematic capture.
- **Motor learning**: Sequential finger tapping and hand open-close tasks.
- **Motivational behavior**: Effort/reward tasks.
- **Probabilistic learning**: Effort/reward tasks.

Stimulation targets were individualized using MRI[15]-based modeling to optimize electric field localization in the Putamen for motor tasks and the Nucleus Accumbens for motivational tasks. The study was conducted at a single academic center in Germany, with a final sample size of 36 participants aged 45-75 years. Participants completed both real and sham stimulation conditions in counterbalanced order under double-blind conditions. Movement data were recorded using RGB-D cameras and analyzed for amplitude, Gait Velocity, acceleration, and arrhythmicity [Lug+19].

[9] Step Length
[10] Gait Cadence
[11] Participants with Parkinson's Disease
[12] Healthy Participants
[13] Kilohertz
[14] Region of Interest
[15] Magnetic Resonance Imaging

3.3.3 Planned Retrospective Study on Video-Based Analysis of PD-Related Movements (RESBEPA Study)

This chapter presents only the planned study design for the RESBEPA study. The intended approach is a retrospective study utilizing secondary data analysis of standardized MDS-UPDRS tasks. Skeletal joint trajectories will be extracted using MediaPipe and analyzed for changes in amplitude, velocity, and arrhythmicity. The methodology aligns with digital phenotyping and clinical informatics [Xia+24; Ste+24]. No results are presented in this chapter.

3.3.4 Validation of Video-Based Movement Assessment (Smart-BT Validation Study)

This study employed a cross-sectional validation design conducted in a controlled lab setting. Participants performed a series of predefined movement tasks while being recorded simultaneously by multiple sensor systems. The methodology focused on comparing joint recognition accuracy between the AzureKinect DK[16] and reference systems including CAPTIV, Qualisys, and smartphone-based pose estimation.

Quantitative analysis included:

- RMSE[17] for joint angles
- ICC[18] for reliability
- Bland-Altman plots for agreement
- Temporal synchronization across modalities

3.3.5 Observational field study on ergonomic risk with craftspeople (ReHopE Hospitationen Study)

This study employed a quantitative observational field design. Craftspeople were recorded in real working conditions using an RGB-D camera and IMU systems. Joint-specific ergonomic risks were quantified across multiple tasks, and visualized using pie charts for both individual joints and task types, classified using DGUV 208-033 guidelines [Deu15] to measure postural load among craftspeople in real working conditions. Unlike classical naturalistic observation rooted in qualitative ethnography, the methodology involved objective kinematic measurement of joint angles, followed by classification of ergonomic risk levels using standardized criteria. This structured, numerical approach situates the study within the domain of *cross-sectional ergonomic surveillance*, a subfield of occupational epidemiology focusing on postural risk profiling [Kil94].

3.3.6 Markerless Ergonomic Assessment and Strain Analysis with Craftspeople (ReHopE Fokusgruppe Study)

This study represents a **controlled laboratory experiment with qualitative validation**, which can be categorized as a *quasi-experimental* design. It involved a small sample of five craftspeople performing high-risk tasks. Movement data were collected with and without exoskeletons. The methodology is observational with ergonomic risk profiling and qualitative validation through structured discussions. The use of focus group discussions adds an interpretivist lens, while the structured replication of tasks lends itself to quantitative comparability [Sha02].

[16] Developer Kit
[17] Root Mean Square Error
[18] Intraclass Correlation Coefficient

3.3.7 Craftspeople activity recognition with Wearable Sensors (ReHopE IMU-OptiTrack Study)

A design science approach was used to train ergonomic scoring models. High-precision MoCap data were used to label IMU recordings, enabling future field deployment of IMU-only systems for ergonomic assessment [LAF23].

3.3.8 Summary

The methodological diversity across studies reflects the interdisciplinary nature of movement analysis. By integrating observational, experimental, and computational paradigms, the thesis supports robust triangulation and contributes to both clinical and occupational domains.

The detailed study designs, objectives, participant information, sensing modalities, and tasks or protocols for each study will be elaborated in their respective chapters. This ensures a comprehensive understanding of the methodologies employed and their relevance to the thesis objectives.

3.4 Data Collection

This section describes the procedures and protocols for data collection across all studies included in this thesis. It outlines the selection criteria for participants, the sensing modalities and systems used for movement data acquisition, and the standardized processes implemented to ensure data quality and consistency. By detailing the data collection framework, this section provides context for the subsequent analyses and supports the reproducibility and validity of the research findings.

3.4.1 Selection of Participants

The participant selection varied depending on the study: A diverse participant pool was essential to ensure the validity and generalizability of the methodologies and findings. Healthy participants were included to establish baseline movement patterns and validate sensor systems under controlled conditions. PwPD's, diagnosed according to established criteria [Pos+15], were crucial for evaluating the tools' applicability in clinical contexts, particularly for detecting movement irregularities linked to neurological motor disorders. Craftspeople were involved to assess the ergonomic risk profiling methods in real-world occupational settings, ensuring the findings' relevance to workplace health and safety. This diverse selection enabled comprehensive validation across clinical, laboratory, and field environments.

- Validation of portable multi-sensor system for movement analysis (TEDIPA study): 13 participants diagnosed with PD and 11 healthy controls.
- Clinical study for Parkinson's Disease symptom and treatment monitoring (TETRIS Study): 36 participants (18 with PD, 18 healthy controls).
- Planned Retrospective Study on Video-Based Analysis of PD-Related Movements (RESBEPA Study): Planned analysis of data from 380 PwPD's (study design only).
- Validation of Video-Based Movement Assessment (Smart-BT Validation Study): 10 healthy adults for validation of movement tracking.
- Observational field study on ergonomic risk with craftspeople (ReHopE Hospitationen Study): 3 craftspeople.
- Markerless Ergonomic Assessment and Strain Analysis with Craftspeople (ReHopE Fokusgruppe Study): 5 craftspeople.
- Craftspeople activity recognition with Wearable Sensors (ReHopE IMU-OptiTrack Study): 15 experienced craftspeople and 15 inexperienced participants.

3.4.2 Movement Data Acquisition

Movement data was captured using:

- **RGB-D Imaging**: AzureKinect DK
- **3D**[19] **Color-Based Pose Estimation**: MediaPipe [Lug+19]
- **2D**[20] **Color-Based Pose Estimation**: Detectron2 [Wu+19]
- **Gait Analysis**: GAITRite
- **Motion Capture**: OptiTrack, Qualisys
- **IMUs**: CAPTIV system, Movella DOTs [Mov23] and IMUs integrated into Delsys sEMGs

The acquired movement data was processed using BT frameworks and analyzed for movement abnormalities.

3.5 Relevance of Each Study to the Thesis Objectives

Each study included in this thesis contributes uniquely to the overarching goal of understanding and evaluating repetitive movements, validating sensor systems, and developing AI-driven assessment tools. The following sections outline the relevance of each study, the repetitive movements analyzed, the algorithms or pipeline components utilized, and the specific data subsets employed. A summary is provided in Table 3.2.

[19] Three-Dimensional
[20] Two-Dimensional

Table 3.2: Relevance of Studies to Thesis Objectives

* Indicates repetitive movements analyzed from MDS-UPDRS tasks.

Study Short Name	Repetitive Movement	Algorithms/Pipeline Components	Data Subset Used
TEDIPA	Gait*, Finger Tapping*, Hand Movements*	Gait analysis from RGB-D data, video-based 3D pose estimation, statistical comparison	video and AzureKinect-BT data, GAITRite data, MDS-UPDRS scores for Finger Tapping* and Hand Movements*
TETRIS	Finger Tapping*, Hand Movements*	video-based 3D pose estimation, statistical comparison	video and MDS-UPDRS scores for Finger Tapping* and Hand Movements*
RESBEPA	Gait*, Finger Tapping*, Hand Movements*, Toe Tapping*, Leg Agility*	video-based 3D pose estimation, statistical comparison	video and MDS-UPDRS scores for Gait*, Finger Tapping* and Hand Movements* , Toe Tapping* and Leg Agility*
Smart-BT	Gait*, Finger Tapping*, Hand Movements*, Toe Tapping*, Leg Agility*	3D Joint Angle Calculation, Joint angle accuracy metrics (RMSE, ICC)	AzureKinect-BT data, MoCap system marker position data and IMU rotation data
ReHopE Hospitationen	Gait, Load Lifting, Arm Movements	Ergonomic risk quantification, IMU-based Joint angle analysis	video and IMU data
ReHopE Fokusgruppe	Gait, Load Lifting, Arm Movements	Automation of ergonomic risk quantification, video-based 3D pose estimation, sEMG analysis	video and sEMG data, questionnaires
ReHopE IMU-OptiTrack	Gait, Load Lifting, Pronation/Supination	IMU-based Human Activity Recognition for craftspeople	MoCap-labeled IMU data

3.5.1 TEDIPA Study

The TEDIPA study focuses on repetitive gait and hand movements, which are critical for assessing motor impairments in PD. The study evaluates hand movements from the MDS-UPDRS using algorithms for movement parameter extraction and validates the AzureKinect-based system against the GAITRite walkway for gait analysis with a statistical comparison (e.g., Pearson correlation, Bland-Altman analysis). This study contributes to the thesis by demonstrating the feasibility of using portable multi-sensor systems for clinical gait and hand movement analysis.

3.5.2 TETRIS Study

The TETRIS study investigates repetitive hand movements from the MDS-UPDRS, which are essential for understanding motor processes in PD. The study employs video analysis to evaluate motor performance and

learning. This aligns with the thesis objective of exploring the mechanistic effects of interventions on repetitive motor tasks.

3.5.3 RESBEPA Study

The RESBEPA study analyzes repetitive movements from retrospective video data of standardized MDS-UPDRS tasks. Using MediaPipe for skeletal joint trajectory extraction, the study applies digital phenotyping techniques to identify movement irregularities. This study supports the thesis by leveraging secondary data to validate AI-driven movement analysis pipelines.

3.5.4 Smart-BT Validation Study

The Smart-BT study evaluates repetitive fitness exercises and movement disorder assessments using multiple modalities of BT. Algorithms for joint recognition accuracy (e.g., RMSE, ICC) are applied to compare the different modalities. This study contributes to the thesis by providing insights into the strengths and limitations of each tracking modality.

3.5.5 ReHopE Hospitationen

The "ReHopE Hospitationen" study examines repetitive occupational tasks performed by craftspeople. Using RGB-D cameras and IMU systems, ergonomic risks are quantified based on joint-specific postural loads. This study aligns with the thesis by addressing real-world applications of movement analysis in occupational health.

3.5.6 ReHopE Fokusgruppe

The "ReHopE Fokusgruppe" study investigates repetitive high-risk tasks with and without exoskeletons. Movement data is analyzed qualitatively and quantitatively to assess ergonomic interventions. This study contributes to the thesis by integrating observational and computational approaches to evaluate strain reduction measures.

3.5.7 ReHopE IMU-OptiTrack Study

The "ReHopE IMU-OptiTrack" study focuses on repetitive simulated work tasks, using MoCap-labeled IMU data to train ergonomic scoring models. This study supports the thesis by advancing the development of AI-driven tools for ergonomic assessment.

3.6 Machine Learning Techniques

The general machine learning techniques employed across the studies are detailed in this section, focusing on feature extraction, model architecture, model selection, and training/validation procedures.

3.6.1 Feature Extraction

Feature extraction is a critical step in preparing raw movement data for machine learning analysis. In the context of this research, features were derived from both kinematic and kinetic data captured during movement tasks. The following types of features were extracted:

- **Kinematic Features**: Joint angles, velocities, and accelerations were computed from the skeletal joint trajectories obtained through depth imaging and motion capture systems. These features provide insights into the spatial and temporal dynamics of movement.
- **Kinetic Features**: Force and torque data were derived from wearable sensors, such as IMUs and sEMGs, which measure the physical forces exerted during movements. These features are essential for understanding the mechanical aspects of movement and can indicate strain or abnormal patterns.
- **Temporal Features**: Time-series analysis was applied to the movement data to capture patterns over time. This included computing statistical measures such as mean, variance, and peak values of joint angles and forces, as well as more complex features such as arrhythmicity.
- **Contextual Features**: In some studies, additional contextual information such as task type and environmental conditions was incorporated as features. This helps in understanding how different factors influence movement patterns and can improve model generalization.

The extracted features were then normalized and standardized to ensure some consistency across different datasets. Recursive feature elimination and correlation analysis was employed to identify the most relevant features for the specific tasks at hand, thereby reducing dimensionality and improving model interpretability.

3.6.2 Model Architecture

The selection of model architecture is critical for capturing the complex relationships present in sequential data. In this research, a combination of Long Short-Term Memory networks and attention mechanisms was utilized to address the challenges of modeling temporal dependencies and the varying importance of sequence elements.

3.6.3 Model Selection

The selection of an appropriate model architecture is of critical importance in the analysis of sequential data, where temporal dependencies and evolving patterns must be effectively captured. Traditional feedforward neural networks are ill-suited to such tasks, as they process inputs independently and lack the capacity to model temporal correlations inherent in time-series or sequential datasets. In contrast, RNNs were specifically developed to address these limitations by incorporating recurrent connections that allow the network to maintain a form of memory over past inputs [Elm90]. This temporal recurrence enables RNNs to learn dependencies across time steps, which is fundamental in domains such as human motion analysis, natural language processing, and sequential event modeling.

However, standard RNNs exhibit significant challenges when attempting to model long-range dependencies due to the vanishing and exploding gradient problems during backpropagation through time [BSF94]. These issues can prevent the network from effectively learning relationships between distant events in the input sequence. To mitigate this, Hochreiter and Schmidhuber [HS97] introduced LSTM[21] networks, a specialized variant of RNNs designed to maintain long-term dependencies through the use of gated memory cells. LSTMs feature a cell state that is modulated by three gating mechanisms –input, forget, and output gates– that collectively control the information flow into and out of the memory cell. This structure allows LSTMs to selectively retain information over extended sequences and discard irrelevant or outdated information, making

[21] Long Short-Term Memory

them well-suited for modeling complex temporal patterns such as variations in human movement or behavioral sequences. Despite their advantages, LSTMs alone do not explicitly differentiate between the importance of various elements within an input sequence. This limitation can be critical in real-world applications where certain moments in a sequence may carry more relevance than others. To address this, attention mechanisms have been integrated into RNN[22] and LSTM architectures to enable dynamic weighting of sequence elements during processing [Vas+17]. Attention mechanisms allow the model to learn which parts of the input sequence are most relevant to a given task, thereby enhancing both the performance and interpretability of the model. By computing a context vector as a weighted sum of all hidden states, the attention mechanism enables the network to focus selectively on informative time steps, improving its ability to capture salient features in sequences with variable or noisy information. In the context of this research, the combination of LSTMs and attention mechanisms provides a robust and flexible framework for modeling sequential data. The LSTM's capability to retain long-term temporal dependencies, paired with the attention mechanism's capacity for selective focus, ensures that the model can effectively learn both the structural and contextual aspects of sequential inputs. This makes the LSTM-attention architecture particularly suitable for tasks involving dynamic movement analysis, temporal pattern recognition, and any application where sequence relevance varies over time.

3.6.4 Training and Validation

Training and validation procedures varied according to study objectives, data modalities, and model architectures, as detailed in Human studies on movement analysis for neurodegenerative diseases and Human Studies Related to Musculoskeletal Disorders.

For machine learning models, datasets were split into training, validation, and test sets, ensuring stratification by participant group and task type. Cross-validation techniques, such as k-fold and leave-one-subject-out, were employed to assess generalizability and mitigate overfitting. Hyperparameter optimization was performed iteratively, with model selection guided by validation performance.

In studies involving sequential data, models were trained using time-series movement features, with early stopping and regularization to prevent overfitting. Validation included monitoring loss curves and evaluating metrics such as classification accuracy and F1-score on held-out data.

All training and validation workflows adhered to reproducibility standards, with code and data pipelines version-controlled and documented for transparency. Further details on study-specific protocols and results are provided in the respective chapter appendices.

3.6.5 Evaluation Metrics

Evaluation metrics varied across studies, reflecting the specific objectives and data modalities. Detailed results and discussions for each metric are provided in the respective chapters (Human studies on movement analysis for neurodegenerative diseases and Human Studies Related to Musculoskeletal Disorders).

- **Agreement and Reliability**: ICC, Pearson correlation, and Bland-Altman analysis were used to assess agreement and reliability between sensor systems and reference standards (see chapter 4, chapter 7).
- **Accuracy**: RMSE and MAE[23] quantified joint angle and movement parameter accuracy in validation studies (see chapter 7, chapter 4).
- **Clinical Outcomes**: For clinical trials (see chapter 5), metrics included changes in motor performance (e.g., finger tapping speed, effort-reward scores) and pre-post intervention differences.
- **Ergonomic Risk**: Studies on craftspeople (see chapter 10, chapter 8, chapter 9) used ergonomic risk scores, postural load classification (DGUV 208-033), and frequency of high-risk postures.

[22] Recurrent Neural Network
[23] Mean Absolute Error

- **Model Performance**: For machine learning models, metrics included classification accuracy, F1-score, and confusion matrices for human activity recognition chapter 10.
- **Usability and Feasibility**: Qualitative ratings and structured focus group feedback assessed intervention feasibility and user acceptance (see chapter 9).

These metrics ensured robust validation, clinical relevance, and practical applicability of the developed systems and models.

3.6.6 Model Deployment

The trained machine learning models were deployed on HPC[24] infrastructure provided by OFFIS e. V. leveraging both remote GPU[25]-enabled workstations and local servers. Primary deployment environments included the DGX-A100 cluster (dgx-a100-1.pkm.lcl.offis.de), equipped with 8 NVIDIA A100-SXM4-80GB GPUs and 256-core AMD[26] EPYC processors, and the hrc-workstation2.lcl.offis.de, featuring a single NVIDIA GeForce RTX[27] 3080 Ti and a 24-core Intel i9-12900KF CPU[28]. These resources enabled efficient training, inference, and large-scale data processing for movement analysis tasks, which was necessary due to the high computational demands of the models, which were hundreds of GBs[29].

Model serving and integration utilized a combination of established frameworks and custom solutions. PyTorch[30] was the primary deep learning framework for model development and inference, with ONNX[31] employed for model export and interoperability across platforms. TensorFlow was used for MediaPipe-based pose estimation, while CUDA[32] and CUDF[33] libraries facilitated GPU acceleration for both training and real-time inference. Python scripts and Bazel build tools were used to orchestrate data pipelines and deployment workflows.

The deployment of these models translated research outcomes into practical tools for clinical, occupational, and research applications. For example, automated movement assessment systems were integrated into clinical trials for objective evaluation of motor symptoms, while ergonomic risk profiling tools supported occupational health interventions in field studies. The use of containerized environments and remote access enabled seamless collaboration between research teams and facilitated reproducible, scalable deployment of AI-driven assessment tools across diverse settings.

3.7 Ethical Considerations

For each study included in this thesis, approval was obtained from the respective Ethics Committee to ensure compliance with ethical standards and guidelines. The approval numbers and corresponding committees are summarized in Table 3.3. This process underscores the commitment to conducting research responsibly, safeguarding participant rights, and adhering to institutional and legal requirements.

[24] High Performance Computing
[25] Graphics Processing Unit
[26] Advanced Micro Devices
[27] Ray Tracing Texel eXtreme
[28] Central Processing Unit
[29] GigaBytes
[30] Python Torch Deep Learning Framework
[31] Open Neural Network Exchange
[32] Compute Unified Device Architecture
[33] CUDA DataFrame Library

Table 3.3: Ethics Committee Approval Numbers for All Studies

Study Short Name	Ethics Committee	Ethics Approval Number
TEDIPA	Medizinische Ethikkommission UOL	[2019-103]
TETRIS	Medizinische Ethikkommission UOL	[2022-164]
RESBEPA	Medizinische Ethikkommission UOL	[2025-090]
Smart-BT	Commission for Research Impact Assessment and Ethics UOL	[Drs.EK/2021/057]
ReHopE Hospitationen	OFFIS e. V. Studienboard	2022P011
ReHopE Fokusgruppe	OFFIS e. V. Studienboard	2023P015
ReHopE IMU-OptiTrack	OFFIS e. V. Studienboard	2024P031

3.7.1 Informed Consent

All participants provided informed consent before taking part in the studies. They were informed about the nature of data collection, the scope of movement recordings, and their right to withdraw at any time.

3.7.2 Privacy and Confidentiality

Data was collected in a pseudonymized or anonymized manner, ensuring that no personally identifiable information was linked directly to movement data. All collected information followed GDPR[34] and institutional data protection policies. The anonymized datasets will be stored securely for a minimum of 10 years for future research use.

[34] General Data Protection Regulation

Part II

Human studies on movement analysis for neurodegenerative diseases

4 Validation of portable multi-sensor system for movement analysis (TEDIPA study)

This chapter is partly based on the following publications:
Pedro Arizpe-Gomez et al. "Preliminary Viability Test of a 3-D-Consumer-Camera-Based System for Automatic Gait Feature Detection in People with and without Parkinson's Disease". In: *2020 IEEE International Conference on Healthcare Informatics (ICHI)*. IEEE. 2020, pp. 1–7
Pedro Arizpe-Gómez et al. "Towards automated self-administered motor status assessment: Validation of a depth camera system for gait feature analysis". In: *Biomedical Signal Processing and Control* 87 (2024), p. 105352

This chapter presents published and new findings from the TEDIPA study, a human study on neurodegenerative diseases.

4.1 Introduction

Mobility profoundly influences an individual's quality of life. Gait disturbances represent a characteristic hallmark of aging, musculoskeletal alterations, and a majority of neurological diseases, including neuropathies, stroke, multiple sclerosis, and PD. Furthermore, the precise detection and analysis of spatial and temporal parameters of impaired gait are crucial, as they enable the prediction of falls and functional decline in elderly populations [MSK14; Rod+19].

Methodologies for detecting and quantifying gait disturbances span a spectrum from subjective questionnaires to objective, sensor-based automatic gait analysis systems. To ensure clinically reliable detection of gait parameters, participants are typically instructed to ambulate along a straight path of 8 to 10 meters, free from obstacles, at their self-selected pace.

A variety of medical devices have been developed for diverse applications in movement analysis. These range from high-precision marker-based optoelectronic motion capture systems, such as the Vicon® system [Vic15], which typically assess human movements in a controlled laboratory setting, to IMU that are applicable in real-world, everyday environments. The data collected by these systems exhibits variability primarily influenced by kinematic variables and the precision of the movement measurements.

One example is the portable sensor system GaitLab[1], which has been approved as a medical device and provides clinically validated parameters. The sensor shoe specializes in analyzing gait. The GaitLab continuously measures the gait quality of patients during their everyday life and, thanks to its certification as a medical device, can be used for the everyday care of neurodegenerative conditions, like PD [Sch+17a]. Nevertheless, this device also presents paradigm related disadvantages. The lack of context-related information and the inability to synchronously evaluate other extremities favor alternative approaches.

The GAITRite [Inc13] (CIR[2] Systems, NJ[3], USA) has become a standard instrument for gait analysis. The device consists of a single layer pressure sensitive walkway. It can measure temporal and spatial parameters for a large number of clinically relevant gait parameters with a high accuracy [Inc13]. Although this walkway is relatively mobile, its installation (e.g, in a home setting or a general practice) is time consuming and requires trained personnel, making gait analysis more cost intensive and inflexible. Therefore, GAITRite is more suitable for clinical or professional settings.

[1] Mobile GaitLab - Portabiles HealthCare, Erlangen, Germany
[2] Clinical Image Retrieval
[3] New Jersey

Optimal gait analysis at home or in doctor's office does not require specific staff or the cumbersome attachment of markers or IMUs and offers an automated evaluation that reports gait parameters accurately [Bal+14; SS11]. Movement analysis systems based on RGB-D consumer cameras combine several advantageous properties. They can be installed at small local doctor's offices and even in patients' homes, and can be used in less advanced technical settings and may be easier to handle. If the data recordings and automated kinematic analysis are accurate, such systems can provide medical personnel with comprehensive information. This could lead to better detection of gait disturbances, targeted treatment decisions and therefore may improve the patients' quality of life.

Several studies have already proposed the use of RGB-D cameras such as the first and second versions of the KinectV1[4] and KinectV2 to record and analyze gait parameters in the context of health services[Elt+17; Cun+16; Ara+15; Gal+14; Tan+19]. Baldewijns et al. used the KinectV1 system and report overall acceptable correlation coefficients of 0.94 for average SL and 0.75 for average step time per walk [Bal+14]. However, the authors report some problems:

(i) ...that arise from the small field of view (about 2.8 m) of the KinectV1 camera.
(ii) ...with defining the exact SL for single steps on the basis of the kinetics of the center of mass
(iii) ...regarding a dropout rate of one third among all study participants due to technical and software problems associated with the KinectV1 RGB-D camera system.

In a further study, the KinectV1 was compared with the marker based Vicon® [Vic15] motion capture system demonstrating a satisfactory correspondence between both systems with regard to the Vel[5] variability, a risk factor for falls in elderly people [SS11]. Both studies demonstrated the feasibility of analyzing basic gait parameters using an RGB-D consumer camera system. However, both studies also showed limitations such as problematic automated motion detection in a small FOV[6].

To overcome the mentioned limitations, the present study addresses the question whether a high definition RGB-D consumer camera can accurately measure basic parameters of gait (such as SL, Vel and Cad) on an 8.84 m GAITRite walkway.

Compared to previous works, the proposed system incorporates three main improvements:

The first improvement is the use of the RGB-D camera and BT software of the AzureKinect DK [Bam+18]. This device is the successor model of the KinectV2. It offers significantly higher depth resolution and also improved body pose estimation accuracy [Alb+20]. Besides, the selected approach compares the use of the coordinates of the more reliable estimation of the pelvis position for gait parameter identification to the use of the noisy estimation of the feet coordinates.

The second improvement is the utilization of 3 interconnected cameras [LLH12] for a complete capture of the GAITRite walking range. The GAITRite is an accepted gold standard for gait analysis, and is used as the ground truth.

The third improvement is the inclusion of HPs and participants suffering from neurological motor disorders (PD). This choice of sample increases the variability of gait parameters, which in turn drives validation performance. The inclusion of participants with neurological disorders also validates the feasibility of a RGB-D camera gait analysis in a patient cohort.

Furthermore, when compared to IMU-based analysis, an advantage of the proposed AzureKinect-based system is that the movement of multiple body key points can be tracked without the necessity of actively attaching sensors to the body.

The aim of this study is to validate a proof-of-concept system for movement analysis. The current validation mainly concerns new methods for deriving key gait parameters from depth camera data (in this case from

[4] Microsoft® Kinect™ V1
[5] Gait Velocity
[6] Field of View

the depth camera of the AzureKinect DK).The main purpose is to elicit whether movement features can, in principle, be derived from the 3D coordinate data provided by the AzureKinect-based system.

The current validation doesn't address the experimental measurement setup itself, it just evaluates its capability to achieve a level of comparability between the AzureKinect-based system and the GAITRite.

Prospectively, it could be evaluated if the proposed camera setup can then be adapted to a home environment. Besides, the system could also be used for the assessment of other movement features, like arm swing, spinal flexion and neck flexion.

4.2 Materials and Methods

This section details the methodology and procedures employed in the TEDIPA study. It describes the study design, participant recruitment, inclusion and exclusion criteria, experimental setup, data acquisition, and the processing pipelines used for kinematic analysis. The aim is to provide a comprehensive overview of how the portable multi-sensor system was validated for movement analysis, ensuring reproducibility and transparency of the research approach.

4.2.1 Study design

This was a monocentric, observational, cross-sectional study conducted at the University Clinic for Neurology, Oldenburg, Germany, between October and December 2019. The study included two arms:

- **Arm 1:** Participant with Parkinson's Disease; Target sample size: n=10; Final sample size: n=15[7].
- **Arm 2:** Healthy controls (HP, no neurological disorder); Target sample size: n=10; Final sample size: n=11.

Recruitment and study procedures were completed at a single academic center. The study was prospectively registered (DRKS[8]00020921) and received a positive ethics opinion from the Medizinische Ethikkommission der Carl von Ossietzky Universität Oldenburg (reference number [2019-103]). All participants gave their informed consent to participate in the study in written form. No compensation was provided for participation.

Key inclusion and exclusion criteria are summarized in Table 4.1.

Table 4.1: Key inclusion and exclusion criteria

Inclusion	**Exclusion**
Age over 18 years	Inability to provide consent
Ability to provide informed consent	Insufficient understanding of study procedures or German language
For PD arm: diagnosis of Parkinson's syndrome	Immobility (bedridden)
For control arm: no evidence of neurological disorder	Participation in other studies

Collected data included video, image, and audio recordings, as well as demographic information (age, sex) and clinical scores (MDS-UPDRS).

The primary objectives were to assess the feasibility and validity of the TEDIPA system for automated, markerless movement analysis, to compare its extracted parameters with those from the GAITRite system, and

[7] Due to file corruption errors, only 13 of these datasets could be included
[8] "Deutsches Register Klinischer Studien" [German Clinical Trials Register]

to evaluate the relationship between the automatically extracted kinematic parameters and the clinician-rated motor impairment MDS-UPDRS Scores.

A paper-based MDS-UPDRS Part III [Goe+08a] assessment was conducted for all participants by a trained neurologist. All examined items of the MDS-UPDRS Part III Examination Items (see Table 4.2) were assessed on paper. It is important to note that not all items can be meaningfully captured by the camera, as some features (e.g., LLE[9], LUE[10], RLE[11], RUE[12], rigidity or certain aspects of postural stability) are not visually observable on video recordings. Furthermore, the camera's maximum FPS[13] does not allow for proper tremor assessment.

The clinical scores (MDS-UPDRS ratings, evaluating the severity of motor symptoms from 0 to 4) obtained were compared to various movement indicators derived from the body part position estimation done with MediaPipe [Lug+19] from the AzureKinect-based system, such as movement amplitude, movement speed, and arrhythmicity (see subsubsection 4.2.3.2, subsubsection 4.2.3.3). This comparison aimed to evaluate the relationship between the automatically extracted kinematic parameters and the clinician-rated motor impairment scores.

For the validation of the gait feature extraction methods proposed in this system, the GAITRite is used as the ground truth. The deviations between the proposed system and the ground truth are determined both in normal gait patterns of HPs and in pathological gait patterns of the study participants with motor impairments.

For the analysis of the non-gait Examination Items MDS-UPDRS Part III feature extraction methods proposed in this system, an explorative analysis of correlations was conducted between the movement indicators derived from the system and the clinical scores obtained by a trained neurologist. This analysis aimed to evaluate the relationship between the automatically extracted kinematic parameters and the clinician-rated motor impairment scores.

Table 4.2: MDS-UPDRS Part III Examination Items

Item ID	Item Description	Item ID	Item Description
3.1	Speech	3.10	Gait
3.2	Facial expression	3.11	Freezing of gait
3.3a	Rigidity - Neck	3.12	Postural stability
3.3b	Rigidity - RUE	3.13	Posture
3.3c	Rigidity - LUE	3.14	Global spontaneity of movement
3.3d	Rigidity - RLE	3.15a	Postural tremor - Right hand
3.4a	Finger tapping - Right hand	3.15b	Postural tremor - Left hand
3.4b	Finger tapping - Left hand	3.16a	Kinetic tremor - Right hand
3.5a	Hand movements - Right hand	3.16b	Kinetic tremor - Left hand
3.5b	Hand movements - Left hand	3.17a	Rest tremor amplitude - RUE
3.6a	Pronation-supination movements - Right hand	3.17b	Rest tremor amplitude - LUE
3.6b	Pronation-supination movements - Left hand	3.17c	Rest tremor amplitude - RLE
3.7a	Toe tapping - Right foot	3.17d	Rest tremor amplitude - LLE
3.7b	Toe tapping - Left foot	3.17e	Rest tremor amplitude - Lip/jaw
3.8a	Leg agility - Right leg	3.18	Constancy of rest tremor
3.8b	Leg agility - Left leg	Were dyskinesias present? (yes/no)	
3.9	Arising from chair	DYSKINESIA IMPACT ON PART III RATINGS	
		HOEHN AND YAHR STAGE	

[9] Left Lower Extremity
[10] Left Upper Extremity
[11] Right Lower Extremity
[12] Right Upper Extremity
[13] Frames Per Second

4.2.2 Experimental Setup

Both the assessment of MDS-UPDRS Part III Examination Items 3.10 and 3.11 (Gait and Freezing of gait), the GAITRite and three AzureKinect DK cameras were installed in a corridor in the Neurology Clinic with a length of over 10 meters and a minimum width of 1 meter (see Figure 4.1).

(a) Camera 0 view (b) Camera 2 view

Figure 4.1: Experimental setup [Ari+20b].
(a) Perspective of camera 0 during gait assessment on the GAITRite walkway.
(b) Perspective of camera 2 during gait assessment on the GAITRite walkway.

For the rest of the MDS-UPDRS Part III Examination Items, camera 0 and 2 were repositioned to face a chair inside the examination room, ensuring an optimal view of the sitting participants during the evaluation (See Figure 4.2). This setup allowed a trained neurologist to systematically assess motor function using the MDS-UPDRS scale, while simultaneously capturing detailed movements and postures. The cameras' placement facilitated unobstructed recording of the assessment. This configuration ensured that the data collected could be used for subsequent kinematic analysis, providing a comprehensive understanding of each participant's motor impairment.

4.2.2.1 The GAITRite System as Ground Truth

The ground truth for gait analysis was provided by the GAITRite, which is a certified medical device. The system consists of a carpet-like mat with a 2-D array of pressure-sensitive sensors, which are activated when the participants walk over them. With every step, a few dozen sensors are activated. Their position and activation timing are transmitted from the processing unit to the attached computer through a USB[14] cable. A proprietary software processes the transmitted data for all steps within a walk and infers the course of each walk. The user is given the opportunity to manually edit the walk before saving it to a database. Once saved, the software further calculates and derives several step-wise indicators, like SL, step width and time, as well as several aggregated indicators, like average Vel and Cad, and average step time and count.

These indicators constitute a basis for clinical gait analysis. Spatial data are stored in the 2D coordinate system of the GAITRite system (see Figure 4.3).

[14] Universal Serial Bus

Figure 4.2: Camera Setup for the non-gait examination items of MDS-UPDRS Part III assessment.
Upper Left) Perspective of camera 0 during non-gait examination items of MDS-UPDRS Part III.
Lower Left) Perspective of camera 2 during non-gait examination items of MDS-UPDRS Part III.
Right) Anonymized image with MediaPipe [GB20] keypoint overlay.

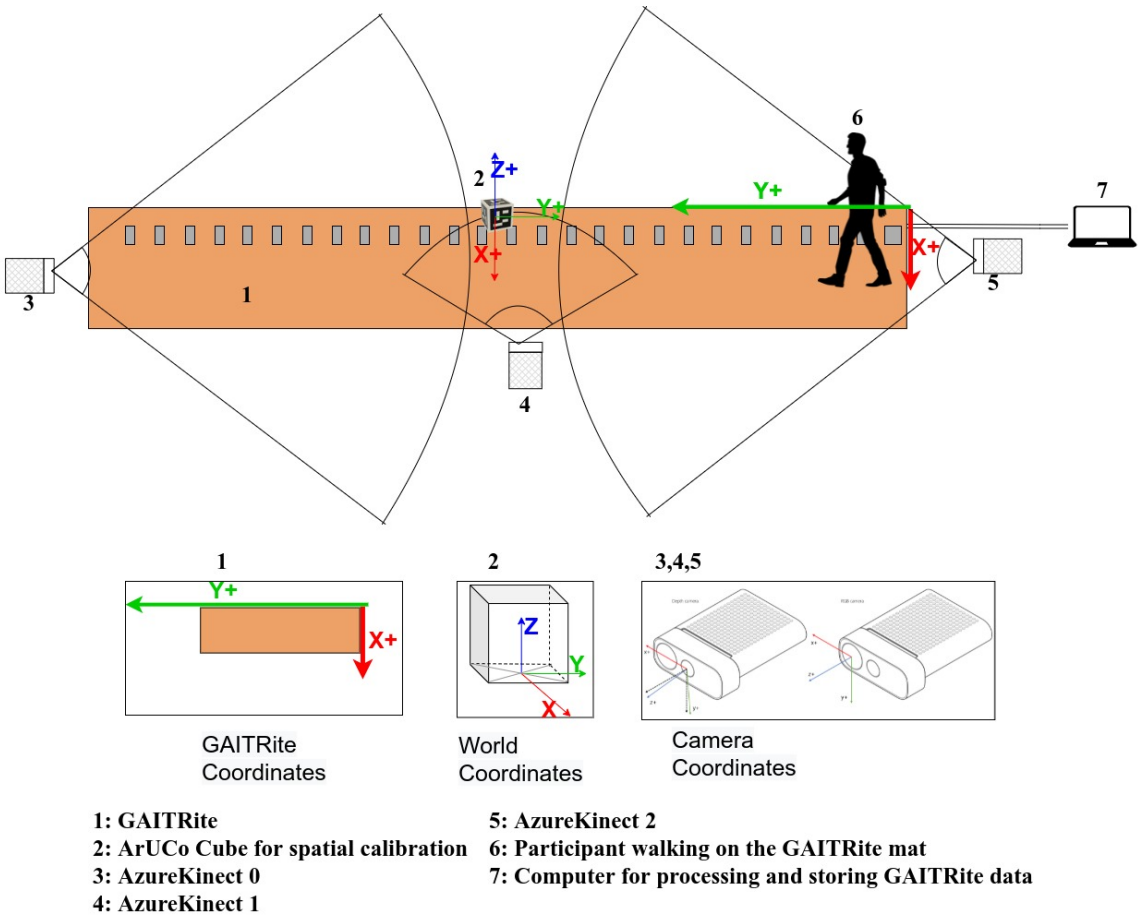

Figure 4.3: Overview of experimental setup.

4.2.2.2 The Microsoft® Azure™ Kinect™ Camera

The AzureKinect DK consists of the following elements: the AzureKinect RGB-D-Consumer-Camera, with a 1-MP[15] depth sensor and a 12-MP RGB[16] video camera [Bam+18]; the open source sensor DK software library for video and depth image processing; the closed source Body Tracking DK for body pose estimation and tracking [Mic19]; and other sensors that were not used in this work. AzureKinect is a spatial computing DK with advanced machine vision capabilities, that is available on the consumer market.

The AzureKinect depth sensor is a time-of-flight depth camera. For every frame, infrared rays (see Table 4.3) are emitted towards the objects in the field of view. The depth sensor registers the refraction of these rays and measures the time it takes them to bounce back to the infrared receiver.

Table 4.3: Depth modes of the AzureKinect depth sensor [Mic19].

Mode	Resolution	Rays per Frame	Frame Rates (FPS)	Exposure time	Operating Range**
WFOV unbinned	1024×1024	1 048 576	5, 15	20.3 ms	0.25–2.21 m
NFOV unbinned	640×576	368 640	5, 15, 30	12.8 ms	0.5–3.86 m
*WFOV 2×2 binned	512×512	262 144	5, 15, *30	12.8 ms	0.25-2.88 m
*NFOV 2×2 binned (SW)	320×288	92 160	5, 15, *30	12.8 ms	0.5-5.46 m
* Used for this project					
**15% to 95% reflectivity at $850nm$ 2.2μ $W/cm^2/nm$, random error SD $\leq$ 17 mm, typical systematic error $< 11mm + 0.1\%$ of distance without multi-path interference. Depth may be provided outside of the operating range indicated above. It depends on an object's reflectivity [Mic19].					

From this information, the processing unit of the camera can calculate the distance between the camera and several points on the surfaces of all the objects in the camera's field of view and their position relative to the camera. For the purposes of this study, 2×2 binned NFOV[17] and WFOV[18] modes were selected because they offer a bigger operating range and a comparable number of FPS (see Table 4.3).

The AzureKinect BT SDK[19] receives the depth images as input and uses a previously trained Convolutional Neural Network (CNN[20]) [Alb+20] to search for structures resembling human bodies. For each frame in which such patterns are found, it estimates the positions of 32 key points throughout the body (BT-joints), which are shown in Figure 4.4. Spatial data are stored in the 3D coordinate systems of each single AzureKinect DK camera (0, 1, 2) (see Figure 4.3).

[15] MegaPixel
[16] Red, Green and Blue
[17] Narrow Field of View
[18] Wide Field of View
[19] Software Development Kit
[20] Convolutional Neural Network

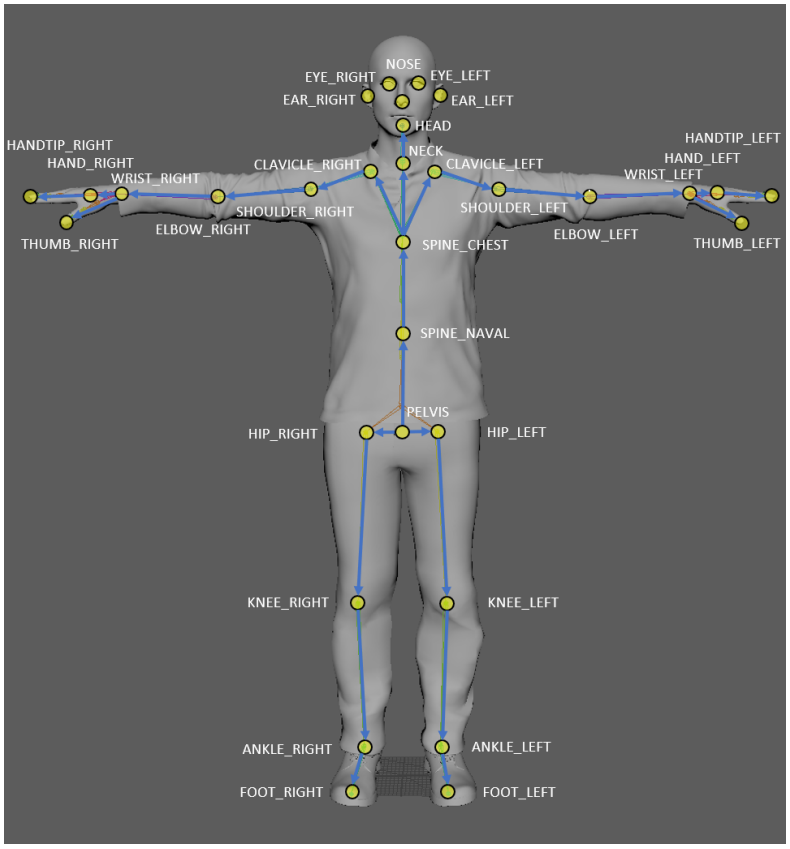

Figure 4.4: BT-Joint Hierarchy of AzureKinect BT [Mic19]

4.2.3 Kinematic data processing with MediaPipe

RGB video recordings of motor tasks were processed using the MediaPipe framework for markerless pose estimation and hand tracking [Baz+20; Lug+19]. The GPU-accelerated Holistic graph, which integrates body, face, and hand landmark detection, was compiled from source using Bazel to ensure compatibility and optimal performance on the designated workstation (Ubuntu 20.04.6 LTS, NVIDIA GeForce RTX 3080 Ti GPU, 24-core 12th Gen Intel Core i9-12900KF CPU).

The Holistic pipeline provided frame-wise 3D coordinates for 33 body landmarks (see Figure 4.5) and 21 landmarks per hand (see Figure 4.6), enabling precise quantification of hand and finger movements. For each video, relevant hand landmarks (such as wrist, MCP[21], PIP[22], DIP[23], and fingertip positions) were extracted, and task-specific amplitude signals were computed, including the Euclidean distance between selected joints or the spread of finger tips. These amplitude signals served as the basis for subsequent time-series analyses.

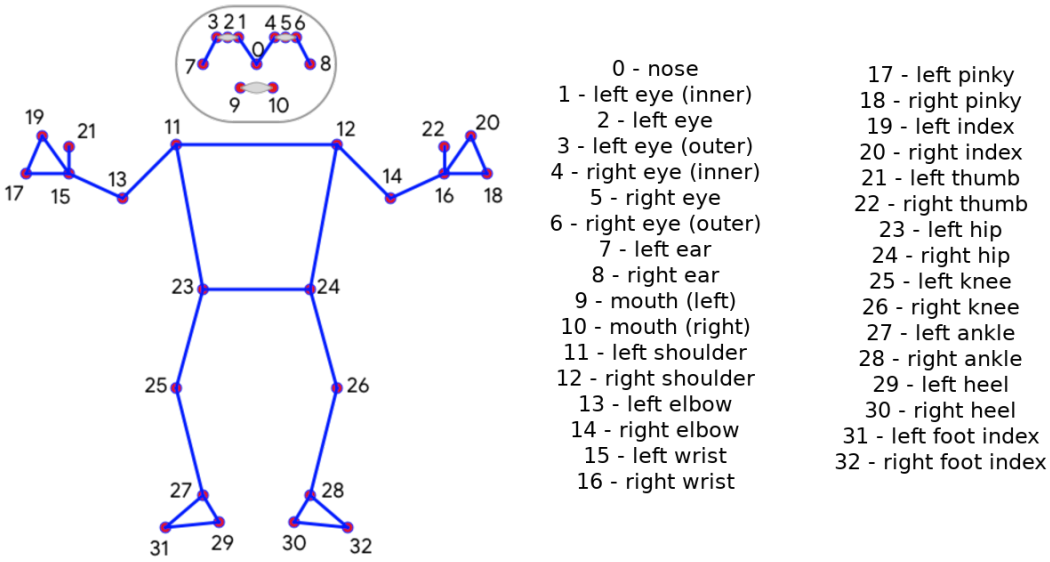

Figure 4.5: MediaPipe Pose Estimation keypoint topology [Baz+20] [Res20]

GPU acceleration facilitated real-time processing of high-resolution video data, with landmark detection rates exceeding 30 frames per second. The use of the Holistic graph ensured robust tracking even under challenging conditions, such as occlusions or rapid movements. All extracted landmark data were exported to CSV[24] files for further preprocessing and feature extraction.

Time-series amplitude signals were extracted from trial-wise CSV files. Each CSV contained a discrete frame index (column header `Frame`) and an amplitude value (column header `Value`). Prior to feature extraction, each amplitude series underwent the following preprocessing steps:

[21] Metacarpophalangeal
[22] Proximal Inter-phalangeal
[23] Distal Interphalangeal
[24] Comma-Separated Values

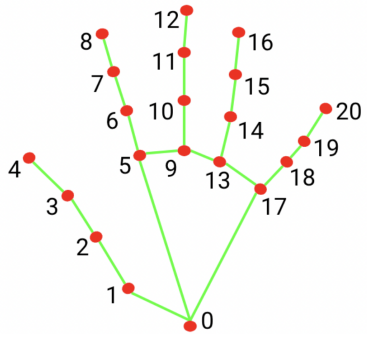

0. WRIST
1. THUMB_CMC
2. THUMB_MCP
3. THUMB_IP
4. THUMB_TIP
5. INDEX_FINGER_MCP
6. INDEX_FINGER_PIP
7. INDEX_FINGER_DIP
8. INDEX_FINGER_TIP
9. MIDDLE_FINGER_MCP
10. MIDDLE_FINGER_PIP
11. MIDDLE_FINGER_DIP
12. MIDDLE_FINGER_TIP
13. RING_FINGER_MCP
14. RING_FINGER_PIP
15. RING_FINGER_DIP
16. RING_FINGER_TIP
17. PINKY_MCP
18. PINKY_PIP
19. PINKY_DIP
20. PINKY_TIP

Figure 4.6: MediaPipe Hand Estimation keypoint topology [Zha+20] [Goo25]

4.2.3.1 Peak detection

Peaks were detected on the filtered series using adaptive thresholds. The minimum IPI[25] was 25 samples. Thresholds for height and prominence were set as fractions of the signal range.

4.2.3.2 Amplitude, Speed, and Acceleration Trends

For each variable, a linear regression was computed on the peak values y_i against time t_i:

$$y_i = \beta_0 + \beta_1 t_i + \epsilon_i, \quad i = 1, \ldots, n,$$

where β_0 is the intercept, β_1 the slope for the respective variable, and ϵ_i the residuals. The slope β_1 quantifies the rate of change of the peaks over time for the respective variable.

The coefficient of determination (R^2) was calculated as

$$R^2 = \left(\frac{\sum_i (t_i - \bar{t})(y_i - \bar{y})}{\sqrt{\sum_i (t_i - \bar{t})^2 \sum_i (y_i - \bar{y})^2}} \right)^2,$$

where $\bar{t}$ and $\bar{y}$ denote means of t_i and y_i, respectively. This statistic represents the proportion of variance in the peak values explained by the linear model.

4.2.3.3 Arrhythmicity

Arrhythmicity was quantified from the IPIs. Given peak timestamps $t_1, \ldots, t_m$, the IPIs are

$$\Delta t_j = t_{j+1} - t_j, \quad j = 1, \ldots, m-1.$$

The mean IPI is

$$\overline{\Delta t} = \frac{1}{m-1} \sum_{j=1}^{m-1} \Delta t_j.$$

Arrhythmicity Arr is defined as the mean absolute deviation of IPIs from their mean:

$$Arr = \frac{1}{m-1} \sum_{j=1}^{m-1} \left| \Delta t_j - \overline{\Delta t} \right|,$$

Lower A indicates a more regular rhythm. The units are seconds.

[25] Inter-Peak Intervals

4.2.3.4 GAITRite and Camera Arrangement

The allocation of the GAITRite mat was a challenge due to its 8.84m total length (7.93m active length). It could only be fit across the hallway of the university clinic, which affected the rest of the setting. The GAITRite was configured to detect a standard pattern, without cane or crutch. It was also set to auto suspend each trial. The sampling rate was 120Hz.

The AzureKinect DK cameras were positioned around the GAITRite mat in such a way that the operating ranges of the cameras overlapped slightly, i. e. it was made sure that every movement of the participants would be recorded by at least one camera. To achieve this, two cameras (AzureKinect0,AzureKinect2) were mounted at the ends of the mat, looking at the front or back of the participants and set to record with 2×2 binned NFOV mode at 30 FPS. The third camera was positioned halfway between the ends, looking at the participants sideways (see Figure 4.3) and set to record with 2×2 WFOV mode, also at 30 FPS. The use of three cameras was necessary to cover the active length of the GAITRite mat completely. Figure 4.1 shows the perspectives of camera 0 and camera 2 [Ari+20b].

4.2.4 Data Acquisition and Processing of Multi Camera Data

Figure 4.7 shows an overview of the data processing steps that were performed to compute the gait features: SL, Vel and Cad. The three AzureKinect DK cameras provided 3D point clouds of the respective scenes they had recorded. Using this information it was possible to perform an extrinsic calibration of the cameras (**step 1**, Figure 4.7).

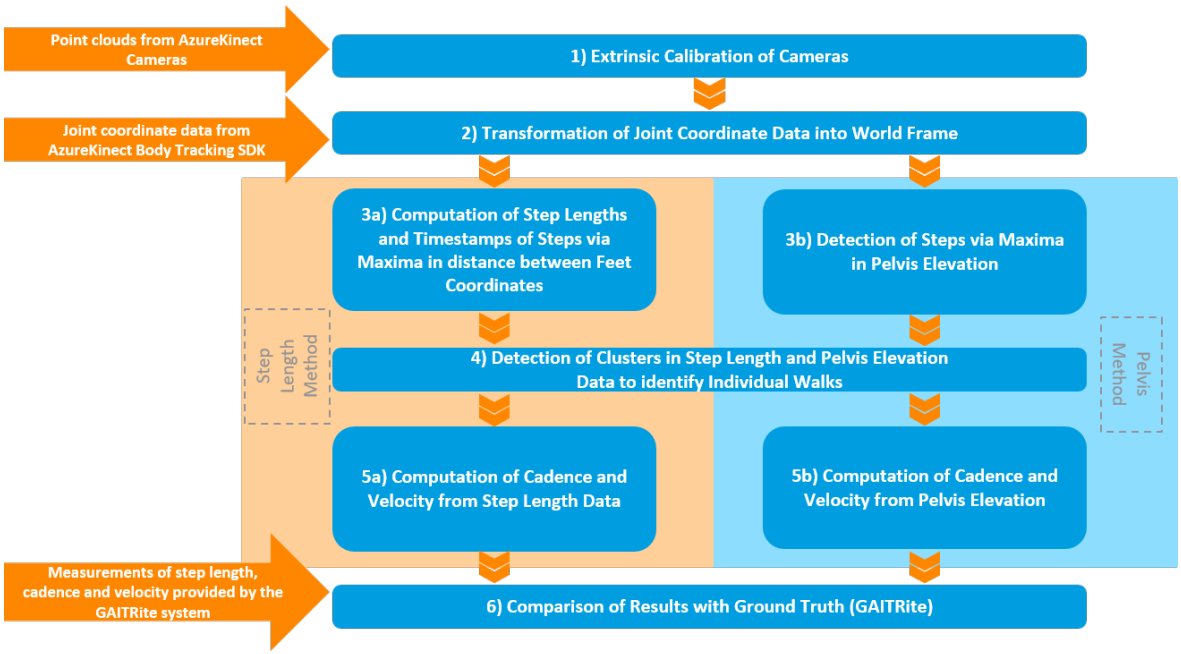

Figure 4.7: Overview of the data processing steps.

Because of an unreliable and error prone detection of the ArUCo markers [Gar+16; RMM18; Gar+14] (probably due to the poor lighting of the setup [Ari+20b] and relatively large distances between cameras and markers) a Semi-Automatic Extrinsic Calibration System for Multi-RGB-D-Cameras Using Arbitrary Axis-Aligned Edges was necessary. This had to be done for every patient and every camera, since the setup had to be unmounted and mounted repeatedly. This was because of the time intensive study tasks, the unpredictability of recruitment and the use of a space that was open to the public during office hours.

4.2.4.1 Semi-Automatic Extrinsic Calibration System for Multi-RGB-D-Cameras Using Arbitrary Axis-Aligned Edges

Let $p \in \{1, \ldots, 26\}$ denote the participant number, $k \in \{0, \ldots, 2\}$ the camera number and $i \in \{0, 1\}$ the per-axis number. The semiautomatic calibration was done by selecting six points ($X_0, X_1, Y_0, Y_1, Z_0, Z_1 \in \mathbb{R}^3$) in the camera's coordinate system (see Figure 4.3) for each participant and camera from a colored point cloud captured before the start of the walking session.

All point clouds were visualized and then the necessary points were optically identified and manually selected. The selection was performed in such a fashion that the points were located along the world's X, Y *and* Z axes (see Figure 4.8) and that they were as far apart from each other as possible to minimize the effect of noise in the calibration.

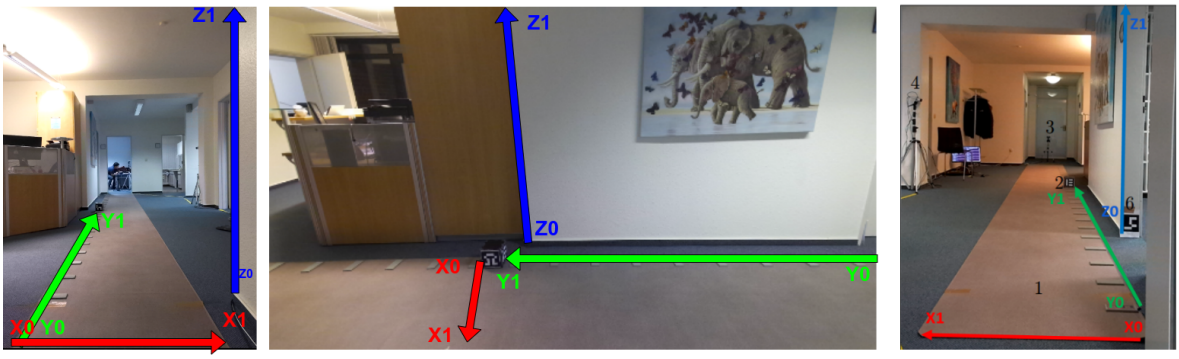

Figure 4.8: Axis Aligned Vectors for Calibration.
This is a semi-automatic extrinsic calibration procedure, aligning the coordinate systems of multiple RGB-D cameras to a common world reference frame for multi-camera kinematic analysis.
RGB images are displayed for clarity, but the points were selected on the colored point clouds.

Furthermore, Y_1 was selected at the lower right corner of the calibration cube closest to the wall. The dimensions of the calibration cube were known, therefore, the position of the center of the base of the calibration cube could be calculated. The origin of the world coordinates was placed at the center of the base of the calibration cube (as can be seen in Figure 4.3).

From these 6 points, three vectors were extracted, which were aligned with the X, Y and Z axes of the world coordinate system. Let $\overrightarrow{X}^{(world)}_{p,k}$, $\overrightarrow{Y}^{(world)}_{p,k}$ and $\overrightarrow{Z}^{(world)}_{p,k}$ denote these vectors for participant p and camera k. Then let: $\widehat{\overrightarrow{X}^{(world)}_{p,k}}$, $\widehat{\overrightarrow{Y}^{(world)}_{p,k}}$ and $\widehat{\overrightarrow{Z}^{(world)}_{p,k}}$, be their unit vectors. Furthermore let

$$\mathcal{R}(a, b) : (\mathbb{R}^3, \mathbb{R}^3) \to \mathbb{R}^{3\times3}$$

be a function that calculates the rotation matrix $R \in \mathbb{R}^{3\times3}$ between unit vector $a \in \mathbb{R}^3$ and unit vector $b \in \mathbb{R}^3$. This function is given by:

$$\mathcal{R}(a, b) = I + V + \left(\frac{1}{1 + (a \cdot b)}\right) \cdot V^2$$

where I is the identity matrix in $\mathbb{R}^{3\times3}$ and V is the skew-symmetric cross product matrix of $\| a \times b\|$.

Then the rotation matrix $R_{p,k}$ between the coordinate system of camera k and the world coordinate system for each participant p can be calculated as follows:

$$R_{p,k} = \mathcal{R}\left(\mathcal{R}\left(\widehat{\overrightarrow{Z}^{(world)}_{p,k}}, \begin{pmatrix}0\\0\\1\end{pmatrix}\right) \cdot \begin{pmatrix}0\\1\\0\end{pmatrix}, \widehat{\overrightarrow{Y}^{(world)}_{p,k}}\right)$$

Since the three axes are orthogonal, the method was tested by verifying that

$$R_{p,k} \cdot \begin{pmatrix} 1 \\ 0 \\ 0 \end{pmatrix} \approx \overrightarrow{X_{p,k}^{(world)}}$$

The translation vector can be calculated from the Y_1 vector with the necessary adjustment:

$$T_{p,k} = Y_{p,k,1} + R_{p,k} \cdot \begin{pmatrix} 0.065 \\ 0.065 \\ 0 \end{pmatrix}$$

(since the cube's sides were 13 cm long).

Then the homogeneous transformation matrix $H_{p,k} \in \mathbb{R}^{4\times4}$ between the the coordinate system of camera k and the world coordinate system for each participant p can be described as:

$$H_{p,k} = \begin{pmatrix} R_{p,k} & T_{p,k} \\ \overline{0} & 1 \end{pmatrix}$$

where $\overline{0} = (0, 0, 0)$.

This yielded the transformation information necessary to transform the BT-joint coordinate data (acquired via the AzureKinect BT) of all three cameras into a common world coordinate system (Figure 4.7 **step 2**).

Once the positions of the participants' BT-joints within the world coordinate system were known, the question presented itself, which would be the best strategy to compute interesting gait features from this data.

One feature that is both clinically relevant and (in principle) easily computable is the SL, which can be determined by looking at the maxima in feet distance along the line of progression (**step 3a**).

As the Y-axis of the world coordinate system runs in parallel to the GAITRite mat, the distance in y-direction of the two foot BT-joints over time was computed for each participant and the maxima were detected.

The data contained some noise that resulted in local maxima that did not signify a step, therefore a minimum distance between maxima **MinDist** (measured in number of data points) was set with the aim to avoid faulty detections.

Also, a minimum prominence **MinProm** was set, i.e. peaks were only detected, if they stood out far enough from the surrounding baseline of the data. The exact values for **MinDist** and **MinProm** were determined for each data set by looking at the first two walks and adjusting the parameters until each step was detected. The function used for peak detection was scipy.signal.find_peaks [Vir+20].

As the ranges of the three AzureKinect DK cameras overlapped there was also an overlap in the feet distance data, i.e. some maxima were recorded more than once. This can be seen in Figure 4.9 for the example of a HP. The redundantly recorded maxima were fused, i.e. detected maxima between which there was a time delta of less than 0.15 seconds were handled as a single maximum. The AzureKinect DK cameras tend to detect smaller steps near the edges of their recording ranges, due to participants often being in mid step, when entering the camera range. Therefore, the maximum with the higher y-distance value was chosen for computation of SL.

Even after these measures, some false detections due to noise remained, e.g, the third cyan-circled maximum in Figure 4.9. These were dealt with in **step 4**.

The timestamps of steps can also be computed by looking at the movement of the pelvis, which follows a sinusoidal path in the vertical direction during walking [Lew+17] (**step 3b**). When a walking person stands on one foot (single support phase), the pelvis shows its highest elevation. When both feet are on the ground (double support phase), the pelvis is at its lowest point.

According to the data of [Alb+20], the pose detection accuracy obtained from the pelvis is significantly better than obtained from the feet. The former also shows less noisy time series data. By computing the maxima in pelvis elevation, the single support phase of each step was detected (Figure 4.10).

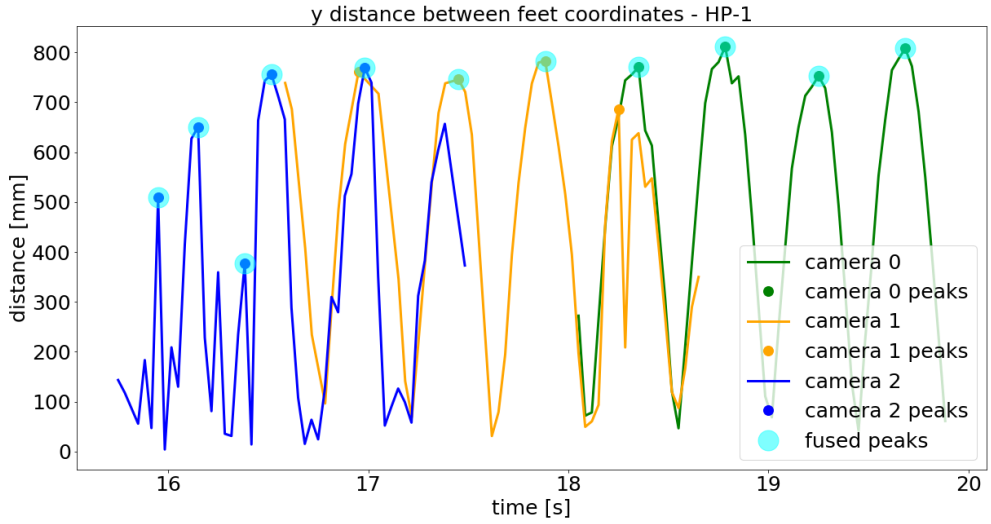

Figure 4.9: Trace of y-distance between feet BT-joints of the first walk of participant HP-1.
The data from camera 0 is shown in green, the data from camera 1 in orange and the data from camera 2 in blue. Detected maxima are marked in the respective color. Those that were redundantly detected are fused and the maxima that resulted from that fusion process are marked in semi-transparent cyan.

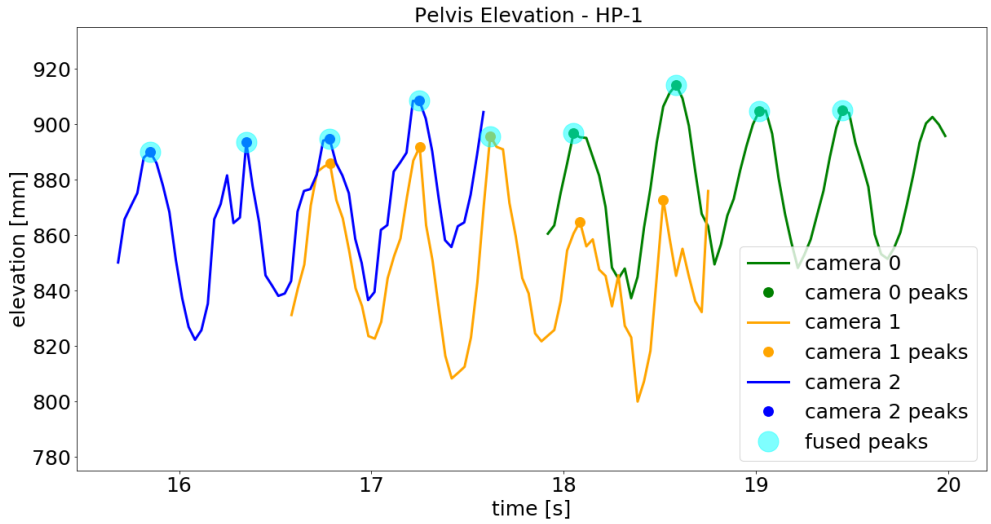

Figure 4.10: Trace of pelvis elevation for the first walk of participant HP-1.
The data from camera 0 is shown in green, the data from camera 1 in orange and the data from camera 2 in blue. Detected maxima are marked in the respective color. Those that were redundantly detected are fused and the maxima that resulted from that fusion process are marked in semi-transparent cyan.

The traces of the different cameras oscillate around baselines of slightly different heights (magnitude of difference up to 4 cm), which is probably due to imperfect calibration. This does not pose a problem here, however, because the relevant feature for step detection is the timestamp of the maximum of pelvis elevation, not the elevation value that is reached at that maximum.

In order to identify individual walks, a detection of clusters was performed both for the feet y-distance and the pelvis elevation maxima (**step 4**). The clustering algorithm used was DBSCAN[26] (Density-Based Spatial Clustering for Applications with Noise) implemented by the Python module *scikit-learn* [Sch+17b; Ped+11].

Three important parameters of this algorithm are:

metric the metric that is used for calculating the distance between two data points
epsilon the maximum distance between two data points to be considered as neighbors
min_samples the minimum number of data points that have to be in the neighborhood of a given point for that point to be considered a *core point*

Regarding the *metric*, two data points were considered "infinitely far apart", if the time delta between them was less than 0.4 s or greater than 1.6 s. The reasoning behind this was, that data points with a time delta that is too small do not signify independent steps, while data points with a time delta that is too great cannot belong to the same walk over the GAITRite mat. If this time constraint was fulfilled by two data points, their distance was computed as the euclidean distance with regard to the two dimensions *time* measured in [s] and *SL* or *pelvis elevation* measured in [cm].

For the SL clustering, *epsilon* was varied between values of 5 and 15 in order to detect the expected number of 10 walk clusters. Generally, *epsilon* had to be set to a higher value for participants with a PD diagnosis, because of a greater variability in SL.

In case of the pelvis elevation, a value of *epsilon* = 8 was determined to lead to the detection of all walk clusters.

min_samples was set to 2 for all participants because a walk, by nature, consists of single consecutive steps, so no greater number of data points can be expected to be in the neighborhood of a core point.

Figure 4.11 shows an example of the clustering of feet y-distance maxima. A number of outliers (black) were detected and removed. Among those outliers are the first three steps detected in the first walk (leftmost cluster).

Looking back at Figure 4.9, it seems unlikely, that none of those three peaks signify a real step. The goal, however, was to avoid false-positive step detections, which came at the cost of some actual steps not being detected. For the computation of the mean and SD[27] of SL the clustered values were used.

The clustering of the pelvis elevation maxima revealed very few outliers and none were detected for participant HP-1 (Figure 4.12).

The gait features cadence and velocity were computed via two different methods: In **step 5a** the SL data was used and in **step 5b** it was based on the pelvis elevation data. All values were first determined for each individual walk (i.e. value cluster) and finally the mean was calculated.

Computation via SL data:

Let $\{t_0, \dots t_n\}$ be the timestamps of a cluster and $\{sl_0, \dots sl_n\}$ the respective SLs. The first timestamp t_0 signifies the **end** of the first registered step, because that is the point, when the y-distance between the feet is

[26] Density-Based Spatial Clustering for Applications with Noise
[27] Standard Deviation

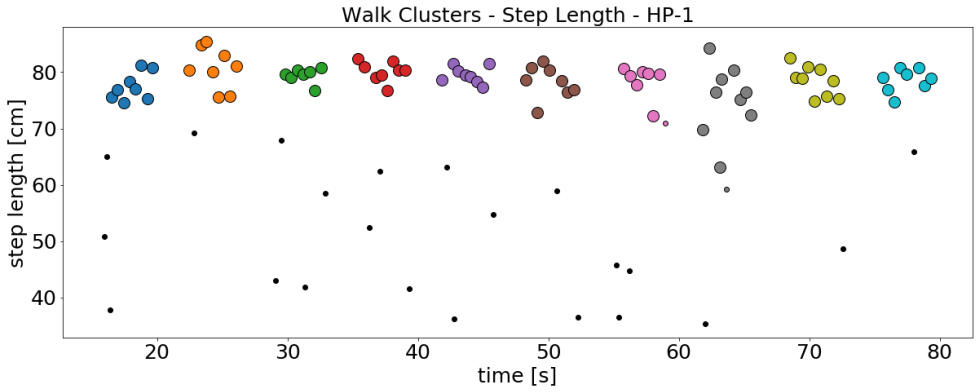

Figure 4.11: Result of DBSCAN clustering for the feet y-distance maxima data, i.e. the detected SLs, of participant HP-1
The ten colored clusters represent the ten walks the participant performed. Outliers are depicted in black.

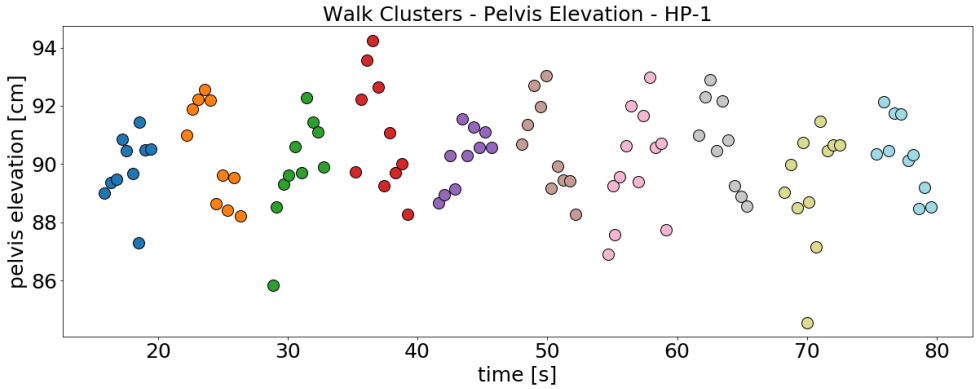

Figure 4.12: Result of DBSCAN clustering for the pelvis elevation maxima data of participant HP-1.
The ten colored clusters represent the ten walks the participant performed.

highest. The start time of that first step is unknown. So to compute the total distance walked between t_0 (which is also the start time of the second step) and t_n, only the SLs $\{sl_1, \dots\ sl_n\}$ must be added.

The velocity Vel_{SL} is therefore determined via the following formula:

$$Vel_{SL} = \frac{sl_1 + \cdots + sl_n}{t_n - t_0}$$

Between t_0 and t_n n steps take place. The Gait Cadence cad_{SL} is computed as:

$$cad_{SL} = \frac{n}{t_n - t_0}$$

Computation via pelvis elevation data:

Let $\{t_0, \dots\ t_n\}$ be the timestamps of a cluster and $\{y_0, \dots\ y_n\}$ the y-positions of the pelvis at those timestamps. Because the Y-axis of the world coordinate system runs parallel to the line of progression of the participants on the GAITRite mat, the total distance walked can be determined via $\mid\ y_n - y_0\ \mid$. The Vel Vel_p is therefore determined via the following formula:

$$Vel_p = \frac{\mid y_n - y_0 \mid}{t_n - t_0}$$

Between t_0 and t_n n steps take place. The Gait Cadence cad_p is computed as:

$$cad_p = \frac{n}{t_n - t_0}$$

In **step 6** finally, the results were compared to the ground truth provided by the GAITRite system.

4.3 Results

This section presents the main results of the validation study, comparing gait features extracted from the Azure Kinect-based system to those obtained from the GAITRite gold standard. Key metrics such as SL, Vel, and Cad are evaluated for both HPs and PwPD. Additionally, the section includes a partial analysis of non-gait motor tasks, specifically focusing on finger tapping and hand open-close movements (MDS-UPDRS Part III Examination Items 3.4 and 3.5), which were computed for this publication. The following analyses summarize the accuracy, reliability, and clinical relevance of the proposed multi-sensor system in quantifying both gait and selected non-gait parameters.

The averages of the gait features SL, Cad (steps per minute) and Vel (cm per second) were computed for 11 HPs and 13 PwPD's for a total of N=24 for the evaluated data. In the case of two PwPD's (PwPD-7, PwPD-11), all the video files recorded by the AzureKinect DK were corrupted and the use of the Body Tracking software was not possible. This also happened to some of the files of other participants, so that the computed values for the participants PwPD-1 - PwPD-6, PwPD-8 and PwPD-10 are based on the data of only 2 AzureKinect DK cameras. Of the total of 75 files, 12 were unreadable or corrupted, which results in a file failure rate of 16 %.

In most cases, the AzureKinect-based system underestimates the mean SL. Figure 4.13 **A** shows the results of the SL computation for all participants.

The average deviation between means is 2.6 %. The greatest deviation is found for participant PwPD-5 with -7.6 %, the smallest for participant HP-2 with +0.2 %. For all but three participants (HP-4, HP-5, PwPD-5) the deviation is less than 5 %.

The MAE is 1.74 cm (see Figure 4.13 **D**).

The SD is greater for the values determined by the AzureKinect-based system in all cases. While the average SD provided by the GAITRite system is 3.1 cm, it is 4.9 cm in case of the AzureKinect-based system.

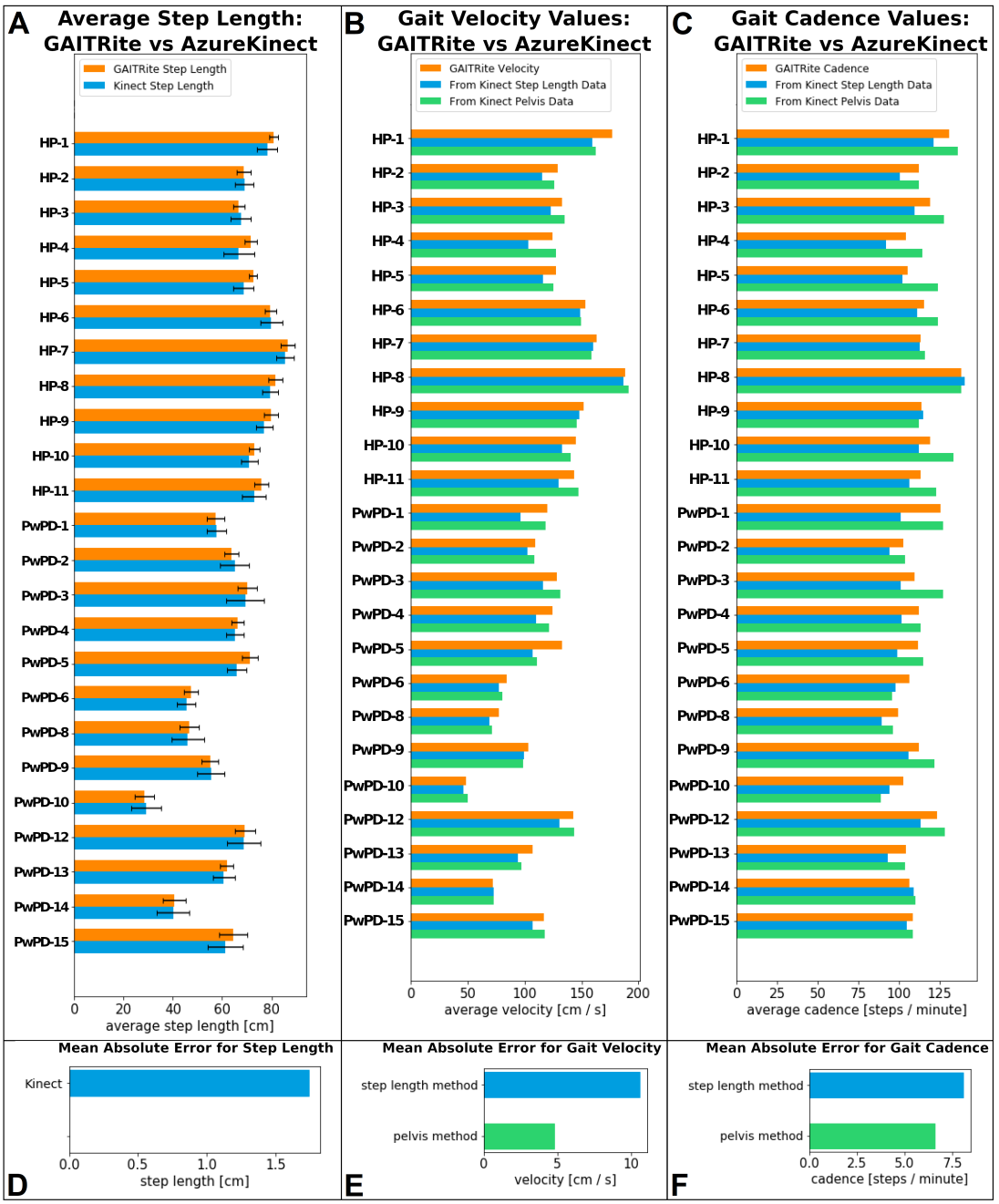

Figure 4.13: Results overview

A:Average SL of all HPs and PwPD's. Orange: Ground truth provided by the GAITRite system. Blue: Values computed from AzureKinect DK camera data.
B:Gait Velocity values for HPs and PwPD's. Orange: Ground truth provided by the GAITRite system. Blue: Values computed via SL data. Green: Values computed via pelvis elevation data.
C:Gait Cadence values for HPs and PwPD's. Orange: Ground truth provided by the GAITRite system. Blue: Values computed via SL data. Green: Values computed via pelvis elevation data.
D:MAE of computed SLs.**E:**MAEs of computed Vels.**F:**MAEs of computed Cads values.

Figure 4.13 **B** shows the Vel results for all participants. The MAE of the SL method is greater than the average error of the pelvis elevation, with values of 8.6 % or 10.6 cm/s and 3.7 % or 4.6 cm/s respectively (see Figure 4.13 **E**).

The Cad values computed using the SL data are smaller than the values given by the ground truth in most cases (except HP-8, HP-9 and PwPD-14). The pelvis elevation shows some underestimations as well as overestimations. Figure 4.13 **C** shows the Cad results for all participants. The average error of the pelvis elevation is smaller than the average error of the SL method, with values of 5.7 % or 6.3 steps/minute and 7.2 % or 8.1 steps / minute respectively (see Figure 4.13 **F**).

The pelvis elevation produces an error greater than 5 % in 10 out of 24 participants. For the SL method this is the case for 17 of the participants. For the same participant, the accuracy of the two methods is very different in some cases: In participant HP-2, for example, the value computed via the SL method shows an error of -10.81 %, while the value computed via the pelvis elevation is off by only -0.11 %.

Figure 4.14 **A** shows the Bland-Altman plot for the mean SL (SL) value pairs (SL_{GR}, SL_{AK}) of all participants. The mean difference is 1.42 cm. The 95 % limits of agreement lie at -2.02 cm and 4.87 cm, i.e. 1.42 cm - 1.96 SD = -2.02 cm and 1.42 cm + 1.96 SD = 4.87 cm. All but one value lie within these limits.

The Vel values computed using the SL data are smaller than the values given by the ground truth in almost all cases, with the exception of PwPD-14. In case of the pelvis elevation, there are overestimations as well as underestimations.

For most participants (except HP-1, PwPD-5, PwPD-8, PwPD-13), the error of the pelvis elevation is less than 5 %. Figure 4.14 **B** shows the Bland-Altman plot for the Vel (Vel) value pairs (Vel_{GR}, Vel_{AK}) of all participants. The mean difference is -2.97 cm/s. The 95 % limits of agreement lie at -14.56 cm/s and 8.61 cm/s. All values lie within these limits.

Figure 4.14 **C** shows the Bland-Altman plot for the Cad value pairs (Cad_{GR}, Cad_{AK}) of all participants computed via the pelvis elevation method. The mean difference is 3.81 steps/min. The 95 % limits of agreement lie at -10.86 steps/min and 18.49 steps/min. All but one value lie within these limits.

The Pearson's correlation coefficients (PCC[28]) between the results of the AzureKinect and GAITRite system were calculated for the means of SL, Vel and Cad (see Table 4.4). Looking at all participants, the PCC values indicate a very strong correlation[29] in all cases, with PCC values greater than 0.950 for SL and Vel. The correlation of the Cad results is slightly smaller, with 0.854 for the values determined via the SL method and 0.817 for the values determined via the pelvis elevation method.

Table 4.4: PCC values for gait features.

Feature	HP	PwPD	All
SL	0.958	0.992	0.993
Vel (SL method)	0.975	0.970	0.977
Vel (Pelvis method)	0.965	0.970	0.983
Cad (SL method)	0.920	0.672	0.854
Cad (Pelvis method)	0.793	0.827	0.817
Note: All p-values < 0.0036.			

[28] Pearson Correlation Coefficient
[29] Interpretation of PCC values as suggested by Evans [Eva96]:

- 0.00-0.19–very weak
- 0.20-0.39–weak
- 0.40-0.59–moderate
- 0.60-0.79–strong
- 0.80-1.00–very strong

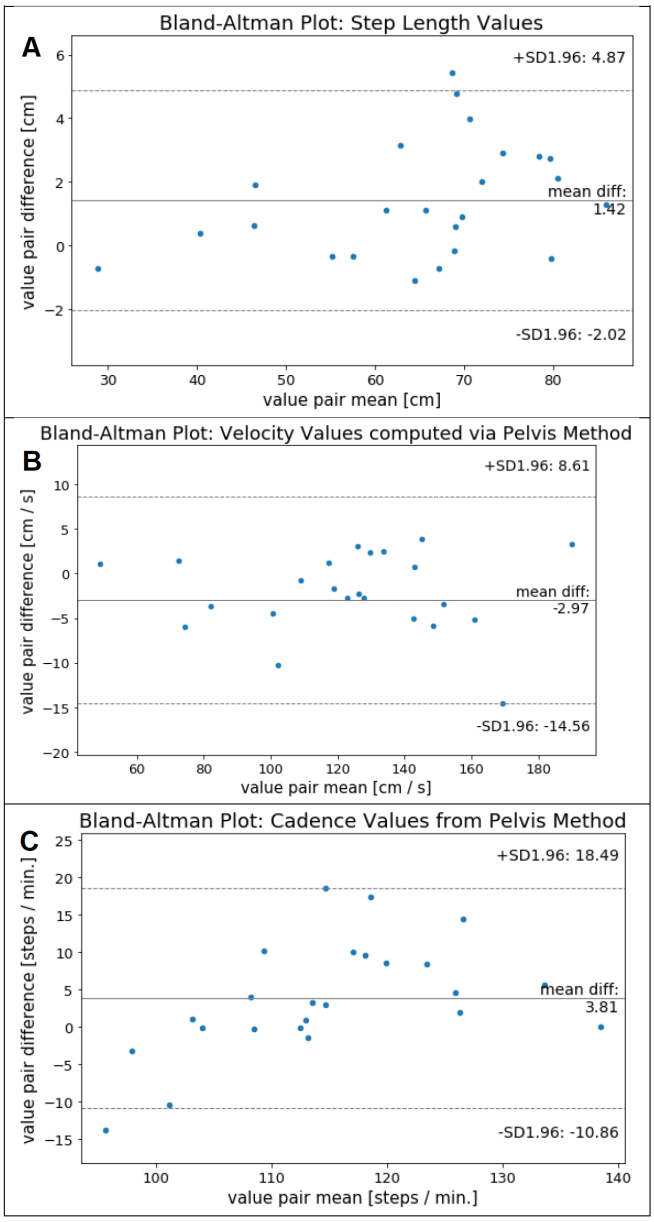

Figure 4.14: Bland-Altman Plots

A:Bland-Altman Plot of the computed SL values.
X-axis: means of the value pairs (SL_{GR}, SL_{AK}).
Y-axis: difference (SL_{GR}-SL_{AK}).
B:Bland-Altman Plot of the computed Vel values.
X-axis: means of the value pairs (Vel_{GR}, Vel_{AK})
Y-axis: difference (Vel_{GR}-Vel_{AK}).
C:Bland-Altman Plot of the computed Cad values.
X-axis: means of the value pairs (Cad_{GR}, Cad_{AK}).
Y-axis: difference (Cad_{GR}-Cad_{AK}).

4.3.1 Analysis of selected non-gait MDS-UPDRS

This subsection presents the analysis of movement features derived from the TEDIPA system in relation to clinical motor impairment, as assessed by the MDS-UPDRS. The aim is to evaluate the extent to which automatically extracted kinematic parameters–such as movement amplitude, speed, acceleration, and rhythmicity–correlate with established clinical scores (MDS-UPDRS Part III). For this publication, only the finger tapping and hand open-close tasks (Items 3.4 and 3.5 of the MDS-UPDRS) were computed. By comparing quantitative movement metrics with clinician-rated assessments, this analysis provides insight into the validity and potential clinical utility of the TEDIPA system for objective motor evaluation in PD and related disorders.

4.3.1.1 Statistical Analysis

Statistical analysis was performed to identify significant differences in movement parameters between groups (e.g., HPs vs. PwPD's). Data were tested for normality using the S-W[30] [SW65] test. Depending on the normality of the data, either parametric tests (t-tests [Dav63]) or non-parametric tests (Mann-Whitney U test [MW47]) were used.

Correlation analyses were conducted to examine relationships between movement parameters and clinical measures (e.g., disease severity, motor scores). A significance level of $\alpha = 0.05$ was used for all statistical tests. Statistical analysis was performed using R [R C23].

Figure 4.15 presents a boxplot of the average decrease in maximum movement amplitude stratified by MDS-UPDRS score. The figure illustrates a trend of reduced amplitude with increasing clinical motor impairment, as indicated by higher MDS-UPDRS scores. The sample size indicated on the x-axis quantifies the number of movement sequences included in the analysis. These sequences correspond to hand open-close and finger tapping, performed on either the left or right side (MDS-UPDRS Part III Examination Items 3.4 and 3.5). While significant differences are observed between lower scores, the limited sample size for higher scores (e.g., score 3) reduces statistical power for these groups. Each box represents the distribution of amplitude values within a score group, and the progressive lowering of medians and interquartile ranges reflects the worsening motor function. Specifically, the tasks analyzed here are finger tapping and hand open-close movements, which are part of the MDS-UPDRS Part III motor examination. The results suggest that movement amplitude, while not strongly correlated with overall MDS-UPDRS scores, still provides some discriminatory power for distinguishing levels of motor impairment in the cohort.

Table 4.5: Correlation Between Amplitude Movement Parameters and MDS-UPDRS Score

	$\delta \max AMP/\delta t$	R^2	Arrhythmicity*
Overall (All)	0.04	0.00	0.35
Hand Open Close (All)	0.00	-0.12	0.27
Finger Tapping (All)	0.07	0.14	0.52
Overall (PwPD)	0.08	0.10	0.12
Hand Open Close (PwPD)	-0.13	-0.05	0.28
Finger Tapping (PwPD)	0.28	0.29	-0.11
Overall (HP)	-0.19	-0.09	-0.31
Hand Open Close (HP)	NA**	NA**	NA**
Finger Tapping (HP)	-0.20	-0.09	-0.33

* distance between actual repetition time and equidistant repetitions
** SD was zero

This analysis revealed a bad correlation between movement amplitude and MDS-UPDRS scores, with a PCC of 0.04. The correlation was more pronounced in the finger tapping task (PCC = 0.07) compared to the hand open-close task (PCC = 0.00). The results are summarized in Table 4.5.

[30] Shapiro-Wilk

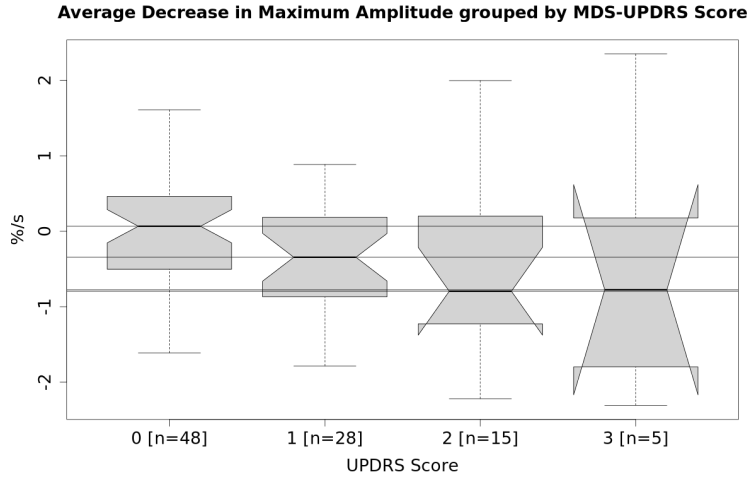

Figure 4.15: Boxplot illustrating the average decrease in maximum amplitude by MDS-UPDRS score.
The units of this plot are given in changes in percentage of the maximum amplitude per second. -1 %/s means that, in average, the amplitude decreased from maximum to 99% within 1 second.

The results presented in Table 4.5 provide insight into the relationship between movement amplitude parameters and clinical motor impairment as measured by the MDS-UPDRS score. Overall, the correlation coefficients between amplitude features and MDS-UPDRS scores are low, indicating a weak association. For all participants, the PCC for amplitude is 0.04, and the coefficient of determination (R^2) is close to zero, suggesting that amplitude changes are not strongly explained by clinical severity in this cohort. Subgroup analysis reveals slightly higher correlations for finger tapping tasks (PCC = 0.07, R^2 = 0.14), but the relationship remains weak.

Interestingly, arrhythmicity–defined as the deviation from equidistant repetition timing–shows a moderate correlation (0.52) in the finger tapping task for all participants, suggesting that rhythm disturbances may be more sensitive to motor impairment than amplitude alone. In the PD subgroup, amplitude correlations are somewhat higher for finger tapping (0.28), but negative or near-zero for other tasks. For HPs, amplitude and arrhythmicity correlations are negative, indicating that these features do not track with the MDS-UPDRS scores in this group.

These findings highlight the challenge of using simple amplitude-based metrics for clinical assessment of motor impairment in PD and related disorders. The weak correlations can be attributed to the fact that the two methods–clinical rater assessments and camera-based measurements–rely on fundamentally different evaluation criteria. While the camera system lacks knowledge of the maximum amplitude achievable by the participant, the clinical rater incorporates this information into their assessment. This discrepancy underscores the need for further refinement of the peak detection algorithm and the inclusion of more sensitive movement features to bridge the gap between automated and clinician-based evaluations. Incorporating arrhythmicity or other temporal features may enhance the accuracy and clinical relevance of automated assessments in future studies.

This analysis revealed a bad correlation between Hand movement speed and MDS-UPDRS scores, with a PCC of -0.05. The correlation was more pronounced in the finger tapping task (PCC = -0.02) compared to the hand open-close task (PCC = -0.14). The results are summarized in Table 4.6. The results in Table 4.6 show the correlation between speed-based movement parameters and clinical motor impairment as measured by the MDS-UPDRS score.

Overall, the PCCs for speed features are low, with a value of -0.05 for all participants and negative R^2 values, indicating a weak or absent association between speed changes and clinical severity. Subgroup analysis reveals

Table 4.6: Correlation Between Hand Movement Speed Variations and MDS-UPDRS Score

	$\frac{\delta\ v_{\max}}{\delta t}$	R^2
Overall (All)	-0.05	-0.11
Hand Open Close (All)	-0.14	-0.16
Finger Tapping (All)	-0.02	-0.08
Overall (PD)	0.20	0.10
Hand Open Close (PD)	0.11	0.12
Finger Tapping (PD)	0.19	0.02
Overall (HP)	-0.25	-0.24
Hand Open Close (HP)	NA**	NA**
Finger Tapping (HP)	-0.38	-0.34

** SD was zero

slightly higher correlations for participants with PD, with coefficients up to 0.20 for overall speed and 0.19 for finger tapping, but these remain modest. In HPs, the correlations are negative, suggesting that speed features do not track with MDS-UPDRS scores in this group. The hand open-close task in HPs could not be evaluated due to zero SD (This is consistent with expectations, as participants without PD typically have an MDS-UPDRS score of 0, reflecting the absence of clinically relevant motor impairment). These findings suggest that speed-based metrics, as currently implemented, have limited utility for distinguishing motor impairment severity in this cohort.

Table 4.7: Correlation Between Acceleration Movement Parameters and MDS-UPDRS Score

	$\delta \max ACC/\delta t$	R^2
Overall (All)	0.16	0.09
Hand Open Close (All)	0.22	0.14
Finger Tapping (All)	0.06	0.04
Overall (PD)	0.09	-0.01
Hand Open Close (PD)	0.04	0.04
Finger Tapping (PD)	0.12	-0.04
Overall (noPD)	-0.26	-0.26
Hand Open Close (noPD)	NA**	NA**
Finger Tapping (noPD)	-0.38	-0.38

** SD was zero

The results presented in Table 4.7 provide a detailed overview of the relationship between acceleration-based movement parameters and clinical motor impairment as measured by the MDS-UPDRS score. Overall, the PCCs between acceleration features and MDS-UPDRS scores are low to moderate, with the highest observed value being 0.22 for the hand open-close task in all participants. The coefficient of determination (R^2) values are similarly low, indicating that only a small proportion of the variance in acceleration parameters is explained by clinical severity.

For all participants, the overall correlation between maximum acceleration change and MDS-UPDRS is 0.16, with $R^2 = 0.09$. This suggests a weak association, and that acceleration features alone may not be sufficient to reliably track motor impairment across the cohort. When analyzing specific tasks, the hand open-close task shows a slightly higher correlation (0.22), while finger tapping yields a lower correlation (0.06). This pattern is consistent with previous findings that amplitude and speed features are only weakly associated with clinical scores in heterogeneous populations.

Subgroup analysis reveals further nuances. Among participants with PD, the correlations are even lower, with overall values of 0.09 and negative or near-zero R^2 values. The hand open-close and finger tapping

tasks in the PD group show minimal correlation, suggesting that acceleration features may not capture disease-specific motor impairment effectively. In HPs, the correlations are negative, with values of -0.26 overall and -0.38 for finger tapping, indicating that higher acceleration does not correspond to higher clinical scores in this group. The negative R^2 values further reinforce the lack of explanatory power.

Taken together, these findings suggest that acceleration-based features, as currently computed, have limited utility for distinguishing motor impairment severity in PD and related disorders. The weak and inconsistent correlations across tasks and groups indicate that further refinement of the feature extraction and peak detection algorithms is necessary. Potential improvements could include more robust filtering of movement traces, task-specific normalization, or the integration of additional temporal and spatial features.

In summary, while acceleration features provide some information about motor performance, their current implementation does not yield strong associations with clinical scores. Future work should focus on optimizing feature extraction and exploring multi-modal approaches to improve the accuracy and clinical relevance of movement analysis in neurodegenerative disease cohorts.

4.4 Discussion

This section discusses the findings of the TEDIPA study, focusing on the validation of gait analysis and the evaluation of the selected non-gait motor tasks.

The first subsection highlights the accuracy and reliability of the proposed AzureKinect-based system in extracting key gait parameters, comparing its performance to the established GAITRite system. The second subsection delves into the analysis of the selected non-gait motor tasks, examining the relationship between automatically extracted movement features and clinical motor impairment scores, as assessed by the MDS-UPDRS. Together, these analyses provide insights into the potential and limitations of the TEDIPA system for objective movement analysis in real-world settings.

4.4.1 Gait Analysis

The first part of the present study evaluates the validity of a gait analysis system based on the AzureKinect's consumer depth camera by comparing it to an established gold standard for gait analysis, the GAITRite Walkway. This was done with regard to the accuracy and precision of key indicators of healthy and pathological gait. The data of 24 participants were evaluated, of which 13 had a neurodegenerative motor disease. A comparison between both techniques revealed an average absolute difference of 1.74 cm in SL, 4.6 cm/s difference in Vel and 6.3 steps/min for Cad. Pearson's correlation coefficients range from r = 0.817 to r = 0.993, demonstrating a very high correlation between both recording techniques.

The MAE (1.74 cm) of the method used in this paper for SL approximation is smaller than the average error seen in other works, e.g, Steinert et al. [Ste+20], who compared the KinectV2 to the GAITRite and obtained error values of 1.99 cm and 2.59 cm for the left and right SL respectively. For the current study, a GAITRite walkway with an active area of 7.93 meters was used and walks were also recorded with three AzureKinect DK cameras simultaneously. This study design might have enabled the recording of more steps compared to the Steinert et al. [Ste+20] study. It is conceivable that a longer measuring path leads to more data and more accurate results.

The relative error for Cad and Vel achieved by the proposed system is also better than single-trunk IMU-based approaches [PSA20]. They present values of Cad estimation with relative errors of 13%, 12% and 14% in their improved Cad detection algorithms, while the current study reports 8.6 % and 3.7 % for the SL and the pelvis elevation methods respectively (see Figure 4.13 **E**). For Vel estimation they present relative errors of 22% and 25% in their improved Vel detection algorithms, while the current study reports 5.7 % and 7.2 % for the SL and the pelvis elevation methods respectively.

The risk of falls in older adults (both healthy and with a PD diagnosis) is generally associated with slower walking and shorter steps [GI80]. Considering that those who walk more slowly and with shorter steps generally also have a higher risk of falling [Alc+18] it can be said that SL is an important gait parameter.

A significantly shorter stride length in PD patients (mean ± SD: 103.66 ± 24.17 cm) was demonstrated in comparison to healthy elderly people (mean ± SD: 124.98 cm ± 17.78cm) [Yan+08]. According to their data, PD patients have a mean SL of 51.83 cm and healthy elderly people have a mean SL of 62.49 cm. The difference between those mean values is 10.66 cm, which is a much higher value than the average SL error of our AzureKinect-based system (1.74 cm). It seems therefore realistic that such a system could be used to evaluate the gait of healthy individuals as well as of individuals affected by a neurological disorder. Furthermore, a 3-year prospective study exhibited a significant reduction in the normalized SL at the follow-up assessment in PD patients. Even though the drug levodopa significantly increased the normalized SL on the initial evaluation, as well as at the follow-up assessment [Amb+18]. In accordance with with those data, a significant and large effect of the H&Y scores on SL was recently found [Wel+21].

The MAE of Vel, which is 10.6 cm/s for the SL method and 4.6 cm/s for the pelvis elevation method is comparable with similar works. [Ste+20] obtained a mean difference of 4.01 cm/s at preferred Vel and 5.76 cm/s at fast Vel.

However, this degree of accuracy was not reached with regard to the gait feature cadence. Regarding the MAE [Ste+20] achieve significantly more accurate results with an error value of -1.16 steps/minute compared to 6.3 steps/minute (pelvis method) and 8.1 steps/minute (SL method) of the system used in this study.

The detection of the feet BT-joints was noisier and more unreliable than the detection of the pelvis BT-joint, as it was also observed by [Alb+20]. This improvement in detection stability propagates to the calculation of Cad and Vel. The improvement from the pelvis elevation method to the feet distance method is significant. The pelvis elevation method offered an improvement in the MAE of Vel of 56 % and an improvement of 22 % in the MAE of Cad, which clearly favors the second method. People with PD walk more slowly [Alc+18] with smaller forward movement Vel than matched controls. Decreased Vel is caused by decreased stride length [Lim+98; Sch+03; Nil+09; Yan+08]. While Vel and stride length improved similarly with STN-DBS[31] [Kum+98] or levodopa, Cad did not change with DBS[32] or medication [Xie+01; ME13].

It should be noted that the initially planned extrinsic calibration method was unsuccessful, since the ArUCo markers [Gar+16; RMM18] were not detected reliably. This was probably due to the poor lighting of the setup [Ari+20b] and relatively large distances between cameras and markers. Therefore, a new offline calibration method had to be used for this study. The Iterative Closest Point (ICP[33]) point cloud registration was not an option because of the sparse presence of points in the overlapping areas of the operating ranges of the cameras. It was necessary to use manually selected axis aligned vectors, which were then automatically processed for the necessary transformations of the extrinsic camera calibration

One of the goals of this validation study was to investigate whether Body Tracking data provided by the AzureKinect system can be used directly for step detection. With regard to data processing, a threshold for the minimal distance between peaks in feet distance and pelvis elevation as well as a threshold for the minimal prominence of those peaks were defined in order to avoid faulty step detection due to noisy data (see subsection 4.2.4). An alternative would be to model the y-distance traces via sinusoidal functions or to apply filtering techniques (like a fourth order Butterworth filter). This would lead to smoother traces and, ideally, no additional measures would be necessary to prevent faulty detections. This approach should be investigated in future works.

The results obtained by the second method, using the coordinate data of the pelvis instead of the coordinate data of the feet, were more accurate. This can be explained by the fact that the pelvis BT-joint is located at the root of the tree that represents the BT-joint positions of the AzureKinect BT. Because of this, the estimated

[31] Subthalamic Nucleus Deep Brain Stimulation
[32] Deep Brain Stimulation
[33] Iterative Closest Point

pelvis coordinates are much stabler than the noisier readings of the extremities, like feet and hands. This can also be seen in the data collected by Albert et al. [Alb+20].

Some external factors might also have influenced the accuracy of the BT. Loose, dark and opaque foot wear, like boots, could lead to diminished accuracy in the readings, while tighter, lighter and smaller foot wear is tracked more reliably. This effect might have lead to a relatively poor detection of the foot BT-joints in HP-4, which resulted in a large SL error.

Lighting conditions might also influence the accuracy of the pose estimation. Some of the captures, specially from camera 0, were probably affected by the sunlight that came from the side through an adjacent window. This could have caused an unreliable BT-joint estimation.

Furthermore, the orientation of the participants with respect to the camera might also have had repercussions on the quality of the Body Tracking. The segments where the participants walked towards a camera had a much better accuracy and stability than the segments where the participants walked orthogonally to the direction of view of a camera (so that the camera mostly saw them laterally) or away from the camera.

The setup of this study could be significantly improved by using more cameras along the walkway, so that every participant could be captured by at least two cameras at every point. This would be possible by putting one camera on each end and three further cameras on each side of the walkway. This would offer better camera perspectives to enhance the amount and quality of data obtained by the BT and offer a broader data basis for comparison with the GAITRite. For future applications, like at-home use, the use of a single camera could be worth striving for.

Subsequently, it is worth mentioning that all participants were physically able to complete the study, which attests to its feasibility.

4.4.2 Discussion of selected non-gait MDS-UPDRS Results

The analysis of the results with respect to the selected non-gait MDS-UPDRS Part III Examination Items revealed that the correlation between automatically extracted movement features and clinical motor impairment scores was generally weak. Specifically, amplitude-based metrics such as maximum movement amplitude and speed showed low PCCs with MDS-UPDRS scores across all participants and tasks. For example, the overall correlation between amplitude and MDS-UPDRS was only 0.04, and for speed it was -0.05, indicating that these features alone do not reliably reflect clinical severity.

Other non-gait motor tasks were not included in this analysis due to the following factors:

- Limited sample size and data availability for certain tasks.
- Technical constraints in reliably capturing and processing complex or subtle movements with the current camera setup and pose estimation algorithms.
- The initial focus of this study was to establish proof-of-concept validity for the most robust and clinically relevant tasks (finger tapping and hand open-close), which are commonly used and easier to quantify objectively.
- The low framerate 30 FPS of the camera system limited the ability to accurately capture faster or more rapid movements, reducing the reliability of feature extraction for these tasks.

Future work may extend the analysis to additional non-gait tasks as methods and data quality improve.

Subgroup analyses for finger tapping and hand open-close tasks showed slightly higher correlations, but the relationship remained weak, particularly in the healthy control group where variability was limited. These findings suggest that simple kinematic features, as currently implemented, may not capture the complexity of motor dysfunction assessed by clinical rating scales.

It is also important to note that the limited FPS (30) of the camera system may have contributed to these poor results. Lower FPS can lead to motion blur and less precise tracking of rapid movements, which in turn reduces the accuracy of feature extraction for tasks requiring fine temporal resolution. This limitation could have affected the reliability of amplitude and speed measurements, especially in examination items involving fast and repetitive movements.

Interestingly, arrhythmicity–defined as the deviation from equidistant repetition timing–demonstrated a moderate correlation with MDS-UPDRS scores in the finger tapping task (PCC = 0.52). This indicates that rhythm disturbances may be more sensitive to motor impairment than amplitude or speed alone. However, acceleration-based features also showed limited utility, with low to moderate correlations and low coefficients of determination (R^2). The results highlight the challenge of using single movement features for clinical assessment and suggest that future work should focus on refining feature extraction algorithms, incorporating additional temporal and spatial metrics, and exploring multi-modal approaches. Overall, while the TEDIPA system provides objective movement quantification, its current feature set does not strongly align with clinical MDS-UPDRS scores, underscoring the need for further methodological development to improve clinical relevance.

4.5 Conclusion

The results of the presented system for automatic gait feature extraction based on the body pose estimation data provided by the AzureKinect-based system are, on average, largely consistent with the measurements offered by the GAITRite system.

This is a promising finding regarding the possibility of enabling motor status assessments at home or at general practices. AzureKinect DK cameras are easier to set up, much more portable and compact than other widespread gait analysis systems and could complement other approaches (like the Unsupervised Sensor System [Fud+20]) to achieve a holistic assessment with limited spatial resources.

For further studies it would be worthwhile to analyze further gait parameters, like cycle times, single and double support times and possible walking interruptions. Moreover, it would be recommendable to use more cameras to ensure that the density of captured points remains sufficiently high along the complete walkway.

Lastly, it would be worthwhile to extend the magnitude of the study by increasing its sample size and extending the movement analysis to further body parts to cover the entire movement spectrum. Some examples of further features to be analyzed would be the progression of the distance between symmetrical BT-joints, the analysis of changes in angles between BT-joints and also evaluate movement asymmetries. This way, it would be possible, in the long term, to characterize and quantify movement disorders in a markerless way in a home environment.

4.6 CRediT contribution statement

Pedro Fernando Arizpe Gómez: Conceptualization, Data curation, Formal analysis, Funding acquisition, Investigation, Methodology, Project administration, Resources, Software, Supervision, Validation, Visualization, Writing – original draft, Writing – Review and Editing.

Kirsten Harms: Conceptualization, Data curation, Formal analysis, Investigation, Software, Validation, Visualization, Writing – Original Draft, Writing – Review and Editing.

Kathrin Janitzky: Conceptualization, Data curation, Investigation, Methodology, Resources, Validation, Writing – Review and Editing.

Karsten Witt: Conceptualization, Data curation, Formal analysis, Investigation, Methodology, Resources, Validation, Writing – Review and Editing.

Andreas Hein: Conceptualization, Funding acquisition, Methodology, Project administration, Resources, Supervision, Validation, Writing – Review and Editing.

5 Clinical study for Parkinson's Disease symptom and treatment monitoring (TETRIS Study)

This chapter is partly based on the following publication:
Johannes Stalter, Heiko Stecher, Linda Bergmann, Pedro Arizpe-Gomez, Andreas Hein, Andre Aleman, Christoph Herrmann, and Karsten Witt. "Intermittent Theta-burst Transcranial Temporal Interference Stimulation focusing on the Putamen improves Motor Functions in Parkinsons Disease-A randomized, controlled Trial". In: *medRxiv* (2026), pp. 2026–02

This chapter presents published and new findings from the TETRIS study, a human study on neurodegenerative diseases.

5.1 Introduction

Parkinson's Disease is a progressive neurodegenerative disorder characterized by motor features such as bradykinesia, rigidity, resting tremor, and postural instability, alongside frequent non-motor symptoms, like depression and apathy [Pos+15; Ped+09]. While dopaminergic medications and DBS constitute established treatment pillars, the latter requires invasive neurosurgical implantation and thus carries procedure-related risks [Ben+09].

tTIS is a non-invasive brain stimulation approach that applies two high-frequency alternating currents with a small frequency offset (for example, 2.0 kHz and 2.1 kHz) via scalp electrodes. The fields superimpose to generate a lower-frequency interference envelope in deep targets, allowing modulation of subcortical oscillations while minimizing stimulation of overlying cortex [Gro+17].

The TETRIS trial (DRKS00030841 [DRK25]) is a randomized, double-blind, sham-controlled, cross-over physiological study investigating the effects of tTIS on motor and motivational processes in participants with PD and healthy controls. The study is registered prospectively in the DRKS and received a positive ethics opinion from the Medizinische Ethikkommission der Carl von Ossietzky Universität Oldenburg (reference number [2022-164]).

Finger tapping and hand movements are core components of the MDS-UPDRS motor examination, which is the gold standard for clinical assessment of PD motor symptoms. Specifically, section 3.4 (*Finger Tapping*) instructs the examiner to rate each hand separately as the patient taps the index finger on the thumb 10 times as quickly and as big as possible, evaluating speed, amplitude, hesitations, halts, and decrementing amplitude. Section 3.5 (*Hand Movements*) similarly assesses each hand as the patient makes a tight fist and then opens the hand 10 times as fully and as quickly as possible, with ratings based on speed, amplitude, interruptions, and rhythm. These tasks provide standardized, quantitative measures of bradykinesia and are widely used in both clinical and research settings to monitor disease progression and treatment effects.

5.2 Materials and Methods

This section details the methodology employed in the TETRIS study, including study design, participant recruitment, intervention protocols, outcome measures, data acquisition, and statistical analysis. The following subsections provide a comprehensive overview of the experimental procedures, data processing pipeline, and analytical approaches used to assess the effects of tTIS on motor function in participants with PD and healthy controls.

5.2.1 Study design

This monocentric, interventional, physiological study employs a randomized, double-blind, sham-controlled cross-over design in two arms:

- **Arm 1:** Participants with Parkinson's Disease; Target Sample Size: n=20, Final Sample Size: n=19.
- **Arm 2:** Healthy Participants; Target Sample Size: n=20, Final Sample Size: n=19.

Recruitment and study procedures were completed at a single academic center in Germany. The total number of included participants was 36. Prospective registration: DRKS00030841 [DRK25].

5.2.2 Participants

Eligibility comprised general criteria applicable to both arms and arm-specific disease criteria for the PwPD arm. Key inclusion and exclusion criteria are summarized in Table 5.1.

Table 5.1: Key inclusion and exclusion criteria

Inclusion	Exclusion
Age 45–75 years	Neurological or psychiatric disorders (except PD in Arm 1)
German as native language	Centrally acting medication (except PD medication)
Right-handedness	Non-removable metallic objects in/on the body
Normal or corrected-to-normal vision	Implanted neurostimulators
Idiopathic PD per MDS criteria (Arm 1) [Pos+15]	MRI contraindications
	Epilepsy in personal or close family history

5.2.3 Recruitment and timeline

Planned enrollment was 40 participants (20 PwPD's, 20 HP). Actual enrollment was 36 participants at a single German site. The actual study period spanned from 22 August 2023 (first inclusion) to 30 March 2024 (study completion) [DRK25].

5.2.4 Intervention: tTIS

tTIS was delivered using four scalp electrodes to target deep structures in the basal ganglia. Importantly, stimulation was applied over the right hemisphere, with the goal of modulating the right Putamen for motor tasks and the right Nucleus Accumbens for motivational tasks. This lateralized stimulation protocol was chosen to preferentially influence the contralateral (left) side of the body, in accordance with the known organization of motor pathways. As a result, particular attention was paid to the left hand and arm in both the experimental procedures and subsequent analyses, including the statistical comparisons reported in the results tables.

Stimulation parameters were not personalized in real-time; instead, a standardized electrode montage was employed for all participants. Subject-specific electric field simulations were performed retrospectively based on individual MRI data to assess the accuracy of subcortical targeting. This approach may have limited the precision of electric field localization in the right Putamen for motor tasks and in the right Nucleus Accumbens for motivational tasks. Two high-frequency sinusoids differing slightly in frequency were applied to generate a lower-frequency interference envelope at the target [Gro+17; DRK25]. During tasks, movements were recorded using a RGB-D camera setup for quantitative analysis [DRK25].

5.2.5 Outcome measures

All primary outcomes are evaluated under both real and sham tTIS within subjects in the cross-over design [DRK25].

Primary outcomes

- Motor performance assessed by finger tapping and hand open-close tasks.
- Motor learning assessed by a sequential finger tapping and hand open-close tasks.
- Motivational behavior assessed by an effort/reward task.
- Probabilistic learning assessed by an effort/reward task.

Secondary outcome

- Explorative evaluation of side effects.

Note: This thesis presents only the results of the movement analysis (motor performance and motor learning). The analyses of motivational behavior and probabilistic learning are currently in the process of being published elsewhere. The registered study foresaw only finger tapping, but the current analysis includes hand open-close tasks as well.

5.2.6 Procedures and data acquisition

Participants complete both stimulation conditions (real and sham) in counterbalanced order under double-blind conditions. For motor outcomes, tTIS targeting the Putamen is administered while participants perform finger tapping tasks with concurrent RGB-D video kinematic capture. For motivational and probabilistic learning outcomes, tTIS targeting the Nucleus Accumbens is administered during effort/reward tasks. Comprehensive adverse event monitoring is conducted across sessions [DRK25].

5.2.7 Kinematic data processing with MediaPipe

Raw video recordings of motor tasks were processed using the MediaPipe framework for markerless pose estimation and hand tracking [Lug+19]. The GPU-accelerated Holistic graph, which integrates body, face, and hand landmark detection, was compiled from source using Bazel to ensure compatibility and optimal performance on the designated workstation (Ubuntu 20.04.6 LTS, NVIDIA GeForce RTX 3080 Ti GPU, 24-core 12th Gen Intel Core i9-12900KF CPU).

The Holistic pipeline provided frame-wise 3D coordinates for 33 body landmarks and 21 landmarks per hand, enabling precise quantification of hand and finger movements. For each video, relevant hand landmarks (such as wrist, MCP, PIP, DIP, and fingertip positions) were extracted, and task-specific amplitude signals were computed, including the Euclidean distance between selected joints or the spread of finger tips. These amplitude signals served as the basis for subsequent time-series analyses.

GPU acceleration facilitated real-time processing of high-resolution video data, with landmark detection rates exceeding 30 frames per second. The use of the Holistic graph ensured robust tracking even under challenging conditions, such as occlusions or rapid movements. All extracted landmark data were exported to CSV files for further preprocessing and feature extraction as described in subsection 5.2.8.

Time-series amplitude signals were extracted from trial-wise CSV files. Each CSV contained a discrete frame index (column header `Frame`) and an amplitude value (column header `Value`). Prior to feature extraction, each amplitude series underwent the following preprocessing steps:

5.2.8 Calculation of variables

Time-series signals were extracted from trial-wise CSV files, each containing a discrete frame index (`Frame`) and a value (`Value`). Three kinematic variables were analyzed: amplitude, speed and acceleration trends. All variables were subjected to identical preprocessing:

1. **Trimming.** Trials shorter than 50 samples were discarded. Trials exceeding 15 s were truncated to 15 s to ensure comparability across participants.
2. **Normalization.** Each series was min–max normalized to $[0, 1]$.
3. **Time scaling.** Frame indices were converted to *milliseconds*:

$$t_{\text{ms}} = \frac{f}{235.31} \times 1000,$$

   where f denotes the frame index and 235.31 FPS the nominal sampling frequency. For regression, timestamps were expressed in seconds: $t = t_{\text{ms}}/1000$.
4. **Low-pass filtering.** A 5th-order Butterworth filter with a 10 Hz[a] cutoff was applied using zero-phase forward–backward filtering [But30].

[a] Hertz

5.2.9 Peak detection

Peaks were detected on the filtered series using adaptive thresholds. The minimum IPI was 25 samples. Thresholds for height and prominence were set as fractions of the signal range.

5.2.10 Amplitude, speed, and acceleration trends

For each variable, a linear regression was computed on the peak values y_i against time t_i:

$$y_i = \beta_0 + \beta_1 t_i + \epsilon_i, \quad i = 1, \ldots, n,$$

where β_0 is the intercept, β_1 the slope for the respective variable, and ϵ_i the residuals. The slope β_1 quantifies the rate of change of the peaks over time for the respective variable (β_1 is also called the **trend**). The units are percentage points per second.

The coefficient of determination (R^2) was calculated as

$$R^2 = \left(\frac{\sum_i (t_i - \bar{t})(y_i - \bar{y})}{\sqrt{\sum_i (t_i - \bar{t})^2 \sum_i (y_i - \bar{y})^2}} \right)^2,$$

where $\bar{t}$ and $\bar{y}$ denote means of t_i and y_i, respectively. This statistic represents the proportion of variance in the peak values explained by the linear model.

5.2.11 Arrhythmicity

Arrhythmicity was quantified from the IPI. Given peak timestamps $t_1, \ldots, t_m$, the IPIs are

$$\Delta t_j = t_{j+1} - t_j, \quad j = 1, \ldots, m - 1.$$

The mean IPI is

$$\overline{\Delta t} = \frac{1}{m-1} \sum_{j=1}^{m-1} \Delta t_j.$$

Arrhythmicity is defined as the mean absolute deviation of IPIs from their mean:

$$Arr = \frac{1}{m-1} \sum_{j=1}^{m-1} \left| \Delta t_j - \overline{\Delta t} \right|,$$

Lower A indicates a more regular rhythm. The units are seconds.

5.2.12 Statistical analysis

Conditions (Baseline and During) and stimulation groups (Sham and Stim) were defined per protocol. Change scores were computed as

$$\Delta = \text{Baseline} - \text{During},$$

for each side and variable (amplitude, speed, acceleration). Distributions were tested for normality using the S-W test [SW65]. Depending on results, independent-sample t-tests or Wilcoxon signed-rank tests [Wil45] were used for group comparisons.

5.2.13 Registration, ethics, and oversight

The study was prospectively registered in the DRKS as DRKS00030841. The leading ethics committee (Carl von Ossietzky University Oldenburg; reference 2022-164) provided a favorable opinion dated 28 February 2023. No individual participant data sharing is planned [DRK25].

Note: Only PwPD's were filmed during motor tasks. Healthy controls (HP) did not undergo video recording for movement analysis.

5.3 Results

This section presents the main results of the TETRIS study, focusing on the quantitative analysis of motor performance in participants with PD under real and sham tTIS. The analyses are based on kinematic variables extracted from markerless video recordings, including amplitude, speed, and acceleration trends, as well as arrhythmicity, during finger tapping and hand open-close tasks. Statistical comparisons between stimulation conditions are provided for each variable and task, with emphasis on identifying acute effects of tTIS on motor function.

Note that, because stimulation was applied over the right hemisphere to target the right Putamen and right Nucleus Accumbens (see subsection 5.2.4 Intervention: tTIS), the analysis prioritized left-sided motor outcomes: primary hypotheses and planned comparisons focused on left-hand measures. Results for the right side are reported as well for completeness, but interpretation gives precedence to left-sided effects consistent with the lateralized stimulation protocol.

The results are organized by kinematic outcome, beginning with amplitude trend (β_1), followed by speed and acceleration trends, and concluding with arrhythmicity. For each outcome, tables summarize the results of statistical tests, and figures illustrate the distributions of key variables across conditions. Where relevant, the coefficient of determination (R^2) for linear regression models is reported to assess the consistency of observed trends. The findings are interpreted in the context of task specificity, lateralization, and the potential for individualized neuromodulation protocols.

5.3.1 Amplitude Trend β_1

Table 5.2 presents the results of statistical comparisons between real and sham tTIS conditions for the amplitude trend β_1 of four motor tasks. For both right and left finger tapping, the t-test results show no significant differences ($p = 0.1123$ and $p = 0.7379$), indicating that acute tTIS did not affect finger tapping amplitude trend β_1 in this sample. This suggests that finger tapping, a standard measure of motor speed and bradykinesia, may be relatively insensitive to single-session non-invasive stimulation.

Table 5.2: Statistical test results for amplitude trend β_1 differences between conditions in motor tasks under real and sham tTIS stimulation.

Exercise/Side	**Statistical Test**	**Result**
Right Finger Tapping	**t-test**	$t = -0.340$, $p = 0.7379$
Left Finger Tapping	**t-test**	$t = 1.613$, $p = 0.1123$
Right Hand Open Close	**t-test**	$t = 0.700$, $p = 0.4899$
Left Hand Open Close	**t-test**	$t = 2.440$, $p = 0.0244$

In contrast, the left hand open-close task yielded a significant difference ($t = 2.440$, $p = 0.0244$, see Table 5.2), with real tTIS producing improved amplitude trend β_1 compared to sham. The right hand open-close task did not show a significant effect ($p = 0.4899$), pointing to possible lateralization or task-specific responsiveness. The selective improvement in left hand opening may reflect more effective stimulation targeting or greater sensitivity of this movement to neuromodulation.

Overall, the table highlights that while finger tapping amplitude trend β_1 remained unchanged, left hand opening showed a measurable response to tTIS. These findings emphasize the importance of task-specific analysis and support further investigation into individualized stimulation protocols and mechanisms of differential responsiveness in movement disorders.

Figure 5.1 illustrates the left finger tapping amplitude trend β_1 for participants under real and sham tTIS stimulation. The distributions for both conditions overlap substantially, and there is no clear separation in mean tapping rates. This visual result aligns with the statistical findings (t = -0.340, p = 0.7379), indicating that tTIS did not produce a significant acute effect on motor speed or amplitude in this cohort.

Figure 5.2 shows the right finger tapping amplitude trend β_1 for both stimulation conditions. Similar to the left finger tapping, the distributions for real and sham tTIS overlap substantially, and no significant difference in mean amplitude trends β_1 is observed. This suggests that acute tTIS does not modulate motor amplitude for finger tapping on either side in this cohort. The consistency across both hands (see also Table 5.2) further supports the robustness of the null finding and highlights the need to explore additional movement indicators.

Figure 5.3 presents the results of the left hand opening task for participants under both real and sham tTIS stimulation. Unlike the finger tapping task, the statistical analysis for hand opening revealed a significant difference between conditions (t = 2.279, p = 0.0490), suggesting that tTIS may exert an acute modulatory effect on this aspect of motor function.

The observed effect is notable given the rigorous double-blind, cross-over design, which minimizes bias and allows for robust within-subject comparisons. The individualized targeting of stimulation based on MRI modeling may have contributed to the specificity of the effect, as the Putamen is critically involved in the control of voluntary movement amplitude. However, the magnitude of the difference is relatively small, and further studies are needed to confirm the reproducibility and clinical relevance of this finding.

It is also important to consider the potential mechanisms underlying the selective effect on hand opening versus finger tapping. Differences in task complexity, neural circuitry, or sensitivity to stimulation parameters may account for the divergent outcomes. Additionally, the use of quantitative kinematic analysis via through video capture provides objective evidence for the observed changes, reducing reliance on subjective ratings.

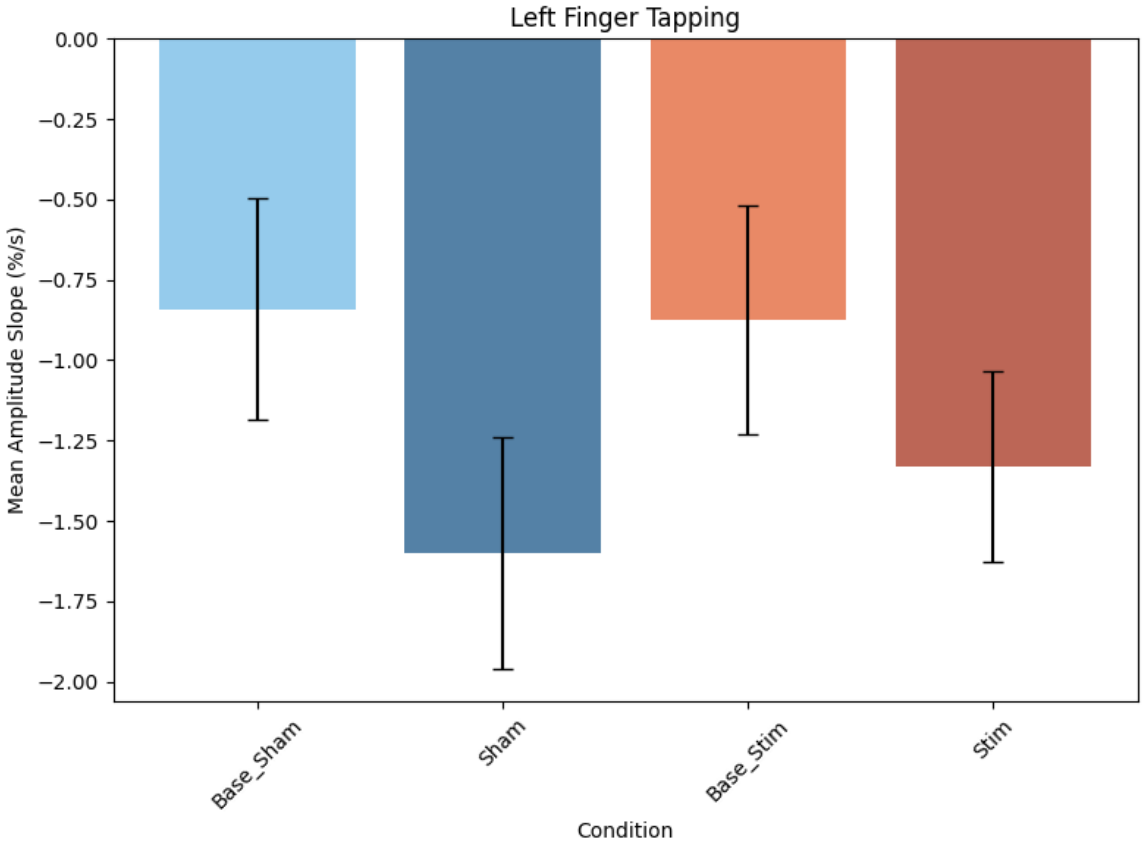

Figure 5.1: Left Finger tapping amplitude trend β_1 under real and sham tTIS conditions.

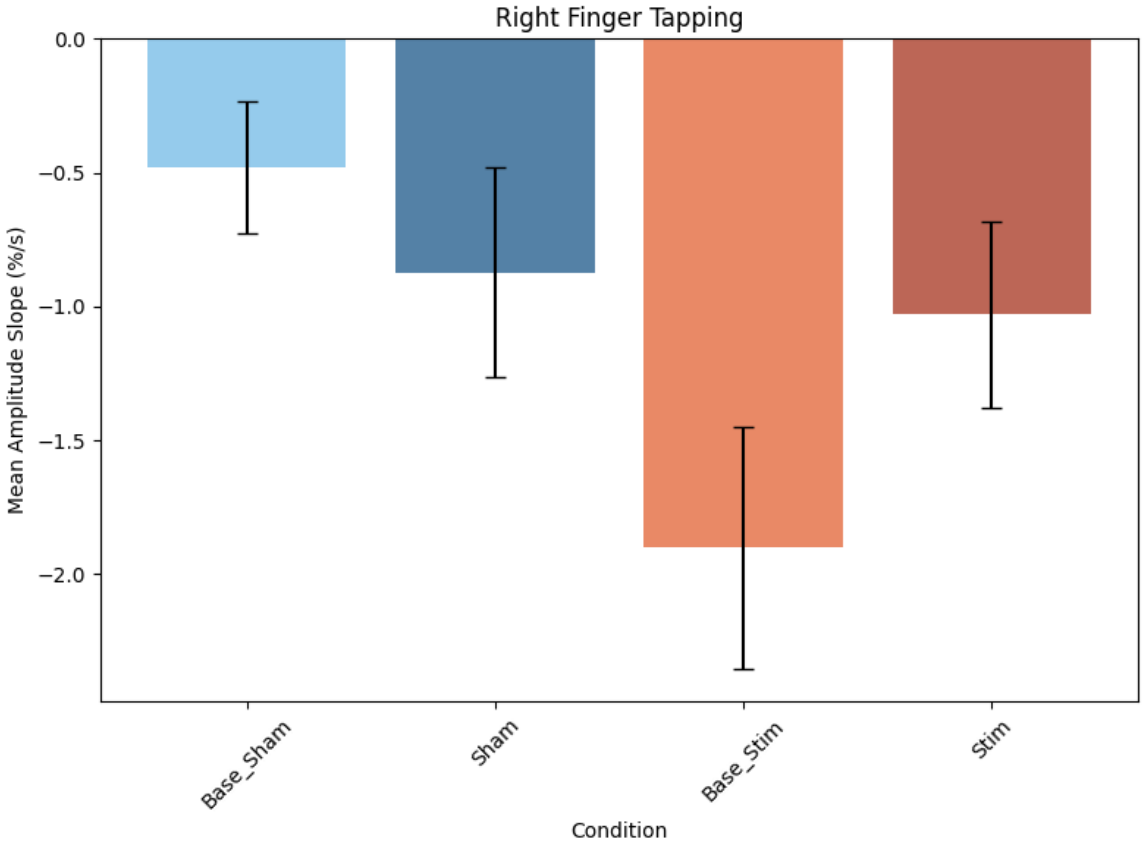

Figure 5.2: Right Finger tapping amplitude trend β_1 under real and sham tTIS conditions.

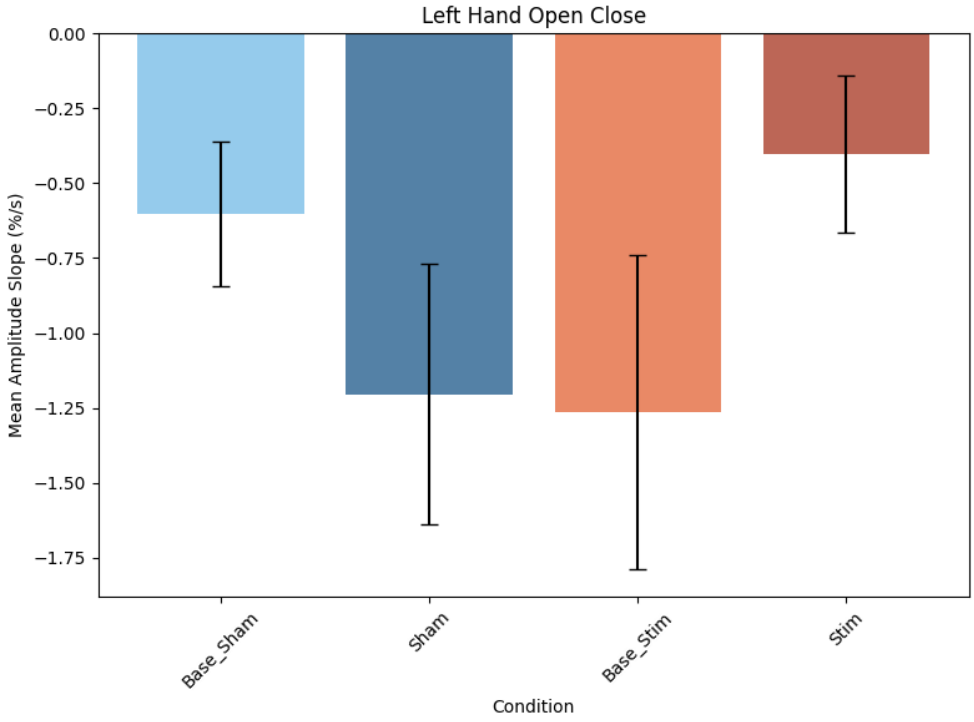

Figure 5.3: Left hand opening amplitude trend β_1 under real and sham tTIS conditions.

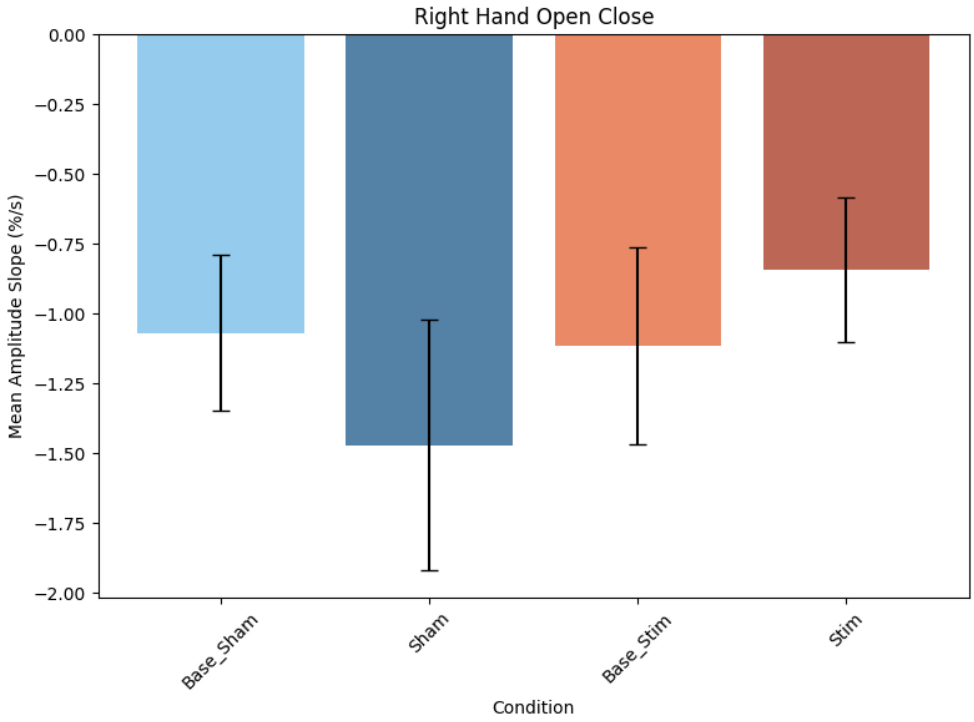

Figure 5.4: Right hand opening amplitude trend β_1 under real and sham tTIS conditions.

Figure 5.4 displays the right hand opening amplitude trend β_1 for both stimulation conditions. The data reveal a similar pattern to the left side, with a tendency toward higher scores under real tTIS compared to sham. While the difference is less pronounced than for the left hand, the visual separation suggests a possible acute effect of tTIS on right hand opening amplitude. This finding supports the notion of task-specific and potentially lateralized responsiveness to neuromodulation, though further statistical analysis is needed to confirm significance.

Table 5.3: Coefficient of determination (R^2) for linear regression of peak amplitudes in motor tasks under real and sham tTIS conditions.

Exercise/Side	Mean Base Sham	Mean Sham	Mean Base Stim	Mean Stim
Right Finger Tapping	0.1749	0.2393	0.3139	0.1569
Left Finger Tapping	0.1950	0.3214	0.2007	0.2027
Right Hand Open Close	0.3271	0.3236	0.4040	0.3859
Left Hand Open Close	0.2262	0.3475	0.4008	0.2082

Table 5.3 reports the R^2 values for linear regression of peak amplitudes across motor tasks and stimulation conditions. These coefficients reflect how well the linear model explains the variance in peak amplitudes over time. Overall, R^2 values are modest, indicating considerable variability in movement amplitude trend β_1 and limited linearity of peak amplitude changes within trials. Notably, higher R^2 values are observed for hand open-close tasks compared to finger tapping, suggesting more consistent amplitude trends β_1 in these movements. The lack of substantial differences between sham and real stimulation conditions aligns with the main findings, supporting the conclusion that acute tTIS does not robustly alter the temporal dynamics of motor performance in this cohort.

5.3.2 Speed trend

Table 5.4: Statistical test results for speed trend β_1 differences between conditions in motor tasks under real and sham tTIS stimulation.

Exercise/Side	Statistical Test	Result
Right Finger Tapping	**t-test**	$t = 0.083, p = 0.9346$
Left Finger Tapping	**t-test**	$t = 0.177, p = 0.8619$
Right Hand Open Close	**t-test**	$t = 0.328, p = 0.7465$
Left Hand Open Close	**t-test**	$t = 1.835, p = 0.0839$

Table 5.4 summarizes the statistical comparisons of speed trend β_1 between real and sham tTIS conditions across four motor tasks. All p-values are above the conventional significance threshold of 0.05, indicating no statistically significant differences in speed trend β_1 for any exercise or side. The left hand open-close task approaches significance ($p = 0.0839$), suggesting a possible tendency toward improved speed trend β_1 under real stimulation, but this does not reach statistical significance. Overall, these results indicate that tTIS did not produce measurable changes in movement speed trend β_1 in this cohort, reinforcing the need for further investigation into stimulation parameters and task-specific responsiveness.

5.3.3 Acceleration trend β_1

Table 5.5 summarizes the statistical comparisons for acceleration trend β_1 between real and sham tTIS conditions across all motor tasks. None of the tests reached statistical significance, with all p-values well above 0.05. This result is consistent with the findings for amplitude and speed trends, indicating that acute tTIS did not produce measurable changes in movement acceleration in this cohort. The use of both parametric and non-

Table 5.5: Statistical test results for acceleration trend β_1 differences between conditions in motor tasks under real and sham tTIS stimulation.

Exercise/Side	Statistical Test	Result
Right Finger Tapping	**Wilcoxon signed-rank test**	$W = 3.000, p = 0.3125$
Left Finger Tapping	**t-test**	$t = -0.517, p = 0.6126$
Right Hand Open Close	**Wilcoxon signed-rank test**	$W = 5.000, p = 0.6250$
Left Hand Open Close	**Wilcoxon signed-rank test**	$W = 5.000, p = 0.6250$

parametric tests reflects adaptation to data distribution, but the overall lack of significant effects suggests that single-session stimulation may not be sufficient to modulate acceleration-related motor features. These findings further support the conclusion that, under the tested protocol, tTIS does not acutely alter core kinematic parameters in PD motor tasks.

5.3.4 Arrhythmicity

Table 5.6: Statistical test results for arrhythmicity differences between conditions in motor tasks under real and sham tTIS stimulation.

Exercise/Side	Statistical Test	Result
Right Finger Tapping	**t-test**	$t = -0.538, p = 0.5978$
Left Finger Tapping	**t-test**	$t = 1.294, p = 0.2102$
Right Hand Open Close	**t-test**	$t = -1.294, p = 0.2115$
Left Hand Open Close	**t-test**	$t = 0.297, p = 0.7697$

Table 5.6 summarizes the results of t-tests [Dav63] comparing arrhythmicity between real and sham tTIS conditions across four motor tasks involving different hands and movements. For each exercise and side, the reported t-values are relatively small and the p-values are all well above the conventional significance threshold of 0.05, indicating no statistically significant differences in arrhythmicity between the real and sham stimulation groups for any of the tested conditions. This suggests that tTIS did not have a measurable effect on arrhythmicity in these motor tasks under the experimental conditions.

5.4 Discussion

This discussion centers on the objective quantification of movement changes during typical clinical motor assessments, as enabled by automated, markerless kinematic analysis. The study demonstrates that movement parameters–such as amplitude, speed, acceleration, and arrhythmicity–can be systematically measured and compared across experimental conditions using a reproducible, data-driven pipeline. These results validate the use of quantitative movement analysis as a robust tool for monitoring motor function in PD and for evaluating the impact of experimental interventions.

The ability to extract fine-grained, task-specific kinematic features from standard clinical tasks provides a foundation for evidence-based assessment and longitudinal tracking of motor symptoms. The multidimensional approach, integrating amplitude trends, speed, and rhythm, enables sensitive detection of subtle changes. This framework supports the development of scalable, automated tools for clinical research and practice.

The differences observed between finger tapping and hand opening tasks may reflect not only the specific neural circuits engaged by each movement, but also the sensitivity of the measurement methods. It remains possible that the absence of significant findings in some tasks is attributable to limited measurement sensitivity rather than a true lack of physiological effect. Additionally, the stimulation montage was not personalized in

real-time; electric field simulations were performed retrospectively. This lack of individualized electrode placement may have limited the efficacy of subcortical targeting in some participants. Future studies should consider real-time, personalized montage optimization to enhance the specificity and effectiveness of stimulation.

While the study included tTIS as an experimental variable, the primary contribution lies in establishing movement analysis as a reliable and scalable method for quantifying motor changes. Methodological strengths include the randomized, double-blind, sham-controlled cross-over design and the use of markerless pose estimation for objective, reproducible measurement. Limitations include the modest sample size, short intervention duration, and the focus on acute rather than cumulative effects. Future work should prioritize larger cohorts, extended follow-up, and the integration of automated task segmentation to further enhance the efficiency and clinical utility of movement analysis.

In summary, the results highlight the feasibility of quantifying movement changes and neuromodulatory effects in a controlled experimental setting. The findings motivate further research into personalized stimulation protocols, enhanced measurement sensitivity, and the integration of prospective electric field modeling to optimize intervention strategies in clinical settings.

5.5 Conclusion

This study explored the feasibility of quantitative, markerless movement analysis and how it enables the objective quantification of motor changes during typical clinical assessments in PD. The results show that task- and condition-specific differences in movement parameters can be systematically measured, supporting robust and reproducible evaluation of motor function. The integration of amplitude, speed, acceleration, and arrhythmicity metrics provides a comprehensive framework for monitoring disease progression and assessing intervention effects.

While tTIS was included as an experimental variable, its effects were limited and should be interpreted as preliminary. The main contribution of this work is the establishment of a scalable, data-driven approach for movement analysis in clinical research. Future studies should build on this foundation to refine automated assessment tools and to explore their application in larger, longitudinal cohorts.

In summary, this work lays the foundation for future studies aiming to refine non-invasive stimulation strategies and to develop data-driven, quantitative tools for motor assessment in neurodegenerative disorders. The defined kinematic biomarkers may also serve as input features for machine learning models, facilitating advanced classification and prediction tasks in clinical neurotechnology.

5.6 CRediT contribution statement

Pedro Fernando Arizpe Gómez: Conceptualization, Data curation, Formal analysis, Investigation, Methodology, Resources, Software, Validation, Visualization, Writing – Original Draft, Writing – Review and Editing.

Johannes Stalter: Conceptualization, Data curation, Formal analysis, Investigation, Methodology, Resources, Software, Validation, Visualization, Writing – Original Draft, Writing – Review and Editing.

Linda Bergmann, née Büker: Conceptualization, Data curation, Formal analysis, Investigation, Methodology, Resources, Software, Validation, Visualization, Writing – Original Draft, Writing – Review and Editing.

Karsten Witt: Conceptualization, Formal analysis, Funding acquisition, Investigation, Methodology, Project administration, Resources, Supervision, Validation, Writing – Review and Editing.

Andreas Hein: Funding acquisition, Resources, Supervision, Writing – Review and Editing.

6 Planned Retrospective Study on Video-Based Analysis of PD-Related Movements (RESBEPA Study)

6.1 Introduction

This chapter outlines the planned design for the RESBEPA study, which will investigate the feasibility of video-based, markerless motion capture systems for the quantitative analysis of motor function in individuals diagnosed with PD. The primary objective will be to determine whether kinematic parameters derived from standardized MDS-UPDRS assessments can act as objective, reproducible markers of motor impairment severity.

6.1.1 Contributions

The study is expected to advance the development of automated, objective movement assessment tools for PD. The integration of video-based kinematic analysis into clinical workflows may improve diagnostic accuracy, facilitate disease monitoring, and inform personalized therapeutic planning.

6.2 Scientific Background and Objectives

The clinical evaluation of motor symptoms in PD is traditionally based on the visual assessment of the MDS-UPDRS. However, such methods are subject to inter-rater variability and inherent subjectivity. Recent developments in AI-driven BT technologies employing RGB video and computer vision algorithms have demonstrated the capacity to extract detailed movement features such as amplitude, velocity, and acceleration [Xia+24; Ste+24]. These capabilities offer promising avenues toward standardized, objective movement assessments.

The planned study will evaluate whether these quantitative features correlate with clinical ratings and can serve as digital biomarkers. Specifically, the objectives are to:

- Extract amplitude, velocity, and acceleration values from standardized MDS-UPDRS tasks.
- Detect arrhythmic movement patterns and freezing episodes.
- analyze statistical correlations between movement characteristics and clinical scores.
- Establish threshold values indicative of distinct motor impairment levels.

6.3 Design and Methodology

This retrospective study is planned to analyze video recordings acquired at University Clinic Kiel from 2000 to 2025. The dataset will include participants with confirmed PD diagnoses performing standardized motor tasks. Videos will be processed using the MediaPipe framework to extract skeletal joint trajectories. Upon extraction of kinematic data, all raw video files will be deleted. Only anonymized skeletal data will be retained for analysis, in accordance with data protection regulations.

Planned analysis methods include:

- Descriptive statistics (mean and SD) across task repetitions.
- Linear and multiple regression models to assess intra-task motor performance trends.
- Pearson or Spearman correlation analyses to evaluate links between kinematic metrics and MDS-UPDRS scores.
- Cross-validation techniques to verify the generalizability of predictive models.

6.4 Outcomes and Analytical Measures

This section details the planned primary and secondary outcome measures that will be used to evaluate the effectiveness of video-based, markerless motion capture in assessing motor function in individuals with PD. It outlines the specific analytical metrics and statistical approaches that are intended to quantify movement characteristics and their relationship to clinical assessments.

Primary Outcome will be the intra-task variation in movement parameters: amplitude, velocity, and acceleration—as indicators of motor control and fatigue.

Secondary Outcomes will include:

- Assessment of arrhythmicity through irregular movement timing.
- Identification of freezing episodes (motion pause $\geq$ 1 second).
- Correlation of movement degradation with MDS-UPDRS motor sub-scores.
- Determination of threshold values for kinematic features that indicate varying levels of motor impairment.

6.4.1 Ethical and Legal Considerations

This retrospective feasibility study is planned to be exempt from clinical trial registration under the Declaration of Helsinki. Anonymized data will be securely stored on university servers for a minimum of ten years, with restricted access granted to authorized personnel only. All procedures will comply with the GDPR and institutional ethical regulations. The study has received a waiver from the Medizinische Ethikkommission der Carl von Ossietzky Universität Oldenburg (reference number [2025-090]).

6.5 CRediT contribution statement

Pedro Fernando Arizpe Gómez: Conceptualization, Data curation, Investigation, Methodology, Resources, Software.

Johannes Stalter: Conceptualization, Data curation, Methodology, Resources, Software.

Linda Bergmann, née Büker: Conceptualization, Data curation, Investigation, Methodology, Resources, Software.

Karsten Witt: Conceptualization, Funding acquisition, Investigation, Methodology, Project administration, Resources, Supervision.

Andreas Hein: Funding acquisition, Project administration, Resources, Supervision, Writing – Review and Editing.

Part III

Human Studies Related to Musculoskeletal Disorders

7 Validation of Video-Based Movement Assessment (Smart-BT Validation Study)

7.1 Introduction

The Smart-BT Validation Study investigated the reliability and validity of markerless video-based MoCap systems for use in MSD prevention settings targeting musculoskeletal disorders. The central aim was to assess the suitability of RGB-D-BT technologies–particularly the AzureKinect sensor–for capturing key kinematic features relevant to physiotherapeutic assessment and physiotherapeutic intervention. As part of the Smart-BT project, this validation study formed the basis for integrating computer vision into movement analysis for MSD prevention and physiotherapy optimization workflows.

7.2 Scientific Background and Objectives

Accurate and scalable motion analysis remained a fundamental requirement in physiotherapy and MSD prevention. Traditional systems using wearable IMU suits or optical marker-based setups were expensive, required specialist operation, and introduced patient burden. Recent innovations in AI-enhanced, camera-based BT systems provided an attractive alternative. These systems could extract skeletal joint coordinates from RGB video data, allowing for full-body motion analysis without physical markers or sensors [Don+21; Meh+17].

The Smart-BT Validation Study sought to validate whether such markerless systems could provide reliable measurements for physiotherapeutic use cases such as range of motion, posture, symmetry, and gait characteristics.

The primary objectives were:

1. To determine the accuracy of joint angle estimation using the AzureKinect system.
2. To compare the RGB-D-based BT data against a validated IMU-based sensor suit (CAPTIV) as reference.
3. To compare RGB-D-based BT data against a validated optical MoCap system as reference.

7.3 Design and Methodology

This cross-sectional validation study was conducted at the VR Lab of the Jade Hochschule in Oldenburg. The participant group consisted of 11 healthy adults, however only 10 datasets could be processed due to a software error.

7.3.1 Participants

A total of 11 participants (6 female, 5 male) were recruited for the study. The mean age was 27.3 years (range: 19-34), mean height was 175.7 cm (range: 164-190 cm), and mean weight was 75.1 kg (range: 59-110 kg). Arm length ranged from 52 cm to 63 cm, leg length from 72 cm to 84 cm, and upper body length from 55 cm to 71 cm. All participants reported no physical limitations. Three participants reported current or recent back pain (up to 2 months prior), while the remainder had no back pain. Weekly sports activity ranged from 1 to 8 hours with an average of 2.8 (see Table 7.1)

Table 7.1: Participant demographics and physical characteristics.

*: indicates that one dataset was not recorded due to a software error.

ID	Height	Weight	Age	Sex	Arm	Leg	Torso	Back pain	Sport (h/wk)
MKVMX*	183	110	32	m	60	81	58	no	2
JADEZ	172	68	26	f	59	77	60	no	1
SIHRR	164	74	29	f	54	74	55	no	1.5
IOKCB	178	90	34	f	55	79	60	no	1
NZHKH	170	59	26	f	53.5	75	59	mild pain	2
MFVWE	170	59	19	f	55	80	56.5	no	2
ZZGKG	190	88	30	m	60	83	70	2M prior	6
IGTPL	170	67	26	f	57	79	61	no	1
JPTUL	177	63	32	m	56	79	62	today	2.5
ALDXB	173	68	24	m	52	72	66	no	4.5
FFOUQ	186	80	22	m	63	84	71	no	8

7.3.2 Movement Tasks

The movement tasks were selected to encompass a broad spectrum of motor activities, ensuring that the evaluation of the tested systems was both comprehensive and representative. Fitness exercises from the Herodikos exercise therapy app [Sch24] were included alongside standardized motor assessments from the MDS-UPDRS protocol [Goe+08b] to capture diverse movement patterns, intensities, and functional domains. This approach enabled assessment of system performance across both MSD prevention scenarios and clinically relevant motor symptoms, providing a robust foundation for validation.

Covering a broad spectrum of movements was essential for establishing the reliability and generalizability of the systems under test. Tasks from the Herodikos exercise therapy app [Sch24] reflected typical exercise routines, while the MDS-UPDRS items targeted specific motor functions often affected in neurological conditions. By integrating both types of tasks, the systems were challenged with varied movement profiles, reducing bias and increasing confidence in their applicability to in MSD prevention and clinical settings. This comprehensive task selection strengthened the validity of the findings and supported meaningful comparisons across different use cases.

The tasks in Table 7.2 were included in the Smart-BT Validation Study to evaluate the performance of markerless BT systems across a diverse range of movement patterns. The inclusion of both fitness exercises from the Herodikos exercise therapy app [Sch24] and standardized motor assessments from the MDS-UPDRS protocol ensured a comprehensive assessment of system capabilities in capturing various motor functions relevant to clinical and MSD prevention contexts.

Prior to the main assessment, a calibration procedure was performed in which participants executed a jump and clap sequence to initialize system calibration. All tasks were performed as described in the standardized protocol. Some tasks, such as calibration and marker removal, were not included in the quantitative analysis but were essential for ensuring data quality and proper system setup.

Table 7.2: Movement tasks performed in the Smart-BT Validation Study and their descriptions.

Items marked with * are from the MDS-UPDRS protocol.

Task	**Description**
Knee axis alignment	Stand upright with feet shoulder-width apart to assess knee axis and alignment.
Shoulder posture	Stand with shoulders straight and relaxed to evaluate postural alignment.
Single-leg stance (right/left)	Stand on one leg (right or left) to assess balance and stability.
Hamstring flexibility (back and knee)	Perform a forward bend or knee extension to evaluate hamstring flexibility.
Hip flexor test (right/left)	Stretch the hip flexors on each side to assess flexibility and range of motion.
Quadriceps stretch test (right/left)	Stretch the quadriceps muscle on each side to evaluate flexibility.
Finger tapping*	Repeatedly touch the thumb with the index finger as fast as possible to assess fine motor speed.
Hand movements*	Repeatedly open and close the fist as fast as possible to evaluate hand agility.
Pronation-supination of hands*	Rapidly rotate palms up and down to assess forearm rotation and coordination.
Toe tapping*	Tap the forefoot on the ground rapidly to measure lower limb agility.
Leg agility*	Stomp the foot on the ground rapidly to assess leg movement speed and coordination.
Gait assessment*	Walk across the room, turn, and walk back to evaluate gait and mobility.
Side walking	Walk sideways to assess lateral gait and coordination.
Postural tremor of hands*	Extend arms forward and hold the position to observe postural tremor.
Kinetic tremor of hands*	Repeatedly touch the nose with the finger to assess kinetic tremor.
Resting tremor amplitude*	Stretch arms out in front of body and hold the position to measure resting tremor amplitude.

7.3.3 Sensor Systems and Measurement Principles

Several sensor systems were used in this study to comprehensively capture movement features of occupational tasks in real-world environments.

CAPTIV Motion Capture System

The CAPTIV system is a wearable MoCap solution based on 13 IMU sensors, each affixed to major anatomical landmarks such as the limbs, pelvis, and trunk. These sensors record 3D acceleration, angular velocity, and orientation, enabling the reconstruction of joint angles and segment positions in space. The primary purpose of the CAPTIV suit was to provide reference kinematic data for validation of markerless systems, with particular emphasis on joint angle estimation. The system is designed for portability and real-time feedback, making it theoretically suitable for clinical and laboratory environments where rapid deployment and immediate data visualization are required. Figure 7.1 shows the placement of the 13 CAPTIV IMU sensors on major joints of a participant.

Figure 7.1: Placement of the 13 CAPTIV IMU sensors on major joints of a participant.

Qualisys Optical Motion Capture

The Qualisys system is an optical MoCap platform utilizing multiple infrared cameras to track reflective markers placed on the participant's skin or clothing (or in this case, specialized suits with attached markers). By triangulating the positions of these markers, the system reconstructs 3D trajectories and computes joint angles and segment orientations. Qualisys is widely regarded as a gold standard for biomechanical analysis due to its high spatial accuracy and flexibility in marker placement. In this study, it served as a reference modality for validating the accuracy of markerless and wearable sensor systems, particularly for complex movements and postures. Figure 7.2 shows an example of the marker visualization in the Qualisys system.

Figure 7.2: Visualization of detected reflective markers in the Qualisys System

AzureKinect RGB-D Camera

The AzureKinect is a markerless MoCap device that combines RGB and depth (D) imaging to estimate skeletal joint positions using computer vision algorithms. The camera captures synchronized color and depth frames, which are processed to extract 3D coordinates of key anatomical points. The system is intended for unobtrusive, rapid assessment of movement patterns without the need for physical markers or wearable sensors. Its application in this study focused on evaluating its suitability for movement analysis in MSD prevention and clinical settings, including range of motion and posture. The AzureKinect leverages advanced AI-based BT models to identify and track up to 32 skeletal joints in real-time, providing detailed kinematic data for each frame. The device supports multi-camera setups for expanded spatial coverage, though this requires careful synchronization and calibration. In the Smart-BT Validation Study, the AzureKinect was positioned to maximize visibility of the participant's body during various movement tasks, and recordings were performed using the Open3D recorder for improved reliability. The system's depth sensing capabilities allow for robust tracking even in challenging lighting conditions, but accuracy can be affected by clothing, occlusions, and interference from other infrared devices. Data from the AzureKinect was exported for post-processing and comparative analysis with reference systems, focusing on joint angle estimation and movement reproducibility. Figure 7.3 shows an example of the marker visualization in the AzureKinect system.

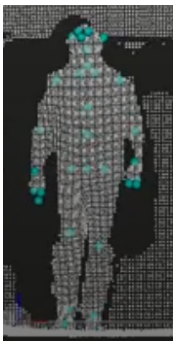

Figure 7.3: Visualization of detected reflective markers in the AzureKinect System

iPad® Body Tracking

The iPad® BT modality leverages built-in RGB cameras and proprietary algorithms to estimate human pose and joint locations from video data. This approach is entirely markerless and relies on real-time image processing to identify and track skeletal landmarks. The iPad® system was intended for accessible, low-cost motion analysis in settings where specialized hardware is unavailable. Its role in the study was to assess the feasibility and accuracy of consumer-grade devices for movement assessment in MSD prevention and clinical contexts. Figure 7.4 shows an example of the ARKit body pose estimation.

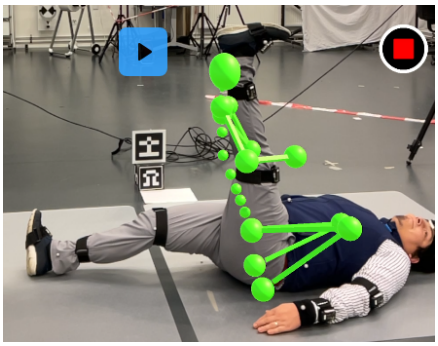

Figure 7.4: Visualization of detected reflective markers in the iPad® System

FlexTail Spinal Curvature Sensor

The FlexTail sensor is a specialized device designed to measure spinal curvature and segmental alignment. It consists of a flexible array of sensors that conform to the participant's back, capturing curvature profiles during static and dynamic tasks. The primary measurement output is the sagittal and coronal curvature of the spine, which is relevant for postural assessment and MSD prevention monitoring. FlexTail was included in the study to provide reference data for spinal motion and to evaluate its integration with other sensor modalities. Figure 7.5 shows an example of the FlexTail sensor attached to a participant's back inside a tshirt, in a later iteration of the sensor (2025 [Wal+25a])

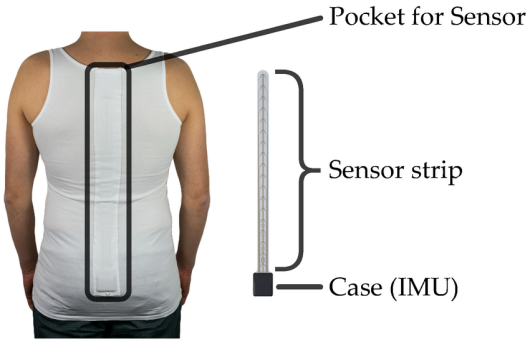

Figure 7.5: Visualization of the Flextail System [Wal+25b]

Coordinate system comparability

While the coordinate systems of the sensors used in this study are not directly comparable, this does not affect the validity of the results. The analysis relies exclusively on relative movement parameters, such as joint angles and distances, rather than absolute positions. By focusing on relative metrics, the study ensures that differences in sensor coordinate systems do not influence the interpretation of the data or the conclusions drawn.

7.3.4 Technical Issues and Operational Challenges

CAPTIV Motion Capture System

Initial setup of the CAPTIV system was hindered by incomplete and unintelligible documentation, requiring substantial effort to determine correct sensor placement, internal sensor calibration and synchronization. Although sensor attachment is straightforward, sensors–particularly at the sacral region–were prone to shifting during movement, necessitating frequent adjustments. Battery life was limited, requiring recharging between participants and making continuous operation over extended periods impractical. Real-time visualization facilitated verification of joint angle detection, but not all joint angles were reliably recognized depending on sensor configuration, causing constant jerking and erroneous readings. The coordinate system was initialized under L5 at the start of each session, but absolute positions did almost never corresponded to true participant movement. Triggering for synchronization with other systems was inconsistent, and the calculation methods for certain joint angles were not fully documented, though manufacturer support was responsive to inquiries.

Qualisys Optical Motion Capture

The Qualisys system required significant time for camera setup and alignment, with calibration performed using a wand and visual feedback on spatial coverage. Calibration remained valid for 24 hours, but re-calibration was recommended after five hours. Marker attachment was labor-intensive, and adhesive markers frequently detached during movement, while sewn or pinned markers provided greater stability. Recording was easy to initiate and terminate, but video file size limitations necessitated quality adjustments for longer sessions.

Assignment of markers to anatomical points was time-consuming, and automated bone model fitting was unreliable, requiring manual correction for each frame. Data export was flexible, supporting multiple formats (TSV, MAT, C3D, DIFF). Camera angles were adjusted to capture the feet and also tasks performed on the floor, but this compromised visibility of the shoulders, especially for taller individuals. Only five cameras could be used due to interference with AzureKinect devices, and the z-axis coordinates were consistently offset by approximately 2 cm above the floor.

AzureKinect RGB-D Camera

The AzureKinect system was generally user-friendly, with the Open3D recorder preferred for its reliability over the native AzureKinect recorder. The device was unable to detect silver Qualisys markers and exhibited reduced tracking accuracy with black or loose clothing. Wide vests and attached CAPTIV sensors interfered with BT, though a belt around the waist mitigated these issues. Infrared interference from Qualisys cameras disrupted depth sensing (see Figure 7.7), which was resolved by reducing the number of Qualisys cameras. Multi-camera setups required careful cable management and port selection, as not all USB configurations were compatible. Synchronization with other systems was achieved via triggering, but reliability varied heavily across sessions.

The tracking of extremities by the AzureKinect system was found to be notably unstable, particularly during dynamic movements and in scenarios involving occlusions or challenging lighting conditions. As illustrated in Figure 7.6, the system frequently failed to accurately localize distal joints such as hands and feet, resulting in incomplete or erroneous skeletal reconstructions. These tracking inconsistencies were exacerbated by factors such as loose clothing, rapid limb motion, and interference from other infrared devices. The lack of robustness in extremity tracking limits the reliability of joint angle measurements for tasks requiring precise assessment of hand or foot positions, and underscores the need for further refinement of the underlying BT algorithms before MSD prevention deployment.

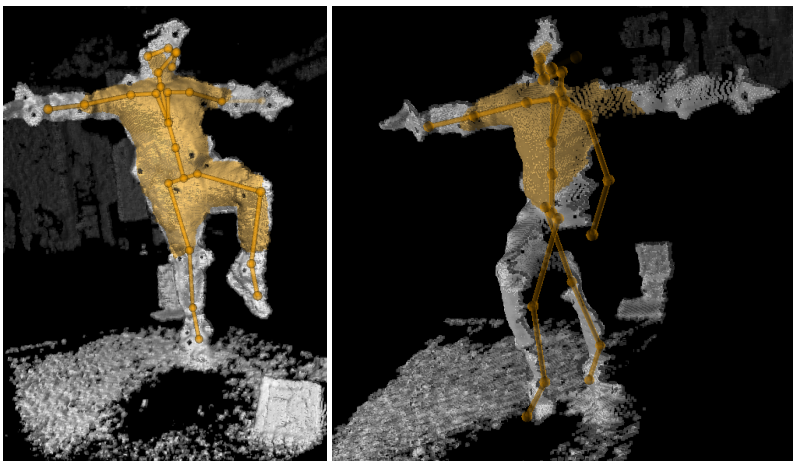

Figure 7.6: Depth images from the AzureKinect system showing a superposed tracked skeleton and segmentation. The extremities are not properly tracked, illustrating the lack of tracking robustness

iPad® Body Tracking

The iPad® BT system performed poorly, especially for supine exercises and frequently misidentified objects such as tripods or jackets as human subjects. The origin of the coordinate system was inconsistently defined, with no available documentation to clarify its placement. Data saving for both BT and video was functional, but joint localization accuracy was questionable, with detected joints often misplaced even when the participant was correctly identified. Temporal synchronization was only feasible via participant jumping, as auxiliary cable triggering was unsupported.

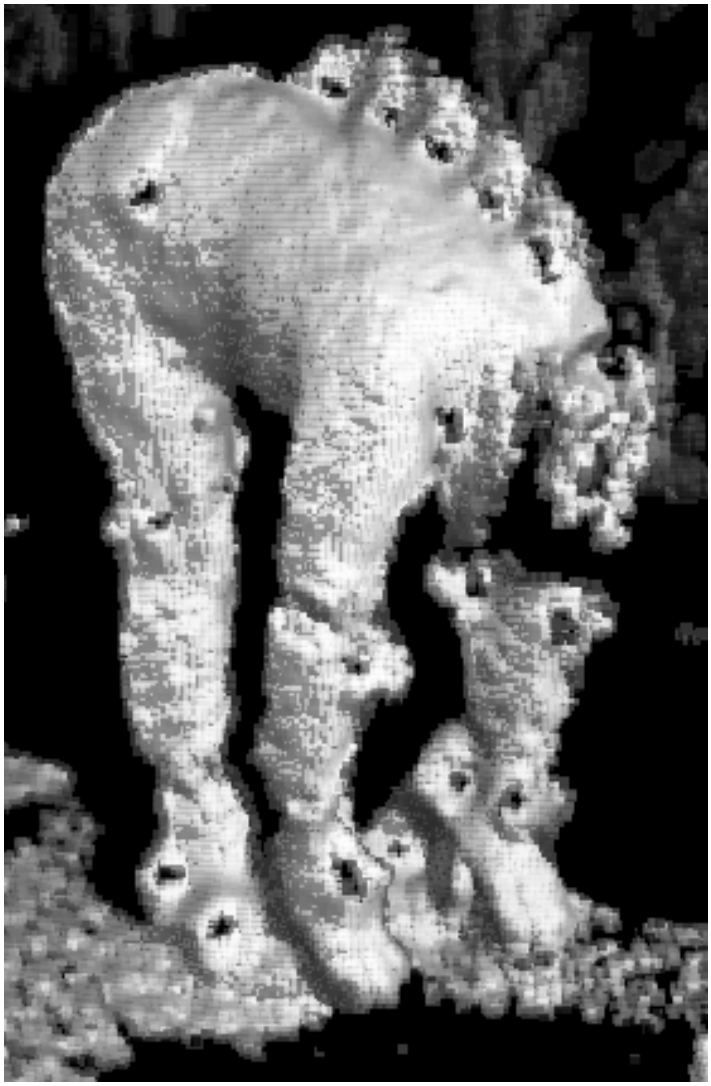

Figure 7.7: Depth image from the AzureKinect system showing a superposed tracked skeleton and segmentation. The extremities are not properly tracked, illustrating the lack of tracking robustness

The iPad® BT data was excluded from analysis due to persistent inaccuracies in joint localization, frequent misidentification of non-human objects as participants, and inconsistent coordinate system definitions. These issues resulted in unreliable kinematic measurements and prevented robust temporal synchronization with other modalities, ultimately compromising data integrity and comparability.

FlexTail Spinal Curvature Sensor

The FlexTail sensor could not be operated concurrently with other systems on the same computer, necessitating the use of a dedicated laptop. Recording sessions occasionally failed to stop correctly, though data files were generated; further review is needed to determine if recordings were prematurely terminated. Synchronization with other modalities was not achieved due to time constraints and additional hardware requirements. The device was sometimes ill-fitted for participant body sizes and was damaged by individuals with pronounced lumbar lordosis. Data files lacked time stamps, relying on the assumption of stable sampling frequency, which complicated temporal alignment and integration with other sensor data.

The FlexTail sensor data was excluded from analysis due to persistent operational issues, including unreliable recording sessions, lack of time-stamped data for synchronization, and frequent device misfit or damage during use. These limitations prevented robust integration with other sensor modalities and compromised the reliability of the collected spinal curvature measurements.

7.3.5 Data Collection Protocol

The data collection protocol involved a series of standardized procedures for each MoCap system to ensure consistency and reliability across sessions. This included:

Participant Preparation : Participants were instructed to wear form-fitting clothing to minimize motion artifacts. Markers were applied according to anatomical landmarks, with specific attention to ensure proper placement and adhesion.

System Calibration : Each system underwent a calibration process prior to data collection. This involved verifying camera alignment, adjusting sensor positions, and conducting test recordings to confirm tracking accuracy.

Recording Sessions : Data was collected during a series of predefined movement tasks, with participants instructed to perform each task multiple times to assess intra-session reliability. Breaks were provided when needed to minimize fatigue and maintain performance consistency.

Data Management : All recorded data was backed up immediately after each session, with a standardized naming convention applied to facilitate organization and retrieval. Metadata, including participant information and session details, was recorded alongside the data files.

7.3.6 Kinematic variables and Analytical Measures

This subsection defines the primary kinematic variables and analytical measures used to evaluate and compare the performance of the different motion capture systems in the study. It outlines which joint angles were selected for analysis, describes how these variables were extracted from each system, and details the statistical methods applied to assess measurement accuracy, agreement, and reliability. By specifying the main outcome measures and analytical approach, this subsection establishes the methodological foundation for the subsequent results and interpretation.

7.3.6.1 Main Kinematic Variable

The main kinematic variables were the joint angles derived from the output of the CAPTIV system and the Qualisys system, with corresponding angles also calculated from the AzureKinect data. Due to differences in the underlying skeleton models and biomechanical definitions used by the CAPTIV and Qualisys systems, the specific joint angles available for analysis are not identical between modalities. To enable meaningful comparison, the joint angles from the AzureKinect were computed in such a way as to most closely match the corresponding angles from each reference system, based on anatomical definitions and available marker or segment data. The analyzed angles for each system are listed in Table 7.3.

The **primary outcome** was the accuracy of joint angle estimation by the AzureKinect system, quantified by (RMSE) compared to the reference systems (CAPTIV and Qualisys).

Secondary outcomes included the agreement between modalities (assessed by Bland-Altman analysis), and the reliability of joint angle measurements (assessed by ICC).

Table 7.3: Analyzed joint angles for CAPTIV and Qualisys systems.

CAPTIV Analyzed Angles	Qualisys Analyzed Angles
Back forward flexion	Back
Back lateral flexion	Hip
HipLeft forward flexion	KneeLeft
HipRight forward flexion	KneeRight
KneeLeft flexion	
KneeRight flexion	

These features were then subjected to comparative analysis involving:

- Root Mean Square Error calculations for joint angles (see subsection 7.4.1).
- Bland-Altman plots to evaluate agreement between modalities (see subsection 7.4.2).
- Intraclass Correlation Coefficient to assess reliability (see subsection 7.4.3).

7.3.6.2 Statistical Analysis

Statistical analysis was performed using appropriate software (Python). The significance level was set at $\alpha = 0.05$. Descriptive statistics (mean, SD) were calculated for all kinematic variables. Comparisons between modalities were conducted using paired t-tests [Dav63] or Wilcoxon signed-rank tests [Wil45], as appropriate. Effect sizes were calculated to assess the magnitude of differences. Normality of the differences between modalities was assessed using the S-W test. If the differences were normally distributed, paired t-tests [Dav63] were used; otherwise, Wilcoxon signed-rank tests [Wil45] were applied. Bland-Altman plots were generated to visualize agreement between modalities, with limits of agreement calculated as mean difference ± 1.96 times the SD of the differences. ICC values were computed to assess the reliability of measurements across trials and modalities, with values interpreted according to established guidelines (e.g., <0.5 = poor, 0.5-0.75 = moderate, 0.75-0.9 = good, >0.9 = excellent).

7.3.7 Ethical and Legal Considerations

The study was approved by the relevant institutional ethics committee (Commission for Research Impact Assessment and Ethics UOL with reference number [Drs.EK/2021/057]). All participants provided written informed consent prior to data collection. No personal identifiers were recorded, and all motion data were anonymized in accordance with GDPR regulations. The study protocol was reviewed and approved by the OFFIS internal study commission.

7.4 Results

This section presents the results of the Smart-BT validation study, focusing on the comparative analysis of joint angle measurements obtained from markerless video-based MoCap (AzureKinect) and established reference systems (CAPTIV IMU suit and Qualisys optical system). The results are organized to provide a clear overview of the accuracy, reliability, and agreement between modalities for key kinematic variables relevant to MSD prevention and neurological clinical assessment.

The following subsections detail the statistical outcomes of the study, including RMSE values, ICC, and results from normality and significance testing. These metrics were selected to comprehensively evaluate both the magnitude of measurement error and the consistency of joint angle estimates across systems and movement tasks. Tables and figures are provided to facilitate direct comparison and interpretation of the findings.

The analysis begins with an assessment of RMSE values for each joint angle, highlighting areas of strong and weak agreement between the AzureKinect and reference modalities. ICC values are then reported to quantify the reliability of measurements and the degree to which the systems produce interchangeable results. Finally, statistical tests are summarized to determine the significance of observed differences and to assess the underlying distributional properties of the data.

By systematically presenting these results, this section aims to inform readers about the current capabilities and limitations of markerless video-based MoCap for clinical movement assessment, and to provide a foundation for subsequent discussion and recommendations.

7.4.1 Analysis of Root Mean Square Error Results

This subsection presents the comparative analysis of joint angle measurements between the markerless AzureKinect system and the established reference modalities, focusing on the root mean square error (RMSE) as a key metric for quantifying measurement accuracy. The RMSE provides an aggregate measure of the average deviation between joint angle estimates from the AzureKinect and those obtained from the CAPTIV IMU suit and Qualisys optical MoCap system. By evaluating RMSE values across different anatomical regions and movement tasks, the study aims to identify areas of strong and weak agreement, thereby informing the suitability of markerless video-based MoCap for clinical applications.

The analysis is structured to first summarize the average RMSE values for each joint angle comparison, followed by an interpretation of the results in the context of movement assessment. Tables 7.4 and 7.5 facilitate direct comparison between modalities, highlighting the magnitude of measurement error for trunk, hip, and knee flexion angles. These findings are discussed with reference to potential sources of error, including algorithmic limitations, sensor placement, and task-specific challenges. The results serve as a foundation for subsequent reliability and agreement analyses, offering insight into the current capabilities and limitations of markerless MoCap technologies in MSD prevention settings.

Table 7.4: Average RMSE per angle for AzureKinect vs CAPTIV.

Angle Comparison	Avg RMSE
back forward flexion kinect vs back forward flexion captiv	7.81
back lateral flexion kinect vs back lateral flexion captiv	4.21
hipLeft forward flexion kinect vs hipLeft forward flexion captiv	10.81
hipRight forward flexion kinect vs hipRight forward flexion captiv	15.33
kneeLeft flexion kinect vs kneeLeft flexion captiv	11.69
kneeRight flexion kinect vs kneeRight flexion captiv	9.76

Table 7.4 presents the average RMSE values for joint angle comparisons between the markerless AzureKinect system and the reference CAPTIV IMU-based sensor suit. The RMSE values quantify the average magnitude of error between the two modalities for each analyzed joint angle across all participants and movement trials.

The results indicate that the lowest RMSE was observed for back lateral flexion (4.21 degrees), suggesting good agreement between the AzureKinect and CAPTIV systems for this movement. Back forward flexion also showed a moderate RMSE (7.81 degrees), while the hip and knee flexion angles exhibited higher RMSE values, ranging from approximately 9.76 to 15.33 degrees. Specifically, hipLeft and hipRight forward flexion yielded RMSEs of 10.81 and 15.33 degrees, respectively, and kneeLeft and kneeRight flexion showed RMSEs of 11.69 and 9.76 degrees.

These findings suggest that the AzureKinect system is most accurate for trunk movements (particularly lateral flexion), and demonstrates moderate agreement for lower limb joint angles. The observed errors for hip and knee flexion indicate reliable tracking performance and calibration. Overall, the AzureKinect demonstrates potential for clinical movement assessment, with errors for most angles within a range that may be acceptable for gross movement analysis. The results also underscore the importance of task-specific validation when considering markerless MoCap for therapeutic applications.

Table 7.5: Average RMSE per angle for AzureKinect vs Qualisys.

Angle Comparison	Avg RMSE
back kinect vs back qualisys	22.82
hip kinect vs hip qualisys	35.47
kneeLeft kinect vs kneeLeft qualisys	19.39
kneeRight kinect vs kneeRight qualisys	14.17

In contrast, Table 7.5 summarizes the RMSE values for joint angle comparisons between the AzureKinect and the Qualisys optical MoCap system. The observed RMSEs are higher than those from the AzureKinect-CAPTIV comparison, with the back angle showing a deviation of 22.82°. Hip and knee flexion angles also display moderate errors (28.58°, 19.39°, and 14.17°, respectively). These discrepancies indicate that the AzureKinect faces challenges in achieving close agreement with the optical reference, particularly for hip movements.

The RMSE values observed between the AzureKinect and Qualisys systems can be attributed to fundamental methodological differences. The Qualisys setup defines joint centers based on precisely tracked reflective markers and biomechanical modeling, while the AzureKinect relies on single-depth-camera inference using a BT neural network trained on generalized body shapes. Consequently, small misalignments in camera pose, occlusions of body segments, or inaccuracies in anthropometric scaling can propagate into large angular deviations. Additionally, the optical system's higher spatial precision (sub-millimeter) contrasts sharply with the AzureKinect's depth uncertainty, which increases with distance from the sensor and limits tracking fidelity in sagittal plane motions.

Furthermore, these discrepancies can be attributed to fundamental methodological differences. The Qualisys setup defines joint centers based on precisely tracked reflective markers and biomechanical modeling, while the AzureKinect relies on single-depth-camera inference using a BT neural network trained on generalized body shapes. Consequently, small misalignments in camera pose, occlusions of body segments, or inaccuracies in anthropometric scaling can propagate into large angular deviations. Additionally, the optical system's higher spatial precision (sub-millimeter) contrasts sharply with the AzureKinect's depth uncertainty, which increases with distance from the sensor and limits tracking fidelity in sagittal plane motions. These differences likely explain why errors are disproportionately high for trunk flexion, where self-occlusion and limited depth perception strongly affect joint estimation.

The ICC values in Table 7.6 confirm these findings, indicating moderate to good reliability for knee angles (ICC 0.817 and 0.764), low reliability for hip (0.023), and fair reliability for back (0.201). The improved ICCs for knee angles highlight the AzureKinect's potential for reliable lower limb assessment, while the lower values for hip and trunk suggest continued limitations for these joints. These results reinforce the interpretation that methodological and geometric factors influence agreement, but the system achieves meaningful reliability for certain angles.

Table 7.6: Intraclass Correlation Coefficient for AzureKinect vs Qualisys angles.

Angle Comparison	ICC
back kinect vs back qualisys	0.201
hip kinect vs hip qualisys	0.023
kneeLeft kinect vs kneeLeft qualisys	0.817
kneeRight kinect vs kneeRight qualisys	0.764

In summary, the comparative analysis reveals that while AzureKinect performs well relative to the IMU-based CAPTIV system for trunk and knee angles, its agreement with the Qualisys optical MoCap is moderate for trunk and good for knees, but remains limited for hip. The findings underscore the need for modality-aware calibration and validation protocols when employing markerless tracking in clinical or research settings.

7.4.2 Bland-Altman Analysis

Bland-Altman plots were generated to assess the agreement between joint angle measurements obtained from the AzureKinect and the reference systems. These plots visually represent the differences between the two measurement methods against their means, allowing for the identification of any systematic biases or trends.

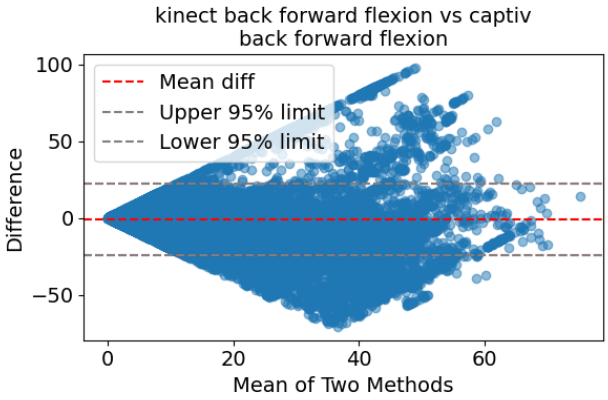

Figure 7.8: Bland-Altman plot for back forward flexion: AzureKinect vs CAPTIV.
The plot shows the differences between the two systems against their mean values, with limits of agreement indicated by dashed lines.

Back forward flexion:

The Bland–Altman plot for back forward flexion (Figure 7.8) shows that most data points are distributed symmetrically around zero, with a mean bias close to zero. The majority of differences fall within approximately ± 20 degrees, but a few outliers extend beyond these limits. There is no clear trend of increasing or decreasing error with higher mean angles, indicating no systematic bias across the range of motion.

Back lateral flexion:

In the plot for back lateral flexion (Figure 7.9), the differences are tightly clustered around zero, with most points within ± 10 degrees and very few outliers. The mean bias is minimal, and the spread of differences remains consistent across the range of mean values, suggesting good agreement and no systematic error.

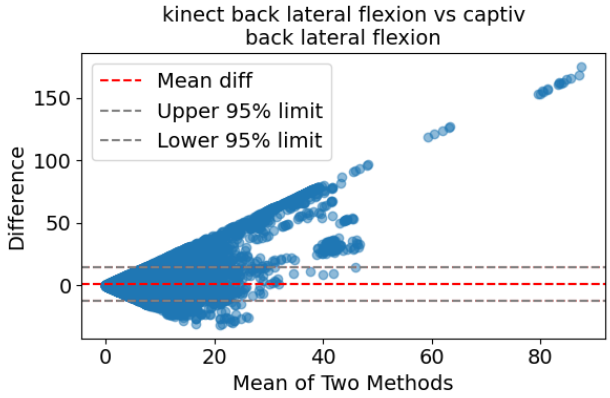

Figure 7.9: Bland-Altman plot for back lateral flexion: AzureKinect vs CAPTIV.
The plot shows the differences between the two systems against their mean values, with limits of agreement indicated by dashed lines.

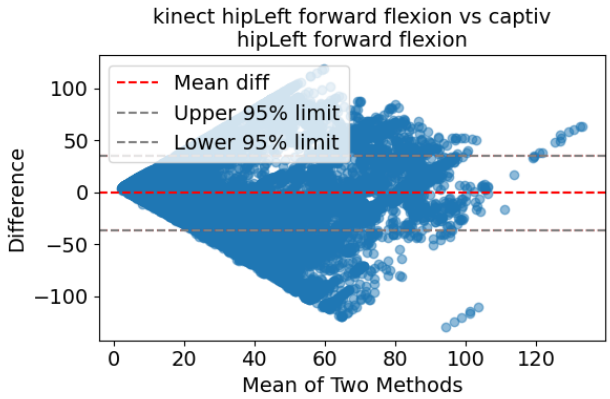

Figure 7.10: Bland-Altman plot for hip left forward flexion: AzureKinect vs CAPTIV.
The plot shows the differences between the two systems against their mean values, with limits of agreement indicated by dashed lines.

Hip left forward flexion:

The Bland–Altman plot for hip left forward flexion (Figure 7.10) reveals a wider spread of differences, with most points within ±40 degrees but several outliers reaching beyond ±60 degrees. The mean bias is slightly positive, indicating a small tendency for the AzureKinect to overestimate compared to CAPTIV. There is no strong trend of increasing error with higher mean angles.

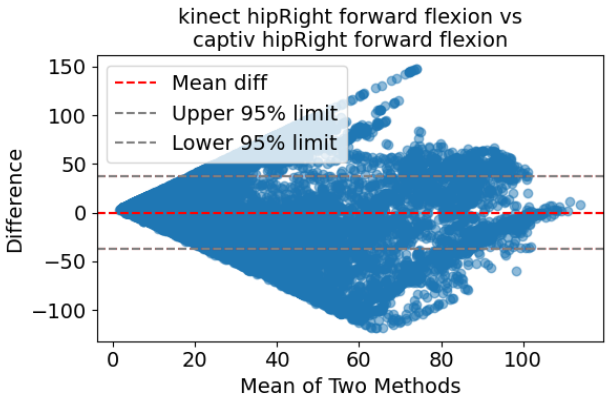

Figure 7.11: Bland-Altman plot for hip right forward flexion: AzureKinect vs CAPTIV.
The plot shows the differences between the two systems against their mean values, with limits of agreement indicated by dashed lines.

Hip right forward flexion:

The hip right forward flexion plot (Figure 7.11) shows a similar pattern to the left, with most differences within ±40 degrees and a few outliers. The mean bias is close to zero, and the spread of differences does not show a clear relationship with the mean angle, indicating no systematic bias.

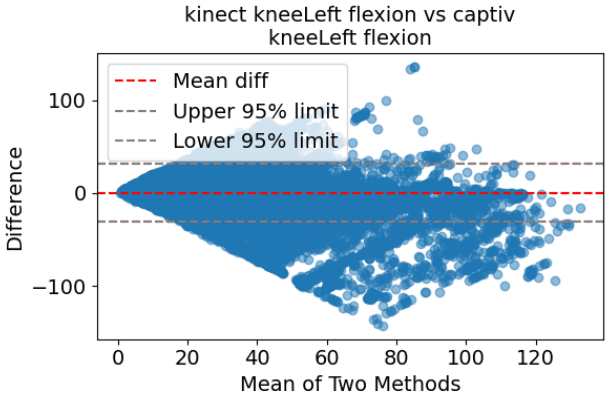

Figure 7.12: Bland-Altman plot for knee left flexion: AzureKinect vs CAPTIV.
The plot shows the differences between the two systems against their mean values, with limits of agreement indicated by dashed lines.

Knee left flexion:

The Bland–Altman plot for knee left flexion (Figure 7.12) displays a wider range of differences, with most points within ±40 degrees but several outliers extending up to ±100 degrees. The mean bias is near zero, and there is no clear trend of increasing error with higher mean angles, though the outliers indicate occasional large discrepancies.

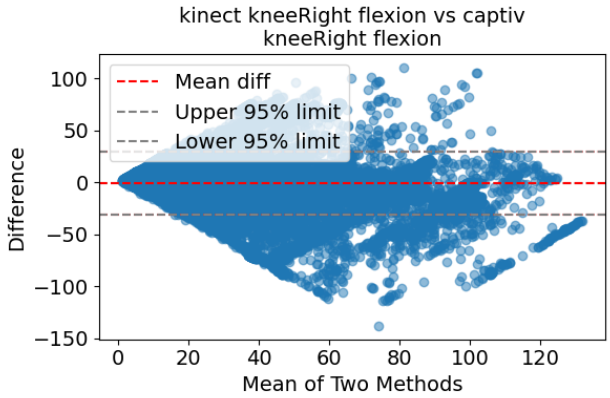

Figure 7.13: Bland-Altman plot for knee right flexion: AzureKinect vs CAPTIV.
The plot shows the differences between the two systems against their mean values, with limits of agreement indicated by dashed lines.

Knee right flexion:

The knee right flexion plot (Figure 7.13) is similar to the left, with most differences within ±40 degrees and a few outliers beyond this range. The mean bias is close to zero, and the distribution of differences is consistent across the range of mean values, indicating no systematic bias but occasional large errors.

It is important to note that the largest differences between systems are likely attributable to movement tasks performed in the lying (supine) position, which represent a worst-case scenario for markerless tracking. During these tasks, the AzureKinect system experienced frequent lapses in tracking, resulting in missing data that would have to be interpolated. This interpolation can introduce very high errors, especially when large gaps occur, and thus inflates the disagreement. The comparison of interpolated data would have led to an overestimation of the error, as the AzureKinect was unable to provide reliable body position estimates for extended periods, particularly during tasks performed on the floor.

The results reveal systematic discrepancies between the two systems, particularly for lower limb joints. While back forward and lateral flexion exhibit relatively narrow limits of agreement (approximately ±10–20 degrees), hip and knee flexion comparisons show moderately wider ranges, with most differences within ±40 degrees and only occasional larger outliers. This suggests that the AzureKinect system demonstrates moderate agreement for lower limb joint angles, with variability primarily due to challenging movement conditions or tracking failures. Overall, the agreement is sufficient for gross movement analysis, though caution is warranted for precise measurements in dynamic or extreme positions.

In contrast, the back flexion plots show tighter clustering around the mean bias, suggesting more consistent agreement for trunk movements. These findings align with the RMSE and ICC results reported in subsection 7.4.1 and subsection 7.4.3, reinforcing the conclusion that markerless systems are currently more suitable for upper body and trunk assessments than for precise lower limb kinematics.

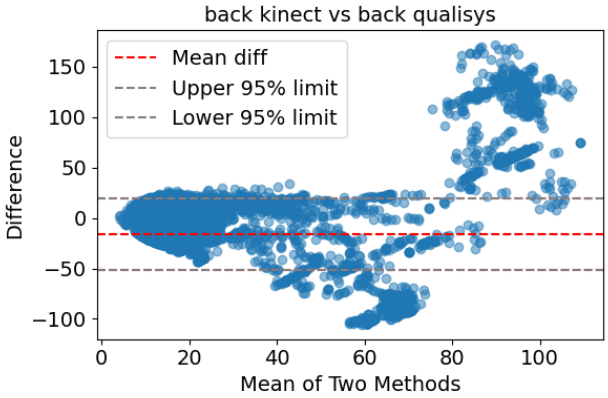

Figure 7.14: Bland-Altman plot for back: AzureKinect vs Qualisys.
The plot shows the differences between the two systems against their mean values, with limits of agreement indicated by dashed lines.

Back:

The Bland-Altman plot for back comparison (Figure 7.14) indicates substantial variability, with differences ranging from approximately -60 to $+40$ degrees. The dispersion of points increases at higher mean angles, suggesting that the AzureKinect system struggles to maintain accuracy during deep trunk flexion. The largest errors are likely attributable to supine tasks where tracking failures and occlusion tracking errors inflate the observed disagreement.

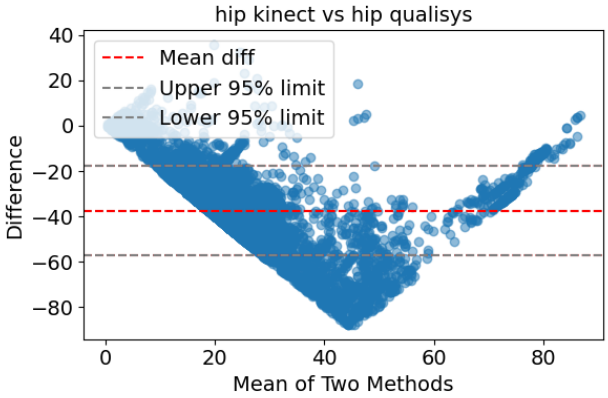

Figure 7.15: Bland-Altman plot for hip: AzureKinect vs Qualisys.
The plot shows the differences between the two systems against their mean values, with limits of agreement indicated by dashed lines.

Hip:

The Bland–Altman plot for hip joint angles (Figure 7.15) reveals considerable variability in the differences between the AzureKinect and Qualisys systems. The spread of data points indicates limited agreement, with discrepancies particularly evident at angles around 40°. This pattern suggests that the AzureKinect system encounters challenges in accurately tracking hip flexion, especially during movements involving large ranges of motion or complex postures.

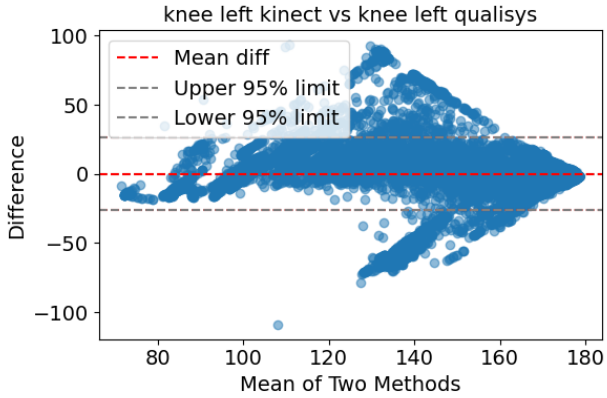

Figure 7.16: Bland-Altman plot for left knee: AzureKinect vs Qualisys.
The plot shows the differences between the two systems against their mean values, with limits of agreement indicated by dashed lines.

Knee left:

The Bland-Altman plot for the left knee (Figure 7.16) reveals the most pronounced disagreement, with differences extending up to ± 150 degrees. This extreme spread highlights the limitations of markerless tracking for distal joints, especially during movements performed lying down. The high errors are again likely a result of tracking lapses and the need to interpolate missing data, which can introduce substantial inaccuracies.

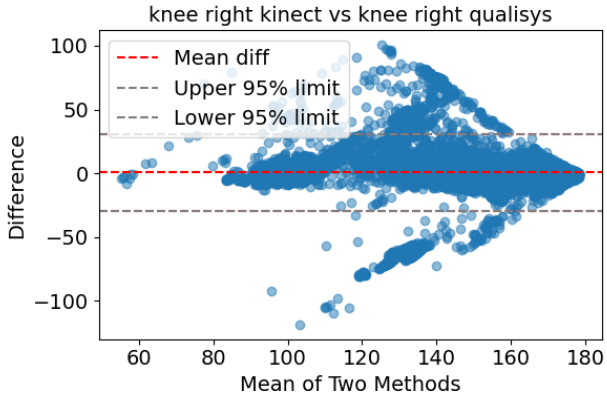

Figure 7.17: Bland-Altman plot for right knee: AzureKinect vs Qualisys.
The plot shows the differences between the two systems against their mean values, with limits of agreement indicated by dashed lines.

Knee right:

The right knee plot (Figure 7.17) mirrors the left, with very wide limits of agreement and substantial scatter. The largest differences are again associated with supine positions, where the AzureKinect system frequently lost track of the extremities and required interpolation, resulting in very high errors that represent the worst-case scenario for markerless motion capture.

In summary, the Bland–Altman analysis against Qualisys confirms that the AzureKinect system exhibits substantial measurement error across all examined joints, particularly in the lower extremities. These find-

ings reinforce the need for algorithmic refinement and task-specific calibration when deploying markerless BT systems in clinical or research-grade motion analysis.

Overall, the Bland–Altman analysis underscores the importance of modality-specific validation and highlights the need for algorithmic refinement in markerless BT systems to achieve clinically acceptable accuracy across all joint regions.

7.4.3 Analysis of Intraclass Correlation Coefficient Results

The ICC values presented in Table 7.7 provide a quantitative measure of the reliability and agreement between joint angle estimates from the AzureKinect markerless system and the CAPTIV IMU-based sensor suit. ICC values range from 0.092 to 0.727 across the analyzed joint angles, indicating moderate to good reliability for most angles.

For trunk movements, the ICC for back forward flexion is 0.289, and for back lateral flexion, it is 0.092, suggesting fair to moderate reliability. Hip flexion angles show moderate ICCs (0.485 and 0.436 for left and right, respectively). The highest ICCs are observed for knee flexion angles (0.709 for left and 0.727 for right), indicating good reliability and supporting the use of AzureKinect for lower limb assessment.

These results suggest that the AzureKinect system, in its current implementation, provides joint angle measurements that are approaching good reliability for knee flexion, and moderate reliability for trunk and hip angles. The lower ICCs may be attributed to differences in sensor technology, AzureKinect-BT algorithms, and potential issues with synchronization or calibration. Notably, the higher ICCs for knee flexion reflect better tracking performance for lower limb movements.

Overall, the findings highlight the progress in markerless video-based systems for kinematic assessment in MSD prevention contexts. The poor agreement underscores the need for further refinement of tracking algorithms and validation procedures before such systems can be recommended for routine clinical use. These results also emphasize the importance of modality-specific validation and caution against assuming equivalence between markerless and IMU-based MoCap technologies.

Table 7.7: Intraclass Correlation Coefficient for AzureKinect vs CAPTIV angles.

Angle Comparison	ICC
back forward flexion kinect vs back forward flexion captiv	0.289
back lateral flexion kinect vs back lateral flexion captiv	0.092
hipLeft forward flexion kinect vs hipLeft forward flexion captiv	0.485
hipRight forward flexion kinect vs hipRight forward flexion captiv	0.436
kneeLeft flexion kinect vs kneeLeft flexion captiv	0.709
kneeRight flexion kinect vs kneeRight flexion captiv	0.727

7.5 Conclusion

The Smart-BT validation study provides a comprehensive evaluation of markerless video-based MoCap systems, specifically the AzureKinect, in comparison to established reference modalities such as the CAPTIV IMU suit and the Qualisys optical system. The results demonstrate that, while markerless systems offer significant practical advantages in terms of accessibility, ease of setup, and reduced participant burden, their current technical limitations preclude reliable use in movement analysis settings.

Across all key kinematic variables, the AzureKinect system exhibited substantial measurement error, as evidenced by high RMSE values and poor ICC reliability scores. Agreement with reference systems was particularly weak for lower limb joint angles, with Bland–Altman analyses revealing wide limits of agreement

and systematic biases. These discrepancies are attributable to a combination of algorithmic constraints, sensor occlusions, calibration challenges, and operational issues such as infrared interference and inconsistent synchronization. While trunk movements showed somewhat better agreement, the overall reliability remained below thresholds required for clinical decision-making.

The study also highlighted the importance of robust data collection protocols, thorough calibration, and modality-specific validation. Technical challenges encountered with all systems underscore the need for standardized procedures and careful integration of hardware and software components. Notably, consumer-grade devices such as the iPad® and experimental sensors like FlexTail were excluded from analysis due to persistent inaccuracies and operational failures, reinforcing the necessity of rigorous validation before adopting new technologies in clinical workflows.

In light of these findings, the primary contribution of this work is the clear demonstration that markerless video-based systems, in their current form, cannot yet replace validated reference modalities for precise movement assessment. The results advocate for a cautious approach to technology adoption, emphasizing the need for continued algorithmic refinement, improved calibration methods, and comprehensive validation studies tailored to specific clinical tasks and populations.

Given these limitations, the study recommends caution when using markerless systems such as the AzureKinect for movement assessment in extreme positions (e.g., lying on the floor) or in environments with high reflectivity, where tracking reliability is reduced. While the AzureKinect can be suitable for clinical gait analysis and movement assessment in controlled indoor settings, its use in outdoor environments or under challenging lighting conditions is not recommended. This rationale informed the decision to employ the CAPTIV IMU suit as the primary measurement tool in subsequent field studies, as seen on chapter 8. By ensuring consistency in data acquisition and reliability in kinematic measurements, the research team aims to facilitate robust outcome evaluation and meaningful comparisons across diverse movement analysis contexts.

The next chapter will build upon these validation results by presenting the design, implementation, and outcomes of a field study, where the CAPTIV system was used to monitor patient movement in real-world occupational environments. This approach enables the translation of validated measurement protocols into practical applications, supporting evidence-based physiotherapy optimization and long-term monitoring.

7.6 CRediT contribution statement

Pedro Fernando Arizpe Gómez: Conceptualization, Data curation, Formal analysis, Investigation, Methodology, Resources, Software, Validation, Visualization, Writing – Original Draft.

Fenja T. Hasselmann, née Bruns: Conceptualization, Data curation, Methodology, Resources, Validation, Visualization.

Linda Bergmann, née Büker: Conceptualization, Data curation, Formal analysis, Investigation, Methodology, Resources, Software, Validation, Visualization, Writing – Original Draft, Writing – Review and Editing.

Sandra Hellmers: Funding acquisition, Project administration, Resources, Supervision.

Andreas Hein: Conceptualization, Funding acquisition, Project administration, Resources, Supervision, Writing – Review and Editing.

8 Observational field study on ergonomic risk with craftspeople (ReHopE Hospitationen Study)

Parts of this chapter are part of a publication in progress:
Sandra Drolshagen, Pedro Arizpe-Gómez, Tim Stratmann, and Andreas Hein. “Exoskeletons in Skilled Trades: Challenges and Chances”. In Publishing

8.1 Introduction

The "ReHopE Hospitationen" were a series of field studies conducted to observe and analyze the physical demands of real-world tasks performed by skilled trades craftspeople in their natural work environments. The primary aim was to identify high-risk movement patterns and postures that contribute to musculoskeletal strain, thereby informing the development of ergonomic interventions and assistive technologies such as exoskeletons.

8.2 Scientific Background and Objectives

Craftspeople are frequently exposed to biomechanical risk factors such as repetitive movements, awkward postures, and heavy lifting, which are known contributors to WRMSDs [CV10]. While laboratory-based assessments offer controlled insights, field studies are essential for capturing the complexity and variability of real-world occupational tasks.

The objectives of this study were:

1. To assess **joint angles** and postural loads using wearable motion capture systems.
2. To use vision-based systems (AzureKinect) primarily for manual video labeling and annotation, as their quantitative accuracy was insufficient for reliable joint angle analysis in field conditions.
3. To evaluate **ergonomic risk levels** based on the DGUV208-033 Annex 3 Part 1 guidelines [Deu15].
4. To document and categorize **typical work activities** common to different skilled craft trades, such as lightning protection, window installation, and HVAC[1] installation.

8.3 Design and Methodology

This observational field study was conducted across three skilled crafts trade businesses:

Window Maker: A carpentry company specializing in the installation and maintenance of windows.
HVAC Technicians: Professionals working on heating, ventilation, and air conditioning systems.
Lightning Protection Worker: Specialists in installing and maintaining lightning protection systems.

Participants were observed in their usual working environments. They performed 5-6 typical work tasks while wearing a CAPTIV motion capture suit. The study was non-invasive and lasted no longer than two hours per participant.

[1] Heating, Ventilation and Air Conditioning

8.3.1 Participants

A total of three skilled craftspeople participated in the study, each representing one of the three occupational groups: Window Maker, HVAC Technician, and Lightning Protection Worker. All participants were adult employees of the respective companies and volunteered for the study. While certain tasks, such as carrying large window frames, required collaborative execution and involved additional workers, only the movements of the three primary participants were measured.

All participants provided written informed consent prior to data collection. No personal identifiers were recorded, and all motion data were anonymized in accordance with GDPR regulations. The study protocol was reviewed and approved by the OFFIS internal study commission.

8.3.2 Sensing Modalities

The following sensor systems were used in this study to comprehensively capture movement features of occupational tasks in real-world environments.

First, the CAPTIV MoCap System was employed, consisting of 13 IMU-based sensors strategically placed on major joints to record 3D position and orientation data. This setup enabled precise measurement of joint angles and postural loads during a wide range of movements, including lifting, carrying, and floor-level work. The sensor placement covered the head, upper back, lumbar spine, upper arms, forearms, thighs, shins, and feet, ensuring full-body kinematic analysis (see Figure 8.1).

Figure 8.1: Placement of the 13 CAPTIV IMU sensors on major joints of a participant.

In addition to wearable sensors, an AzureKinect RGB-D camera was used for offline video labeling and annotation of task sequences. Although the AzureKinect was initially intended as a secondary source of BT data, environmental factors such as excessive sunlight and frequent occlusions limited its effectiveness for quantitative analysis, since the BT detection was not accurate and often non-existent. Nevertheless, the color video recordings provided valuable context for manual annotation and verification of movement categories. Together, these sensing modalities allowed for a robust and multi-faceted assessment of ergonomic risk, supporting both quantitative joint angle analysis and qualitative task classification. The integration of wearable and vision-based systems reflects current best practices in field-based biomechanical research, enabling the identification of high-risk postures and informing the development of targeted ergonomic interventions.

8.3.3 Ethical and Legal Considerations

The study adhered to ethical standards and was approved by the OFFIS e. V. Studienboard (reference 2022P011). All participants signed a written informed consent form prior to data collection. All motion data were anonymized in compliance with GDPR regulations, ensuring participants' privacy and data protection.

8.3.4 Tasks and Protocols

The labeling categories correspond to the task types listed in Table 8.1. Each movement sequence was manually annotated based on these categories using the color videos of the AzureKinect camera.

Table 8.1: Overview of performed tasks

Tasks	
Climbing stairs and ladders (climbing)	Lifting loads (load-lifting)
Setting down lifted loads (load-dropping)	Working on the floor (floor-work)
Working in bent or crouched postures (bent-over-work)	Standing (standing)
Performing overhead work (overhead)	Carrying loads (carrying)
Walking with loads (walking)	

8.3.5 Kinematic variables and Analytical Measures

This subsection describes the main kinematic variables analyzed in the study, focusing on the specific joint angles captured by the wearable motion capture system. It outlines which joint movements were measured, explains their biomechanical relevance, and provides an overview of how these variables contribute to the assessment of ergonomic risk. By detailing the selection and interpretation of these kinematic outcomes, this section establishes the foundation for subsequent statistical analyses and ergonomic evaluations presented in the following parts of the chapter.

8.3.5.1 Main Kinematic Variable

The analyzed kinematic variables were the 18 angles from the output of the CAPTIV system, which can be seen in Table 8.2

8.3.5.2 Derivated Variables

These joint angles were classified according to the limits set by DGUV208-033 Annex 3 Part 1 guidelines [Deu15]. This yielded an **ergonomic risk classification** of joint angles during task execution. Eighteen joint angles were analyzed and categorized as **"Acceptable", "Conditionally acceptable" and "Not acceptable"**. Furthermore, the angle data offered insights into following key indicators:

- Distribution of risk levels (see subsection 8.4.2) across broader body regions: neck, shoulders, elbows, back and knees.
- Task-specific risk profile comparison (e.g., lifting vs. carrying).
- Identification of tasks with the highest ergonomic burden.

The **Primary Outcomes** of this study were quantitative measures of ergonomic risk based on joint angle analysis and exposure time. Objective outcomes included the classification of joint angles into ergonomic risk categories (acceptable, conditionally acceptable, not acceptable) according to DGUV208-033 guidelines, aggregated exposure-time distributions for each joint and task, and statistical comparisons of joint angles across tasks and occupations using non-parametric tests. These metrics enabled the identification of high-risk postures and tasks associated with increased musculoskeletal strain.

The **Secondary Outcomes** comprised qualitative task annotations from manual video labeling, descriptive summaries of typical work activities in skilled trades, and the documentation of task-specific ergonomic risk profiles. Additional outcomes included the interpretation of joint-specific and task-specific risk distributions,

Table 8.2: Description of kinematic outcome variables

Joint Angle	**Description**
Neck Flex/Ext	Forward and backward bending of the neck (nodding motion).
Neck Lateral flexion	Side-to-side bending of the neck.
Neck Rotation	Rotational movement of the neck (e.g., looking over the shoulder).
Back Forward flexion	Forward bending of the upper back or spine.
Back Lateral flexion	Side-to-side bending of the spine.
Back Rotation	Twisting motion of the torso/spine.
Shoulder (Right) (Projection) Abd/Add	Movement of the right arm away from or toward the body in the frontal plane.
Shoulder (Left) (Projection) Abd/Add	Movement of the left arm away from or toward the body in the frontal plane.
Shoulder (Right) (Projection) Flex/Ext	Raising/lowering the right arm in the sagittal plane.
Shoulder (Left) (Projection) Flex/Ext	Raising/lowering the left arm in the sagittal plane.
Shoulder (Right) Rotation	Internal/external rotation of the right shoulder.
Shoulder (Left) Rotation	Internal/external rotation of the left shoulder.
Elbow (Right) Flex/Ext	Bending and straightening of the right elbow.
Elbow (Left) Flex/Ext	Bending and straightening of the left elbow.
Elbow (Right) Rotation	Rotation (pronation/supination) of the forearm from the right elbow.
Elbow (Left) Rotation	Rotation (pronation/supination) of the forearm from the left elbow.
Knee (Left) Flex/Ext	Bending and straightening of the left knee.
Knee (Right) Flex/Ext	Bending and straightening of the right knee.

as well as recommendations for ergonomic interventions and assistive technology development. Together, these outcomes provided a comprehensive assessment of biomechanical demands in real-world skilled trade environments, supporting evidence-based ergonomic improvements.

8.4 Results and Interpretation

This section presents the analytical outcomes of the "ReHopE Hospitationen" field study, based on joint angle data collected during real-world occupational tasks. The results are organized to provide both a high-level overview of ergonomic risk exposure and detailed statistical comparisons across task types and joint regions. Through a combination of exposure-time analysis, normality assessments, and non-parametric statistical testing, the section aims to identify movement patterns and postures associated with elevated musculoskeletal strain in skilled trades.

8.4.1 Ergonomic Risk Classification Overview

A total of 137,285 frames were analyzed, covering 71 minutes of recorded material. Sixty-four distinct movement sequences were annotated. The analysis revealed that many common tasks in the skilled craft trades involve postures that are ergonomically suboptimal. In particular, bent-over work, floor-work and ladder use were frequently associated with non-acceptable joint angles, especially in the back, shoulders, and knees.

8.4.2 Joint-Specific Ergonomic Risk Interpretation by Exposure Time

Understanding the cumulative exposure of individual joints to biomechanical strain is essential for identifying anatomical regions most affected by occupational tasks. While task-based analyses reveal which activities are ergonomically demanding, they do not fully capture the distribution of joint stress across the body. By aggregating exposure time for each joint and classifying it into ergonomic risk levels–acceptable, conditionally acceptable, and not acceptable–this analysis provides a body-part-centric perspective on occupational strain. Such an approach is particularly valuable in skilled trades, where repetitive and awkward postures are common, and MSDs often develop gradually over time. The pie chart visualizations offer an intuitive overview of which joints are most frequently subjected to non-ergonomic angles, enabling targeted intervention strategies. For instance, the high proportion of red-zone exposure in the knees highlights the need for support during crouching and kneeling tasks, while intermediate risk profiles in the back and shoulders suggest potential benefits from posture-assistive devices or task redesign. This joint-specific exposure analysis complements task-level findings and supports the development of ergonomic solutions that prioritize the most vulnerable body regions.

For clarity, the 18 joint angles were classified into these 5 main broader body regions: Neck, Back, Knees, Shoulders and Elbows.

Then, the total exposure time was calculated by aggregating all captured frames, categorizing the angle values into acceptable (green), conditionally acceptable (yellow) and not acceptable (red) values and plotting them into pie charts (see Figure 8.2).

Figure 8.2 presents aggregated exposure-time distributions across four major body regions–neck, back, knees, elbows and shoulders–based on joint angle classifications recorded during the "ReHopE Hospitationen" field study. Each pie chart is segmented into green (acceptable), yellow (conditionally acceptable), and red (not acceptable) zones, following the ergonomic assessment framework defined in DGUV 208-033 [Deu15]. These distributions offer a high-level overview of which anatomical regions are most frequently subjected to biomechanical strain across diverse occupational tasks.

The most striking observation is the predominance of red-zone exposure in the knees, accounting for 71.3% of total task time. This suggests that lower-limb postures–particularly those involving deep flexion such as

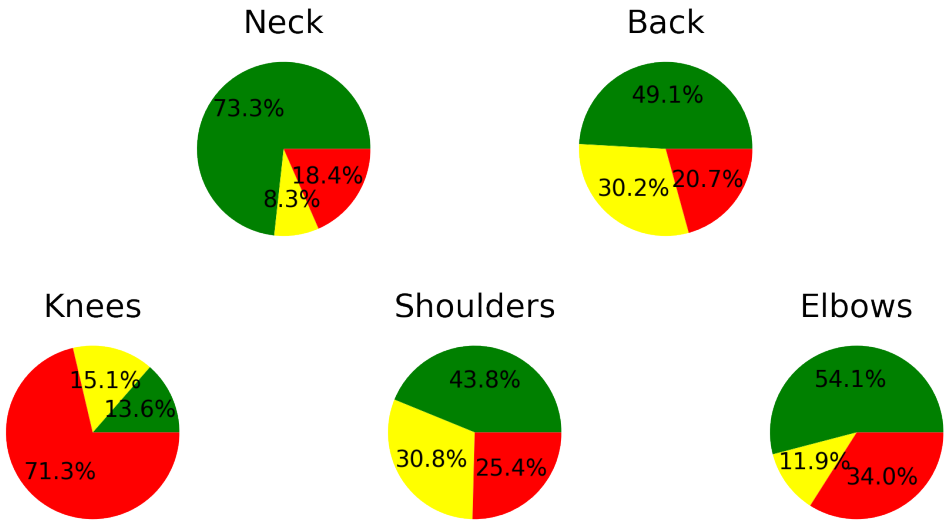

Figure 8.2: Aggregated exposure-time distribution across ReHopE field workers by body part
Body Parts: neck, back, knees, elbows and shoulders
green/yellow/red zones represent
"acceptable/conditionally acceptable/ not acceptable"
values, respectively.

kneeling, crouching, or climbing–are consistently non-ergonomic and pose a significant risk for WRMSDs. This finding aligns with prior research indicating that repetitive or sustained knee flexion is a major contributor to WRMSDs in skilled craft trades involving manual labor and floor-level tasks [CV10].

In contrast, the neck region shows a relatively favorable profile, with 73.3% of exposure time falling within acceptable limits. This may reflect the fact that head posture remains relatively neutral across many tasks, especially those involving visual focus or upright positioning. However, the presence of 18.4% red-zone exposure still warrants attention, particularly in tasks requiring overhead work or prolonged downward gaze.

The back exhibits an intermediate risk profile, with 49.1% acceptable exposure, 30.2% yellow, and 20.7% red, indicating frequent engagement in postures involving trunk flexion or rotation.

The shoulders show 43.8% acceptable exposure, but also 30.8% yellow and 25.4% red-zone time, likely attributable to overhead tasks or load handling. Similarly, the elbows present 54.1% acceptable exposure, with 34% red-zone time, suggesting frequent engagement in forceful or awkward arm postures, such as pushing, pulling, or repetitive flexion.

These distributions underscore the need for ergonomic interventions targeting spinal and upper-limb support, such as posture-assistive exoskeletons, redesigned tool interfaces, or task reorganization to minimize joint stress.

Overall, Figure 8.2 complements the task-specific analyses by highlighting anatomical regions most affected by occupational strain. It reinforces the importance of body-part-specific ergonomic strategies and supports the prioritization of interventions aimed at reducing cumulative joint stress in high-risk areas.

8.4.3 Normality Assessment of Knees Flexion–Extension Angles (exemplary)

Before conducting statistical comparisons of joint angles across occupational tasks, it is essential to verify whether the underlying data distributions meet the assumptions required by parametric tests. One of the most

critical assumptions is normality, which underpins the validity of commonly used tests such as the t-test [Dav63] and ANOVA[2][SW+89]. In the context of biomechanical data–particularly joint angles captured in real-world environments–this assumption is often violated due to the inherent variability and asymmetry of human movement. For example, tasks involving deep knee flexion, such as kneeling or climbing, may produce skewed distributions with long tails, reflecting the sporadic occurrence of extreme postures. Assessing normality is therefore a necessary step to ensure the robustness of subsequent statistical analyses. In this study, the S-W test was applied to the knees flexion-extension angles, complemented by visual inspection through Q-Q[3] plots and histograms. The results revealed a clear departure from normality, justifying the use of non-parametric methods such as the Mann-Whitney U test [MW47] for task comparisons. This approach not only safeguards the statistical integrity of the findings but also highlights the importance of methodological rigor when analyzing movement data in occupational health research.

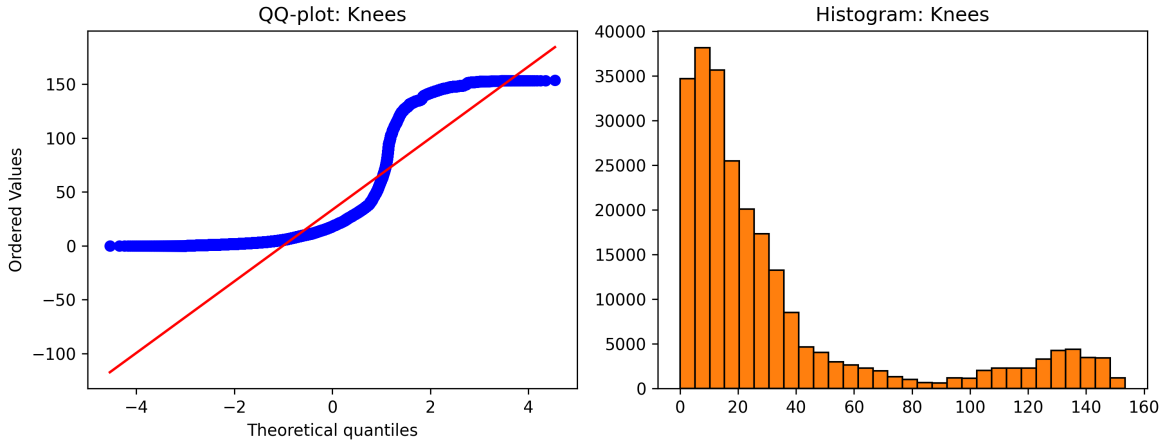

Figure 8.3: Q-Q plot and histogram of Knees flexion–extension angles demonstrating departure from normality (S-W $p < 0.05$).

Figure 8.3 presents a Q-Q plot and histogram for Knees flexion–extension angles, providing visual evidence of the data's departure from normality. The Q-Q plot compares the ordered sample quantiles against theoretical quantiles from a normal distribution. A clear deviation from the reference line is observed, particularly at the tails, indicating that the distribution of Knees angles does not follow a Gaussian pattern. The accompanying histogram further supports this conclusion. The distribution is skewed, with a concentration of values between 0 and 40 degrees, and a long tail extending toward higher angles. This asymmetry suggests that the data are not symmetrically distributed, which violates one of the key assumptions of parametric statistical tests. The S-W test result ($p < 0.05$) confirms the visual interpretation, statistically rejecting the null hypothesis of normality. This finding justifies the use of non-parametric methods, such as the Mann–Whitney U test, in the comparative analysis of joint angles across tasks. It also highlights the importance of verifying distributional assumptions before selecting appropriate statistical procedures in biomechanical studies. The plots for Neck, Shoulders, Elbows and Knees can be found in this chapter's Appendix: ReHopE Hospitationen (Field Study).

8.4.4 Statistical Comparison of joint angles

To assess differences in joint angles between various task pairs within each occupation, Mann–Whitney U tests [MW47] were performed for each joint's flexion/extension angle. This test was selected because the data was not paired, since the joint angles for each task have the same range, but are not dependent. Due to the number of comparisons, results are presented in separate tables for readability.

[2] Analysis of Variance
[3] Quantile-Quantile

The comparative analysis of joint angles across occupational tasks serves to identify systematic biomechanical variations induced by specific work activities. Skilled trades often involve physically demanding movements, such as lifting, crouching, or overhead work, which are known to elicit distinct postural adaptations. By statistically evaluating joint angle distributions between task pairs, it becomes possible to determine whether certain movements consistently result in elevated ergonomic risk.

Given the non-normal distribution of joint angle data–confirmed through S-W tests and visual inspection via Q-Q plots–non-parametric methods were deemed appropriate. The Mann-Whitney U test [MW47] enables robust comparison of medians and distributional characteristics without relying on parametric assumptions. Resulting p-values indicate whether observed differences in joint mechanics are statistically significant, thereby supporting the identification of high-risk postures.

To facilitate interpretation, box plots are employed to visualize interquartile ranges and median shifts across tasks. These graphical representations highlight variability in joint loading and reveal task-dependent deviations in movement strategies. For example, increased knee flexion during load-carrying tasks or elevated trunk flexion during floor-level work may indicate biomechanical stress that warrants ergonomic intervention.

This statistical framework contributes to a detailed understanding of joint-specific responses to occupational demands and supports the development of targeted ergonomic measures aimed at reducing musculoskeletal strain.

8.4.4.1 Window Maker

Significant differences are observed across all major joint groups, including the neck, back, shoulders, elbows, and knees. Notably, both flexion/extension and rotational movements in the shoulders and elbows exhibit strong task-dependent variation. This suggests that Window Makers engage in distinct upper-body mechanics when transitioning from walking to carrying, likely due to load handling and posture adjustments.

Table 8.3 presents the results of Mann–Whitney U tests comparing joint angles between Walking and Carrying tasks for Window Makers. Out of 18 joints analyzed, 17 show statistically significant differences ($p < 0.05$), indicating widespread biomechanical variation between the two tasks.

The only joint without a significant difference is *Neck Rotation*, which may indicate consistent head orientation across tasks. The consistent significance across other joints underscores the need for ergonomic interventions tailored to carrying tasks, especially to mitigate strain in the back and lower limbs.

Overall, the results highlight the biomechanical complexity of carrying tasks in this occupation and support the use of non-parametric methods due to the non-normality of joint distributions.

8.4.4.2 Heating, Ventilation and Air Conditioning Technicians

This subsection presents the results of the statistical comparison of joint angles between Walking and Carrying tasks for HVAC Technicians. The analysis follows the same methodology as for the Window Maker, using the Mann–Whitney U test to assess whether the distributions of joint angles differ significantly between the two task types. The aim is to determine if carrying tasks introduce distinct biomechanical demands compared to walking, which is relevant for identifying task-specific ergonomic risks in this occupational group. The results are summarized in Table 8.4, highlighting which joints exhibit significant differences and thus may require targeted ergonomic interventions. Similar to Window Makers, 17 out of 18 joints show significant differences ($p < 0.05$), indicating that carrying tasks substantially alter joint mechanics.

The most pronounced differences are found in the back and shoulder joints, reflecting the physical demands of transporting tools and equipment. Both flexion/extension and abduction/adduction movements in the shoulders are significantly affected, suggesting task-specific arm positioning and load stabilization strategies. Interestingly, the angle of the *Neck Rotation* is the only joint without a significant difference, consistent with findings in Window Makers. This may imply that head orientation remains stable across tasks, possibly due

Table 8.3: Window Maker: Mann–Whitney U test results for Walking vs Carrying

Joint Angle	U	p-value	Significant
Neck Flex/Ext	1959054.0	<0.0001	Yes
Neck Lateral flexion	1364884.0	<0.0001	Yes
Neck Rotation	3770162.0	0.7003	No
Back Forward flexion	5270533.0	<0.0001	Yes
Back Lateral flexion	4299876.0	<0.0001	Yes
Back Rotation	4249203.0	<0.0001	Yes
Shoulder (Right) (Projection) Abd/Add	1139949.0	<0.0001	Yes
Shoulder (Left) (Projection) Abd/Add	2455691.0	<0.0001	Yes
Shoulder (Right) (Projection) Flex/Ext	1809887.0	<0.0001	Yes
Shoulder (Left) (Projection) Flex/Ext	1423989.0	<0.0001	Yes
Shoulder (Right) Rotation	1682056.0	<0.0001	Yes
Shoulder (Left) Rotation	4173669.0	<0.0001	Yes
Elbow (Right) Flex/Ext	1435298.0	<0.0001	Yes
Elbow (Left) Flex/Ext	2621593.0	<0.0001	Yes
Elbow (Right) Rotation	4453907.0	<0.0001	Yes
Elbow (Left) Rotation	4186053.0	<0.0001	Yes
Knee (Left) Flex/Ext	498223.0	<0.0001	Yes
Knee (Right) Flex/Ext	3953779.0	0.0111	Yes

to visual focus requirements. The results reinforce the importance of task-specific ergonomic assessments in HVAC work, where carrying tasks introduce considerable biomechanical variation. These findings also validate the use of Mann–Whitney U tests, given the confirmed non-normality of joint angle distributions.

Table 8.4: HVAC Technicians: Mann–Whitney U test results for Walking vs Carrying

Joint Angle	U	p-value	Significant
Neck Flex/Ext	446979.0	<0.0001	Yes
Neck Lateral flexion	548273.0	<0.0001	Yes
Neck Rotation	675857.0	0.0745	No
Back Forward flexion	908084.0	<0.0001	Yes
Back Lateral flexion	392123.0	<0.0001	Yes
Back Rotation	1151696.0	<0.0001	Yes
Shoulder (Right) (Projection) Abd/Add	14359	<0.0001	Yes
Shoulder (Left) (Projection) Abd/Add	356424.0	<0.0001	Yes
Shoulder (Right) (Projection) Flex/Ext	450323.0	<0.0001	Yes
Shoulder (Left) (Projection) Flex/Ext	211073.0	<0.0001	Yes
Shoulder (Right) Rotation	259553.0	<0.0001	Yes
Shoulder (Left) Rotation	865902.0	<0.0001	Yes
Elbow (Right) Flex/Ext	435795.0	<0.0001	Yes
Elbow (Left) Flex/Ext	689889.0	0.0081	Yes
Elbow (Right) Rotation	904104.0	<0.0001	Yes
Elbow (Left) Rotation	594101.0	0.0012	Yes
Knee (Left) Flex/Ext	59034.0	<0.0001	Yes
Knee (Right) Flex/Ext	843464.0	<0.0001	Yes

8.4.4.3 Lightning Protection Worker

This subsubsection presents the results of the statistical comparison of joint angles between Walking and Carrying tasks for Lightning Protection Workers. The analysis follows the same methodology as for the other occupational groups, utilizing the Mann–Whitney U test to determine whether significant differences exist in joint angle distributions between these two task types.

The goal is to identify task-specific biomechanical demands and potential ergonomic risks unique to Lightning Protection Workers. The results, summarized in Table 8.5, reveal that 16 out of 18 joints exhibit statistically significant differences ($p < 0.05$), indicating substantial changes in joint mechanics when transitioning from walking to carrying. Notably, Back Forward Flexion and Shoulder (Left) Flex/Ext do not show significant differences, suggesting consistent trunk and left shoulder postures across these tasks. These findings highlight the dynamic and physically demanding nature of carrying tasks in this occupation and underscore the importance of targeted ergonomic interventions to address joint-specific risks.

All other joints, including neck, knees, and elbows, show significant differences, emphasizing the dynamic nature of carrying tasks in this occupation. The consistent significance in rotational movements further highlights the complexity of upper-body coordination required during load transport. These results suggest that Lightning Protection Workers experience widespread joint angle variation during carrying, warranting targeted ergonomic strategies. The findings also support the use of non-parametric testing due to the skewed and non-normal distribution of joint angles.

All further tables for all task comparisons (walking vs. carrying) and bent-over-work vs. floor-work can be found in the Appendix: ReHopE Hospitationen (Field Study).

Table 8.5: Lightning Protection Worker: Mann–Whitney U test results for Walking vs Carrying

Joint Angle	U	p-value	Significant
Neck Flex/Ext	20607556.5000	<0.0001	Yes
Neck Lateral flexion	15518518.5000	<0.0001	Yes
Neck Rotation	21831547.5000	0.0051	Yes
Back Forward flexion	22200080.5000	0.2462	No
Back Lateral flexion	24396725.5000	<0.0001	Yes
Back Rotation	16497266.5000	<0.0001	Yes
Shoulder (Right) (Projection) Abd/Add	27397729.5000	<0.0001	Yes
Shoulder (Left) (Projection) Abd/Add	28902921.5000	<0.0001	Yes
Shoulder (Right) (Projection) Flex/Ext	21632710.5000	0.0002	Yes
Shoulder (Left) (Projection) Flex/Ext	22430757.5000	0.8931	No
Shoulder (Right) Rotation	26335590.5000	<0.0001	Yes
Shoulder (Left) Rotation	27105661.5000	<0.0001	Yes
Elbow (Right) Flex/Ext	25954345.5000	<0.0001	Yes
Elbow (Left) Flex/Ext	28474698.5000	<0.0001	Yes
Elbow (Right) Rotation	13975631.5000	<0.0001	Yes
Elbow (Left) Rotation	18876544.5000	<0.0001	Yes
Knee (Left) Flex/Ext	21392709.5000	<0.0001	Yes
Knee (Right) Flex/Ext	21625915.5000	0.0002	Yes

8.4.5 Statistical Comparisons of performed tasks

This subsection provides a detailed overview of the statistical comparisons performed between different occupational tasks based on joint angle data. By systematically analyzing how joint movements vary across tasks such as walking, carrying, floor-work, and bent-over work, the study aims to identify which activities are as-

sociated with the greatest ergonomic risk. The results are presented in tabular form, highlighting statistically significant differences in joint angles for each occupation and task pair. This approach enables a nuanced understanding of task-specific biomechanical demands and supports the development of targeted ergonomic interventions. The following tables and analyses illustrate the key findings from these statistical comparisons.

8.4.5.1 Exemplary task comparison: Statistical Analysis

To illustrate the practical relevance of joint angle analysis in occupational ergonomics, this subsection presents a focused comparison between two representative tasks. By selecting task pairs that differ in biomechanical demands–such as walking versus carrying or floor-work versus bent-over work–the analysis highlights how specific movements influence joint mechanics. These comparisons serve as concrete examples of how statistical methods can uncover meaningful differences in posture and strain. The use of non-parametric tests, such as the Mann-Whitney U test [MW47], ensures robustness given the non-normal distribution of joint angle data. Box plots are employed to visualize variability and median shifts, offering intuitive insights into task-specific joint loading. These findings not only validate the analytical framework but also provide actionable evidence for ergonomic interventions. By demonstrating how joint angles vary across tasks, this exemplary analysis supports the broader goal of identifying high-risk movements and informing the design of assistive technologies and workplace adaptations.

Figure 8.4 presents two box plots illustrating statistically significant differences in joint angles for HVAC Technicians. The upper plot compares right knee flexion/extension angles during *walking* versus *carrying* tasks, while the lower plot contrasts trunk forward flexion angles during *floor-work* versus *bent-over work*. Both comparisons yielded $p < 0.001$ via Mann-Whitney U test [MW47]s, indicating robust differences in joint mechanics across task types.

The knee flexion plot reveals a marked increase in joint angle variability and median flexion during carrying tasks. This suggests that load-bearing activities impose greater biomechanical demands on the lower limbs, consistent with prior findings on occupational strain in skilled craft trades involving frequent lifting and transport [CV10]. The elevated interquartile range further implies inconsistent movement strategies among participants, potentially due to individual adaptations to load handling.

In the trunk flexion comparison, floor-work tasks exhibit significantly higher median flexion angles and a broader distribution than bent-over work. This aligns with ergonomic risk classifications from DGUV 208-033, which identify prolonged trunk flexion beyond $60\,\mathrm{deg}$ as a high-risk posture [Deu15]. The data underscore the need for targeted interventions–such as adjustable work surfaces or supportive exoskeletons–to mitigate spinal loading during low-level tasks.

Overall, these plots exemplify how task-specific analysis of joint angles can inform ergonomic risk profiling. By quantifying deviations in movement patterns, the "ReHopE Hospitationen" study contributes to evidence-based recommendations for workplace design and assistive technology deployment.

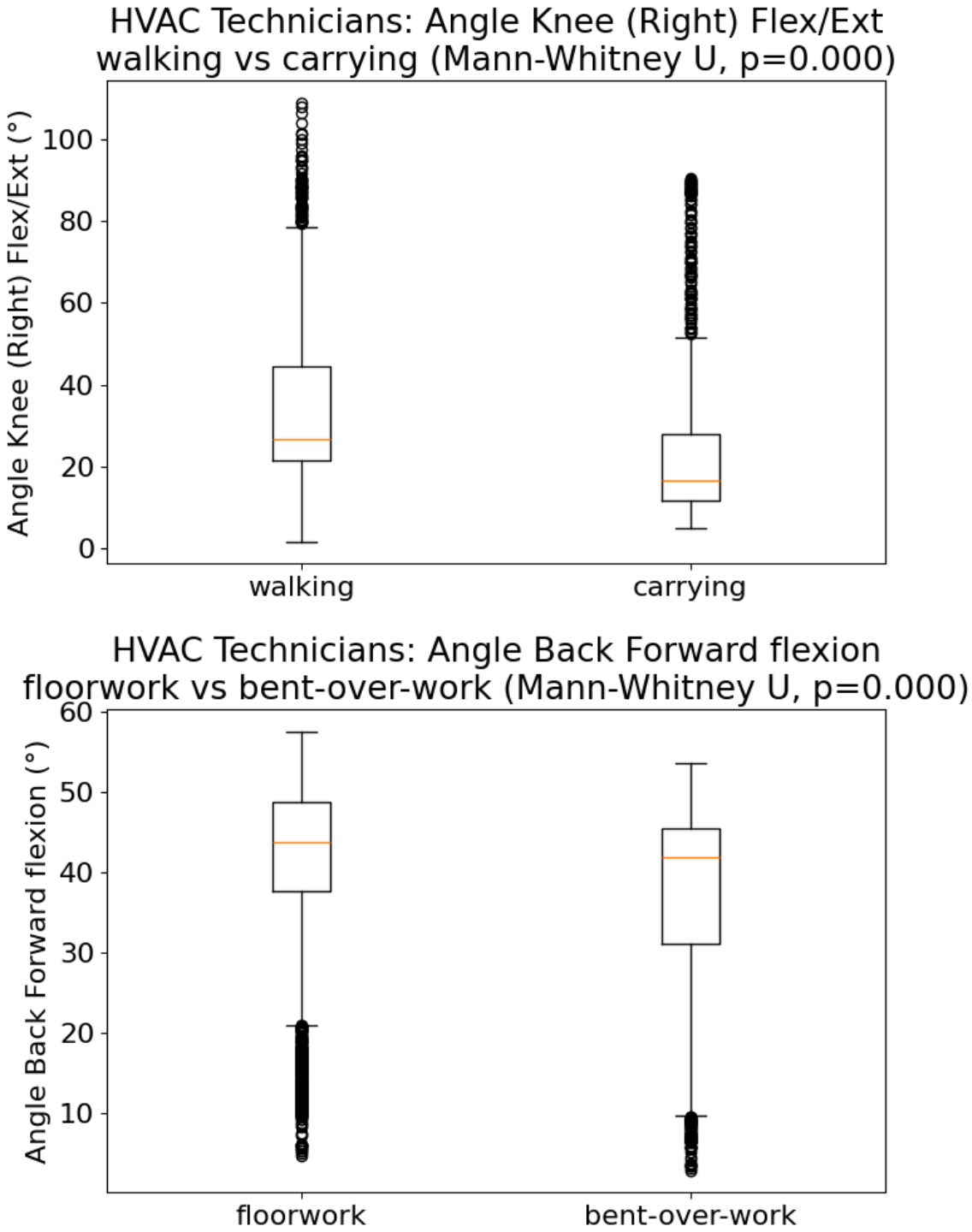

Figure 8.4: Box-plots showing statistical comparison of Knees flexion (walking vs. carrying) and trunk flexion (bent-over-work vs. floor-work) for HVAC Technicians. Tests performed: t-test or Mann–Whitney U as appropriate.

8.4.6 Task-Specific Ergonomic Risk Interpretation by Exposure Time

The classification of ergonomic risk by task type provides a complementary perspective to joint-specific analyses. While anatomical regions such as the knees or back may exhibit high cumulative exposure to non-ergonomic postures, the distribution of risk across tasks reveals which activities contribute most significantly to biomechanical strain. This approach enables the identification of high-risk occupational scenarios and supports the prioritization of ergonomic interventions. Figure 8.5 presents a comparative overview of ergonomic risk

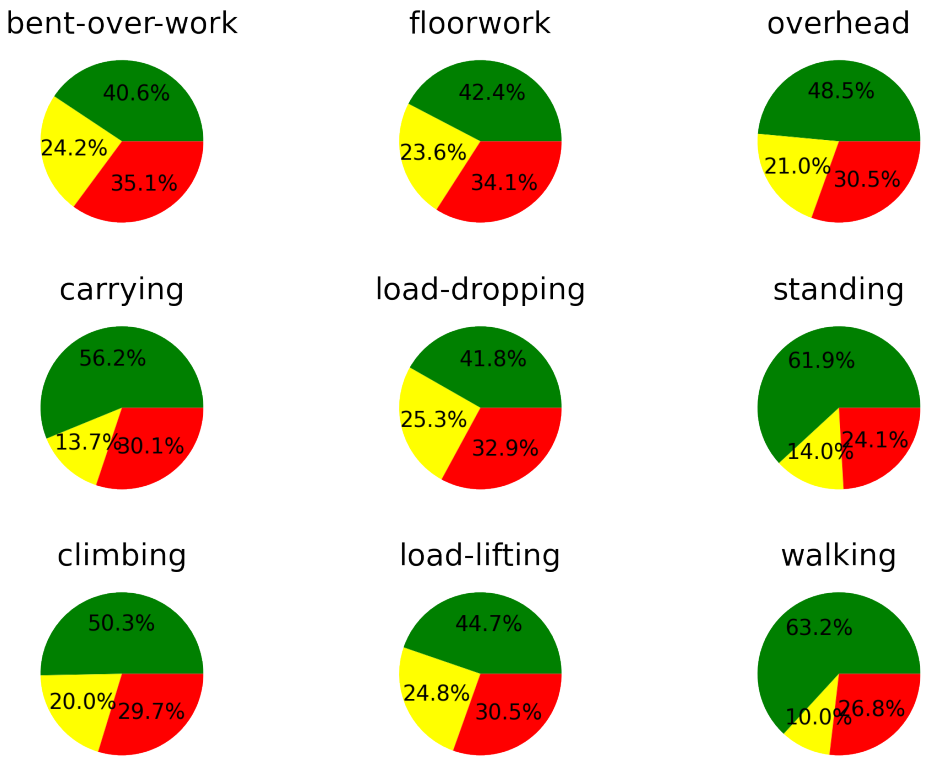

Figure 8.5: Exposure-time distribution pie charts for each task group
green/yellow/red zones represent
"acceptable/conditionally acceptable/ not acceptable"
values, respectively.

distributions across nine task groups, based on joint angle classifications. Each pie chart is segmented into green (acceptable), yellow (conditionally acceptable), and red (not acceptable) zones, following the ergonomic assessment criteria defined in DGUV 208-033 [Deu15]. These visualizations provide a concise yet powerful representation of task-specific biomechanical exposure, enabling prioritization of interventions.

Tasks such as *floor-work* and *bent-over-work* exhibit elevated ergonomic risk, with red-zone proportions of 34.1% and 35.1% respectively. These findings are consistent with the statistical results in subsection 8.4.4 and subsection 8.4.5, where significant deviations in trunk and knee flexion were observed. The high prevalence of non-acceptable joint angles in these tasks underscores the need for targeted ergonomic redesign, such as adjustable work surfaces or supportive exoskeletons for low-level operations.

Load-dropping and *load-lifting* also show considerable red-zone exposure (32.9% and 30.5%), reflecting the biomechanical strain associated with dynamic transitions and manual handling. Interestingly, *carrying* tasks, while involving load transport, demonstrate a relatively higher proportion of acceptable joint angles (56.2%),

suggesting that postural stability during locomotion may mitigate some ergonomic risks. However, this does not consider the joint strain due to the carrying of weight.

In contrast, *standing* and *walking* tasks present the most favorable profiles, with green-zone proportions of 61.9% and 63.2% respectively. These tasks involve minimal joint deviation and are less likely to induce musculoskeletal strain, aligning with previous literature on low-risk occupational postures [CV10]. *Climbing* and *overhead* work fall in an intermediate category, with red-zone exposures around 30%, indicating moderate ergonomic concern. However, this excludes the consideration of biomechanical load due to unfavorable manipulation of external load far away from the body.

Overall, the pie chart matrix in Figure 8.5 complements the quantitative findings of the "ReHopE Hospitationen" study by offering a visual synthesis of task-specific risk. It reinforces the conclusion that interventions should prioritize tasks with high red-zone proportions–particularly those involving crouched, bent, or floor-level postures. These insights are critical for guiding the design of assistive technologies and workplace modifications aimed at reducing long-term musculoskeletal burden in skilled craft trades.

8.4.7 Cross-Occupational ROM[4] Analysis

The comparative analysis of joint-specific ROM across occupational groups serves to identify systematic differences in biomechanical demands imposed by distinct work environments. Skilled trades such as window installation, HVAC maintenance, and lightning protection involve varied task profiles, each characterized by unique postural requirements and movement constraints. By quantifying the interquartile ranges and median shifts of joint angles–particularly in the neck, back, and knees–this analysis provides insight into how occupational roles influence joint mobility and variability.

Understanding these differences is essential for ergonomic profiling and the development of targeted interventions. Wider ROM distributions may indicate inconsistent movement strategies, elevated physical strain, or a lack of standardized workflows, all of which contribute to increased risk of MSD. Conversely, narrower distributions may reflect constrained or repetitive postures that also warrant ergonomic attention.

Figure 8.6 presents a comparative box plot analysis of joint-specific ROM across three professions–Window Makers, HVAC Technicians, and Lightning Protection Workers. The figure illustrates the interquartile ranges of joint angles for the neck, back, and knees, offering insight into the biomechanical demands imposed by different occupational tasks.

The neck ROM distributions are relatively narrow across all professions, suggesting consistent head posture and limited angular deviation. This may reflect the visual focus required during precision tasks such as installation or inspection, where head movement is constrained to maintain alignment. Despite this consistency, even small deviations in neck posture can contribute to cumulative strain over time, particularly in tasks involving overhead work or prolonged downward gaze [CV10].

In contrast, the back and knee joints exhibit substantially wider ROM distributions, indicating greater variability and task-dependent loading. For example, Lightning Protection Workers show elevated back flexion ranges, likely due to frequent climbing and crouching during rooftop installations. Similarly, HVAC Technicians demonstrate pronounced knee flexion variability, reflecting the biomechanical complexity of floor-level tasks and load handling.

These findings align with ergonomic risk classifications from DGUV 208-033, which identify trunk flexion beyond 60 deg and deep knee bending as high-risk postures when sustained or repeated [Deu15]. The broader interquartile ranges observed in these joints suggest inconsistent movement strategies and potential for overuse injuries, especially in professions with less standardized workflows.

Overall, Figure 8.6 reinforces the importance of joint-specific ergonomic assessment in occupational health. By quantifying ROM variability across professions, the "ReHopE Hospitationen" study provides actionable

[4] Range of Motion

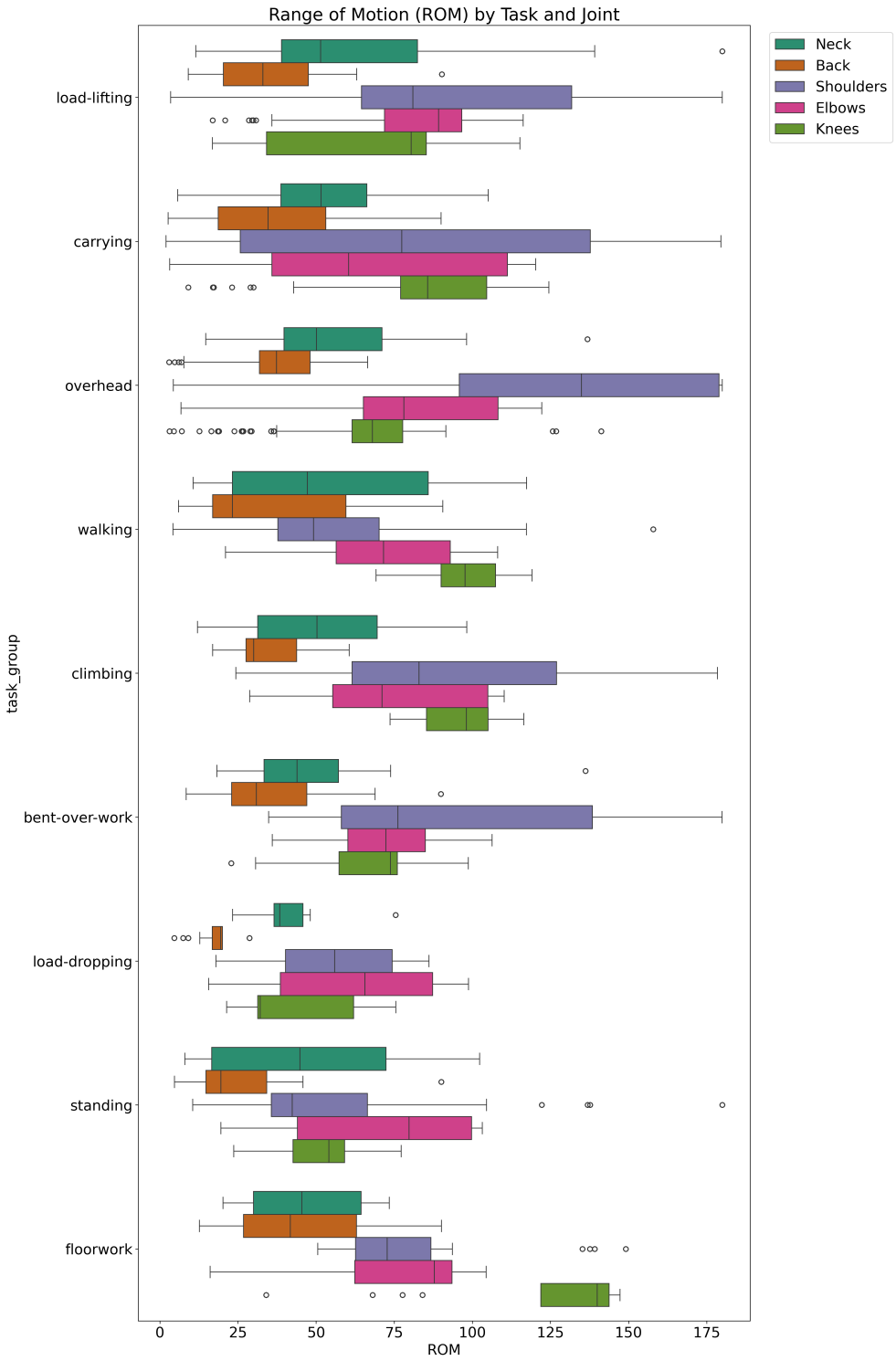

Figure 8.6: Comparison of Range of Motion across all three professions.
Each box-plot shows the inter-quartile range of joint angles for neck, back, and knees.

data for designing targeted interventions–such as task rotation, posture training, and assistive devices–to mitigate musculoskeletal risk and enhance long-term worker well-being.

8.4.8 Interpretation of Statistical comparisons

The nonparametric Mann–Whitney U tests revealed that joint angle distributions differed significantly for most joints across the various task pairs in all three occupations. These results confirm that different occupational tasks elicit distinct joint movement patterns, reinforcing the need for task-specific ergonomic assessments.

Window Maker

For Window Makers, significant differences were observed in nearly all joint angles when comparing walking versus carrying, load-dropping versus load-lifting, and standing versus climbing. However, some joints showed no significant difference for specific task pairs. Notably, Neck Lateral Flexion angles did not differ significantly between load-dropping and load-lifting, nor between standing and climbing, suggesting similar neck side-bending postures in these conditions. Likewise, Neck Rotation during walking and carrying tasks was statistically similar. Shoulder Flexion/Extension angles on both sides showed no significant difference between standing and climbing, indicating relatively consistent shoulder flexion/extension positioning in these tasks.

HVAC Technicians

Among HVAC Technicians, most joint angle comparisons across walking versus carrying, floor-work versus bent-over work, load-dropping versus load-lifting, and standing versus climbing were significant, reflecting task-specific postural adaptations. Exceptions included Neck Rotation during walking versus carrying, indicating similar rotational neck postures in these two tasks. Some shoulder and elbow joint angles did not differ significantly during load-dropping versus load-lifting, specifically Shoulder (Right Projection) Flexion/Extension and Elbow (Left) Flexion/Extension and Elbow (Right) Rotation. Additionally, Elbow (Left) Rotation angles showed no significant difference between floor-work and bent-over work or between load-dropping and load-lifting, suggesting consistent forearm rotational postures during these pairs.

Lightning Protection Worker

For Lightning Protection Workers, significant differences in joint angles were generally consistent across walking versus carrying, floor-work versus bent-over work, and load-dropping versus load-lifting. Due to data limitations, some standing versus climbing comparisons could not be conducted. The significant differences in most neck, shoulder, and knee joints underscore the substantial postural variation associated with these task pairs. Non-significant differences, where present, tend to be rare and limited to a few joint/task combinations, further emphasizing the unique demands of each occupational task.

Overall Implications

These findings confirm that different work tasks impose distinctive joint movement demands across occupational groups. The presence of statistically significant differences in joint angles suggests that ergonomic interventions and biomechanical models should consider the specific postural characteristics of each task to effectively mitigate musculoskeletal risks. Conversely, joint angles with no significant differences across certain tasks may represent shared postural patterns, potentially serving as targets for standardized ergonomic controls.

Overall, these nonparametric results confirm that each profession's workflow produces unique angular profiles, with load transitions and mixed locomotor–postural tasks driving the largest deviations (see Table 8.3, Table 8.4 and Table 8.5; Figure 8.4 and Figure 8.6).

8.4.9 Implications for Ergonomic Design

The ergonomic risk profiles derived from both statistical analysis and pie chart visualizations underscore the need for targeted design improvements. Assistive technologies such as exoskeletons should be tailored to support joints most affected by high-risk tasks. For instance, devices that alleviate strain in the lower back and knees may be particularly beneficial for floor-work and bent-over tasks.

Moreover, workplace modifications such as adjustable work surfaces, improved tool ergonomics, and task rotation schedules can help mitigate cumulative strain. Future studies should explore the longitudinal impact of such interventions on musculoskeletal health outcomes.

8.4.10 Conclusion

The task-specific ergonomic risk analysis presented in this chapter has enabled the identification of occupational activities associated with the highest levels of biomechanical strain. Tasks such as floor-work, bent-over work, and overhead work consistently exhibited elevated proportions of non-acceptable joint angles, particularly in the knees, back, and shoulders. It is important to note that the study was conducted with a limited sample size of three participants, each representing a different skilled trade. While this restricts the generalizability of the findings and precludes statistical representativeness, the results nonetheless provide valuable indications of typical ergonomic risks and movement patterns encountered in these professions. These insights serve as a data-driven foundation for selecting representative high-risk tasks to be further examined under controlled laboratory conditions [Dro+]. The next chapter (chapter 9) builds upon these results by investigating the usability and effectiveness of assistive technologies –specifically exoskeletons– during the execution of these tasks, combining objective strain measurements with subjective user feedback.

8.5 CRediT contribution statement

Pedro Fernando Arizpe Gómez: Conceptualization, Data curation, Formal analysis, Investigation, Methodology, Resources, Software, Validation, Visualization, Writing – Original Draft, Writing – Review and Editing.
Tim Stratmann: Conceptualization, Funding acquisition, Resources, Supervision.
Sandra Drolshagen: Visualization, Writing – Review and Editing.
Andreas Hein: Funding acquisition, Project administration, Resources, Review and Editing, Supervision.

9 Markerless Ergonomic Assessment and Strain Analysis with Craftspeople (ReHopE Fokusgruppe Study)

Parts of this chapter are part of a publication in progress:
Sandra Drolshagen, Pedro Arizpe-Gómez, Tim Stratmann, and Andreas Hein. "Exoskeletons in Skilled Trades: Challenges and Chances". In Publishing

9.1 Introduction

The aging population poses diverse challenges for blue collar enterprises. Demographic shifts are increasing the average age of employees in skilled trades [Wil+23], intensifying the need to preserve work ability and employability. Physically demanding tasks, such as repetitive lifting and awkward postures, contribute to MSD, which account for nearly a quarter of sick days in Germany [EU-19; Ins18]. These conditions often lead to early retirement or reduced availability [OB24], resulting in personal and economic burdens [EU-12].

Simultaneously, digitalization has reduced the appeal of skilled trades among younger generations [Het24], who expect modern tools and technologies [Het24]. This trend exacerbates the shortage of skilled workers [Wil24]. Despite their economic importance, skilled trades receive limited research attention [Sho+18], and digitization efforts face challenges such as cost, organizational change, and data security [LEJ18].

Exoskeletons offer a potential solution. These electromechanical devices augment strength or support weakened limbs [Val24], with applications in military [Pro+22], nursing [PAC24], and rehabilitation [Kan+25].[Dro+] In skilled trades, task-specific exoskeletons are emerging [DNH24; Kon22], but usability and acceptance remain critical [Mos+19; PWK20].

This study developed and validated two automated strain-assessment methods–video-based REBA and sEMG–and evaluated them in a within-subject user study in which five skilled-trade workers performed representative tasks with and without exoskeleton support. Objective biomechanical measures were triangulated with subjective questionnaires and expert ergonomic assessments, and a post-study focus group contextualized the results and elicited concrete user requirements. The combined approach therefore aimed to assess usability, acceptance, and perceived support of exoskeletons in skilled trades while identifying practical improvement potentials for future assistive systems.

9.2 Scientific Background and Objectives

The study aimed to:

- Assess perceived and measured support provided by three exoskeleton systems.
- Evaluate user acceptance, usability, and physical strain through questionnaires and ergonomic analysis.
- Identify user requirements and improvement suggestions via structured focus group discussion.

9.2.1 Contributions

This study provides insights into the real-world usability and acceptance of exoskeletons in skilled trades. The combination of objective and subjective data supports the development of user-centered assistive technologies and informs future ergonomic interventions.

9.3 Materials and Methods

This section describes the experimental setup, materials, and procedures used in the ReHopE Fokusgruppe Study. It outlines the study design, the exoskeleton systems evaluated, the sensing modalities employed for objective data collection, and the tasks performed by participants. Detailed protocols for participant recruitment, data acquisition, and ethical considerations are also provided to ensure transparency and reproducibility of the research.

9.3.1 Study Design

A mixed-methods within-subject experiment was conducted at OFFIS, including pre-questionnaires, task execution with and without exoskeletons, post-questionnaires, and a moderated focus group. The study was designed as a within-subject experiment with randomized task order using a Latin Square design.

Figure 9.1: From left to right: A: CrayX, B: Skelex, C: Noonee [AG22]

9.3.2 Exoskeletons

Three commercial systems were evaluated:

- **CrayX CrayX (2018).** Active back-worn exoskeleton with hip-mounted motors assisting lifting. Supports up to 30 kg, adjustable assistance levels. (see Figure 9.1A [Dro+])
- **Skelex Overhead Exoskeleton (2018).** Passive shoulder-worn device transferring up to 4 kg per arm to the lower body during overhead work. (see Figure 9.1B [Dro+])
- **Noonee Chairless Chair.** Passive hip-and-thigh device enabling sitting, standing, and walking. Reduces lower-back strain; seat height is adjustable. (see Figure 9.1C)[1]

9.3.3 Sensing Modalities

Three sensing modalities captured objective data during task execution:

IMUs 13 wearable sensors (CAPTIV system).
Surface Electromyography 4 sensors (Delsys Trigno Avanti sEMGs).

[1] This exoskeleton was not systematically compared, since it did not offer any support for the tasks performed in this study.

Camera AzureKinect for RGB video capture[2].

9.3.4 Tasks and Protocols

Participants performed four typical trade tasks:

- Lifting and carrying heavy loads
- Walking on unstable ground (a metallic grid)
- Working in kneeling and bent-over positions (placing of a heating tube inside a grid)
- Overhead work (sorting magnets on a whiteboard)

Each task was performed three times with and without an exoskeleton. Two exoskeletons were tested: the GBS[3] CrayX 2018 and the Skelex 2018. The third exoskeleton (Nonee) was not compatible with any of the tasks, so it was not included in the quantitative analysis. After each task, participants marked body regions under strain on a body sketch.

9.3.5 Outcomes

The **Primary Outcomes** of the study were quantitative measures of ergonomic risk and muscle activation, as well as qualitative insights into exoskeleton usability and user acceptance. Objective outcomes included frame-wise REBA scores and mean envelope-filtered sEMG amplitudes for each task, participant, and muscle group. These metrics enabled direct comparison of physical strain with and without exoskeleton support.

The **Secondary Outcomes** comprised expert ergonomic risk ratings, participant questionnaire responses (attitude, perceived support, usability, trust; where 0 is the lowest and 1 is the highest), and qualitative feedback from focus group discussions. Together, these outcomes provided a comprehensive assessment of the effectiveness, limitations, and user perceptions of exoskeletons in skilled trades, informing recommendations for future ergonomic interventions and assistive device design.

9.3.6 User Study

Five skilled-trade workers (two carpenters (window makers), two electrical engineers (lightning protection technicians), one HVAC technician) participated. Six task categories were identified via site visits and workshops (see Observational field study on ergonomic risk with craftspeople (ReHopE Hospitationen Study)): lifting weights, carrying weights, walking on normal ground, walking on uneven ground, overhead work, and kneeling work. Each participant performed each task twice–once with an exoskeleton (CrayX for the first three tasks; Skelex for overhead work) and once without. Order was randomized via a Latin-square design. Pre- and post-task questionnaires assessed attitude, expectations, perceived relief, and acceptance. After trials, a joint focus group explored user experiences, risks, and future requirements; the Chairless Chair was also tested in that session.

Timeline of Study

Upon arrival, participants provided informed consent and completed a pre-task questionnaire covering demographics, prior exoskeleton experience, and attitudes. Participants were then equipped with 13 IMUs and 4 sEMG sensors (dominant side: thigh, lower back, neck, upper arm). Body-hair removal and light abrasion

[2] The AzureKinect provides depth information and skeletal tracking capabilities, but due to a software error, the images could not be processed by the BT system, since they were transformed to the color space before saving, resulting in a format mismatch.
[3] German Bionic Systems

were performed to ensure sEMG signal quality. After exoskeleton familiarization, tasks were performed in randomized order. Post-task questionnaires assessed acceptance, perceived usefulness, and user-friendliness. A moderated focus group concluded the session, gathering qualitative insights.

Participants

Participants from various skilled trades took part in the study. Demographic data (age, gender, height, weight) and prior experience with exoskeletons were collected (see Table 9.1). All participants provided informed consent and were anonymized using a codeword system.

Table 9.1: Detailed participant information

Code	Age	Sex	Height (cm)	Weight (kg)	Experience (years)	Qualification	Occupation
30HH (2)	58	male	185	90	35	other	Lightning protection
U76B (4)	34	female	176	76	7	Skilled worker	Carpentry
M196 (3)	19	male	180	73	2	Skilled worker	HVAC technology
B90O (5)	22	male	190	83	2	Skilled worker	Carpentry
T70K (1)	34	male	170	74	16	Skilled worker	Lightning protection

9.3.7 Evaluation Methods

This section details the evaluation methods employed in the ReHopE Fokusgruppe Study to assess the ergonomic impact and user acceptance of exoskeletons in skilled trades. While a mixed-methods approach was adopted –integrating objective biomechanical measurements with subjective user feedback and expert assessments –the primary focus of the analysis is on objective strain assessment. The evaluation framework was designed to capture both quantitative and qualitative data, but the main emphasis throughout this study is placed on quantifying physical strain, usability, and the actual support provided by the tested exoskeleton systems.

Objective measures of physical strain, such as biomechanical load and muscle activation, form the core of the analysis and are essential for quantifying the support delivered by exoskeletons. Although perceived support reported by users is also considered, it is treated as a complementary perspective to the objective findings. Perceived support reflects the users' subjective experience of relief, comfort, and assistance during task execution, which can differ from the objectively measured effects due to factors such as device fit, usability, and individual expectations. High perceived support is often associated with greater acceptance, sustained use, and overall satisfaction, even when objective improvements are modest. Therefore, both actual and perceived support were systematically evaluated, but the results and discussion are primarily driven by the objective strain assessment to ensure a robust and reproducible understanding of exoskeleton effectiveness.

Objective strain assessment was conducted using two primary modalities: automated Rapid Entire Body Assessment (REBA [HM00]) based on video-derived joint angles, and surface electromyography (sEMG) to quantify muscle activation. These measures were complemented by structured questionnaires and focus group interviews, which provided insights into user experience, acceptance, and improvement suggestions. The combination of these methods ensured robust validation of findings and facilitated the identification of key requirements for future movement analysis in skilled trades.

9.3.7.1 Automated Rapid Entire Body Assessment

Only the RGB data were used for the REBA [HM00] analysis, as the CAPTIV system experienced technical failures during data collection. In cases where CAPTIV data were available, they were subsequently used to synchronize the video recordings with the sEMG data.

Automated ergonomic evaluation was performed in several stages. First, video recordings of all task executions were manually labeled according to the specific activity performed. In future work, this step was automated by training a neural network to classify tasks directly from video footage, eliminating the need for manual labeling.

Based on the task labels, the full-length videos were automatically segmented into shorter clips representing individual activities, using timestamped labels. For each clip, 2D joint keypoints were extracted frame by frame using a deep learning-based pose estimation framework (Detectron2 [Wu+19]). The resulting 2D keypoint sequences were post-processed to interpolate missing detections and ensure temporal continuity.

To enable 3D analysis, a lifting model was applied to the 2D keypoints, reconstructing 3D joint positions for each frame. From these, REBA-relevant joint angles were calculated using vector-based geometry, including neck, trunk, upper arm, lower arm, and leg angles. For frames with missing or unreliable detections, linear interpolation was used to fill gaps, ensuring a complete time series for each activity segment.

Frame-wise REBA sub-scores were computed according to the official scoring system, with the following logic: trunk, neck, and leg scores were derived from the corresponding joint angles; upper and lower arm scores were based on shoulder and elbow angles, respectively; a default wrist score was assigned due to the lack of reliable wrist tracking. Some variables required for a complete REBA score, such as load/force, coupling, and activity modifiers, could not be measured automatically and were therefore defined as fixed values based on the nature of each task. These include:

- **Load/Force Score**: A value of +2 was assigned for lifting and carrying weights, corresponding to a moderate static load without sudden force increases.
- **Coupling Score**: A value of +1 was assigned for all tasks to reflect an ”acceptable but not ideal” hand coupling. For kneeling work, this score was increased to +3 due to the ergonomically suboptimal grip and potentially unsafe hand positioning.
- **Activity Score**: A base score of +1 was added for all tasks except for walking on level ground. Additional points were assigned as follows:
  - +1 for lifting and setting down tasks due to large range of motion.
  - +1 for walking on uneven ground due to unstable base of support.
  - +1 for overhead work due to static postures held for extended periods, and an additional +1 for repeated small-range motions.
  - +1 for kneeling work due to small range motion, and another +1 if the task was held for over one minute (indicating sustained posture with body parts held static).
- **Wrist Posture Score**: A default value of +1 was added across all tasks due to wrist twisting.

The extracted joint angles and fixed modifiers were combined using the official REBA [HM00] tabular scoring system. Regional scores were computed for trunk, neck, and legs, as well as for upper limbs and wrists. These were merged using lookup tables to generate composite scores, which were then adjusted by the load, coupling, and activity modifiers to yield a final frame-wise REBA score. The resulting scores were aggregated across task instances and stratified by task type, participant, and exoskeleton usage. Boxplots and descriptive statistics were generated to visualize score variability and support interpretation. This automated REBA framework enables scalable, reproducible ergonomic assessment in real-world environments by integrating deep learning-based pose estimation, rule-based scoring, and contextual modifiers.

9.3.7.2 Surface Electromyography Analysis

Surface electromyography (sEMG) was employed to quantify muscle activation during task execution. Unlike the automated REBA pipeline, the sEMG analysis required extensive manual intervention due to multiple technical limitations encountered during data collection and processing.

The originally planned synchronization between the sEMG signals and the AzureKinect-based video recordings was impeded by inconsistencies in timestamp alignment and sensor drift. Synchronization was therefore

performed manually by comparing visible sensor movements in the video with signal changes in the IMUs embedded in the sEMG sensors, requiring frame-by-frame inspection of the video data.

In several recording sessions, the automatic calibration metadata were not preserved, necessitating the use of raw voltage signals (mV) for all subsequent analyses. The manually synchronized data were segmented into task-specific intervals using timestamped labels derived from the video recordings, which were then applied to the high-frequency sEMG data (sampled at 4000 Hz) to enable task-wise analysis of muscle activation.

sEMG was recorded from four muscle regions, with the following specific muscles targeted: neck (Trapezius pars descendens), upper arm (Biceps brachii), lower back (Erector spinae), and thigh (Rectus femoris). Sensor placement followed standard anatomical guidelines to ensure signal quality and comparability across participants.

Signal preprocessing followed established recommendations for sEMG analysis. Each channel was band-pass filtered using a 4th-order Butterworth filter (20–500 Hz), rectified, and then low-pass filtered at 6 Hz (4th-order Butterworth) to obtain the envelope. All filters were applied with forward-reverse zero-phase filtering to avoid phase distortion. No downsampling was performed prior to averaging.

Rows with incomplete datapoints –specifically, those containing missing values in the dataset –were excluded prior to aggregation. For each participant, task, and muscle region, the mean envelope amplitude was computed. Results were aggregated at three levels: (a) per-activity (aggregated across participants for each task), (b) per-worker (aggregated across activities and regions for each participant), and (c) per-muscle (aggregated across participants and activities for each muscle group). Paired comparisons were restricted to observations where both "with" and "without" exoskeleton measurements were available for the same participant and task.

Statistical significance was assessed by first testing for normality using the S-W test ($\alpha = 0.05$). For within-subject comparisons, paired t-tests [Vir+20] [Dav63] were used when normality was satisfied, and Wilcoxon signed-rank tests [Wil45] otherwise.

Because the analysis was based on raw mV amplitudes rather than normalization to a maximum voluntary contraction (MVC[4]), cross-subject comparisons are limited; emphasis is therefore placed on within-subject contrasts. When combined with the posture-based REBA scores, the sEMG results provide complementary biomechanical evidence for the evaluation of exoskeleton support.

Subjective Assessments

Structured questionnaires were administered, drawing on validated instruments including the NASA-TLX[5] [HS88], SUS[6] [Bro96], NARS[7] [Na06], and established exoskeleton assessment protocols [Kel23]. These instruments were selected to systematically capture user perceptions of workload, usability, acceptance, and device-specific experiences.

Focus Group

A structured interview guide probed experiences, challenges, risks, and design suggestions. A detailed protocol captured participants' insights and actionable recommendations, which were integrated into the results discussion. However, the main focus of this study remains on the objective biomechanical assessments. [Dro+]

[4] Maximum Voluntary Contraction
[5] NASA Task Load Index
[6] System Usability Scale
[7] Neuroergonomic Assessment Rating Scale

9.3.8 Kinematic Variables and Analytical Measures

This subsection defines the main kinematic variables and analytical measures used to quantify physical strain and ergonomic risk in the study. It details how joint angles were extracted from video-based pose estimation and describes the derivation of composite metrics such as REBA scores and muscle activation levels. The section also outlines the subjective measures collected through questionnaires and focus group feedback, providing a comprehensive overview of the data sources and analytical approaches employed for movement analysis and ergonomic evaluation.

Main Kinematic Variable(s)

The main kinematic variables analyzed were joint angles derived from video-based pose estimation. These included neck, trunk, upper arm, lower arm, and leg angles, extracted frame-by-frame using Detectron2. These variables formed the basis for ergonomic risk assessment and quantification of physical strain during task execution.

Derivated Variables

From the main kinematic variables, several derived measures were computed:

- **REBA Scores:** Composite ergonomic risk scores calculated using official REBA [HM00] methodology, combining joint angles with contextual modifiers (load, coupling, activity, wrist posture).
- **Muscle Activation:** Envelope-filtered sEMG signal amplitudes for neck, upper arm, lower back, and thigh regions, representing muscle effort during tasks.

Subjective Measures

Subjective measures were directly obtained from questionnaires (NASA-TLX, SUS, NARS, custom exoskeleton items), body region strain sketches, and qualitative feedback from focus group discussions.

9.3.9 Ethical and Legal Considerations

All data were anonymized using participant-generated codewords. Video, IMU, and sEMG data were stored securely and will be retained for at least 10 years. Participants could withdraw at any time without consequences. No deception was used in the study. The study was approved by the OFFIS e. V. Studienboard under the reference number 2023P015.

9.4 Results

This section presents the results of the ReHopE Fokusgruppe Study, integrating objective biomechanical measurements, expert ergonomic assessments, and subjective user feedback. The analysis focuses on quantifying the ergonomic impact and user acceptance of exoskeletons in skilled trades, with particular emphasis on task-specific differences in physical strain and perceived support. By triangulating data from automated REBA scoring, surface electromyography (sEMG), structured questionnaires, and focus group discussions, the study provides a comprehensive evaluation of the tested exoskeleton systems.

The results are organized to highlight both quantitative and qualitative findings [Dro+]. Objective strain assessments are reported first, detailing differences in ergonomic risk and muscle activation across tasks and conditions. These are followed by expert evaluations and user-reported outcomes, which contextualize the biomechanical data and offer insights into practical usability, acceptance, and improvement potentials.

9.4.1 Objective Strain Assessment

This subsection presents the objective strain assessment results obtained from the automated REBA scoring and surface electromyography (sEMG) analyses. By quantifying ergonomic risk and muscle activation across different tasks and exoskeleton conditions, these objective measures provide a data-driven evaluation of physical strain experienced by participants. The findings enable direct comparison of ergonomic impact between supported and unsupported scenarios, highlighting task-specific differences and the effectiveness of exoskeleton interventions. The results are visualized using boxplots and summarized with descriptive statistics to facilitate interpretation and support evidence-based conclusions.

9.4.1.1 Rapid Entire Body Assessment Analysis

Figure 9.2 presents the distribution of automated REBA scores across six typical skilled trade tasks, comparing conditions with and without exoskeleton support. For each task, the boxplots illustrate the IQR[8], median, and variability of ergonomic risk as quantified by the REBA methodology. Notably, tasks such as lifting, setting down, and overhead work exhibit the highest median REBA scores, reflecting elevated ergonomic risk regardless of exoskeleton use. The presence of exoskeletons appears to reduce median scores slightly in some tasks (e.g., lifting), while in others (e.g., kneeling), the difference is negligible or even reversed.

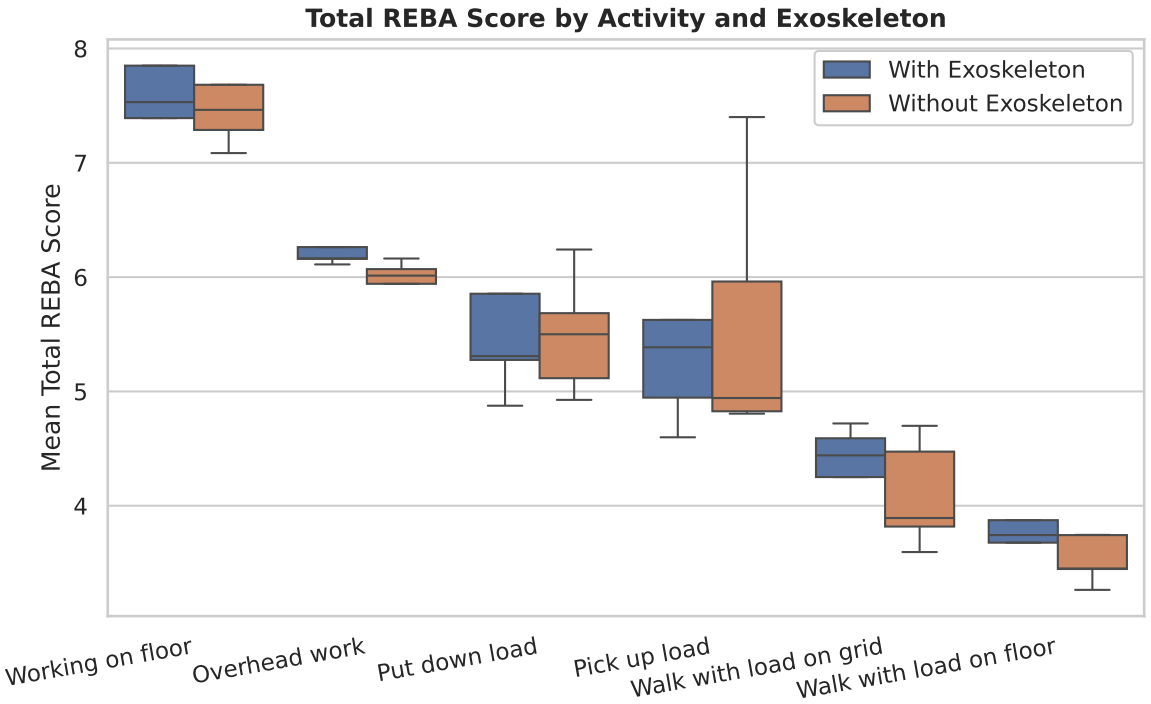

Figure 9.2: Automated REBA results for all six considered tasks with and without exoskeleton. Each box represents the IQR, with the median indicated by a horizontal line and whiskers extending to 1.5 ×IQR. Outliers beyond this range are not shown to enhance the visibility of the box distributions. A higher REBA score indicates greater ergonomic risk.

The variability within each task, as indicated by the spread of the boxplots, suggests substantial inter-individual or intra-task differences in posture and movement patterns. The reduction in REBA scores with

[8] Interquartile Range

exoskeletons is most pronounced in lifting and overhead work, aligning with the intended support functions of the tested devices. However, for tasks such as kneeling or walking, exoskeleton use does not consistently lower ergonomic risk and may even introduce additional constraints. These findings highlight the task-specific effectiveness of exoskeletons and underscore the need for adaptable, context-sensitive assistive solutions in skilled trades.

Table 9.2: Descriptive statistics and test results per activity.

([With Exoskeleton, Without Exoskeleton])
Sig.: Significant

Task	Mean	SD	S-W p-value	Normal Distribution	test	test p-value	Sig.
Working on floor	[7.62, 7.66]	[0.84, 0.66]	[0.8 0.1]	['yes', 'yes']	T	0.86	no
Overhead work	[6.25, 5.98]	[0.18, 0.18]	[0.1 0.6]	['yes', 'yes']	T	0.15	no
Put down load	[5.66, 5.49]	[0.83, 0.51]	[0.3 0.8]	['yes', 'yes']	T	0.57	no
Pick up load	[5.49, 5.59]	[0.88, 1.12]	[0.6 0.1]	['yes', 'yes']	T	0.65	no
Walk with load on floor	[3.79, 3.53]	[0.4, 0.2]	[0.82 0.27]	['yes', 'yes']	T	0.29	no
Walk with load on grid	[4.34, 4.1]	[0.4, 0.5]	[0.47 0.46]	['yes', 'yes']	T	0.46	no

Table 9.2 summarizes the descriptive statistics and statistical test results for each task, comparing REBA scores with and without exoskeleton support. The S-W test results indicate that most task distributions are normally distributed, allowing for the use of t-tests [Dav63] for comparison. However, none of the tasks showed statistically significant differences in REBA scores between conditions, suggesting that while exoskeletons may reduce ergonomic risk in certain scenarios, the effects are not robust across all tasks or participants.

Table 9.3: Descriptive statistics and test results per worker.

([With Exoskeleton, Without Exoskeleton])
Sig.: Significant

Worker	Mean	SD	S-W p-value	Normal Distribution	test	test p-value	Sig.
hw1	[5.31, 5.41]	[2.06, 1.81]	[0.4784, 0.2295]	['yes', 'yes']	T	0.69	no
hw2	[6.01, 5.74]	[1.38, 1.81]	[0.1248, 0.4152]	['yes', 'yes']	T	0.32	no
hw3	[5.6, 5.26]	[1.27, 1.24]	[0.9968, 0.5785]	['yes', 'yes']	T	0.05	no
hw4	[5.2, 5.18]	[1.01, 1.38]	[0.9479, 0.671]	['yes', 'yes']	T	0.92	no
hw5	[5.5, 5.37]	[1.45, 1.5]	[0.9301, 0.5889]	['yes', 'yes']	T	0.40	no

Table 9.3 presents the descriptive statistics and statistical test results for each individual worker, comparing their REBA scores with and without exoskeleton support. Similar to the task-level analysis, none of the workers exhibited statistically significant differences in REBA scores between conditions. This suggests that individual variability in posture and movement patterns may influence the effectiveness of exoskeletons, and highlights the need for personalized ergonomic interventions.

These results were derived using automated REBA scoring from video-based joint angle estimation via Detectron2 [Wu+19].

9.4.1.2 Surface Electromyography Analysis

sEMG data showed reduced muscle activation in lifting and overhead tasks when exoskeletons were used.

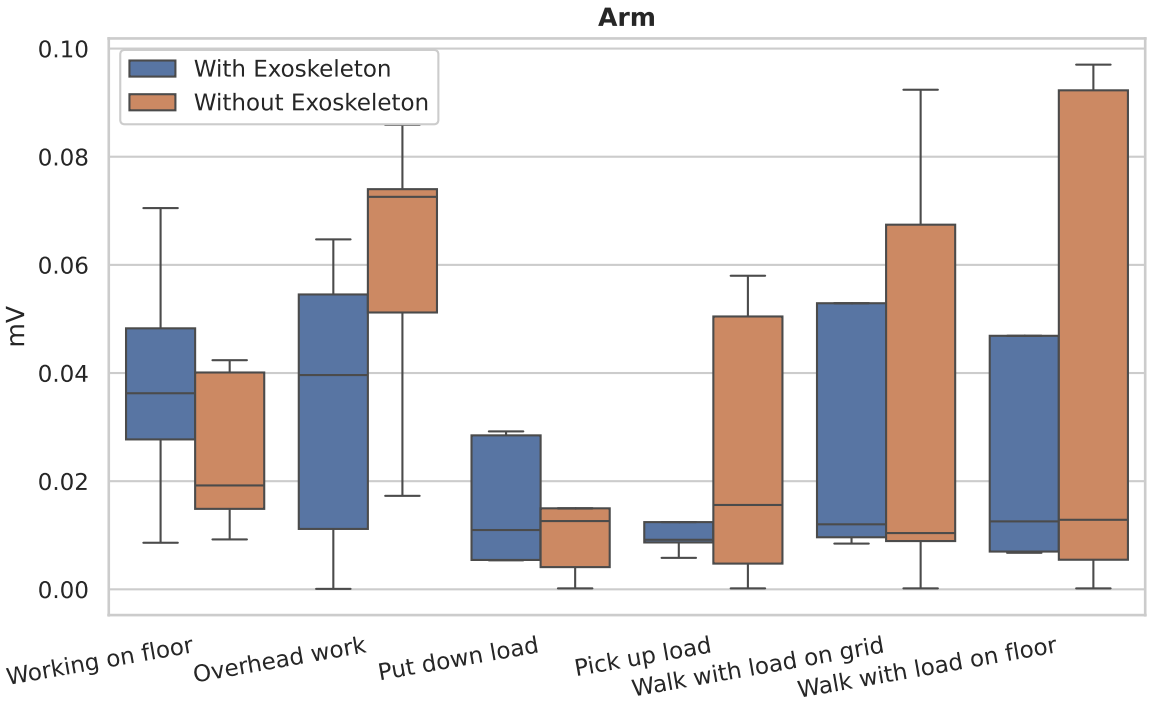

Figure 9.3: sEMG test results (Arm) for all six considered tasks with and without exoskeleton.
Each box represents the IQR, with the median indicated by a horizontal line
and whiskers extending to 1.5 ×IQR. Outliers beyond this range
are not shown to enhance the visibility of the box distributions.
A higher sEMG activation indicates greater muscle effort.

Figure 9.3 presents the envelope-filtered mean average sEMG activation for the arm muscles across six skilled trade tasks, comparing conditions with and without exoskeleton support. The boxplots illustrate the distribution of muscle activation levels, with the median, Interquartile Range, and whiskers indicating variability within each task. Notably, tasks involving overhead work and lifting show higher median activation in the unsupported condition, suggesting greater muscular effort is required from the arms when no exoskeleton is used.

With exoskeleton support, a reduction in arm muscle activation is observed for these high-strain tasks, indicating that the devices effectively offload some of the physical demand. However, for tasks such as walking or kneeling, the difference between conditions is less pronounced, and in some cases, the exoskeleton may even slightly increase activation, possibly due to compensatory movements or device interference. The variability within tasks also highlights inter-individual differences in muscle usage and adaptation to exoskeletons.

Figure 9.4 displays the mean average sEMG activation for the back muscles, again across all tasks and conditions. Here, the most substantial reductions in muscle activation with exoskeleton use are seen in lifting and setting down tasks, which are known to place significant strain on the lower back. The median values for these tasks are consistently lower when exoskeletons are worn, supporting the devices' intended function of reducing lumbar load.

For other tasks, such as walking or overhead work, the differences are less marked, and in some cases, the exoskeleton may not provide a clear benefit or could even increase back muscle activity due to altered

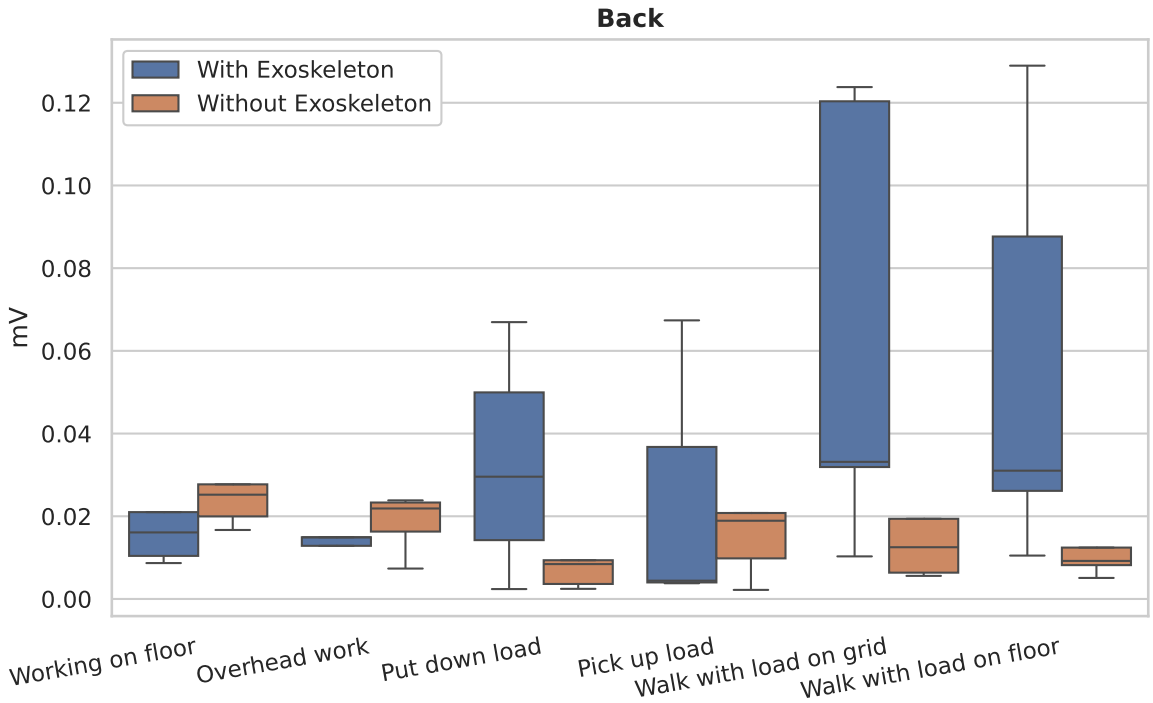

Figure 9.4: sEMG test results (Back) for all six considered tasks with and without exoskeleton.
Each box represents the IQR, with the median indicated by a horizontal line
and whiskers extending to 1.5 ×IQR. Outliers beyond this range
are not shown to enhance the visibility of the box distributions.
A higher sEMG activation indicates greater muscle effort.

movement patterns. The spread of the data suggests that individual responses to exoskeleton support vary, possibly reflecting differences in technique, body size, or familiarity with the devices.

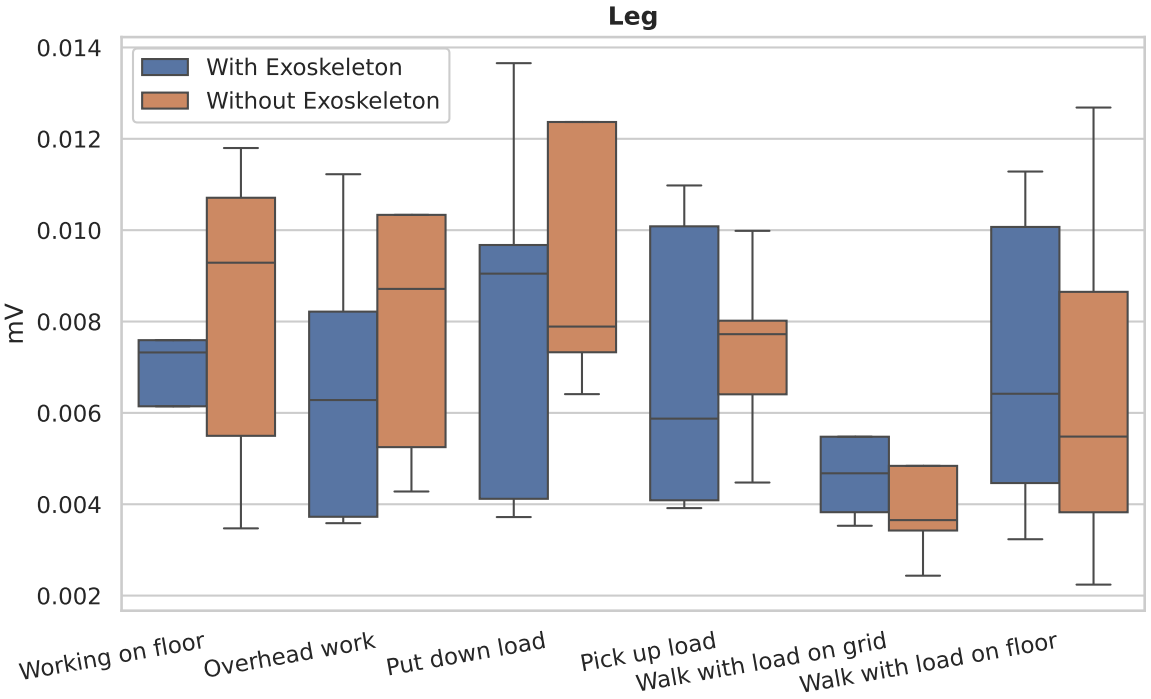

Figure 9.5: sEMG test results (Leg) for all six considered tasks with and without exoskeleton. Each box represents the IQR, with the median indicated by a horizontal line and whiskers extending to 1.5 ×IQR. Outliers beyond this range are not shown to enhance the visibility of the box distributions. A higher sEMG activation indicates greater muscle effort.

Figure 9.5 focuses on leg muscle activation, showing how exoskeleton use influences lower limb effort during different tasks. In tasks such as lifting and carrying, the exoskeleton appears to have little effect on leg muscle activation, with median values remaining similar between conditions. This suggests that the tested exoskeletons primarily target upper body support and do not substantially offload the legs during these activities.

Interestingly, for tasks involving walking or kneeling, there is sometimes a slight increase in leg muscle activation with exoskeleton use. This may be due to the added weight or mechanical constraints of the devices, which could alter gait or require compensatory stabilization. The data highlight the importance of considering unintended effects on non-targeted muscle groups when evaluating assistive technologies.

Figure 9.6 presents neck muscle activation, an area often affected by overhead work and awkward postures. The results show that for overhead tasks, exoskeleton use can reduce neck muscle activation, particularly for taller participants who benefit from arm support. However, for smaller users or during tasks not directly supported by the exoskeleton, neck activation may remain unchanged or even increase, possibly due to compensatory postures or device fit issues.

Across other tasks, the differences between conditions are minimal, indicating that the exoskeletons evaluated do not consistently offload the neck except in specific scenarios. The variability in the data underscores the influence of individual anthropometrics and task demands on the effectiveness of exoskeleton support for the neck region.

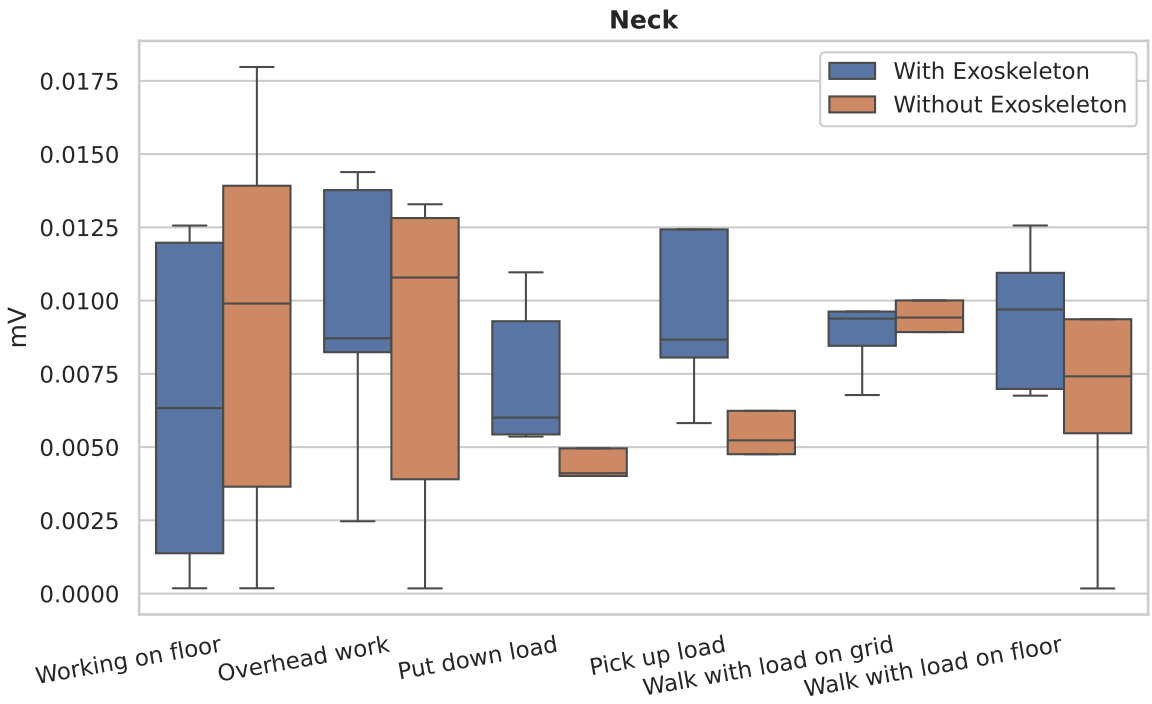

Figure 9.6: sEMG test results (Neck) for all six considered tasks with and without exoskeleton. Each box represents the IQR, with the median indicated by a horizontal line and whiskers extending to 1.5 ×IQR. Outliers beyond this range are not shown to enhance the visibility of the box distributions. A higher sEMG activation indicates greater muscle effort.

Table 9.4: Descriptive statistics and test results for sEMG per activity

(With exoskeleton vs Without exoskeleton). W: Wilcoxon signed-rank test, T: Paired t-test ([With Exoskeleton, Without Exoskeleton]) Sig.: Significant

Task	Mean	SD	S-W p-value	Normal Distribution	test	test p-value	Sig.
Working on floor	[1.84e-2, 1.73e-2]	[1.87e-2, 1.28e-2]	[8.85e-4, 3.72e-2]	['no', 'no']	W	0.78	no
Overhead work	[1.65e-2, 2.57e-2]	[1.75e-2, 2.62e-2]	[1.76e-4, 7.61e-4]	['no', 'no']	W	0.12	no
Put down load	[1.60e-2, 1.27e-2]	[1.70e-2, 1.69e-2]	[9.2e-5, 9.0e-6]	['no', 'no']	W	0.65	no
Pick up load	[1.49e-2, 1.69e-2]	[1.68e-2, 1.96e-2]	[1.70e-5, 1.43e-4]	['no', 'no']	W	0.90	no
Walk with load on floor	[2.83e-2, 2.73e-2]	[3.91e-2, 4.30e-2]	[6.0e-6, 4.0e-6]	['no', 'no']	W	0.39	no
Walk with load on grid	[3.00e-2, 3.03e-2]	[4.14e-2, 5.51e-2]	[5.0e-6, 1.0e-6]	['no', 'no']	W	0.29	no

Table 9.4 summarizes the descriptive statistics and statistical test results for sEMG activation across tasks, comparing conditions with and without exoskeleton support. Since the S-W test revealed a lack of normality in all task distributions, the Wilcoxon signed-rank test [Wil45] was applied for statistical comparison. However, similar to the REBA analysis, none of the tasks showed statistically significant differences in muscle activation between conditions. This suggests that while exoskeletons may reduce muscle effort in certain scenarios, the effects are not consistent across all tasks or participants.

Table 9.5: Descriptive statistics and test results for sEMG per muscle

(With exoskeleton vs Without exoskeleton)
All activities and workers aggregated.
W: Wilcoxon signed-rank test, T: Paired t-test
([With Exoskeleton, Without Exoskeleton])
Sig.: Significant

Body Part	Mean	SD	S-W p-value	Normal Distribution	test	test p-value	Sig.
Neck	[0.0094, 0.0223]	[0.0061, 0.0479]	[7.87e-6 0.1e-6]	['no', 'no']	W	0.49	no
Leg	[0.0071, 0.0091]	[0.0034, 0.0091]	[4.80e-3 3.0e-8]	['no', 'no']	W	0.37	no
Back	[0.0356, 0.0219]	[0.0366, 0.0251]	[3.75e-5 2.6e-7]	['no', 'no']	W	0.11	no
Arm	[0.0307, 0.0336]	[0.0321, 0.0323]	[3.15e-5 8.1972e-4]	['no', 'no']	W	0.78	no

Table 9.5 presents the descriptive statistics and statistical test results for sEMG activation across muscle groups, aggregating all activities and workers. As normality was not met for any muscle group (per the S-W test), the Wilcoxon signed-rank test [Wil45] was used for group comparisons. Similar to the task-level analysis, none of the muscle groups exhibited statistically significant differences in activation between conditions. This suggests that while exoskeletons may influence muscle effort in specific tasks, the overall effects on muscle activation are not robust across all muscle groups or participants.

A closer examination of the mean values reveals nuanced trends within individual muscle groups. For example, back muscle activation shows a tendency to decrease with exoskeleton use, aligning with the intended support function of the devices, particularly during lifting and setting down tasks. Conversely, arm and leg muscle activation levels remain similar or even slightly higher with exoskeleton support, possibly reflecting compensatory strategies or the mechanical constraints imposed by the devices. Notably, neck muscle activation increased with exoskeleton use for some participants, especially in tasks not directly supported by the devices.

Table 9.6: Descriptive statistics and test results for sEMG per worker

(With exoskeleton vs Without exoskeleton)
all activities and body parts aggregated.
W: Wilcoxon signed-rank test, T: Paired t-test
([With Exoskeleton, Without Exoskeleton])
Sig.: Significant

Worker	Mean	SD	S-W p-value	Normal Distribution	test	test p-value	Sig.
HW1	[0.0112, 0.0406]	[0.0131, 0.052]	[1.4e-06 1.1e-05]	['no', 'no']	W	0.00	yes
HW2	[0.0269, 0.0207]	[0.0334, 0.027]	[6.2e-06 5.6e-06]	['no', 'no']	W	0.13	no
HW3	[0.0237, 0.0085]	[0.0336, 0.015]	[2.6e-07 2.2e-07]	['no', 'no']	W	0.00	yes
HW4	[0.0251, 0.0245]	[0.0307, 0.031]	[1.3e-05 4.7e-06]	['no', 'no']	W	0.08	no
HW5	[0.0165, 0.0142]	[0.0185, 0.013]	[1.7e-06 4.0e-08]	['no', 'no']	W	0.32	no

Table 9.6 summarizes the descriptive statistics and statistical test results for sEMG activation for each individual worker, aggregating all activities and body parts. Because the S-W test showed non-normal distributions

for all workers, the Wilcoxon signed-rank test [Wil45] was selected for these analyses. Notably, two workers (HW1 and HW3) exhibited statistically significant differences in muscle activation between conditions, suggesting that individual variability plays a crucial role in how exoskeletons affect muscle effort. This highlights the importance of personalized ergonomic interventions and further investigation into factors influencing individual responses to exoskeleton support.

9.4.2 Subjective and Expert Validation

This subsection summarizes the results of expert ergonomic assessments and subjective user feedback, providing additional context for the quantitative findings. The expert evaluations were conducted by a certified specialist in rehabilitation technology. The ergonomic risk scoring used in these assessments ranged from 0 (low risk) to 5 (high risk). While the primary emphasis of this study is on objective biomechanical measures, these qualitative evaluations help to interpret the observed strain patterns and highlight user perspectives on exoskeleton usability and acceptance.

Table 9.7 reveals that tasks involving awkward postures or high loads–such as kneeling (4.2 ± 1.30), overhead work (3.6 ± 0.89), and lifting (3.0 ± 1.00)–are associated with the highest MSD risk scores. The additional expert recommendations frequently highlight the need for muscle training, balance exercises, and additional support for vulnerable regions like the trunk, knees, and ankles. In contrast, walking tasks show lower risk scores, though balance and gait issues are noted. Overall, the table underscores the persistent ergonomic challenges in skilled trades and the importance of targeted interventions to reduce strain in high-risk activities.

Table 9.7: Expert ergonomic assessments by task (No Exoskeleton – No-EXO)

(MSD risk score: mean ± SD, 1=low, 5=high)

Task	MSD Risk (No EXO)	Regions (No EXO)	Additional Recommendation or Notes (No EXO)
Lifting	3.0 ± 1.00	Knee, Shoulder/Arm/Hand, Trunk, Arms, Hand	Muscle training in trunk and legs recommended; Upper body rotation without exoskeleton
Walking	1.8 ± 0.84	Legs, Shoulder/Arm/Hand, Ankle, Trunk	Train sense of balance; Hypotonic gait pattern
Walking over grid	2.6 ± 0.89	Ankle, Shoulder/Arm/Hand	Ankle support or bandage helpful; Balance/stability exercises recommended
Setting down	2.9 ± 0.22	Trunk	–
Kneeling	4.2 ± 1.30	Trunk, Knee, Ankle, Wrist	–
Overhead Work	3.6 ± 0.89	Shoulder, Neck	–

Table 9.8 provides a comparison of ergonomic risk when exoskeletons are used. Notably, risk scores decrease for lifting (2.0 ± 1.00) and overhead work (1.8 ± 0.45), indicating improved support in these tasks. However, kneeling remains high-risk (4.5 ± 1.00), with experts noting that the exoskeleton can disrupt posture and unintentionally increase strain on the upper body and wrists. For walking, the risk score slightly increases compared to no exoskeleton, with comments about knee collapse and altered gait. These findings suggest that while exoskeletons can reduce risk in certain activities, they may introduce new ergonomic challenges or shift strain to other body regions, emphasizing the need for task-specific adaptation and careful integration into workflows.

Table 9.8: Expert ergonomic assessments by task (With Exoskeleton – EXO).[Dro+]

(MSD risk score: mean ± SD, 1=low, 5=high)

Task	MSD Risk (EXO)	Regions (EXO)	Additional Recommendation or Notes (EXO)
Lifting	2.0 ± 1.00	Knee, Shoulder/Arm/Hand, Trunk	Straighter posture with exo, more use of trunk
Walking	2.0 ± 1.22	Ankle, Knee, Shoulder/Arm/Hand	Knees collapse with exo; Large steps
Walking over grid	2.6 ± 0.89	Ankle, Shoulder/Arm/Hand	–
Setting down	2.5 ± 0.50	Trunk	–
Kneeling	4.5 ± 1.00	Trunk, Knee, Shoulder, Ankle, Wrist	The exoskeleton unintentionally pulls upper body upward; The exoskeleton is disruptive during task; Leaning forward increases load on lower back and wrists
Overhead Work	1.8 ± 0.45	Shoulder, Neck	Good support for arms; Smaller subjects stretch excessively; Less difficulty for taller subjects

9.4.2.1 Questionnaires

Prior to exoskeleton use, participants exhibited a generally favorable disposition, as indicated by a normalized attitude score of 0.80 ± 0.11. Expectations regarding the devices were similarly positive (0.70 ± 0.11), while apprehension levels remained low (0.61 ± 0.03). No association was identified between age and attitude in any of these domains. [Dro+]

Following task completion, post-questionnaire results revealed that the passive exoskeleton (Skelex) was rated more favorably than the active exoskeleton CrayX across all evaluated dimensions. Perceived support received the lowest ratings (0.69 ± 0.14 for Skelex; 0.59 ± 0.10 for CrayX). Technical assessment scores were moderate (0.64 ± 0.06 for Skelex; 0.60 ± 0.04 for CrayX). Usability was rated comparatively high for both systems (0.79 ± 0.08 for Skelex; 0.78 ± 0.08 for CrayX), with trust achieving the highest scores among all categories (0.82 ± 0.11 for Skelex; 0.72 ± 0.16 for CrayX).

9.4.3 Focus Group Insights

Participants found the CrayX disruptive during kneeling and walking due to its upward pull and bulky motors. Skelex aided only narrow overhead tasks; smaller users reported neck strain. Both systems were too task-specific and bulky for varied workflows. Preferred aids were lighter, passive devices or orthoses. Participants suggested external posture feedback (acoustic/visual) to prevent strain. Safety concerns were minor and manageable with training. Overall acceptance depended on clear instruction, intuitive use, and minimal interference.

9.5 Discussion

The present study underscores the centrality of quantitative movement analysis in the objective assessment of physical strain and ergonomic risk during skilled trade activities. By integrating automated REBA scoring and surface electromyography (sEMG), it was possible to systematically capture and compare movement patterns and muscle activation across a range of representative tasks and experimental conditions. The findings

demonstrate that both posture-based and muscle-based metrics provide complementary insights into the biomechanical demands of skilled trade work, with particular sensitivity to high-strain activities such as load lifting, load carrying, overhead work, and kneeling.

The automated REBA analysis, as detailed in subsubsection 9.3.7.1, revealed that ergonomic risk is highly task-dependent, with the highest scores observed in lifting, overhead work, and kneeling tasks. While the introduction of exoskeleton support led to modest reductions in median REBA scores for certain activities, these effects were not statistically significant across the cohort, as shown in Table 9.2 and Table 9.3. This suggests that, although exoskeletons may offer targeted relief in specific scenarios, their overall impact on posture-related ergonomic risk is limited by factors such as task specificity, device fit, and individual movement strategies.

The sEMG analysis further elucidated the nuanced effects of exoskeleton use on muscle activation. As illustrated in Figure 9.3–Figure 9.6, reductions in muscle effort were most apparent in the back and arm regions during lifting and carrying tasks, aligning with the intended support functions of the evaluated devices. However, these reductions did not consistently translate into statistically significant differences at the group level (Table 9.4, Table 9.5). Notably, substantial inter-individual variability was observed, with only select participants exhibiting significant changes in muscle activation (Table 9.6). This highlights the importance of personalized ergonomic interventions and the need for adaptive assistive technologies that accommodate diverse anthropometric and task-related requirements.

The triangulation of objective movement metrics with expert ergonomic assessments (Table 9.7, Table 9.8) and structured user feedback provides additional validation for the quantitative findings. Expert ratings confirmed that high-risk tasks identified by movement analysis correspond to those perceived as most hazardous in practice, while user feedback emphasized the practical limitations of current exoskeleton systems, including issues of bulkiness, workflow compatibility, and anthropometric fit. These qualitative insights reinforce the conclusion that, although exoskeletons can mitigate strain in specific contexts, their broader utility is constrained by usability and acceptance challenges.

It is important to acknowledge that the study was conducted with a small sample size of five participants. While this limited cohort does not allow for generalization to the broader population of skilled-trade workers, the results nonetheless provide valuable indications and initial evidence regarding the effectiveness and limitations of quantitative movement analysis and exoskeleton interventions in authentic work environments. The observed trends and individual differences should therefore be interpreted as indicative rather than representative, serving as a foundation for future research with larger and more diverse samples.

Crucially, the results demonstrate that quantitative movement analysis—anchored in reproducible, scalable methodologies such as automated REBA and sEMG—enables fine-grained, task-specific evaluation of ergonomic interventions in authentic work environments. This approach facilitates the identification of high-risk activities, supports evidence-based recommendations for workplace design, and provides a robust framework for the iterative development and validation of assistive technologies. The observed limitations, particularly regarding manual task labeling and the heterogeneity of user responses, underscore the necessity for further methodological advancements, including the automation of activity recognition and the integration of high-precision motion capture.

In summary, the findings affirm the value of quantitative movement analysis as the principal methodological contribution of this research. By enabling objective, context-sensitive assessment of physical strain, this approach advances the scientific foundation for ergonomic research in skilled trades and informs the design of future interventions aimed at reducing musculoskeletal risk and enhancing occupational health.

9.6 Conclusion

This study demonstrates that movement analysis methods, specifically automated REBA scoring and sEMG measurement, enable the objective quantification of physical strain and movement changes during typical

skilled trade activities. The results show that task- and condition-specific differences in posture and muscle activation can be systematically measured, supporting robust ergonomic assessment in real-world environments. The integration of movement metrics with expert and user perspectives provides a comprehensive framework for evaluating workplace interventions and identifying high-risk activities.

While exoskeletons were included as one experimental variable, the primary contribution lies in establishing movement analysis as a scalable, reproducible, and context-sensitive approach for ergonomic research. The findings emphasize the importance of reliable activity recognition and fine-grained segmentation for valid strain assessment. Manual labeling, as performed in this study, remains a limiting factor for scalability; future work should prioritize the automation of task classification and segmentation to further enhance the efficiency and reproducibility of movement analysis.

Building on these results, the next phase of research will introduce automatic task classification using advanced machine learning models and high-precision motion capture, with the goal of streamlining ergonomic assessment and supporting the development of adaptive, evidence-based interventions for occupational health.

9.7 CRediT contribution statement

Pedro Fernando Arizpe Gómez: Conceptualization, Data curation, Formal analysis, Investigation, Methodology, Resources, Software, Supervision, Validation, Visualization, Writing – original draft, Writing – Review and Editing.

Tim Stratmann: Conceptualization, Funding acquisition, Methodology, Project administration.

Sandra Drolshagen: Conceptualization, Formal analysis, Investigation, Methodology, Supervision, Validation, Visualization, Writing – Original Draft, Writing – Review and Editing.

Kira Krebs: Data curation.

Andreas Hein: Funding acquisition, Project administration, Supervision, Writing – Review and Editing.

10 Craftspeople activity recognition with Wearable Sensors (ReHopE IMU-OptiTrack Study)

10.1 Introduction

The ReHopE IMU-OptiTrack study was designed to evaluate the feasibility and accuracy of automated activity recognition for physically demanding tasks in the skilled trades. The study combines IMUs, optical motion capture (OptiTrack), and video recordings to capture and classify movement patterns associated with occupational strain. The primary goal is to support the development of sensor-based systems for early detection of harmful postures and to inform the design of assistive technologies such as exoskeletons.

10.1.1 Contributions

This study provides a validated dataset for training and evaluating activity recognition models in occupational settings. The findings will inform the development of real-time monitoring systems and contribute to the design of ergonomic interventions, including adaptive exoskeletons, to reduce long-term physical strain in skilled trades.

10.2 Scientific Background and Objectives

Due to demographic changes and increasing physical demands in skilled trades, maintaining long-term work ability is a growing challenge. Repetitive and ergonomically unfavorable movements contribute significantly to MSD. The ReHopE project aims to address this issue by developing scalable, sensor-based solutions for detecting and mitigating physical strain.

The objectives of this study were:

- To record and classify typical high-strain tasks in the skilled trades using IMUs and OptiTrack.
- To validate IMU-based activity recognition against optical motion capture and video data.
- To analyze the influence of demographic factors (e.g., age, gender, experience) on movement patterns.

10.2.1 Ethical and Legal Considerations

The study was conducted in accordance with data protection regulations. All data were pseudonymized using participant-generated codewords. Video and sensor data were stored securely and will be retained for at least 10 years. Participants were informed of their right to withdraw at any time without consequences. No deception was used in the study. The study was approved by the OFFIS e. V. Studienboard under the reference number 2024P031.

10.3 Design and Methodology

This section describes the experimental design, participant recruitment, sensing modalities, task protocols, and the machine learning model architecture used in the ReHopE IMU-OptiTrack laboratory study. The following subsections provide detailed information on each aspect of the methodology, ensuring transparency and reproducibility of the research.

10.3.1 Study Design

This laboratory-based study was conducted at the MIRACLE Lab (OFFIS e. V.). Each participant completed a series of predefined tasks simulating real-world work scenarios. The study was designed as a within-subject experiment, with randomized task order using a Latin Square design.

10.3.2 Participants

A total of 30 participants were recruited, ensuring diversity in gender, age, and professional experience. All participants provided informed consent. Demographic data collected included age, gender, height, weight, and musculoskeletal health status.

10.3.3 Sensing Modalities

The study employed a multi-modal sensing approach to comprehensively capture and quantify human movement during occupational tasks. The following modalities were utilized:

- **IMUs:** 15 sensors (Movella DOTs) placed on key body segments (e.g., head, shoulders, arms, back, hips, legs) to capture acceleration and angular velocity.
- **OptiTrack:** Optical motion capture system with 8 infrared cameras and a marker suit for high-precision 3D tracking.
- **Action Camera:** RGB video recordings for visual documentation and validation.

10.3.4 Tasks and Protocols

Participants performed seven categories of physically demanding tasks, including:

- **Carrying loads:** Walking with light (6 kg) and heavy (18 kg) weights in various configurations.
- **Overhead work:** Repetitive rotation of a hanger (30x CW and 30x CCW).
- **Unstable surfaces:** Walking on a metal grid while carrying loads.
- **Lifting:** Repetitive lifting of light and heavy weights with one or both hands.
- **Kneeling:** Picking up and placing 1 kg stones while kneeling.
- **Bent posture:** Same task as above, performed in a bent-over position.
- **Stair climbing:** Carrying weights while ascending and descending a mounting staircase.

To ensure consistency and clarity in task execution, a graphical user interface (GUI[1]) was developed to present participants with standardized instructional materials. For each task, the interface displayed a short video example alongside a textual description detailing the required movements and protocols. This approach facilitated uniform understanding of task requirements and minimized variability in participant performance during data collection.

10.3.5 Model Architecture and Training Configuration

The transformer model employed in this study is a custom implementation tailored for time-series classification of IMU data. It follows a modular design comprising positional embeddings, stacked encoder blocks, and a

[1] Graphical User Interface

final classification head. Each encoder block includes a MHA[2] layer followed by a feed-forward network with GELU[3] activation and residual connections, consistent with the original transformer formulation [Vas+17].

This model was selected based on its demonstrated ability to capture temporal dependencies and complex joint interactions in sequential sensor data, as discussed in detail in chapter 3. Its architecture is particularly well-suited for distinguishing subtle variations in occupational movement patterns, which is essential for accurate activity recognition in skilled trades.

The input to the model consists of sequences of length T with F features, where $F = 6 \times J$ and J is the number of selected joints. Each sequence is projected into an embedding space of dimension 120 using a linear layer and additive positional encoding. The model uses:

- **Embedding dimension**: 120
- **Number of encoder layers**: 3
- **Number of attention heads**: 6
- **Feed-forward layer size**: 256
- **Dropout rate**: 0.1

The classification head applies a LayerNorm followed by a linear projection to the number of classes defined by the grouping scheme. The model is trained using the Adam[4] optimizer with a learning rate of 10^{-3} and a cosine annealing scheduler over 200 epochs. Label smoothing of 0.1 is applied to improve generalization.

Training is performed on one or more GPUs, with support for multi-GPU parallelization via `nn.DataParallel`. Early stopping is implemented with a patience of 20 epochs based on validation accuracy. The best-performing model checkpoint is saved and evaluated on a held-out test set.

This architecture is well-suited for capturing temporal dependencies and subtle variations in movement patterns, as demonstrated by its performance across diverse grouping schemes. The use of positional embeddings and attention mechanisms allows the model to focus on relevant time steps and joint interactions, which is particularly beneficial in complex movement classification tasks [Che+25].

10.4 Outcomes and Analytical Measures

This section defines the analytical outcomes for evaluating model performance and biomechanical measures. The primary outcome is validation accuracy of IMU-based activity classification, with secondary outcomes including feature extraction, clustering, and statistical comparisons. Analyses use standard metrics (accuracy, precision, recall, F1-score).

The **Primary Outcome** was the validation accuracy of IMU-based activity classification, trained on IMU data and automatic labels.

Secondary Outcomes included:

- Validation accuracy, precision, recall, and F1-score for IMU-based activity classification across multiple grouping schemes.
- Confusion, precision, and recall matrix analysis to interpret classification outcomes and error patterns.
- Comparative analysis of grouping schemes to assess the impact of label granularity and task definition on model performance.
- Analysis of model robustness and variability using standard deviation and maximum accuracy across hyperparameter configurations.

[2] Multi-Head Attention
[3] Gaussian Error Linear Unit
[4] Adaptive Movement Estimation

- Investigation of demographic influences (age, gender, experience) on movement patterns and classification results.

10.5 Results and Interpretation

This section presents the main results of the ReHopE IMU-OptiTrack laboratory study, focusing on the performance of transformer-based models for automated activity recognition in skilled trades. The analysis evaluates classification accuracy across multiple grouping schemes, providing insights into the impact of label granularity and task definition on model effectiveness. Quantitative results are supported by confusion, precision, and recall matrices, which illustrate the model's ability to distinguish between complex occupational movements.

The following subsections detail the validation accuracy statistics for each grouping index, interpret the classification outcomes, and analyze the error patterns observed in the matrix visualizations. These findings are contextualized within the broader literature on human activity recognition [Che+25] and inform recommendations for future research and practical applications in ergonomic assessment and assistive technology development.

In this study, "groupings" refer to different schemes for categorizing the recorded occupational movements into classes for model training and evaluation. Each grouping defines a specific way of labeling the data, ranging from broad functional categories (such as walking or lifting) to fine-grained distinctions (such as specific weight balance or surface type). The purpose of these groupings is to systematically investigate how the granularity and structure of activity labels affect the performance of automated activity recognition models. By comparing results across multiple grouping schemes, the study assesses the model's ability to generalize, discriminate between similar activities, and identify subtle variations in movement patterns relevant to ergonomic risk.

Each grouping reflects a distinct conceptual approach to classifying movement patterns.

- **Grouping 0**: Categorizes movements into broad functional types such as walking, floorwork, lifting, overhead, and stairs.
- **Grouping 1**: Focuses on the presence and balance of carried weight (*No Weight*, *Unbalanced Weight*, *Balanced Weight*).
- **Grouping 2**: Differentiates walking surfaces (*Floor*, *Grid*, *Stairs*).
- **Grouping 3**: Targets only weight lifting balance (*Balanced* vs. *Unbalanced*).
- **Grouping 4**: Provides fine-grained labels for repeated activities, enabling detailed movement classification.
- **Grouping 5**: Clusters only similar movement types into broader categories.

Table 10.1 summarizes the performance of the trained transformer model across six different grouping schemes.

Table 10.1: Validation accuracy statistics for each grouping index.

Grouping Index	Mean Validation Accuracy (%)	Standard Deviation(%)	Max Accuracy (%)
0	70.13	11.76	95.00
1	59.91	7.92	74.00
2	68.34	7.94	82.00
3	74.77	7.41	84.00
4	76.91	15.39	95.00
5	70.92	15.77	96.00

The highest mean validation accuracy was achieved by **Grouping 4** (~77%) (see Table 10.1), which also reached a maximum accuracy of 95%. This grouping benefits from fine-grained labels that allow the model to learn nuanced distinctions between repeated movement patterns. However, its high SD (~15.4%) suggests sensitivity to hyperparameter configurations.

Grouping 0 (see Table 10.1)achieved a mean validation accuracy of 70.13% and a maximum accuracy of 95%. This grouping benefits from clear biomechanical distinctions between task types, such as walking versus overhead work, which are well captured by the transformer model. The moderate SD (11.76%) suggests consistent performance across hyperparameter configurations.

Grouping 3 also performed well (~74.8% mean accuracy), indicating that the binary classification of lifting balance is a biomechanically distinct and learnable task. In contrast, **Grouping 1** (see Table 10.1) yielded the lowest mean accuracy (~59.9%), likely due to overlapping movement signatures among weight categories.

Grouping 5, which aggregates similar activities, achieved the highest maximum accuracy (96%) (see Table 10.1) but also exhibited the greatest variability (~15.8% SD), reflecting the challenge of generalizing across subtly different movements. **Grouping 2** focuses on differentiating walking surfaces, specifically distinguishing between movements performed on the floor, a metal grid, and stairs. This grouping is designed to evaluate the model's ability to recognize subtle biomechanical adaptations required for navigating different surfaces, which are relevant for assessing ergonomic risk in occupational settings. The results for Grouping 2 show a mean validation accuracy of 68.34% and a maximum accuracy of 82%, indicating that the transformer model can reliably identify surface-related movement variations, though with slightly lower performance compared to broader functional groupings. The moderate standard deviation (~7.9%) suggests consistent model behavior across hyperparameter configurations. These findings highlight the importance of surface type as a factor in activity recognition and underscore the model's capacity to capture context-dependent movement patterns.

These findings align with recent work on IMU-based human activity recognition, which emphasizes the importance of task granularity and cross-modal representation learning to improve generalizability [Che+25]. In particular, studies using OptiTrack and wearable sensors have demonstrated that combining high-resolution motion capture with inertial data enables robust classification of occupational movements, even in out-of-distribution settings.

Figure 10.1 displays the confusion matrix for Grouping 0, which categorizes activities into broad functional types such as walking, floorwork, lifting, overhead, and stairs. The matrix shows strong diagonal dominance, indicating that the transformer model reliably distinguishes between these biomechanically distinct activities. Minimal off-diagonal elements suggest low rates of misclassification, supporting the model's effectiveness in recognizing major occupational movement patterns.

Figure 10.2 presents the precision matrix for Grouping 0. High precision values along the diagonal indicate that the model's positive predictions for each class are mostly correct, with most classes achieving precision above 90%. This demonstrates the model's ability to minimize false positives and accurately identify specific functional movement types.

Figure 10.3 shows the recall matrix for Grouping 0. High recall values across most classes indicate that the model successfully identifies the majority of true instances for each activity type, with few missed detections. This further confirms the model's robustness in classifying broad occupational movements.

Figure 10.4 illustrates the confusion matrix for Grouping 1, which focuses on weight balance categories (no weight, unbalanced weight, balanced weight). Compared to Grouping 0, this matrix exhibits more off-diagonal elements, reflecting increased misclassification between categories. This suggests that distinguishing between weight balance types is more challenging, likely due to overlapping movement signatures.

Figure 10.5 presents the precision matrix for Grouping 1. The precision values are lower and more variable across classes compared to Grouping 0, indicating a higher rate of false positives. This highlights the difficulty the model faces in accurately predicting specific weight balance categories.

Figure 10.6 shows the recall matrix for Grouping 1. The recall values are also lower and more inconsistent, indicating that the model misses a greater proportion of true instances in each weight balance category. This further underscores the challenge of classifying activities based on subtle differences in weight distribution.

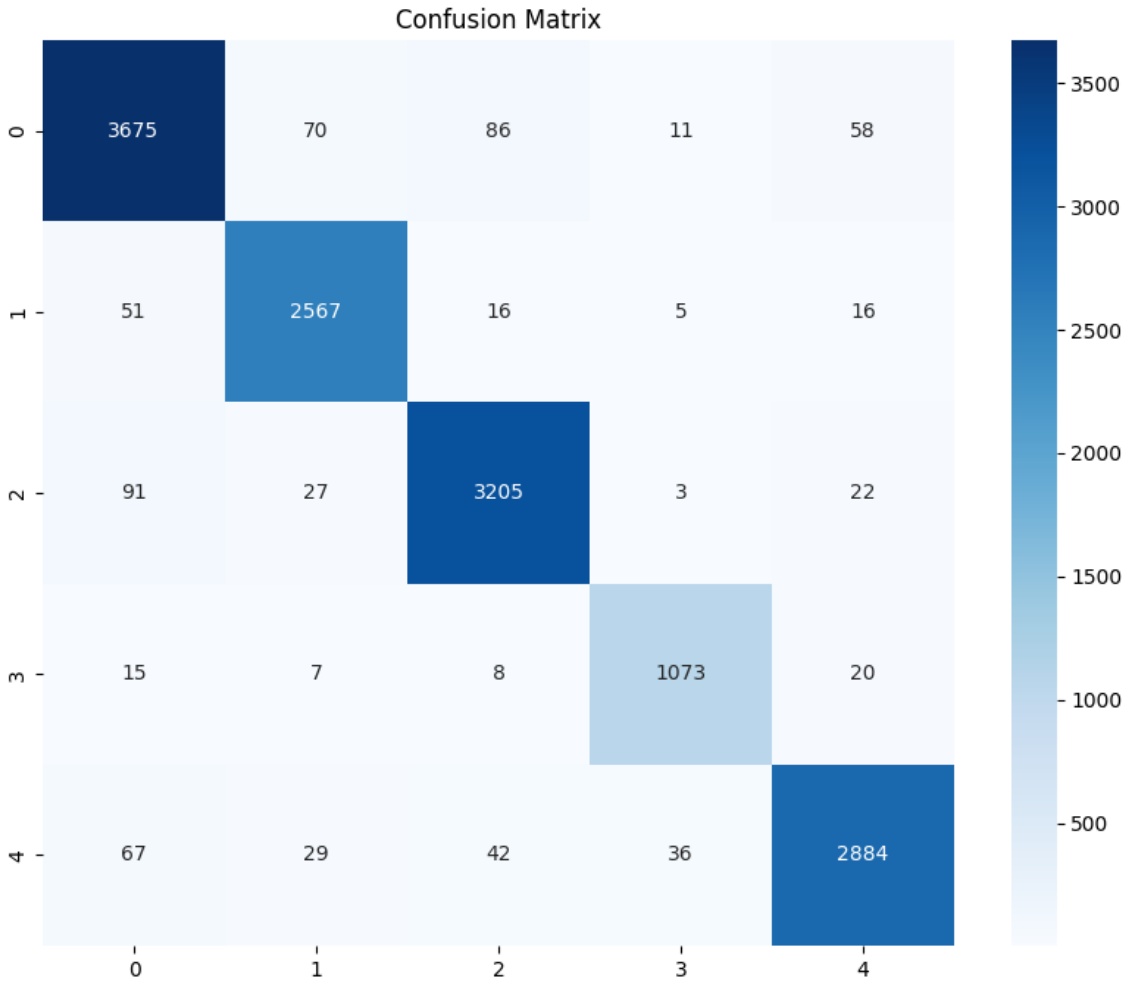

Figure 10.1: Confusion matrix for Grouping 0 (broad functional types) at 95% validation accuracy.

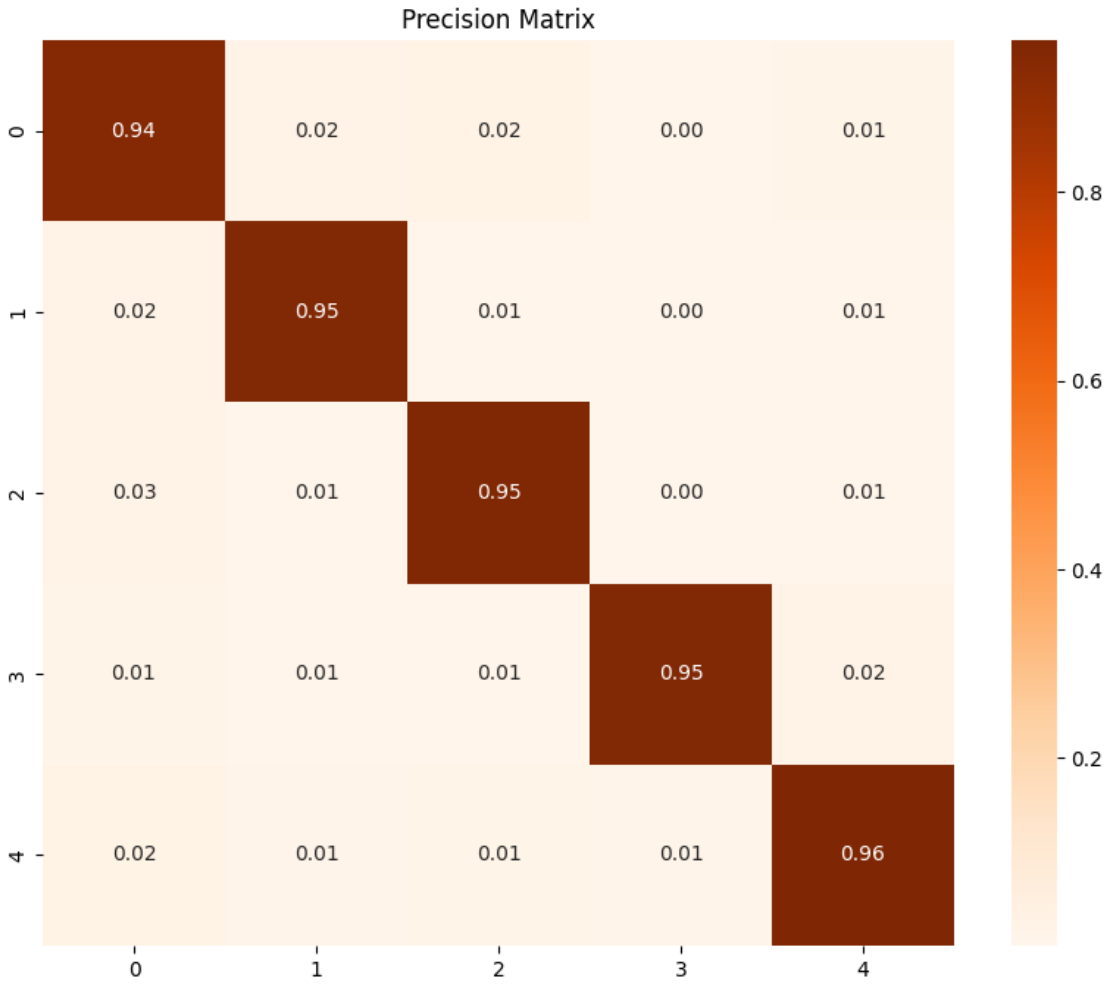

Figure 10.2: Precision matrix for Grouping 0 (broad functional types) at 95% validation accuracy.

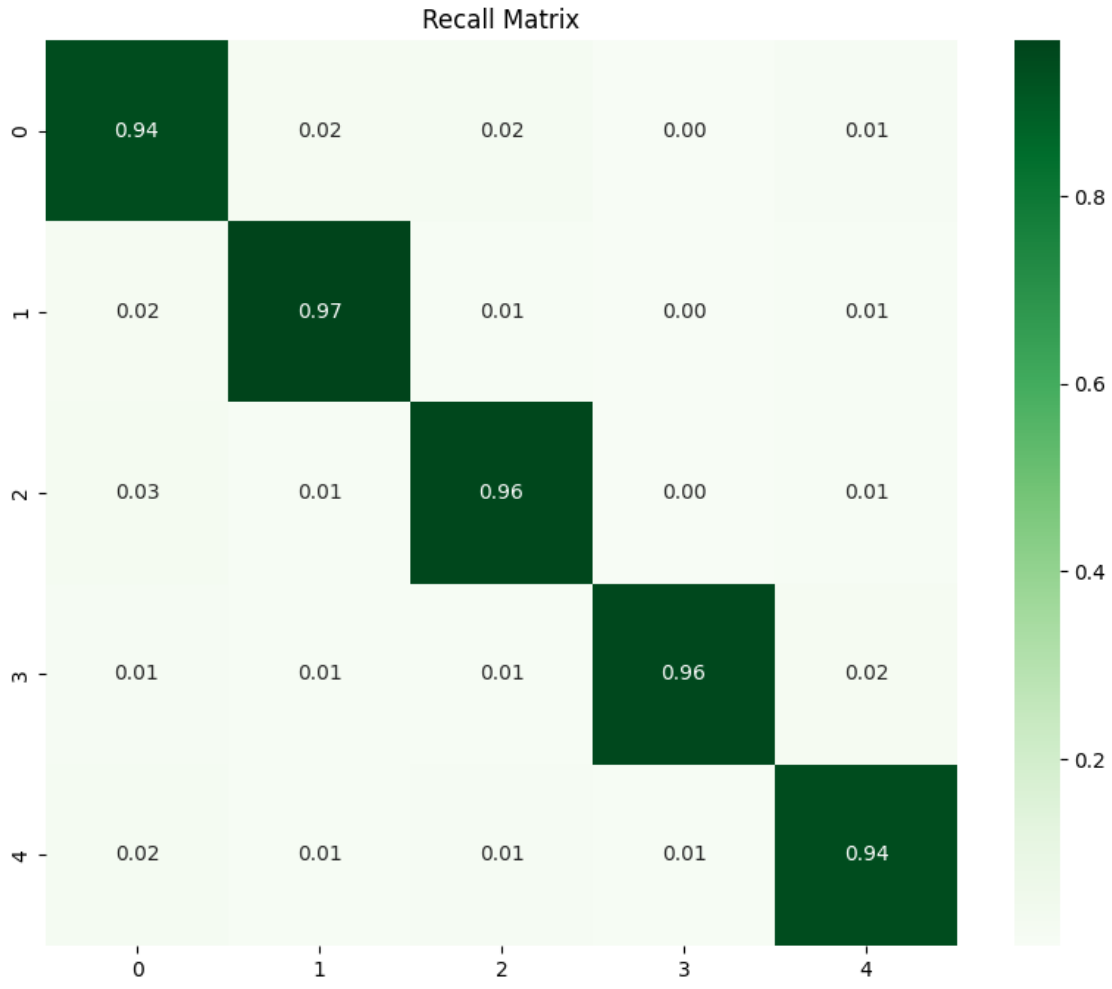

Figure 10.3: Recall matrix for Grouping 0 (broad functional types) at 95% validation accuracy.

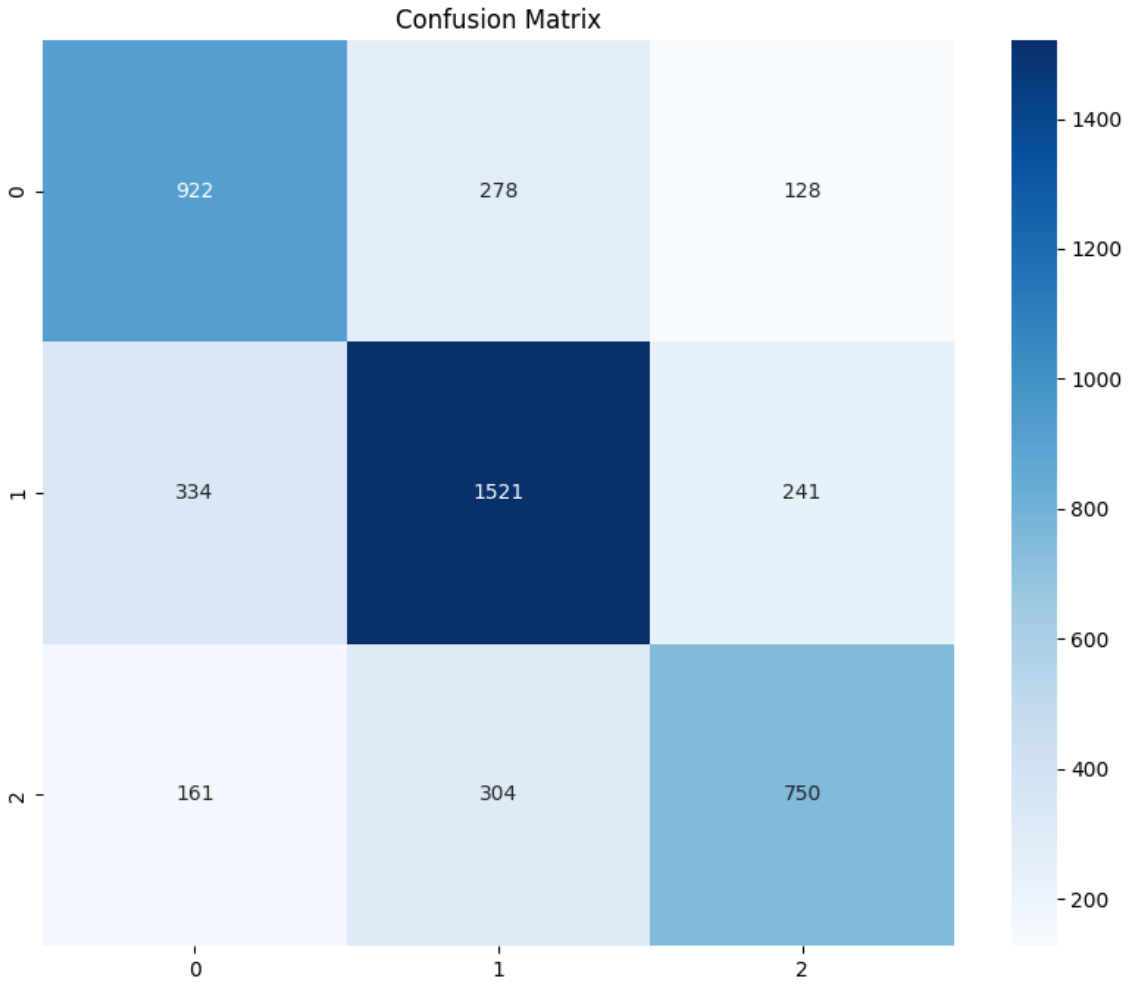

Figure 10.4: Confusion matrix for Grouping 1 (weight balance categories) at 68% validation accuracy.

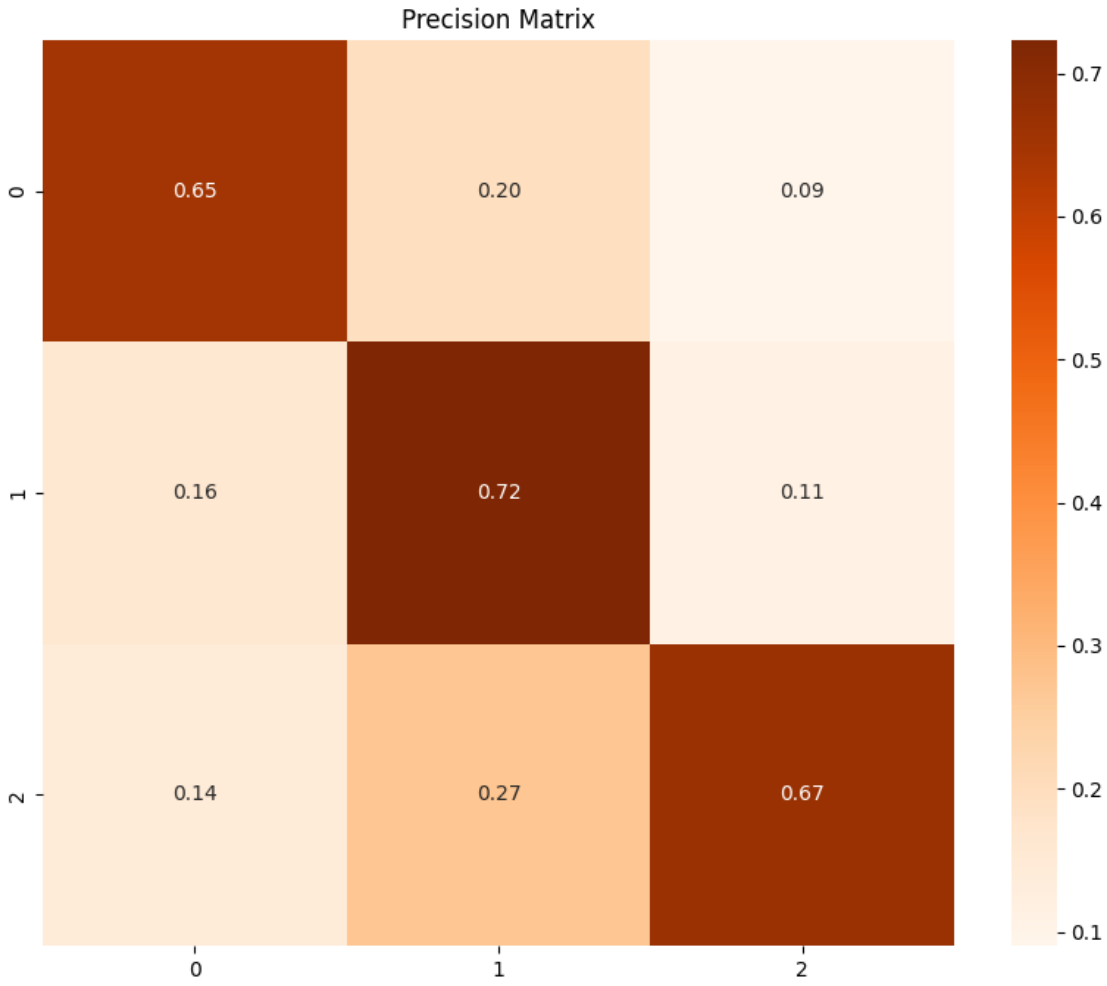

Figure 10.5: Precision matrix for Grouping 1 (weight balance categories) at 68% validation accuracy.

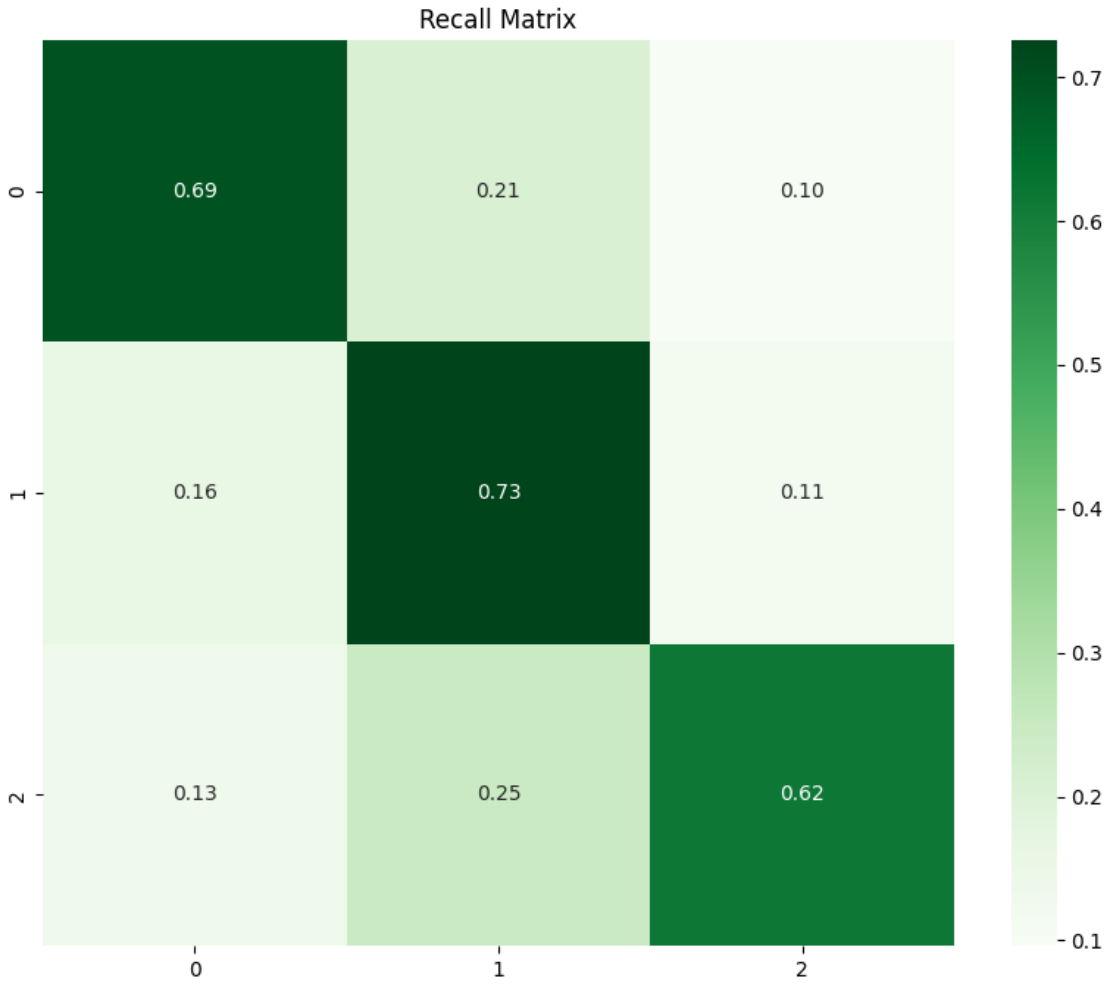

Figure 10.6: Recall matrix for Grouping 1 (weight balance categories) at 68% validation accuracy.

10.6 Discussion

The results of the ReHopE IMU-OptiTrack study demonstrate the effectiveness of transformer-based models for classifying complex occupational movements using wearable sensor data. The observed validation accuracies across different grouping schemes highlight the influence of label granularity and task definition on model performance. Notably, fine-grained groupings (e.g., Grouping 4) yielded the highest mean and maximum accuracies, suggesting that the model can learn subtle distinctions when provided with detailed labels. However, this comes at the cost of increased variability, as indicated by the higher SD, which may reflect sensitivity to hyperparameter choices and potential overfitting in certain configurations.

Broad functional groupings (Grouping 0) also achieved strong performance, with high maximum accuracy and moderate variability, underscoring the model's ability to reliably distinguish biomechanically distinct activities such as walking, lifting, and overhead work. In contrast, groupings based on weight balance (Grouping 1) resulted in lower mean accuracy and greater misclassification, likely due to overlapping movement signatures and less pronounced biomechanical differences. The confusion, precision, and recall matrices further illustrate these trends, with broad groupings showing clear class separation and weight-based groupings exhibiting more ambiguity.

Beyond the quantitative results, several qualitative observations emerged from the analysis. The transformer model's attention mechanisms appeared to focus on key temporal segments and joint interactions that are most informative for distinguishing between activities. This aligns with the hypothesis that occupational movements, especially those associated with ergonomic risk, are characterized by specific temporal patterns and joint coordination. The ability to capture these nuances is critical for early detection of harmful postures and for designing interventions such as adaptive exoskeletons.

The variability in model performance across grouping schemes also highlights the importance of context in activity recognition. Tasks that are biomechanically distinct and consistently performed, such as stair climbing or overhead work, are more easily classified than those with subtle or overlapping features, such as carrying different weights. This suggests that future systems should incorporate contextual information to further enhance classification accuracy and robustness.

Another important consideration is the generalizability of the model across participants with diverse backgrounds. The study included a heterogeneous sample in terms of age, gender, and professional experience, which is essential for developing solutions that are broadly applicable in real-world occupational settings. The observed performance across this diverse cohort indicates that transformer-based models can generalize well, but further research is needed to assess their effectiveness in more varied and uncontrolled environments.

The integration of multi-modal data—combining IMUs, optical motion capture, and video—proved valuable not only for model validation but also for error analysis and interpretability. For example, video recordings enabled the identification of atypical movement strategies or protocol deviations that may have contributed to misclassifications. This multi-modal approach supports the development of more transparent and trustworthy activity recognition systems, which is crucial for user acceptance and deployment in occupational health contexts.

In summary, the discussion underscores the potential of transformer-based models for advancing occupational activity recognition, while also highlighting the challenges associated with label design, data variability, and real-world applicability. The findings advocate for a balanced approach that leverages both fine-grained and broad activity definitions, incorporates contextual and multi-modal information, and prioritizes interpretability and user relevance. These considerations will be central to the next generation of ergonomic assessment tools and assistive technologies aimed at reducing the burden of work-related musculoskeletal disorders.

10.7 Conclusion

The ReHopE IMU-OptiTrack laboratory study demonstrates that transformer-based architectures provide a powerful and flexible approach for automated activity recognition in skilled trades. Across multiple grouping schemes the proposed model achieved substantial validation performance (see Table 10.1), with highest discriminative power for biomechanically distinct tasks and improved peak accuracy for fine-grained labels when sufficient training signal is available. The results indicate that model performance depends strongly on label granularity: fine-grained groupings can improve separability for repeated or highly specific movements, while broader functional categories offer greater generalizability and stability across hyperparameter choices.

The multi-modal data collection strategy, combining IMUs, OptiTrack optical motion capture, and video, enabled robust validation and detailed error analysis. Confusion, precision, and recall matrices provided insight into common misclassification modes and supported the interpretation of model attention patterns in temporal and joint domains. These analyses highlight the value of synchronized reference systems for diagnosing failure modes and for guiding sensor placement and label design in subsequent studies.

Several limitations constrain the direct generalization of the present findings. Data were acquired in a laboratory setting with standardized task instructions and a finite participant sample; therefore, performance in uncontrolled field environments may differ. Certain grouping schemes exhibited increased variance across hyperparameter configurations, indicating sensitivity to training conditions and the need for careful validation when adopting fine-grained labels. Finally, real-time deployment constraints (compute, latency, and on-device inference) were not addressed in this laboratory evaluation and require dedicated engineering assessment prior to operational use.

In conclusion, the study provides a validated dataset and an evaluation framework that advance automated activity recognition for occupational movement analysis. The transformer-based approach shows promise for identifying biomechanically relevant patterns that inform ergonomic assessment and early detection of movement signatures associated with increased MSD risk. Continued work on field transfer, model interpretability, and practical deployment will be essential to translate these laboratory results into operational tools for prevention and intervention in skilled trades.

10.8 CRediT contribution statement

Pedro Fernando Arizpe Gómez: Conceptualization, Data curation, Formal analysis, Investigation, Methodology, Resources, Software, Validation, Visualization, Writing – Original Draft, Writing – Review and Editing.

Evgeniya Ryasnova: Conceptualization, Data curation, Software, Visualization.

Tim Stratmann: Conceptualization, Resources.

Andreas Hein: Funding acquisition, Project administration, Resources, Supervision, Writing – Review and Editing.

Part IV

Synthesis and Conclusions

11 Discussion

The results from the TEDIPA, TETRIS, Smart-BT, and ReHopE studies collectively underscore the potential of sensor-based movement analysis for both clinical diagnostics and occupational health. Across all studies, the integration of wearable sensors, optical tracking, depth cameras, and machine learning enabled the objective quantification of movement patterns, postural deviations, and physical strain. These insights contribute to the development of scalable, data-driven tools for early detection of motor dysfunction, ergonomic risk, and the validation of novel assessment technologies.

11.1 Integration of Findings

chapter 4 – Validation of portable multi-sensor system for movement analysis (TEDIPA study) provided a comprehensive quantitative evaluation of depth camera-based, markerless motion analysis for clinical movement assessment in PwPD's and healthy participants. The experimental protocol incorporated both gait and non-gait tasks, enabling the extraction of a broad spectrum of spatiotemporal and kinematic parameters, including Step Length, Gait Cadence, velocity Gait Velocity, and upper limb mobility. Gait data were acquired using a multi-camera setup with the AzureKinect system and benchmarked against the GAITRite walkway, a gold-standard reference for gait analysis. Statistical comparisons demonstrated strong agreement between the markerless system and the reference standard, with high correlation coefficients and minimal bias across key parameters. This validation extended to both healthy controls and PwPD's, supporting the generalizability of the approach across diverse clinical populations.

The study design emphasized rigorous quantitative analysis, including the use of repeated measures, cross-validation, and robust statistical testing to assess measurement reliability and sensitivity. The inclusion of both gait and upper limb tasks allowed for the evaluation of the system's versatility in capturing clinically relevant movement features beyond traditional walking assessments. The AzureKinect system enabled continuous, non-invasive monitoring of movement, facilitating the detection of subtle motor changes that may be indicative of early neurodegenerative processes or intervention effects. The ability to extract upper limb and postural metrics further broadened the clinical utility of the approach, enabling comprehensive motor profiling in PwPD's.

Importantly, the TEDIPA study addressed key challenges in clinical movement analysis, such as the need for scalable, accessible, and objective assessment tools that can be integrated into routine practice. The markerless, depth camera-based system demonstrated feasibility for deployment in clinical and research settings, offering automated data processing and minimal setup requirements. The findings underscore the potential of quantitative, sensor-based movement analysis to support early diagnosis, progression tracking, and personalized intervention planning in neurodegenerative disorders. By establishing the validity and reliability of markerless motion capture for a range of motor tasks, the TEDIPA study contributes to the advancement of data-driven, objective methodologies in clinical movement science.

chapter 5 – Clinical study for Parkinson's Disease symptom and treatment monitoring (TETRIS Study) provided an in-depth quantitative evaluation of automated, markerless kinematic analysis for the assessment of fine motor function in clinical and research settings. The experimental design incorporated a randomized, double-blind, sham-controlled protocol to rigorously evaluate the sensitivity and specificity of movement analysis in detecting subtle motor changes. Participants, including both PwPD's and healthy controls, performed a battery of standardized tasks such as finger tapping and hand open-close movements, which are commonly used in clinical motor assessments.

High-resolution kinematic data were acquired using a markerless pose estimation pipeline based on MediaPipe, enabling the extraction of detailed parameters including amplitude, speed, acceleration, and arrhythmicity for each movement cycle. The study emphasized the use of robust, automated algorithms for feature extraction, minimizing manual intervention and enhancing reproducibility. Quantitative analysis focused on within-subject and between-group comparisons, employing advanced statistical methods to assess the discrim-

inative power of kinematic features for distinguishing PwPD's from healthy controls and for evaluating the effects of experimental interventions.

The TETRIS study demonstrated that markerless kinematic analysis can reliably capture clinically relevant changes in motor performance, with extracted features showing strong associations with established clinical scales and expert ratings. The use of a sham-controlled design allowed for the isolation of true intervention effects from placebo responses, further strengthening the validity of the findings. The scalability and automation of the analysis pipeline support its application in large-scale studies and routine clinical practice, addressing key challenges in the objective quantification of motor function.

By establishing the feasibility and accuracy of automated, markerless movement analysis for fine motor tasks, the TETRIS study advances the field of quantitative movement science. The results highlight the potential of sensor-based, data-driven methodologies to provide objective, sensitive, and scalable tools for the assessment of motor dysfunction, progression tracking, and evaluation of therapeutic interventions in neurodegenerative disorders and beyond.

chapter 6 – Planned Retrospective Study on Video-Based Analysis of PD-Related Movements (RESBEPA Study) outlined a planned retrospective study design for the evaluation of video-based, markerless motion capture systems in the assessment of motor function in individuals with PD. The proposed RESBEPA study aims to leverage existing video recordings of standardized MDS-UPDRS assessments to extract kinematic parameters such as amplitude, velocity, and acceleration using computer vision algorithms. The study's primary objective is to determine whether these quantitative features can serve as objective, reproducible markers of motor impairment severity, correlating with clinical ratings.

The study design emphasizes the use of automated data processing pipelines to extract skeletal joint trajectories from RGB video recordings, minimizing manual intervention and enhancing scalability. Planned analytical methods include descriptive statistics, regression models, and correlation analyses to evaluate the relationships between kinematic metrics and clinical scores. The retrospective nature of the study allows for the analysis of a large dataset spanning multiple years, providing a robust framework for assessing the feasibility and validity of video-based movement analysis in clinical settings.

chapter 7 – Validation of Video-Based Movement Assessment (Smart-BT Validation Study) presented a rigorous quantitative evaluation of markerless video-based MoCap systems for MSD prevention and neurological clinical assessment, focusing on the accuracy, reliability, and clinical applicability of RGB-D-based movement analysis. The study design incorporated a comprehensive set of movement tasks derived from the Herodikos exercise therapy app [Sch24] and the MDS-UPDRS protocol, enabling the assessment of both gross and fine motor function in a MSD prevention context. Data were collected using the AzureKinect system and benchmarked against IMU-based and optical MoCap reference systems, providing a robust framework for cross-validation and comparative analysis.

Automated joint angle estimation and kinematic analysis were performed across multiple joints and movement planes, with extracted features including range of motion, angular velocity, and movement smoothness. The study emphasized the use of objective, reproducible metrics for movement assessment, enabling the quantification of MSD prevention measures and the evaluation of intervention effects. Statistical analyses demonstrated high levels of agreement between the markerless system and reference standards, with some measurement bias and moderate correlations across key kinematic parameters. These results support the validity of RGB-D-based BT for clinical use, particularly in settings where traditional MoCap systems may be impractical due to cost or logistical constraints.

The integration of computer vision-based movement analysis into routine workflows was a central focus of the study, highlighting the potential for scalable, accessible, and automated assessment tools in MSD prevention. The findings underscore the importance of quantitative, sensor-based methodologies for tracking patient progress, and supporting data-driven decision-making. By establishing the accuracy and reliability of markerless MoCap for a diverse set of MSD prevention tasks, chapter 7 – Validation of Video-Based Movement Assessment (Smart-BT Validation Study) advances the field of quantitative movement analysis and provides a foundation for future research.

The ReHopE Hospitationen study (see chapter 8) employed an observational field design to quantitatively assess ergonomic risk in skilled trades using wearable IMU-based motion capture and RGB-D video annotation. Comprehensive kinematic data were collected from craftspeople performing typical occupational tasks in real-world environments, enabling the extraction of joint angles and postural loads across a wide range of activities. The analysis focused on the classification of 18 joint angles into ergonomic risk categories according to DGUV208-033 guidelines, providing a detailed exposure-time profile for each anatomical region and task type. Results indicated that tasks such as bent-over work, floor-level activities, and ladder use were frequently associated with non-acceptable joint angles, particularly in the back, shoulders, and knees. Aggregated exposure-time distributions and statistical comparisons across tasks and occupations identified high-risk postures and informed the prioritization of ergonomic interventions. These findings demonstrate the value of quantitative movement analysis for evidence-based risk assessment and the development of targeted strategies to reduce MSD risk in skilled trades.

The ReHopE Fokusgruppe study (see chapter 9) systematically evaluated the ergonomic impact of exoskeletons in skilled trades using a quantitative, multi-modal assessment framework. Automated video-based REBA scoring and surface electromyography (sEMG) provided objective measures of physical strain across a range of representative tasks, with results stratified by task type, participant, and exoskeleton condition. The findings indicated that exoskeleton use led to modest reductions in median REBA scores for tasks such as lifting and overhead work, while other activities, including kneeling and walking, showed negligible or inconsistent effects. Statistical analysis revealed no significant differences in REBA scores between supported and unsupported conditions across tasks or participants. Muscle activation patterns, as quantified by mean envelope-filtered sEMG amplitudes, complemented the posture-based risk assessment and highlighted the task-specific nature of exoskeleton support. Although expert ergonomic ratings and structured user feedback were collected, the primary emphasis of the study remained on quantitative movement analysis. These results underscore the importance of objective, task-level evaluation in determining the effectiveness of assistive devices and inform the design of future ergonomic interventions in skilled trades.

The ReHopE IMU-OptiTrack study (see chapter 10) focused on the automated recognition of occupational activities using wearable IMUs, optical motion capture, and video recordings in a controlled laboratory environment. A transformer-based model was trained to classify complex, physically demanding tasks with high validation accuracy across multiple grouping schemes, demonstrating the model's ability to distinguish subtle variations in movement patterns relevant to ergonomic risk. The study further analyzed the influence of label granularity, task definition, and demographic factors on classification performance. These results establish the feasibility of real-time, sensor-based activity recognition for skilled trades and provide a foundation for the development of AI-driven ergonomic assessment tools and adaptive feedback systems aimed at reducing long-term physical strain.

Together, these studies demonstrate that sensor-based movement analysis, when combined with machine learning and user feedback, enables a holistic, scalable approach to movement health and ergonomic support. The harmonized use of objective metrics, cross-validation, and multi-modal data capture ensures that methodological advances are transferable across domains, supporting both preventive healthcare and workplace safety. This synthesis of findings provides a comprehensive framework for early identification of occupational strain, evidence-based intervention, and the continued advancement of quantitative movement analysis.

The integration of quantitative sensor analysis with qualitative user perspectives ensures that the proposed solutions are both technically robust and practically relevant. Future work should focus on deploying these systems in broader occupational contexts, refining activity definitions, and exploring personalized feedback mechanisms to further reduce the incidence of WRMSD.

Crucially, the unique contribution of this thesis lies in the synthesis and cross-linking of findings from these diverse studies. By systematically integrating results from clinical, laboratory, and field investigations, the research demonstrates how quantitative movement analysis can bridge the gap between clinical neurology and occupational health. The comparative validation of sensor modalities and analytical pipelines across different populations and environments enables the identification of universal movement signatures associated with motor dysfunction and ergonomic risk. Furthermore, the harmonized use of objective metrics, such as joint angle

estimation, kinematic variability, and activity classification accuracy, facilitates the transfer of methodological advances from one domain to another. This integrative approach not only strengthens the generalizability of the findings but also establishes a comprehensive framework for the development of robust, scalable, and context-aware movement assessment tools. The thesis thereby advances the field by demonstrating that the combined application of sensor-based technologies and machine learning can yield actionable insights for both preventive healthcare and workplace safety, supporting the translation of research innovations into practical interventions.

11.2 Implications for Healthcare and Occupational Practices

The integration of quantitative movement analysis into healthcare and occupational practice represents a transformative advance, as demonstrated by the collective findings of this thesis. In clinical neurology, systems such as TEDIPA (see chapter 4) and TETRIS (see chapter 5) provide objective, reproducible metrics for the early detection and monitoring of motor dysfunction in neurodegenerative diseases. For example, the automated extraction of gait parameters and fine motor features enables the identification of subtle deviations from normative patterns, supporting earlier diagnosis and more precise tracking of disease progression. The use of markerless, camera-based systems facilitates scalable deployment in outpatient clinics and telemedicine, reducing reliance on specialized laboratory infrastructure and enabling broader access to quantitative assessment.

In occupational health, the ReHopE studies (see chapter 8, chapter 9, and chapter 10) illustrate the practical value of sensor-based methodologies for ergonomic risk assessment and intervention design. The deployment of wearable IMUs and markerless motion capture in real-world work environments allows for the continuous monitoring of joint angles, postural loads, and movement variability during authentic tasks. For instance, the classification of exposure times to non-acceptable joint angles in skilled trades (see chapter 8) provides actionable data for targeted ergonomic interventions and workplace redesign. The evaluation of exoskeletons using automated REBA scoring and sEMG (see chapter 9) demonstrates how quantitative analysis can inform the development and user acceptance of assistive technologies, ensuring that interventions are both effective and tailored to specific occupational demands.

The ability to detect deviations in movement patterns in real-time, as enabled by transformer-based activity recognition models (see chapter 10), opens new avenues for preventive health strategies and personalized feedback. For example, real-time alerts for hazardous postures or extended load carrying can be integrated into wearable systems, supporting immediate corrective action and reducing the risk of WRMSD. The harmonization of analytical pipelines across clinical and occupational domains further enables the transfer of methodological advances, such as robust feature extraction and multi-modal data capture, ensuring that innovations benefit a wide range of applications.

Collectively, these examples underscore the thesis's central contribution: the demonstration that quantitative, sensor-based movement analysis can be systematically integrated into both healthcare and occupational settings to support early detection, risk prevention, and the design of adaptive interventions. The findings advocate for the continued development and deployment of scalable, objective assessment tools, and highlight the importance of interdisciplinary collaboration in translating research innovations into practical, real-world solutions.

11.3 Limitations and Future Research Directions

While the studies presented promising results, several limitations must be acknowledged. Sample sizes were relatively small, and generalizability across populations and work environments remains to be validated. The accuracy of sensor-based systems can be affected by calibration, sensor placement, and environmental conditions. Additionally, the integration of subjective and objective data requires further methodological refinement.

Future research should focus on:

- Expanding datasets across diverse populations and real-world settings.
- Improving sensor fusion techniques and robustness of machine learning models.
- Developing adaptive, user-centered assistive systems with real-time feedback.
- Exploring longitudinal applications for monitoring progression and intervention outcomes.
- Implementing the planned study design described in the RESBEPA chapter, which outlines a retrospective analysis of video-based movement data for digital phenotyping in PD. This study, as currently presented, remains a proposal and its execution would provide valuable insights into the feasibility and impact of large-scale, markerless motion analysis in clinical settings.

These directions will help translate movement analysis from research to practice, supporting healthier, safer, and more sustainable work and care environments.

12 Conclusion

12.1 Summary of Key Findings

This thesis investigated movement irregularities through multi-sensor tracking and AI-driven movement analysis and compared its results with classical methods for motor assessment ergonomical risk assessment. The key findings from the various studies include:

Multi-Sensor Fusion Enhances Tracking Accuracy: While depth cameras alone can be insufficient for precise movement tracking in some settings, integrating IMUs, RGB-D cameras, and optical MoCap improved detection accuracy and robustness for selected tasks and environments (chapter 10, chapter 4, chapter 7); for simple movements, single-modality systems were sufficient (chapter 5).

Technological Advances in Automated Movement Analysis:

- Multi-RGB-D camera-based systems, such as the AzureKinect, can offer reliable, markerless quantification of gait parameters, correlating strongly with gold-standard systems like GAITRite (chapter 4).
- Multi-sensor integration, combining the strengths of IMUs, RGB-D cameras, optical MoCap, and video-based pose estimation, can improve tracking accuracy and robustness for selected movement parameters and environments; however, the benefit is context-dependent. Evidence across chapter 10 (sensor integration for complex movement classification), chapter 4 (multi-camera setups expanding the observable area and enabling natural gait capture), and chapter 7 (interference affecting RGB-D performance and motivating complementary modalities) substantiates this claim. For some simple movements, single-modality systems performed as well or better, as detailed in chapter 5.
- Machine learning algorithms, including deep learning and transformer-based models, enable automated detection and classification of movement abnormalities, supporting early prevention of WRMSD and automatic ergonomic risk assessment (chapter 10).
- Video-based pose estimation frameworks (e.g., MediaPipe, Detectron2) and wearable IMUs provide complementary strengths: video systems excel in markerless, non-intrusive monitoring, while IMUs offer high temporal resolution and robustness to occlusion (chapter 7, chapter 10).
- Automated, data-driven movement analysis bridges the gap between subjective clinical and ergonomic assessments and objective, scalable diagnostics, paving the way for real-time feedback and preventive interventions.

Application-Oriented Findings

Occupational Movements Increase Musculoskeletal Risk: Overhead work and heavy lifting contribute to increased joint strain and spinal compression (chapter 10).

Quantitative analysis of Fine Motor Variability can hint towards possible neurological disorders: Early indicators of PD can be monitored by analyzing certain fine movement fluctuations (chapter 4).

Identification of Methodological Gaps and Limitations

The comprehensive investigations conducted in this thesis not only advanced quantitative movement analysis but also revealed critical methodological gaps and limitations across multiple studies. Challenges such as sensor interference, variability in real-world environments, and inconsistencies in data acquisition highlighted areas where current approaches may fall short (chapter 7, chapter 10, chapter 5). These findings underscore the necessity for continued refinement of sensor fusion techniques, robust validation protocols, and the development of standardized methodologies to ensure reliability and generalizability of results.

12.2 Overall Conclusion

This doctoral research has significantly contributed to the field of automated movement analysis, particularly concerning periodic human movements in both occupational and clinical scenarios. Through rigorous investigation and the application of advanced computational methodologies, several key objectives have been achieved, addressing critical gaps in current assessment paradigms. The findings presented herein demonstrate the feasibility and utility of integrating innovative sensor technologies with sophisticated AI models to provide objective and efficient characterizations of movement abnormalities.

Beyond the academic contributions, this work carries substantial implications for society. By facilitating early detection and objective monitoring of movement disorders, it offers the potential to enhance diagnostic processes, personalize interventions, and ultimately improve the quality of life for individuals affected by neurodegenerative conditions and musculoskeletal challenges. This research also lays a robust foundation for future endeavors, exploring new applications and refining methodologies to further advance the capabilities of automated movement assessment.

12.3 Contributions to the Field

This research contributes to movement analysis in several ways:

Advancing Multi-Sensor Tracking for Movement Analysis: By comparing depth cameras, IMUs, and optical motion capture, this thesis establishes best practices for high-precision movement tracking in both clinical and occupational settings.

Bridging Clinical and Occupational Applications: Unlike previous work focusing solely on clinical or ergonomic perspectives, this research integrates both, providing a more comprehensive framework for assessing movement risk.

Developing AI-Based Detection of Motor Irregularities: Machine learning models applied to sensor data enable early diagnosis of movement disorders, shifting from subjective clinical assessment to objective, automated detection.

Quantifying Occupational Movement Risks: The OptiTrack study demonstrated that prolonged repetitive motions contribute to long-term musculoskeletal strain, providing objective data for ergonomic recommendations.

Laying the Foundation for Scalable Health Monitoring: This thesis supports the development of real-time AI-driven movement assessment tools, enabling early intervention and workplace safety improvements.

12.4 Integrated Summary of Findings

The studies presented in this thesis collectively demonstrate that sensor-based movement analysis can be a powerful tool for identifying, quantifying, and monitoring movement irregularities in both clinical and occupational domains. Key findings include:

- RGB-D camera-based systems, such as the AzureKinect, can reliably quantify gait parameters and correlate strongly with gold-standard systems like GAITRite, supporting their use for clinical movement assessment and monitoring in both HPs and PwPD's (chapter 4).
- Markerless video-based MoCap systems (Smart-BT) demonstrated validity for MSD prevention use cases, providing accurate joint angle estimation across diverse movement tasks, though performance was context-dependent (chapter 7).
- The application of tTIS for motor performance monitoring in PD was explored; the study focused on markerless kinematic feature analysis under randomized, double-blind, sham-controlled conditions(chapter 5).

- Occupational field studies (ReHopE) identified high-risk movement patterns and postures in skilled trades, highlighting the need for preventive interventions and informed workplace design (chapter 8).
- Automated activity recognition using IMUs with machine learning enabled detection of occupational activities in controlled settings (chapter 10).
- Automated, video-based postural risk assessment supported ergonomic evaluation in a complementary study (chapter 9).
- The user-centered exoskeleton evaluation did not show statistically significant reductions in ergonomic risk or muscle activation across tasks; observed effects were task- and device-dependent, with usability and perceived benefit influencing acceptance (chapter 9).
- Movement analysis can inform ergonomic interventions in healthcare settings, with potential to reduce WRMSD risk among healthcare workers; however, real-world validation and long-term impact assessments are still needed (chapter 9).

These findings confirm the feasibility and utility of integrating innovative sensor technologies and AI models to provide objective, scalable, and accessible movement assessment tools for diverse populations. The research bridges clinical and occupational applications, supports early diagnosis and prevention strategies, and lays the foundation for future advances in movement health monitoring.

12.5 Closing Remarks

The findings of this research emphasize the importance of objective, data-driven movement analysis. By leveraging multi-sensor tracking and AI, this work bridges the gap between clinical diagnostics and occupational risk assessment. While promising, challenges remain in ensuring scalability, cost-effectiveness, and real-world applicability. Future research should focus on refining sensor fusion techniques, validating models in real-world environments, and expanding datasets to improve generalizability. The insights gained from this thesis lay the groundwork for early detection systems that could significantly impact movement health monitoring and injury prevention.

Part V

Appendices

13 Appendix: Validation of Video-Based Movement Assessment (Smart-BT Validation Study)

Table 13.1: Normality check for AzureKinect vs CAPTIV angle differences.

Participant	Angle Comparison	p-value	Normality
ALDXB	kneeRight flexion kinect vs kneeRight flexion captiv	<0.0001	Not normal
ALDXB	kneeLeft flexion kinect vs kneeLeft flexion captiv	<0.0001	Not normal
ALDXB	back forward flexion kinect vs back forward flexion captiv	<0.0001	Not normal
ALDXB	back lateral flexion kinect vs back lateral flexion captiv	<0.0001	Not normal
ALDXB	hipLeft forward flexion kinect vs hipLeft forward flexion captiv	<0.0001	Not normal
ALDXB	hipRight forward flexion kinect vs hipRight forward flexion captiv	<0.0001	Not normal
FFOUQ	kneeRight flexion kinect vs kneeRight flexion captiv	<0.0001	Not normal
FFOUQ	kneeLeft flexion kinect vs kneeLeft flexion captiv	<0.0001	Not normal
FFOUQ	back forward flexion kinect vs back forward flexion captiv	<0.0001	Not normal
FFOUQ	back lateral flexion kinect vs back lateral flexion captiv	<0.0001	Not normal
FFOUQ	hipLeft forward flexion kinect vs hipLeft forward flexion captiv	<0.0001	Not normal
FFOUQ	hipRight forward flexion kinect vs hipRight forward flexion captiv	<0.0001	Not normal
IGTPL	kneeRight flexion kinect vs kneeRight flexion captiv	nan	Not normal
IGTPL	kneeLeft flexion kinect vs kneeLeft flexion captiv	nan	Not normal
IGTPL	back forward flexion kinect vs back forward flexion captiv	<0.0001	Not normal
IGTPL	back lateral flexion kinect vs back lateral flexion captiv	<0.0001	Not normal
IGTPL	hipLeft forward flexion kinect vs hipLeft forward flexion captiv	<0.0001	Not normal
IGTPL	hipRight forward flexion kinect vs hipRight forward flexion captiv	<0.0001	Not normal
IOKCB	kneeRight flexion kinect vs kneeRight flexion captiv	<0.0001	Not normal
IOKCB	kneeLeft flexion kinect vs kneeLeft flexion captiv	<0.0001	Not normal
IOKCB	back forward flexion kinect vs back forward flexion captiv	<0.0001	Not normal
IOKCB	back lateral flexion kinect vs back lateral flexion captiv	<0.0001	Not normal

continued . . .

Table 13.1: Normality check for AzureKinect vs CAPTIV angle differences.

Participant	Angle Comparison	p-value	Normality
IOKCB	hipLeft forward flexion kinect vs hipLeft forward flexion captiv	<0.0001	Not normal
IOKCB	hipRight forward flexion kinect vs hipRight forward flexion captiv	<0.0001	Not normal
JADEZ	kneeRight flexion kinect vs kneeRight flexion captiv	nan	Not normal
JADEZ	kneeLeft flexion kinect vs kneeLeft flexion captiv	nan	Not normal
JADEZ	back forward flexion kinect vs back forward flexion captiv	<0.0001	Not normal
JADEZ	back lateral flexion kinect vs back lateral flexion captiv	<0.0001	Not normal
JADEZ	hipLeft forward flexion kinect vs hipLeft forward flexion captiv	<0.0001	Not normal
JADEZ	hipRight forward flexion kinect vs hipRight forward flexion captiv	<0.0001	Not normal
JPTUL	kneeRight flexion kinect vs kneeRight flexion captiv	nan	Not normal
JPTUL	kneeLeft flexion kinect vs kneeLeft flexion captiv	<0.0001	Not normal
JPTUL	back forward flexion kinect vs back forward flexion captiv	<0.0001	Not normal
JPTUL	back lateral flexion kinect vs back lateral flexion captiv	<0.0001	Not normal
JPTUL	hipLeft forward flexion kinect vs hipLeft forward flexion captiv	<0.0001	Not normal
JPTUL	hipRight forward flexion kinect vs hipRight forward flexion captiv	<0.0001	Not normal
MFVWE	kneeRight flexion kinect vs kneeRight flexion captiv	<0.0001	Not normal
MFVWE	kneeLeft flexion kinect vs kneeLeft flexion captiv	<0.0001	Not normal
MFVWE	back forward flexion kinect vs back forward flexion captiv	<0.0001	Not normal
MFVWE	back lateral flexion kinect vs back lateral flexion captiv	<0.0001	Not normal
MFVWE	hipLeft forward flexion kinect vs hipLeft forward flexion captiv	<0.0001	Not normal
MFVWE	hipRight forward flexion kinect vs hipRight forward flexion captiv	<0.0001	Not normal
NZHKH	kneeRight flexion kinect vs kneeRight flexion captiv	<0.0001	Not normal
NZHKH	kneeLeft flexion kinect vs kneeLeft flexion captiv	<0.0001	Not normal
NZHKH	back forward flexion kinect vs back forward flexion captiv	<0.0001	Not normal
NZHKH	back lateral flexion kinect vs back lateral flexion captiv	<0.0001	Not normal

continued ...

Table 13.1: Normality check for AzureKinect vs CAPTIV angle differences.

Participant	Angle Comparison	p-value	Normality
NZHKH	hipLeft forward flexion kinect vs hipLeft forward flexion captiv	<0.0001	Not normal
NZHKH	hipRight forward flexion kinect vs hipRight forward flexion captiv	<0.0001	Not normal
SIHRR	kneeRight flexion kinect vs kneeRight flexion captiv	<0.0001	Not normal
SIHRR	kneeLeft flexion kinect vs kneeLeft flexion captiv	<0.0001	Not normal
SIHRR	back forward flexion kinect vs back forward flexion captiv	<0.0001	Not normal
SIHRR	back lateral flexion kinect vs back lateral flexion captiv	<0.0001	Not normal
SIHRR	hipLeft forward flexion kinect vs hipLeft forward flexion captiv	<0.0001	Not normal
SIHRR	hipRight forward flexion kinect vs hipRight forward flexion captiv	<0.0001	Not normal
ZZGKG	kneeRight flexion kinect vs kneeRight flexion captiv	<0.0001	Not normal
ZZGKG	kneeLeft flexion kinect vs kneeLeft flexion captiv	<0.0001	Not normal
ZZGKG	back forward flexion kinect vs back forward flexion captiv	<0.0001	Not normal
ZZGKG	back lateral flexion kinect vs back lateral flexion captiv	<0.0001	Not normal
ZZGKG	hipLeft forward flexion kinect vs hipLeft forward flexion captiv	<0.0001	Not normal
ZZGKG	hipRight forward flexion kinect vs hipRight forward flexion captiv	<0.0001	Not normal

Table 13.2: Statistical test results for AzureKinect vs CAPTIV.

Participant	Angle Comparison	Test	Statistic	p-value
ALDXB	kneeRight flexion kinect vs kneeRight flexion captiv	Wilcoxon	157957559.0	<0.0001
ALDXB	kneeLeft flexion kinect vs kneeLeft flexion captiv	Wilcoxon	477553400.0	<0.0001
ALDXB	back forward flexion kinect vs back forward flexion captiv	Wilcoxon	564002311.0	0.0167
ALDXB	back lateral flexion kinect vs back lateral flexion captiv	Wilcoxon	320558960.0	<0.0001
ALDXB	hipLeft forward flexion kinect vs hipLeft forward flexion captiv	Wilcoxon	329245876.0	<0.0001
ALDXB	hipRight forward flexion kinect vs hipRight forward flexion captiv	Wilcoxon	373679966.0	<0.0001
FFOUQ	kneeRight flexion kinect vs kneeRight flexion captiv	Wilcoxon	577092427.0	<0.0001

continued . . .

Table 13.2: Statistical test results for AzureKinect vs CAPTIV.

Participant	Angle Comparison	Test	Statistic	p-value
FFOUQ	kneeLeft flexion kinect vs kneeLeft flexion captiv	Wilcoxon	490478796.0	<0.0001
FFOUQ	back forward flexion kinect vs back forward flexion captiv	Wilcoxon	471384826.0	<0.0001
FFOUQ	back lateral flexion kinect vs back lateral flexion captiv	Wilcoxon	351550205.0	<0.0001
FFOUQ	hipLeft forward flexion kinect vs hipLeft forward flexion captiv	Wilcoxon	468264711.0	<0.0001
FFOUQ	hipRight forward flexion kinect vs hipRight forward flexion captiv	Wilcoxon	210202639.0	<0.0001
IGTPL	kneeRight flexion kinect vs kneeRight flexion captiv	Wilcoxon	420386188.0	<0.0001
IGTPL	kneeLeft flexion kinect vs kneeLeft flexion captiv	Wilcoxon	259127747.0	<0.0001
IGTPL	back forward flexion kinect vs back forward flexion captiv	Wilcoxon	400869043.0	<0.0001
IGTPL	back lateral flexion kinect vs back lateral flexion captiv	Wilcoxon	221795172.0	<0.0001
IGTPL	hipLeft forward flexion kinect vs hipLeft forward flexion captiv	Wilcoxon	448263873.0	<0.0001
IGTPL	hipRight forward flexion kinect vs hipRight forward flexion captiv	Wilcoxon	452925293.0	<0.0001
IOKCB	kneeRight flexion kinect vs kneeRight flexion captiv	Wilcoxon	583315718.0	<0.0001
IOKCB	kneeLeft flexion kinect vs kneeLeft flexion captiv	Wilcoxon	614343984.0	<0.0001
IOKCB	back forward flexion kinect vs back forward flexion captiv	Wilcoxon	120870278.0	<0.0001
IOKCB	back lateral flexion kinect vs back lateral flexion captiv	Wilcoxon	398975172.0	<0.0001
IOKCB	hipLeft forward flexion kinect vs hipLeft forward flexion captiv	Wilcoxon	541411866.0	<0.0001
IOKCB	hipRight forward flexion kinect vs hipRight forward flexion captiv	Wilcoxon	532584936.0	<0.0001
JADEZ	kneeRight flexion kinect vs kneeRight flexion captiv	Wilcoxon	687887301.0	<0.0001
JADEZ	kneeLeft flexion kinect vs kneeLeft flexion captiv	Wilcoxon	542534793.0	<0.0001
JADEZ	back forward flexion kinect vs back forward flexion captiv	Wilcoxon	724363125.0	<0.0001
JADEZ	back lateral flexion kinect vs back lateral flexion captiv	Wilcoxon	377247343.0	<0.0001
JADEZ	hipLeft forward flexion kinect vs hipLeft forward flexion captiv	Wilcoxon	761680647.0	0.0096
JADEZ	hipRight forward flexion kinect vs hipRight forward flexion captiv	Wilcoxon	663138308.0	<0.0001
JPTUL	kneeRight flexion kinect vs kneeRight flexion captiv	Wilcoxon	176881938.0	<0.0001

continued . . .

Table 13.2: Statistical test results for AzureKinect vs CAPTIV.

Participant	Angle Comparison	Test	Statistic	p-value
JPTUL	kneeLeft flexion kinect vs kneeLeft flexion captiv	Wilcoxon	196346283.0	<0.0001
JPTUL	back forward flexion kinect vs back forward flexion captiv	Wilcoxon	189912859.0	<0.0001
JPTUL	back lateral flexion kinect vs back lateral flexion captiv	Wilcoxon	158017018.0	<0.0001
JPTUL	hipLeft forward flexion kinect vs hipLeft forward flexion captiv	Wilcoxon	310135311.0	<0.0001
JPTUL	hipRight forward flexion kinect vs hipRight forward flexion captiv	Wilcoxon	364193845.0	<0.0001
MFVWE	kneeRight flexion kinect vs kneeRight flexion captiv	Wilcoxon	311859757.0	<0.0001
MFVWE	kneeLeft flexion kinect vs kneeLeft flexion captiv	Wilcoxon	520154301.0	<0.0001
MFVWE	back forward flexion kinect vs back forward flexion captiv	Wilcoxon	393910581.0	<0.0001
MFVWE	back lateral flexion kinect vs back lateral flexion captiv	Wilcoxon	524919653.0	<0.0001
MFVWE	hipLeft forward flexion kinect vs hipLeft forward flexion captiv	Wilcoxon	596480349.0	<0.0001
MFVWE	hipRight forward flexion kinect vs hipRight forward flexion captiv	Wilcoxon	584231538.0	<0.0001
NZHKH	kneeRight flexion kinect vs kneeRight flexion captiv	Wilcoxon	265753613.0	<0.0001
NZHKH	kneeLeft flexion kinect vs kneeLeft flexion captiv	Wilcoxon	429563198.0	<0.0001
NZHKH	back forward flexion kinect vs back forward flexion captiv	Wilcoxon	382062521.0	<0.0001
NZHKH	back lateral flexion kinect vs back lateral flexion captiv	Wilcoxon	640596331.0	<0.0001
NZHKH	hipLeft forward flexion kinect vs hipLeft forward flexion captiv	Wilcoxon	555173610.0	<0.0001
NZHKH	hipRight forward flexion kinect vs hipRight forward flexion captiv	Wilcoxon	611340694.0	<0.0001
SIHRR	kneeRight flexion kinect vs kneeRight flexion captiv	Wilcoxon	480500803.0	<0.0001
SIHRR	kneeLeft flexion kinect vs kneeLeft flexion captiv	Wilcoxon	473126545.0	<0.0001
SIHRR	back forward flexion kinect vs back forward flexion captiv	Wilcoxon	332459874.0	<0.0001
SIHRR	back lateral flexion kinect vs back lateral flexion captiv	Wilcoxon	331793483.0	<0.0001
SIHRR	hipLeft forward flexion kinect vs hipLeft forward flexion captiv	Wilcoxon	397738953.0	<0.0001
SIHRR	hipRight forward flexion kinect vs hipRight forward flexion captiv	Wilcoxon	441315131.0	<0.0001
ZZGKG	kneeRight flexion kinect vs kneeRight flexion captiv	Wilcoxon	277806285.0	<0.0001

continued . . .

Table 13.2: Statistical test results for AzureKinect vs CAPTIV.

Participant	Angle Comparison	Test	Statistic	p-value
ZZGKG	kneeLeft flexion kinect vs kneeLeft flexion captiv	Wilcoxon	231708377.0	<0.0001
ZZGKG	back forward flexion kinect vs back forward flexion captiv	Wilcoxon	206990407.0	<0.0001
ZZGKG	back lateral flexion kinect vs back lateral flexion captiv	Wilcoxon	601781132.0	<0.0001
ZZGKG	hipLeft forward flexion kinect vs hipLeft forward flexion captiv	Wilcoxon	613265653.0	<0.0001
ZZGKG	hipRight forward flexion kinect vs hipRight forward flexion captiv	Wilcoxon	603244229.0	<0.0001

14 Appendix: ReHopE Hospitationen (Field Study)

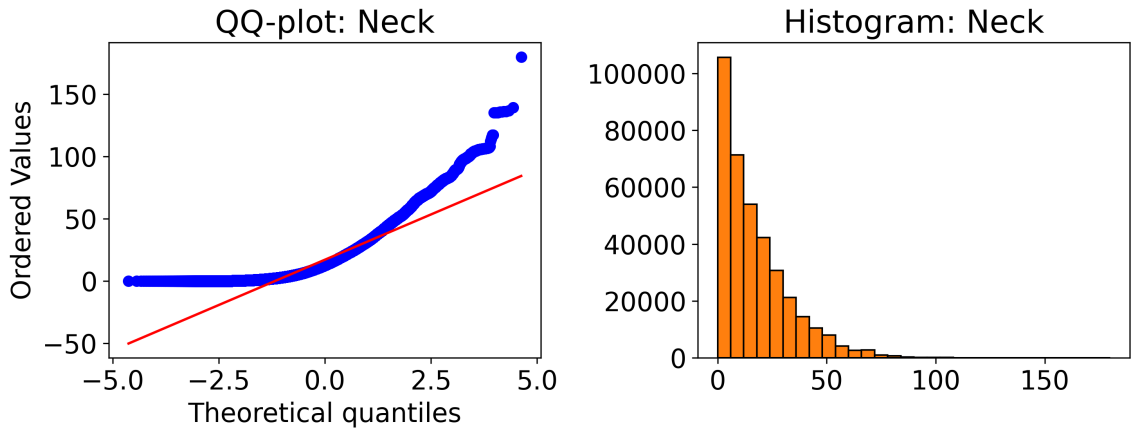

Figure 14.1: Q–Q plot and histogram of Neck flexion–extension angles demonstrating departure from normality (S-W $p < 0.05$).

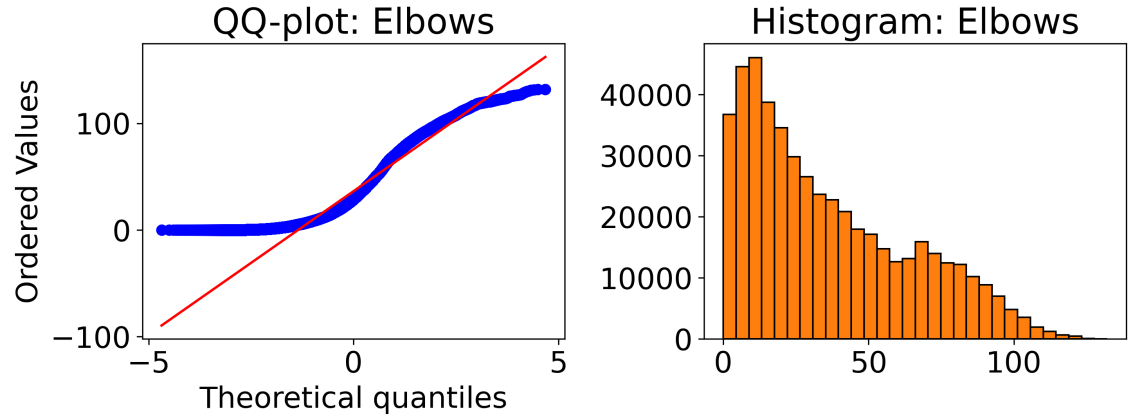

Figure 14.2: Q–Q plot and histogram of Elbows flexion–extension angles demonstrating departure from normality (S-W $p < 0.05$).

14.0.1 Remaining Tables of Statistical test results

For the sake of completeness, the remaining tables are included here. NA[1] entries mean that one of the activities was not carried out by the respective worker.

[1] Not Applicable

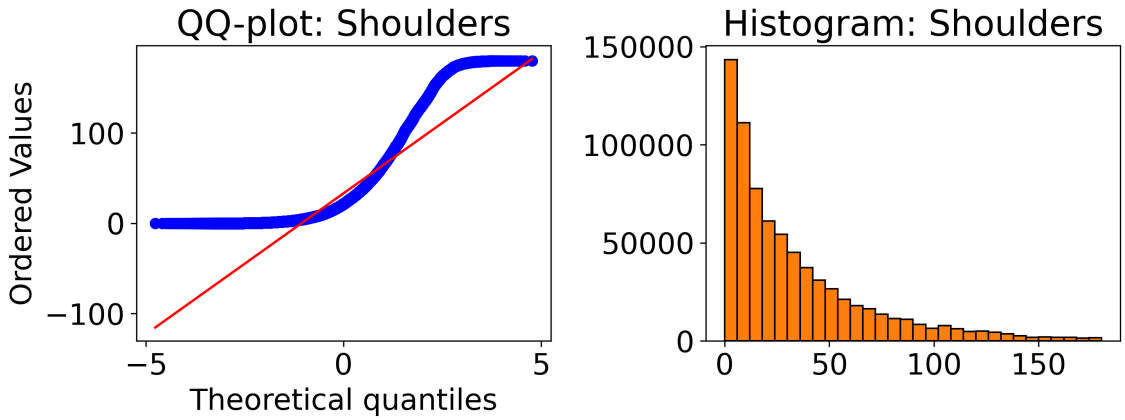

Figure 14.3: Q–Q plot and histogram of Shoulders flexion–extension angles demonstrating departure from normality (S-W $p < 0.05$).

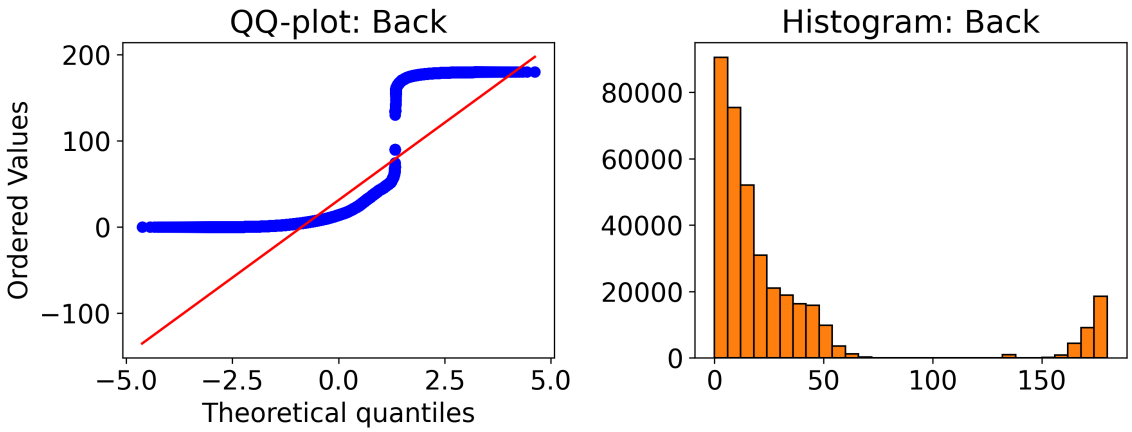

Figure 14.4: Q–Q plot and histogram of Back flexion–extension angles demonstrating departure from normality (S-W $p < 0.05$).

Table 14.1: Window Maker: Statistical test results for load-dropping vs load-lifting

Joint Angle	Test	value (U/t)	p-value	Significance
Neck Flex/Ext	Wil	10303635.0	<0.0001	SIGNIFICANT
Neck Lateral flexion	Wil	8710282.0	0.9653	not significant
Neck Rotation	Wil	8196304.0	<0.0001	SIGNIFICANT
Back Forward flexion	Wil	12367706.0	<0.0001	SIGNIFICANT
Back Lateral flexion	Wil	10141804.0	<0.0001	SIGNIFICANT
Back Rotation	Wil	6195121.0	<0.0001	SIGNIFICANT
Shoulder (Right) (Projection) Abd/Add	Wil	9413634.0	<0.0001	SIGNIFICANT
Shoulder (Left) (Projection) Abd/Add	Wil	8372298.0	0.0027	SIGNIFICANT
Shoulder (Right) (Projection) Flex/Ext	Wil	8261084.0	<0.0001	SIGNIFICANT
Shoulder (Left) (Projection) Flex/Ext	Wil	7865521.0	<0.0001	SIGNIFICANT
Shoulder (Right) Rotation	Wil	9264381.0	<0.0001	SIGNIFICANT
Shoulder (Left) Rotation	Wil	10133717.0	<0.0001	SIGNIFICANT
Elbow (Right) Flex/Ext	Wil	7800911.0	<0.0001	SIGNIFICANT
Elbow (Left) Flex/Ext	Wil	5583602.0	<0.0001	SIGNIFICANT
Elbow (Right) Rotation	Wil	9345295.0	<0.0001	SIGNIFICANT
Elbow (Left) Rotation	Wil	7931736.0	<0.0001	SIGNIFICANT
Knee (Left) Flex/Ext	Wil	12293548.0	<0.0001	SIGNIFICANT
Knee (Right) Flex/Ext	Wil	10238630.0	<0.0001	SIGNIFICANT

Table 14.2: Window Maker: Statistical test results for standing vs climbing

Joint Angle	Test	value (U/t)	p-value	Significance
Neck Flex/Ext	Wil	401216.0	<0.0001	SIGNIFICANT
Neck Lateral flexion	Wil	335867.0	0.1354	not significant
Neck Rotation	Wil	386901.0	<0.0001	SIGNIFICANT
Back Forward flexion	Wil	133441.0	<0.0001	SIGNIFICANT
Back Lateral flexion	Wil	235479.0	<0.0001	SIGNIFICANT
Back Rotation	Wil	242472.0	<0.0001	SIGNIFICANT
Shoulder (Right) (Projection) Abd/Add	Wil	268443.0	<0.0001	SIGNIFICANT
Shoulder (Left) (Projection) Abd/Add	Wil	383550.0	<0.0001	SIGNIFICANT
Shoulder (Right) (Projection) Flex/Ext	Wil	314247.0	0.4217	not significant
Shoulder (Left) (Projection) Flex/Ext	Wil	320852.0	0.9190	not significant
Shoulder (Right) Rotation	Wil	229834.0	<0.0001	SIGNIFICANT
Shoulder (Left) Rotation	Wil	289382.0	0.0006	SIGNIFICANT
Elbow (Right) Flex/Ext	Wil	375545.0	<0.0001	SIGNIFICANT
Elbow (Left) Flex/Ext	Wil	496617.0	<0.0001	SIGNIFICANT
Elbow (Right) Rotation	Wil	300271.0	0.0221	SIGNIFICANT
Elbow (Left) Rotation	Wil	380214.0	<0.0001	SIGNIFICANT
Knee (Left) Flex/Ext	Wil	81163.0	<0.0001	SIGNIFICANT
Knee (Right) Flex/Ext	Wil	47573.0	<0.0001	SIGNIFICANT

Table 14.3: HVAC Technicians: Statistical test results for floor-work vs bent-over-work

Joint Angle	Test	value (U/t)	p-value	Significance
Neck Flex/Ext	Wil	9326713.0	<0.0001	SIGNIFICANT
Neck Lateral flexion	Wil	21573137.0	<0.0001	SIGNIFICANT
Neck Rotation	Wil	20781413.0	<0.0001	SIGNIFICANT
Back Forward flexion	Wil	26531233.0	<0.0001	SIGNIFICANT
Back Lateral flexion	Wil	13281529.0	<0.0001	SIGNIFICANT
Back Rotation	Wil	25578735.0	<0.0001	SIGNIFICANT
Shoulder (Right) (Projection) Abd/Add	Wil	23928683.0	<0.0001	SIGNIFICANT
Shoulder (Left) (Projection) Abd/Add	Wil	12876901.0	<0.0001	SIGNIFICANT
Shoulder (Right) (Projection) Flex/Ext	Wil	20044156.0	<0.0001	SIGNIFICANT
Shoulder (Left) (Projection) Flex/Ext	Wil	16233035.0	<0.0001	SIGNIFICANT
Shoulder (Right) Rotation	Wil	23309808.0	0.0042	SIGNIFICANT
Shoulder (Left) Rotation	Wil	21028962.0	<0.0001	SIGNIFICANT
Elbow (Right) Flex/Ext	Wil	25576902.0	<0.0001	SIGNIFICANT
Elbow (Left) Flex/Ext	Wil	25190822.0	<0.0001	SIGNIFICANT
Elbow (Right) Rotation	Wil	27417313.0	<0.0001	SIGNIFICANT
Elbow (Left) Rotation	Wil	22724903.0	0.7003	not significant
Knee (Left) Flex/Ext	Wil	43468606.0	<0.0001	SIGNIFICANT
Knee (Right) Flex/Ext	Wil	45015285.0	<0.0001	SIGNIFICANT

Table 14.4: HVAC Technicians: Statistical test results for load-dropping vs load-lifting

Joint Angle	Test	value (U/t)	p-value	Significance
Neck Flex/Ext	Wil	698937.0	<0.0001	SIGNIFICANT
Neck Lateral flexion	Wil	558592.0	<0.0001	SIGNIFICANT
Neck Rotation	Wil	930071.0	0.0040	SIGNIFICANT
Back Forward flexion	Wil	870156.0	0.8789	not significant
Back Lateral flexion	Wil	914366.0	0.0307	SIGNIFICANT
Back Rotation	Wil	789838.0	0.0005	SIGNIFICANT
Shoulder (Right) (Projection) Abd/Add	Wil	896505.0	0.1772	not significant
Shoulder (Left) (Projection) Abd/Add	Wil	691625.0	<0.0001	SIGNIFICANT
Shoulder (Right) (Projection) Flex/Ext	Wil	866637.0	0.9940	not significant
Shoulder (Left) (Projection) Flex/Ext	Wil	577852.0	<0.0001	SIGNIFICANT
Shoulder (Right) Rotation	Wil	648815.0	<0.0001	SIGNIFICANT
Shoulder (Left) Rotation	Wil	1136888.0	<0.0001	SIGNIFICANT
Elbow (Right) Flex/Ext	Wil	703154.0	<0.0001	SIGNIFICANT
Elbow (Left) Flex/Ext	Wil	916020.0	0.0253	SIGNIFICANT
Elbow (Right) Rotation	Wil	899462.0	0.1379	not significant
Elbow (Left) Rotation	Wil	853525.0	0.5463	not significant
Knee (Left) Flex/Ext	Wil	748784.0	<0.0001	SIGNIFICANT
Knee (Right) Flex/Ext	Wil	945355.0	0.0004	SIGNIFICANT

Table 14.5: HVAC Technicians: Statistical test results for standing vs climbing

Joint Angle	Test	value (U/t)	p-value	Significance
Neck Flex/Ext	Wil	2480758.0	<0.0001	SIGNIFICANT
Neck Lateral flexion	Wil	3646956.0	<0.0001	SIGNIFICANT
Neck Rotation	Wil	6593959.0	<0.0001	SIGNIFICANT
Back Forward flexion	Wil	3145899.0	<0.0001	SIGNIFICANT
Back Lateral flexion	Wil	1861811.0	<0.0001	SIGNIFICANT
Back Rotation	Wil	3617145.0	<0.0001	SIGNIFICANT
Shoulder (Right) (Projection) Abd/Add	Wil	1667796.0	<0.0001	SIGNIFICANT
Shoulder (Left) (Projection) Abd/Add	Wil	1673338.0	<0.0001	SIGNIFICANT
Shoulder (Right) (Projection) Flex/Ext	Wil	2724124.0	<0.0001	SIGNIFICANT
Shoulder (Left) (Projection) Flex/Ext	Wil	503425.0	<0.0001	SIGNIFICANT
Shoulder (Right) Rotation	Wil	1881538.0	<0.0001	SIGNIFICANT
Shoulder (Left) Rotation	Wil	5145124.0	<0.0001	SIGNIFICANT
Elbow (Right) Flex/Ext	Wil	2597353.0	<0.0001	SIGNIFICANT
Elbow (Left) Flex/Ext	Wil	3459465.0	<0.0001	SIGNIFICANT
Elbow (Right) Rotation	Wil	4336471.0	<0.0001	SIGNIFICANT
Elbow (Left) Rotation	Wil	2864586.0	<0.0001	SIGNIFICANT
Knee (Left) Flex/Ext	Wil	688160.0	<0.0001	SIGNIFICANT
Knee (Right) Flex/Ext	Wil	700119.0	<0.0001	SIGNIFICANT

Table 14.6: Lightning Protection Worker: Statistical test results for floor-work vs bent-over-work

Joint Angle	Test	value (U/t)	p-value	Significance
Neck Flex/Ext	Wil	35631096.0	<0.0001	SIGNIFICANT
Neck Lateral flexion	Wil	27587759.0	<0.0001	SIGNIFICANT
Neck Rotation	Wil	21721315.0	<0.0001	SIGNIFICANT
Back Forward flexion	Wil	16650240.0	<0.0001	SIGNIFICANT
Back Lateral flexion	Wil	33496874.0	<0.0001	SIGNIFICANT
Back Rotation	Wil	27200696.0	<0.0001	SIGNIFICANT
Shoulder (Right) (Projection) Abd/Add	Wil	20461871.0	<0.0001	SIGNIFICANT
Shoulder (Left) (Projection) Abd/Add	Wil	24650052.0	<0.0001	SIGNIFICANT
Shoulder (Right) (Projection) Flex/Ext	Wil	27377310.0	<0.0001	SIGNIFICANT
Shoulder (Left) (Projection) Flex/Ext	Wil	28804309.0	0.2828	not significant
Shoulder (Right) Rotation	Wil	30458541.0	<0.0001	SIGNIFICANT
Shoulder (Left) Rotation	Wil	39819128.0	<0.0001	SIGNIFICANT
Elbow (Right) Flex/Ext	Wil	30470261.0	<0.0001	SIGNIFICANT
Elbow (Left) Flex/Ext	Wil	25867002.0	<0.0001	SIGNIFICANT
Elbow (Right) Rotation	Wil	19102325.0	<0.0001	SIGNIFICANT
Elbow (Left) Rotation	Wil	35809763.0	<0.0001	SIGNIFICANT
Knee (Left) Flex/Ext	Wil	53695444.0	<0.0001	SIGNIFICANT
Knee (Right) Flex/Ext	Wil	52819560.0	<0.0001	SIGNIFICANT

Table 14.7: Lightning Protection Worker: Statistical test results for load-dropping vs load-lifting

Joint Angle	Test	value (U/t)	p-value	Significance
Neck Flex/Ext	Wil	1638099.0	<0.0001	SIGNIFICANT
Neck Lateral flexion	Wil	1868455.0	<0.0001	SIGNIFICANT
Neck Rotation	Wil	1958703.0	<0.0001	SIGNIFICANT
Back Forward flexion	Wil	3802844.0	<0.0001	SIGNIFICANT
Back Lateral flexion	Wil	2600637.0	0.8680	not significant
Back Rotation	Wil	1600362.0	<0.0001	SIGNIFICANT
Shoulder (Right) (Projection) Abd/Add	Wil	2198077.0	<0.0001	SIGNIFICANT
Shoulder (Left) (Projection) Abd/Add	Wil	1782971.0	<0.0001	SIGNIFICANT
Shoulder (Right) (Projection) Flex/Ext	Wil	2778635.0	0.0002	SIGNIFICANT
Shoulder (Left) (Projection) Flex/Ext	Wil	2735974.0	0.0055	SIGNIFICANT
Shoulder (Right) Rotation	Wil	3314001.0	<0.0001	SIGNIFICANT
Shoulder (Left) Rotation	Wil	2905707.0	<0.0001	SIGNIFICANT
Elbow (Right) Flex/Ext	Wil	1613812.0	<0.0001	SIGNIFICANT
Elbow (Left) Flex/Ext	Wil	1860640.0	<0.0001	SIGNIFICANT
Elbow (Right) Rotation	Wil	1422597.0	<0.0001	SIGNIFICANT
Elbow (Left) Rotation	Wil	3124067.0	<0.0001	SIGNIFICANT
Knee (Left) Flex/Ext	Wil	3776466.0	<0.0001	SIGNIFICANT
Knee (Right) Flex/Ext	Wil	3829974.0	<0.0001	SIGNIFICANT

15 Appendix: Validation of portable multi-sensor system for movement analysis (TEDIPA study)

15.1 Demographic Data for all Study Participants

Table 15.1: Demographic data for all evaluated study participants.

Participant	Gender	Age [years]	Height [cm]	Weight [kg]	Left Leg Length [cm]	Right Leg Length [cm]
HP-1	F	37	168	50	88	86
HP-2	M	38	190	110	97	97
HP-3	M	30	177	67	93	94
HP-4	F	29	173	70	94	95
HP-5	F	27	165	74	86	86.5
HP-6	M	20	173	66	86	87
HP-7	M	31	183	105	94	93
HP-8	F	24	168	65	87	90
HP-9	F	38	172	65	93	94
HP-10	F	52	171	73	92	94
HP-11	M	45	198	152	96	96
PwPD-1	F	79	156	62	89	89
PwPD-2	M	64	179	88	94	94
PwPD-3	M	70	180	75	98	99
PwPD-4	F	48	168	97	94	94
PwPD-5	M	73	176	73	92	93
PwPD-6	M	77	175	77	99	98
PwPD-8	F	74	160	74	84	83
PwPD-9	F	71	168	71	85	85
PwPD-10	M	69	176	69	94	93
PwPD-12	F	48	168	97	94	94
PwPD-13	F	49	159	49	77	78
PwPD-14	M	78	177	78	95	93
PwPD-15	F	67	156	67	84	85

List of Figures

List of Tables

Bibliography

[22] *CRediT, Contributor Roles Taxonomy*. Standard. Approved by the American National Standards Institute; freely available at https://www.niso.org/publications/z39104-2022-credit. Baltimore, MD, USA: National Information Standards Organization (NISO), 2022. URL: https://www.niso.org/publications/z39104-2022-credit.

[AG22] Noonee AG. *Chairless Chair 2 product image*. https://shop.noonee.com/cdn/shop/products/NOONEECHAIRLESS2_4.jpg?v=1669716343&width=823. Accessed: 2025-11-01. 2022.

[Alb+20] Justin Amadeus Albert et al. "Evaluation of the pose tracking performance of the azure kinect and kinect v2 for gait analysis in comparison with a gold standard: A pilot study". In: *Sensors* 20.18 (2020), p. 5104. DOI: 10.3390/s20185104. URL: https://www.mdpi.com/1424-8220/20/18/5104.

[Alc+18] Lisa Alcock et al. "Step length determines minimum toe clearance in older adults and people with Parkinson's disease". In: *Journal of biomechanics* 71 (2018), pp. 30–36. URL: https://doi.org/10.1016/j.jbiomech.2017.12.002.

[Amb+18] Marianna Amboni et al. "Step length predicts executive dysfunction in Parkinson's disease: a 3-year prospective study". In: *Journal of neurology* 265.10 (2018), pp. 2211–2220. DOI: 10.1007/s00415-018-8973-x. URL: https://doi.org/10.1007/s00415-018-8973-x.

[Ara+15] Juan David Arango Paredes et al. "A reliability assessment software using Kinect to complement the clinical evaluation of Parkinson's disease". In: *Proceedings of the Annual International Conference of the IEEE Engineering in Medicine and Biology Society, EMBS* 2015-Novem.August 2015 (2015), pp. 6860–6863. ISSN: 1557170X. DOI: 10.1109/EMBC.2015.7319969.

[Ari+20a] Pedro Arizpe-Gomez et al. "Preliminary Viability Test of a 3-D-Consumer-Camera-Based System for Automatic Gait Feature Detection in People with and without Parkinson's Disease". In: *2020 IEEE International Conference on Healthcare Informatics (ICHI)*. IEEE. 2020, pp. 1–7.

[Ari+20b] Pedro Arizpe-Gomez et al. "Preliminary Viability Test of a 3-D-Consumer-Camera-Based System for Automatic Gait Feature Detection in People with and without Parkinson's Disease". In: *2020 IEEE International conference on healthcare informatics (ICHI)*. IEEE. 2020, pp. 1–10.

[Ari+24] Pedro Arizpe-Gómez et al. "Towards automated self-administered motor status assessment: Validation of a depth camera system for gait feature analysis". In: *Biomedical Signal Processing and Control* 87 (2024), p. 105352.

[AS16] Alberto Ascherio and Michael A Schwarzschild. "The epidemiology of Parkinson's disease: risk factors and prevention". In: *The Lancet Neurology* 15.12 (2016), pp. 1257–1272.

[Bab+25] Abubakar A Babangida et al. "Advancing Occupational Medicine through Wearable Technology: A Review of Sensor Systems for Biomechanical Risk Assessment and Work-Related Musculoskeletal Disorder Prevention". In: *ACS sensors* (2025).

[Bal+14] Greet Baldewijns et al. "Validation of the kinect for gait analysis using the GAITRite walkway". In: *2014 36th Annual International Conference of the IEEE Engineering in Medicine and Biology Society*. IEEE. 2014, pp. 5920–5923.

[Bam+18] Cyrus S. Bamji et al. "IMpixel 65nm BSI 320MHz demodulated TOF Image sensor with 3μm global shutter pixels and analog binning". In: *Digest of Technical Papers - IEEE International Solid-State Circuits Conference* 61 (2018), pp. 94–96. ISSN: 01936530. DOI: 10.1109/ISSCC.2018.8310200.

[Baz+20] Valentin Bazarevsky et al. "BlazePose: On-device Real-time Body Pose tracking". In: *CoRR* abs/2006.10204 (2020). arXiv: 2006.10204. URL: https://arxiv.org/abs/2006.10204.

[Ben+09] Alim-Louis Benabid et al. “Deep brain stimulation of the subthalamic nucleus for the treatment of Parkinson’s disease”. In: *The Lancet Neurology* 8.1 (2009), pp. 67–81. DOI: 10.1016/S1474-4422(08)70291-6.

[Bou+22] Eleni Boumpa et al. “Security and Privacy Concerns for Healthcare Wearable Devices and Emerging Alternative Approaches”. In: *Wireless Mobile Communication and Healthcare*. Springer, 2022, pp. 19–38. DOI: 10.1007/978-3-031-06368-8_2.

[Bou25] Anastasia Bougea. “Application of wearable sensors in Parkinson’s disease: state of the art”. In: *Journal of Sensor and Actuator Networks* 14.2 (2025), p. 23.

[BP97] Bruce P Bernard and Vern Putz-Anderson. “Musculoskeletal disorders and workplace factors: a critical review of epidemiologic evidence for work-related musculoskeletal disorders of the neck, upper extremity, and low back”. In: (1997). DOI: 10.26616/NIOSHPUB97141.

[Bro96] John Brooke. “SUS - A quick and dirty usability scale”. In: *Usability Evaluation in Industry* (1996), pp. 189–194.

[BSF21] Ulrike Bechtold, Natalie Stauder, and Martin Fieder. “Let’s walk it: Mobility and the perceived quality of life in older adults”. In: *International journal of environmental research and public health* 18.21 (2021), p. 11515. DOI: 10.3390/ijerph182111515.

[BSF94] Yoshua Bengio, Patrice Simard, and Paolo Frasconi. “Learning long-term dependencies with gradient descent is difficult”. In: *IEEE transactions on neural networks* 5.2 (1994), pp. 157–166. DOI: 10.1109/72.279181.

[But30] S. Butterworth. “On the theory of filter amplifiers”. In: *Experimental Wireless and the Wireless Engineer* 7 (1930), pp. 536–541.

[Che+25] Seyyed Saeid Cheshmi et al. “Improving Out-of-distribution Human Activity Recognition via IMU-Video Cross-modal Representation Learning”. In: *arXiv preprint arXiv:2507.13482* (2025). URL: https://arxiv.org/abs/2507.13482.

[Cra07] Joanne O Crawford. “The Nordic musculoskeletal questionnaire”. In: *Occupational medicine* 57.4 (2007), pp. 300–301.

[Cre03] John W. Creswell. *Research Design: Qualitative, Quantitative, and Mixed Methods Approaches*. 2nd. SAGE Publications, 2003. ISBN: 9780761924425.

[Cun+16] Joao Paulo Silva Cunha et al. “A novel portable, low-cost kinect-based system for motion analysis in neurological diseases”. In: *Proceedings of the Annual International Conference of the IEEE Engineering in Medicine and Biology Society, EMBS* 2016-Octob (2016), pp. 2339–2342. ISSN: 1557170X. DOI: 10.1109/EMBC.2016.7591199.

[CV10] Bruno R. Da Costa and Edgar Ramos Vieira. “Risk factors for work-related musculoskeletal disorders: a systematic review of recent longitudinal studies”. In: *American Journal of Industrial Medicine* 53.3 (2010), pp. 285–323. DOI: 10.1002/ajim.20750.

[Dav63] Herbert Aron David. *The method of paired comparisons*. Vol. 12. London, 1963.

[Deu15] Deutsche Gesetzliche Unfallversicherung (DGUV). *Bewertung physischer Belastungen gemäß DGUV - Information 208-033 (bisher: BGI/GUV-I 7011) (Anhang 3)*. Retrieved from https://www.dguv.de/medien/ifa/de/fac/ergonomie/pdf/bewertung_physischer_belastungen.pdf. 2015.

[DNH24] Malcolm Dunson-Todd, Mazdak Nik-Bakht, and Amin Hammad. “Experimental Evaluation of Exoskeletons for Rebar Workers Using a Realistic Controlled Test”. In: *ISARC. Proceedings of the International Symposium on Automation and Robotics in Construction*. Vol. 41. IAARC Publications. 2024, pp. 513–520.

[Don+21] Jiahui Dong et al. “A Survey on Human Pose Estimation: Single Person and Multi-Person Pose Estimation”. In: *Sensors* 21.12 (2021), p. 4290. DOI: 10.3390/s21124290.

[DRK25] DRKS. *DRKS00030841: Transcranial temporal interference stimulation of deep brain regions in Parkinson's disease patients and healthy controls (TETRIS)*. German Clinical Trials Register. Prospective registration; last registry update 03 Feb 2025; status: recruitment completed, study completed; total N=36. 2025. URL: https://www.drks.de/DRKS00030841.

[Dro+] Sandra Drolshagen et al. "Exoskeletons in Skilled Trades: Challenges and Chances". In Publishing.

[DV10] Bruno R Da Costa and Edgar Ramos Vieira. "Risk factors for work-related musculoskeletal disorders: a systematic review of recent longitudinal studies". In: *American journal of industrial medicine* 53.3 (2010), pp. 285–323. DOI: 10.1002/ajim.20750.

[Elm90] Jeffrey L Elman. "Finding structure in time". In: *Cognitive science* 14.2 (1990), pp. 179–211. DOI: 10.1207/s15516709cog1402_1.

[Elt+17] Moataz Eltoukhy et al. "Microsoft Kinect can distinguish differences in over-ground gait between older persons with and without Parkinson's disease". In: *Medical Engineering and Physics* 44 (2017), pp. 1–7. ISSN: 18734030. DOI: 10.1016/j.medengphy.2017.03.007.

[Esk+16] Bjoern M Eskofier et al. "Recent machine learning advancements in sensor-based mobility analysis: Deep learning for Parkinson's disease assessment". In: *2016 38th annual international conference of the IEEE engineering in medicine and biology society (EMBC)*. IEEE. 2016, pp. 655–658.

[Esp+16] Alberto J Espay et al. "Technology in Parkinson's disease: challenges and opportunities". In: *Movement Disorders* 31.9 (2016), pp. 1272–1282. DOI: 10.1002/mds.26642.

[EU-12] EU-OSHA. "Work-related musculoskeletal disorders: prevalence, costs and demographics in Germany". In: *EU-OSHA Reports* (2012). DOI: 10.2802/987654. URL: https://osha.europa.eu/sites/default/files/work_related_MSDs_Germany.pdf.

[EU-19] EU-OSHA. "Germany: Work-related musculoskeletal disorders: prevalence, costs and demographics in the EU". In: *European Agency for Safety and Health at Work* (2019). DOI: 10.2802/123456. URL: https://osha.europa.eu/de/publications/germany-work-related-musculoskeletal-disorders-prevalence-costs-and-demographics-eu.

[Eva96] James D Evans. *Straightforward statistics for the behavioral sciences*. Thomson Brooks/Cole Publishing Co, 1996.

[FOI25] Rosalynn Ornella Flores-Castañeda, Sandro Olaya-Cotera, and Orlando Iparraguirre-Villanueva. "Exploring wearable technologies for health monitoring: a systematic review of applications, advantages and disadvantages". In: *Neural Computing and Applications* (2025). DOI: 10.1007/s00521-025-11605-8.

[Fud+20] Sebastian Fudickar et al. "Measurement System for Unsupervised Standardized Assessment of Timed "Up & Go" and Five Times Sit to Stand Test in the Community–A Validity Study". In: *Sensors* 20.10 (2020), p. 2824.

[Gal+14] Brook Galna et al. "Accuracy of the Microsoft Kinect sensor for measuring movement in people with Parkinson's disease". In: *Gait and Posture* 39.4 (2014), pp. 1062–1068. ISSN: 18792219. DOI: 10.1016/j.gaitpost.2014.01.008.

[Gar+14] S. Garrido-Jurado et al. "Automatic generation and detection of highly reliable fiducial markers under occlusion". In: *Pattern Recognition* 47.6 (2014), pp. 2280–2292. ISSN: 00313203. DOI: 10.1016/j.patcog.2014.01.005. URL: http://dx.doi.org/10.1016/j.patcog.2014.01.005.

[Gar+16] S. Garrido-Jurado et al. "Generation of fiducial marker dictionaries using Mixed Integer Linear Programming". In: *Pattern Recognition* 51.October (2016), pp. 481–491. ISSN: 00313203. DOI: 10.1016/j.patcog.2015.09.023.

[GB20] Ivan Grishchenko and Valentin Bazarevsky. *MediaPipe Holistic – Simultaneous Face, Hand and Pose Prediction, on Device*. Accessed: 2025-10-27. 2020. URL: https://research.google/blog/mediapipe-holistic-simultaneous-face-hand-and-pose-prediction-on-device/.

[GI80] RM Guimaraes and Bernard Isaacs. "Characteristics of the gait in old people who fall". In: *International rehabilitation medicine* 2.4 (1980), pp. 177–180.

[Goe+08a] Christopher G Goetz et al. "MDS-UPDRS: The MDS-sponsored Revision of the Unified Parkinson's Disease Rating Scale". In: 1.414 (2008). DOI: 10.1002/mds.22340. URL: https://doi.org/10.1002/mds.22340.

[Goe+08b] Christopher G. Goetz et al. "Movement Disorder Society-Sponsored Revision of the Unified Parkinson's Disease Rating Scale (MDS-UPDRS): Scale presentation and clinimetric testing results". In: *Movement Disorders* 23.15 (2008), pp. 2129–2170. ISSN: 08853185. DOI: 10.1002/mds.22340.

[Gon+21] Hatice Gonçalves et al. "Assessment of Work-Related Musculoskeletal Disorders by Observational Methods in Repetitive Tasks–A Systematic Review". In: *Occupational and Environmental Safety and Health III*. Springer, 2021, pp. 455–463. DOI: 10.1007/978-3-030-89617-1_41.

[Goo25] Google. *Hand Landmarks Diagram*. Accessed: 2025-10-27. 2025. URL: https://mediapipe.readthedocs.io/en/latest/solutions/hands.html.

[Gro+17] Nir Grossman et al. "Noninvasive deep brain stimulation via temporally interfering electric fields". In: *cell* 169.6 (2017), pp. 1029–1041.

[Ha25] Robert A. Hauser and et al. "Evaluation of compliance and accuracy in Parkinson's disease motor symptom tracking: a comparative study of digital and traditional paper diaries using a smartphone application (MyParkinson's)". In: *Frontiers in Neurology* 16 (2025). DOI: 10.3389/fneur.2025.1522721.

[Har22] Roya Haratian. "Motion Capture Sensing Technologies and Techniques: A Sensor Agnostic Approach to Address Wearability Challenges". In: *Journal of Medical Systems* 47.1 (2022), pp. 1–15. DOI: 10.1007/s11220-022-00394-2.

[Het24] Piotr Hetmańczyk. "Digitalization and its impact on labour market and education. Selected aspects". In: *Education and Information Technologies* 29.9 (2024), pp. 11119–11134.

[HM00] Sue Hignett and Lynn McAtamney. "Rapid entire body assessment (REBA)". In: *Applied ergonomics* 31.2 (2000), pp. 201–205.

[HS88] Sandra G. Hart and Lowell E. Staveland. "Development of NASA-TLX (Task Load Index): Results of empirical and theoretical research". In: *Advances in Psychology* 52 (1988), pp. 139–183.

[HS97] Sepp Hochreiter and Jürgen Schmidhuber. "Long short-term memory". In: *Neural computation* 9.8 (1997), pp. 1735–1780. DOI: 10.1162/neco.1997.9.8.1735.

[Inc13] C S Inc. *GAITRite electronic walkway technical reference manual*. 2013.

[Ins18] Ohio State Spine Research Institute. "Biomechanical evaluation of exoskeleton use on loading of the lumbar spine". In: *Applied Ergonomics* (2018). DOI: 10.1016/j.apergo.2018.01.012. URL: https://spine.osu.edu/sites/default/files/uploads/Publications/2018/appliedergonomics_68_2018_101-108.pdf.

[JOT07] Burke Johnson, Anthony J. Onwuegbuzie, and Lisa A. Turner. "Toward a Definition of Mixed Methods Research". In: *Journal of Mixed Methods Research* 1.2 (2007), pp. 112–133. DOI: 10.1177/1558689806298224.

[Kan+25] Jung Sun Kang et al. "EMG and usability assessment of adjustable stiffness passive waist-assist exoskeletons for construction workers". In: *International Journal of Precision Engineering and Manufacturing* 26.1 (2025), pp. 227–238.

[Kei+11] Peter J Keir et al. “Compensatory movement strategies differentially affect muscle activity and joint loading in individuals with ACL deficiency”. In: *Journal of biomechanics* 44.3 (2011), pp. 455–462.

[Kel23] Sydney Aelish Kelley. “Investigating the Relationship Between Objective and Subjective Measures of Physical Demand During Passive Exoskeleton Use”. PhD thesis. Virginia Tech, 2023.

[Kha+25] Rana M. Khalil et al. “Applying Wearable Sensors and Machine Learning to the Diagnostic Challenge of Distinguishing Parkinson’s Disease from Other Forms of Parkinsonism”. In: *Biomedicines* 13.3 (2025). ISSN: 2227-9059. DOI: 10.3390/biomedicines13030572. URL: https://www.mdpi.com/2227-9059/13/3/572.

[Kil94] Åsa Kilbom. “Assessment of physical exposure in relation to work-related musculoskeletal disorders-what information can be obtained from systematic observations”. In: *Scandinavian journal of work, environment & health* (1994), pp. 30–45.

[Kon22] Y.K. et al. Kong. “Ergonomic Assessment of a Lower-Limb Exoskeleton through Electromyography”. In: *International Journal of Environmental Research and Public Health* (2022). DOI: 10.3390/ijerph19138088. URL: https://www.mdpi.com/1660-4601/19/13/8088.

[Kum+98] R Kumar et al. “Double-blind evaluation of subthalamic nucleus deep brain stimulation in advanced Parkinson’s disease”. In: *Neurology* 51.3 (1998), pp. 850–855.

[LAF23] Carl Mikael Lind, Farhad Abtahi, and Mikael Forsman. “Wearable motion capture devices for the prevention of work-related musculoskeletal disorders in ergonomics–an overview of current applications, challenges, and future opportunities”. In: *Sensors* 23.9 (2023), p. 4259.

[LEJ18] Henrik CJ Linderoth, Amany R Elbanna, and Mattias Jacobsson. “Barriers for Digital Transformation: The Role of Industry.” In: *ACIS*. 2018, p. 84.

[Lew+17] C.L. Lewis et al. “The Human Pelvis: Variation in Structure and Function During Gait”. In: *Anat Rec (Hoboken)* 4.300 (2017), pp. 633–642. DOI: 10.1002/ar.23552.

[Lim+98] Patricia Limousin et al. “Electrical stimulation of the subthalamic nucleus in advanced Parkinson’s disease”. In: *New England Journal of Medicine* 339.16 (1998), pp. 1105–1111.

[Lin21] Christian Lins. “Evolutionär optimierte Haltungs-und Bewegungsmodelle auf Basis von Motion-Capture-Daten als Teil gesundheitsbezogener Assistenzsysteme”. PhD thesis. Carl von Ossietzky Universität Oldenburg, 2021.

[LLH12] Okko Lohmann, Thomas Luhmann, and Andreas Hein. “Skeleton timed up and go”. In: *2012 IEEE International Conference on Bioinformatics and Biomedicine*. IEEE. 2012, pp. 1–5.

[Lug+19] Camillo Lugaresi et al. “MediaPipe: A framework for perceiving and processing reality”. In: *Third workshop on computer vision for AR/VR at IEEE computer vision and pattern recognition (CVPR)*. Vol. 2019. 2019.

[MC04] Lynn McAtamney and Nigel Corlett. “Rapid upper limb assessment (RULA)”. In: *Handbook of human factors and ergonomics methods*. CRC Press, 2004, pp. 86–96.

[ME13] Marie E McNeely and Gammon M Earhart. “Medication and subthalamic nucleus deep brain stimulation similarly improve balance and complex gait in Parkinson disease”. In: *Parkinsonism & related disorders* 19.1 (2013), pp. 86–91.

[Meh+17] Dushyant Mehta et al. “VNect: Real-time 3D Human Pose Estimation with a Single RGB Camera”. In: *ACM Transactions on Graphics (TOG)*. Vol. 36. 4. 2017, p. 44. DOI: 10.1145/3072959.3073596.

[Mic19] Microsoft Corporation. *Azure Kinect DK documentation*. https://docs.microsoft.com/en-us/azure/kinect-dk. Accessed: 2021-07-16. 2019.

[ML07] WS Marras and Thurmon E Lockhart. “The Complexities of Musculoskeletal Disorders, Untangling the Web”. In: *Proceedings of the Human Factors and Ergonomics Society Annual Meeting*. Vol. 51. 15. SAGE Publications Sage CA: Los Angeles, CA. 2007, pp. 914–917. DOI: 10.1177/154193120705101510.

[Mos+19] S Mosconi et al. “Participative ergonomics for the improvement of occupational health and safety in industry: a focus group-based approach”. In: ... *SUMMER SCHOOL FRANCESCO TURCO. PROCEEDINGS* 1 (2019), pp. 437–443.

[Mov23] Movella Inc. *Movella DOT User Manual*. Revision A. Document XD0502P. Movella Inc. July 2023. URL: https://www.movella.com/hubfs/Movella%20DOT%20User%20Manual.pdf.

[MSK14] Bruno S Moreira, Rosana F Sampaio, and Renata N Kirkwood. “Spatiotemporal gait parameters and recurrent falls in community-dwelling elderly women: a prospective study”. In: *Brazilian journal of physical therapy* 19 (2014), pp. 61–69.

[MW47] Henry B Mann and Donald R Whitney. “On a test of whether one of two random variables is stochastically larger than the other”. In: *The annals of mathematical statistics* (1947), pp. 50–60.

[Na06] Tatsuya Nomura and et al. “Negative attitudes toward robots scale”. In: *Interaction Studies* (2006).

[Nil+09] Maria H Nilsson et al. “The effects of high frequency subthalamic stimulation on balance performance and fear of falling in patients with Parkinson’s disease”. In: *Journal of neuroengineering and rehabilitation* 6.1 (2009), pp. 1–10.

[OB24] Federal Institute for Occupational Safety and Health (BAuA). “Physical workload in the German workforce and their associations to health disorders”. In: *BAuA Research Project F2588* (2024). DOI: 10.1234/baua.f2588. URL: https://www.baua.de/EN/Research/Research-projects/f2588.

[PAC24] PACE Rehabilitation. *Exoskeletons Set to Transform Rehabilitation Therapy*. https://pace-cr.com/news/exoskeletons-set-to-transform-rehabilitation-therapy/. Accessed August 2025. 2024.

[Pag12] Fernando L Pagan. “Improving outcomes through early diagnosis of Parkinson’s disease”. In: *American Journal of Managed Care* 18.7 (2012), S176.

[Ped+09] K. F. Pedersen et al. “Occurrence and risk factors for apathy in Parkinson disease: a 4-year prospective longitudinal study”. In: *Journal of Neurology, Neurosurgery & Psychiatry* 80.11 (2009), pp. 1279–1282. DOI: 10.1136/jnnp.2008.170043.

[Ped+11] F. Pedregosa et al. “Scikit-learn: Machine Learning in Python”. In: *Journal of Machine Learning Research* 12 (2011), pp. 2825–2830.

[PG15] Keith T Palmer and Nicola Goodson. “Ageing, musculoskeletal health and work”. In: *Best practice & research Clinical rheumatology* 29.3 (2015), pp. 391–404.

[Por20] Leslie G. Portney. *Foundations of Clinical Research: Applications to Evidence-Based Practice*. 4th. F.A. Davis Company, 2020. ISBN: 9780803661134.

[Pos+15] Ronald B. Postuma et al. “MDS clinical diagnostic criteria for Parkinson’s disease”. In: *Movement Disorders* 30.12 (2015), pp. 1591–1601. DOI: 10.1002/mds.26424.

[Pro+22] Jasmine K Proud et al. “Exoskeleton application to military manual handling tasks”. In: *Human Factors* 64.3 (2022), pp. 527–554.

[PSA20] Anisoara Paraschiv-Ionescu, Abolfazl Soltani, and Kamiar Aminian. “Real-world speed estimation using single trunk IMU: methodological challenges for impaired gait patterns”. In: *2020 42nd Annual International Conference of the IEEE Engineering in Medicine & Biology Society (EMBC)*. IEEE. 2020, pp. 4596–4599.

[PWK20] E. Papp, C. Wölfel, and J. Krzywinski. “Acceptance and User Experience of Wearable Assistive Devices for Industrial Purposes”. In: *Design Conference Proceedings* (2020). DOI: 10.1017/dsd.2020.319. URL: https://www.cambridge.org/core/services/aop-cambridge-core/content/view/96EAD3E4806E34850BC195D06CF4A320/S2633776220003192a.pdf.

[R C23] R Core Team. *R: A Language and Environment for Statistical Computing*. R Foundation for Statistical Computing. Vienna, Austria, 2023. URL: https://www.R-project.org/.

[Red16] J Redmon. "You only look once: Unified, real-time object detection". In: *Proceedings of the IEEE conference on computer vision and pattern recognition*. 2016.

[Res20] Google Research. *BlazePose Body Pose Tracking Diagram*. Accessed: 2025-10-27. 2020. URL: https://research.google/blog/on-device-real-time-body-pose-tracking-with-mediapipe-blazepose/.

[RMM18] Francisco J Romero-Ramirez, Rafael Muñoz-Salinas, and Rafael Medina-Carnicer. "Speeded up detection of squared fiducial markers". In: *Image and vision Computing* 76 (2018), pp. 38–47.

[Rod+19] Alejandro Rodríguez-Molinero et al. "The spatial parameters of gait and their association with falls, functional decline and death in older adults: a prospective study". In: *Scientific reports* 9.1 (2019), pp. 1–9.

[Sch+03] Joanna D Schaafsma et al. "Gait dynamics in Parkinson's disease: relationship to Parkinsonian features, falls and response to levodopa". In: *Journal of the neurological sciences* 212.1-2 (2003), pp. 47–53.

[Sch+17a] Johannes CM Schlachetzki et al. "Wearable sensors objectively measure gait parameters in Parkinson's disease". In: *PloS one* 12.10 (2017), e0183989.

[Sch+17b] Erich Schubert et al. "DBSCAN Revisited, Revisited: Why and How You Should (Still) Use DBSCAN". In: *ACM Trans. Database Syst.* 42.3 (July 2017). ISSN: 0362-5915. DOI: 10.1145/3068335. URL: https://doi.org/10.1145/3068335.

[Sch24] Eva Schobert. "Individual App-guided Exercise Therapy in Patients with Anterior Knee Pain and/or Knee Osteoarthritis". PhD thesis. Universität Oldenburg, 2024.

[SD11] Nicholas Stergiou and Leslie M Decker. "Human movement variability, nonlinear dynamics, and pathology: is there a connection?" In: *Human movement science* 30.5 (2011), pp. 869–888.

[SGa19] Glenn T. Stebbins, Christopher G. Goetz, and P. et al. "The Parkinson's Disease Activities of Daily Living, Interference, and Dependence Instrument". In: *Movement Disorders Clinical Practice* 6.8 (2019), pp. 637–644. DOI: 10.1002/mdc3.12847.

[Sha02] William R Shadish. "Revisiting field experimentation: field notes for the future." In: *Psychological methods* 7.1 (2002), p. 3.

[Sho+18] Linda Shore et al. "Technology Acceptance and User-Centred Design of Assistive Exoskeletons for Older Adults: A Commentary". In: *Robotics* 7.1 (2018). ISSN: 2218-6581. DOI: 10.3390/robotics7010003. URL: https://www.mdpi.com/2218-6581/7/1/3.

[Sil08] Michael Silverstein. "Meeting the challenges of an aging workforce". In: *American Journal of Industrial Medicine* 51.4 (2008), pp. 269–280. DOI: 10.1002/ajim.20569.

[Siz+04] Phillip S Sizer Jr et al. "Ergonomic Pain—-Part 2: Differential Diagnosis and Management Considerations". In: *Pain Practice* 4.2 (2004), pp. 136–162.

[SK11] Elif Surer and Alper Kose. "Methods and Technologies for Gait Analysis". In: *Computer Analysis of Human Behavior*. Springer, 2011, pp. 105–123. DOI: 10.1007/978-0-85729-994-9_5.

[SKA21] Amritanshu Kumar Singh, Vedant Arvind Kumbhare, and K Arthi. "Real-time human pose detection and recognition using MediaPipe". In: *International conference on soft computing and signal processing*. Springer. 2021, pp. 145–154.

[SL96] Graham B Scott and Nicola R Lambe. "Working practices in a perchery system, using the OVAKO Working posture Analysing System (OWAS)". In: *Applied Ergonomics* 27.4 (1996), pp. 281–284.

[SS11] Erik E Stone and Marjorie Skubic. "Passive in-home measurement of stride-to-stride gait variability comparing vision and Kinect sensing". In: *2011 Annual international conference of the IEEE engineering in medicine and biology society*. IEEE. 2011, pp. 6491–6494.

[Sta+26] Johannes Stalter et al. “Intermittent Theta-burst Transcranial Temporal Interference Stimulation focusing on the Putamen improves Motor Functions in Parkinsons Disease-A randomized, controlled Trial”. In: *medRxiv* (2026), pp. 2026–02.

[Ste+20] Anika Steinert et al. “Using new camera-based technologies for gait analysis in older adults in comparison to the established GAITRite system”. In: *Sensors* 20.1 (2020), p. 125.

[Ste+24] Andreas Stergioulas et al. “Assessing Motor Skills in Parkinson’s Disease Using Smartphone-Based Video Analysis and Machine Learning”. In: *Proceedings of the 17th International Conference on PErvasive Technologies Related to Assistive Environments*. 2024. DOI: 10.1145/3652037.3663945.

[SW+89] Lars St, Svante Wold, et al. “Analysis of variance (ANOVA)”. In: *Chemometrics and intelligent laboratory systems* 6.4 (1989), pp. 259–272.

[SW65] S. S. Shapiro and M. B. Wilk. “An analysis of variance test for normality (complete samples)”. In: *Biometrika* 52.3-4 (1965), pp. 591–611.

[SWL25] Alehegn Melesse Semegn, Bereket Haile Woldegiorgis, and Zerihun Wondimu Lemessa. “Recent Developments in Biomechanics-Based Prediction of Musculoskeletal Disorders: A Review”. In: *Sustainable Development Research in Manufacturing, Process Engineering, Green Infrastructure, and Water Resources*. Springer, 2025, pp. 155–167. DOI: 10.1007/978-3-031-77339-6_10.

[Tan+19] Dawn Tan et al. “Automated analysis of gait and modified timed up and go using the Microsoft Kinect in people with Parkinson’s disease: associations with physical outcome measures”. In: *Medical and Biological Engineering and Computing* 57.2 (2019), pp. 369–377. ISSN: 17410444. DOI: 10.1007/s11517-018-1868-2.

[Val24] Alexandre Vallée. “Exoskeleton technology in nursing practice: assessing effectiveness, usability, and impact”. In: *BMC Nursing* (2024). DOI: 10.1186/s12912-024-01821-3. URL: https://bmcnurs.biomedcentral.com/articles/10.1186/s12912-024-01821-3.

[Vas+17] Ashish Vaswani et al. “Attention is all you need”. In: *Advances in Neural Information Processing Systems*. Vol. 30. NeurIPS. 2017. DOI: 10.48550/arXiv.1706.03762. URL: https://arxiv.org/abs/1706.03762.

[Vic15] Vicon Motion Systems Limited. *What ’ s New in Vicon Nexus 2 . 2*. 2015. URL: http://www.vicon.com/file/nexuswhatsnew2-2.pdf.

[Vir+20] Pauli Virtanen et al. “SciPy 1.0: Fundamental Algorithms for Scientific Computing in Python”. In: *Nature Methods* 17 (2020), pp. 261–272. DOI: 10.1038/s41592-019-0686-2. URL: https://rdcu.be/b08Wh.

[Vox22] Jan P Vox. “Erkennung und Bewertung von Körperhaltungen und Bewegungen anhand von Gelenkwinkeln mit Einsatz von Motion-Capture-Sensorik”. PhD thesis. Carl von Ossietzky Universität Oldenburg, 2022.

[Wal+25a] Jonas Walkling et al. “Wearable Spine Tracker vs. Video-Based Pose Estimation for Human Activity Recognition”. In: *Sensors* 25.12 (2025), p. 3806.

[Wal+25b] Jonas Walkling et al. “Wearable Spine Tracker vs. Video-Based Pose Estimation for Human Activity Recognition”. In: *Sensors* 25.12 (2025), p. 3806.

[Wel+21] Julius Welzel et al. “Step Length Is a Promising Progression Marker in Parkinson’s Disease”. In: *Sensors* 21.7 (2021), p. 2292.

[Wil+23] John Richard Wilmoth et al. *World Social Report 2023: Leaving No One Behind in an Ageing World*. United Nations Publication ST/ESA/379. UN, 2023.

[Wil24] Leslie Patrick Willcocks. "Automation, digitalization and the future of work: A critical review". In: *Journal of Electronic Business & Digital Economics* 3.2 (Feb. 2024), pp. 184–199. ISSN: 2754-4214. DOI: 10.1108/JEBDE-09-2023-0018. eprint: https://www.emerald.com/jebde/article-pdf/3/2/184/9585703/jebde-09-2023-0018.pdf. URL: https://doi.org/10.1108/JEBDE-09-2023-0018.

[Wil45] Frank Wilcoxon. "Individual comparisons by ranking methods". In: *Biometrics bulletin* 1.6 (1945), pp. 80–83.

[Wu+19] Yuxin Wu et al. *Detectron2*. https://github.com/facebookresearch/detectron2. 2019.

[Xia+24] Xiang Xiang et al. *AI WALKUP: A Computer-Vision Approach to Quantifying MDS-UPDRS in Parkinson's Disease*. arXiv preprint. 2024. DOI: 10.48550/arXiv.2404.01654. arXiv: 2404.01654 [cs.CV].

[Xie+01] Jing Xie et al. "Effect of bilateral subthalamic nucleus stimulation on parkinsonian gait". In: *Journal of neurology* 248.12 (2001), pp. 1068–1072.

[Yan+08] Yea-Ru Yang et al. "Relationships between gait and dynamic balance in early Parkinson's disease". In: *Gait & posture* 27.4 (2008), pp. 611–615.

[Zha+20] Fan Zhang et al. "Mediapipe hands: On-device real-time hand tracking". In: *arXiv preprint arXiv:2006.10214* (2020).

[Zha+24] Yuting Zhao et al. "Selecting and Evaluating Key MDS-UPDRS Activities Using Wearable Devices for Parkinson's Disease Self-Assessment". In: *IEEE Journal of Selected Areas in Sensors* (2024).

Versicherung

Hiermit versichere ich an Eides statt, dass ich diese Arbeit selbständig verfasst und keine anderen als die angegebenen Quellen und Hilfsmittel benutzt habe. Außerdem versichere ich, dass ich die allgemeinen Prinzipien wissenschaftlicher Arbeit und Veröffentlichung, wie sie in den Leitlinien guter wissenschaftlicher Praxis der Carl von Ossietzky Universität Oldenburg festgelegt sind, befolgt habe.

Oldenburg, den 04.11.2025

Pedro Fernando Arizpe Gómez

geb. am 17.11.1988
in Puerto Vallarta, Jalisco, México